

AD-A102 282

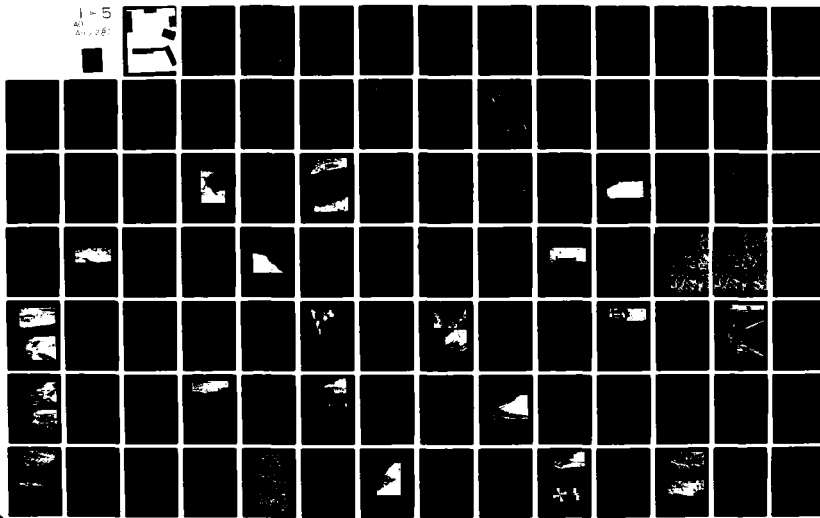
STATE UNIVERSITY OF NEW YORK COLL AT FREDONIA DEPT 0--ETC F/G 8/8
CATTARAUGUS CREEK HARBOR, NEW YORK GENERAL DESIGN MEMORANDUM, P--ETC(U)
MAR 76

DACW49-74-C-0118

NL

UNCLASSIFIED

1-5
40
40, 281



Appendix G for this report is not available per Mr. Thomas Vanwart, Army Corps of Engineers, Buffalo District

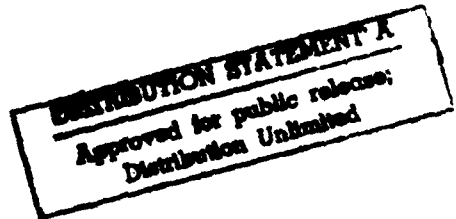
STATEMENT A
for
Hannibal Construction Unlimited

REPORT DOCUMENTATION PAGE		READ INSTRUCTIONS BEFORE COMPLETING FORM
1. REPORT NUMBER	2. GOVT ACCESSION NO.	3. RECIPIENT'S CATALOG NUMBER
		AD-A102282
4. TITLE (and Subtitle) Cattaraugus Creek Harbor, New York General Design Memorandum Phase 11	5. TYPE OF REPORT & PERIOD COVERED Final	
7. AUTHOR(s)	6. PERFORMING ORG: REPORT NUMBER	
9. PERFORMING ORGANIZATION NAME AND ADDRESS U.S. Army Engineer District, Buffalo 1776 Niagara Street Buffalo, New York 14207	10. PROGRAM ELEMENT, PROJECT, TASK AREA & WORK UNIT NUMBERS	
11. CONTROLLING OFFICE NAME AND ADDRESS U.S. Army Engineer District, Buffalo 1776 Niagara Street Buffalo, New York 14207	12. REPORT DATE 1976	
14. MONITORING AGENCY NAME & ADDRESS(if different from Controlling Office)	13. NUMBER OF PAGES 173	
	15. SECURITY CLASS. (of this report)	
	15a. DECLASSIFICATION/DOWNGRADING SCHEDULE	
16. DISTRIBUTION STATEMENT (of this Report) Distribution Unlimited		
17. DISTRIBUTION STATEMENT (of the abstract entered in Block 20, if different from Report)		
18. SUPPLEMENTARY NOTES		
19. KEY WORDS (Continue on reverse side if necessary and identify by block number) Harbors Cattaraugus Creek Flood Control		
20. ABSTRACT (Continue on reverse side if necessary and identify by block number) The purpose of this Phase 11 General Design Memorandum is to present the detailed design of the Cattaraugus Harbor improvements. This report describes the changes in the local cooperation requirements, costs, and benefits that have accrued due to changes in design and price levels since preparation of the Phase 1 General Design Memorandum.		

APPENDIX E

LITTORAL PROCESSES AND SEDIMENTATION
IN THE CATTARAUGUS EMBAYMENT, NEW YORK

Accession For	
NTIS GRA&I	
DTIC TAB	
Unannounced	
Justification	
By _____	
Distribution/	
Availability Codes	
Dist	Avail and/or Special
A	



ERRATA

p. 80 line 5 from bottom. SE rather than NE

p. 90 line 8. 9E rather than NE

p. 100 line 17. above sea level

p. 122 October measurements presented as Chapter 10.

p. 134 in caption of fig. 50. > 6

p. 150 Footnote Refer to Chapter 11 for a preliminary estimate of gravel transport rate.

p. 151 line 18 should read: ...Gowanda Shale. [and] Red sandstone, possibly from outcrops of the Medina Sandstone Granite granite and other... (Delete the words in brackets)

TABLE OF CONTENTS

	<u>Page</u>
Abstract	v
Acknowledgements	v
List of Illustrations	vi
List of Tables	xi
1. Authority and Scope	1
2. Report Outline	2
3. Reconnaissance of the Morphology and Sediments of the Southeast Shoreline of Lake Erie	3
3.1. Introduction	3
3.2. Shoreline Units	9
3.3. Conclusions	98
4. Geomorphic History of Cattaraugus Harbor and Vicinity	100
5. Historic Changes Near the Mouth of Cattaraugus Creek	116
6. Littoral Processes	122
6.1. North American Cyclone Patterns	122
6.2. Wind and Wave Statistics	130
6.3. Littoral Processes at Sunset Bay	138
6.4. Wave Refraction	143
6.5. Observed Process Variability in the Embayment	147
7. Sediment Sources and Dispersal Patterns	151
7.1. Sediment Sources	151
7.2. Beach Sediments	156
7.3. Nearshore Sediments	161

	<u>Page</u>
8. Coastal Morphology	166
8.1. Beach Profiles	166
8.2. River Mouth Spits	175
8.3. Protuberances	180
9. Breakwater Design Alternatives	185
9.1. Changes in the Updrift Beaches	188
9.2. Changes in Downdrift Beaches	188
9.3. Harbor Shoaling Due to Littoral Drift	189
9.4. Harbor Shoaling Due to Fluvial Sediment Supply	190
9.5. Ice Jams and Related Flood Problems	193
9.6. Wave Conditions in the Harbor Entrance	194
9.7. Tentative Recommendations	194
10. Seasonal Changes in Shoreline and River Mouth Form	196
10.1. Introduction	196
10.2. Beach Morphology	196
10.3. Seasonal Changes in Spit Morphology	199
10.4. Lake Erie Wind Patterns	202
11. Gravel Transportation on Cattaraugus Creek	206
11.1. Introduction	206
11.2. Hydraulic Computations	206
11.3. Sediment Discharge Computations	220
11.4. Discussion	222
12. Conclusions	226
References	230
Appendix I. Weather Data for Buffalo, May 7-June 13, 1974	246
Appendix II. Littoral Processes in the Cattaraugus Embayment, May 7-June 13, 1974	247
Appendix III. Lithological Composition of Cattaraugus Beach and Source Materials	255
Appendix IV. Texture of Cattaraugus Beach Sediments	259
Appendix V. Cattaraugus Creek Stage Readings at the Keene Marina Staff Gage	262

	<u>Page</u>
Appendix VI. Recorded Profiles of the Cattaraugus Beach	264
Appendix VII. A. Concentration of Suspended Sediment in Surface Samples from the Breaker Zone Obtained during the Storm of June 11, 1974	275
B. Concentration of Suspended Sediment in Cattaraugus Creek at the Buffalo Rd. Bridge	275
Appendix VIII. Texture Parameters for Nearshore Sand in the Cattaraugus Embayment	276
Appendix IX. Textural Composition of the Cattaraugus Beach Sand Fraction	278

ACKNOWLEDGEMENTS

This study was supported by the U. S. Army Engineer District, Buffalo, New York, by contract No. DACW49-74-C-0118 plus modification P00001 to Robert K. Fahnestock. Thomas Wilkinson, Joan Pope, Robert Johnson, John Koller and James Karsten, all of the U. S. Army Engineers, are acknowledged for guidance and active participation in various phases of the project.

The bulk of the field work in the spring was performed by Robert K. Fahnestock of the State University of New York at Fredonia and Dag Nummedal, Miles Hayes, Robert Clemens, David Shearer and Leita Hulmes of the Department of Geology, University of South Carolina. Field work in the fall was done by Robert Fahnestock, Gary Weir, Hannes Leetaru, Ray Levey, Ignacio Orozco-Martinez, Herb Buxton, Donald Messinger and John Walton, all of the Department of Geology, the State University of New York at Fredonia.

The report was prepared by Dag Nummedal, Miles O. Hayes and Robert K. Fahnestock.

LIST OF ILLUSTRATIONS

<u>Figure</u>	<u>Page</u>
1. Location map showing the area studied during the regional reconnaissance.	5
2. Location of shoreline morphological units (A-N) and zonal study sites (1-20).	7
3. Map and beach profile at zonal site #1.	13
4. Beach southwest of Fairport Harbor structure.	16
5. Photographs of zonal study site #2.	18
6. Sketch and beach profiles measured at zonal site #3, Geneva-on-the-lake, Ohio.	21
7. Photograph of area updrift of the groin at zonal site #4.	23
8. Sketch map and beach profile at zonal site #4.	25
9. Jetties at mouth of Red Brook, Ohio.	28
10. Eroding cliff at zonal site #5.	31
11. Structure at Conneaut Harbor, Ohio.	33
12. Mouth of Elk Creek, Pa.	36
13. Beach profile and sample photographs at zonal site #6.	38
14. Photographs of zonal site #7, near Fairplain, Pa.	40
15. Map of part of groin field at zonal site #8.	43
16. Field sketch of profile B at zonal site #8.	45
17. Photographs of zonal site #8.	47
18. Photographs and beach profiles at mouth of Walnut Creek, Pa. (zonal site #9).	50

<u>Figure</u>	<u>Page</u>
19. Photographs of beach zone at the Walnut Creek jetties.	52
20. Photographs of zonal site #10.	54
21. Photograph and map of zonal site #11, Presque Isle, Pa.	57
22. Photographs and beach profiles at zonal site #11.	59
23. Photograph of zonal site #12, the recurved spit area on Presque Isle, Pa.	62
24. Block diagram of recurved spit area of Presque Isle.	64
25. Photographs of zonal site #14, mouth of Twentymile Creek, Pa.	68
26. Three-dimensional diagram of zonal site #14.	70
27. Gravel samples on profile B at zonal site #14.	72
28. Photograph of rock cliff at zonal site #15, Blue Water Beach, N. Y.	74
29. Photograph and joint pattern diagram, Unit L.	77
30. Photographs of zonal site #16, Van Buren Point, N. Y.	79
31. Field sketch of zonal site #18.	83
32. Three-dimensional diagram of the beach zone at Evangola State Park.	85
33. Photograph of the beach at Evangola State Park.	87
34. Photograph and map of zonal site #19, Big Sister Creek, N. Y.	89
35. Photographs and beach-dune profile at zonal site #19.	92
36. Photograph of structure at Sturgeon Point, N. Y.	94

<u>Figure</u>	<u>Page</u>
37. Photograph of zonal site #20.	96
38. Simplified glacial map of the eastern part of Lake Erie.	102
39. Formation of the Allegheny River from preglacial drainage.	104
40. High-level beaches and moraines of western New York.	107
41. Lake escarpment glaciation. Position of ice-margin and drainage patterns.	109
42. Gowanda glaciation. Position of ice-margin and drainage pattern.	111
43. Lake Whittlesey and associated drainage.	113
44. Maps of Cattaraugus Creek mouth and the adjacent shoreline. From 1875 to 1961.	118
45. Maps of Cattaraugus Creek mouth and the adjacent shoreline. From 1961 to 1971.	120
46. Annual variation in wave characteristics.	124
47. A. Major North American cyclone tracks.	127
B. Generalized cyclonic circulation.	127
C. Variations in wind direction on Lake Erie with passage of a typical cyclone.	127
48. Synoptic charts at 24 h intervals for storm of June 9-12, 1974.	129
49. Wind diagram for Buffalo, N. Y.	132
50. Wave diagrams for Erie, Pa., and Buffalo, N. Y.	135
51. Wave energy diagrams for Erie, Pa., and Buffalo, N. Y.	137

<u>Figure</u>	<u>Page</u>
52. Process parameters at Cattaraugus Beach, Cat. 3, May 7-June 13, 1974.	141
53. A. Location map of the Cattaraugus Embayment.	145
B. Fetch diagram.	145
C. Wave refraction diagram.	145
54. Process variability in the Cattaraugus Embayment.	149
55. A. Lithological variations in Cattaraugus beach gravels.	154
B. Characteristic lithologies of source materials.	154
56. Texture variations in Cattaraugus beach gravels.	158
57. A. Distribution of sediment sizes in the nearshore of the Cattaraugus Embayment.	163
B. Bathymetry of the Cattaraugus Embayment.	163
58. A. Beach profiles Cat. 5 and Cat. 6 superimposed for May 10 and June 11.	168
B. Beach profiles Cat. 3 and Cat. 7 superimposed for May 10 and June 11.	168
59. Beach profiles Cat. 4 and Cat. 5 on May 7, June 11, June 12, and June 13.	171
60. Beach profiles Cat. 6 and Cat. 10 on May 10, June 11, June 12, and June 13.	174
61. Planimetric maps of the Hanover spit.	177
62. Planimetric maps of the Brant spit.	179
63. Map of protuberance between Cat. 6 and Cat. 7 on May 15, 1974.	182
64. Map of protuberance between Cat. 6 and Cat. 7 on May 27, 1974.	184

<u>Figure</u>	<u>Page</u>
65. Alternative structure designs.	187
66. Current pattern near entrance to Little Lake Harbor (Lake Superior) during strong westerly wind with outflow from the harbor.	192
67. A. Beach profiles at Cat. 6 on September 15 and October 26.	198
B. Beach profiles at Cat. 5 superimposed for June 13 and October 26, 1974.	198
68. Changes in the configuration of Cattaraugus Creek mouth in late October 1974.	201
69. Wind diagram for Buffalo, New York, from May 1 to November 1, 1974.	205
70. Map of lower Cattaraugus Creek, Erie and Chautauqua Counties, New York.	208
71. Cross sections of studied reaches at Cattaraugus Creek	210
72. Size-frequency distribution of typical point bar gravel on Cattaraugus Creek.	212
73. Stage-discharge curves.	216
74. Summary of computed hydraulic and sedimentary parameters for the lower Cattaraugus Creek.	218
75. Flow frequency diagrams of Cattaraugus Creek at Gowanda and the mouth.	225

Plate

1. Aerial view of a section of Cattaraugus Creek upstream of Gowanda.	233
2. Aerial view of a Cattaraugus Creek gravel point bar.	233
3. Wide beach. View northward from profile location Cat. 10 towards Lotus Point.	234
4. Oblique aerial photograph of the Cattaraugus Embayment from 1000 feet.	234
5. Beach face at Cat. 6 during storm.	235

	<u>Page</u>
6. Beach face at Cat. 6.	235
7. View towards the north of the beach at profile location Cat. 5.	236
8. View towards the south of the beach at profile location Cat. 5.	236
9. View of the mouth of Cattaraugus Creek during a storm.	237
10. Aerial photo of the mouth of Cattaraugus Creek right after a storm.	237
11. Oblique aerial view of the mouth of Cattaraugus Creek on October 26, 1974.	238

LIST OF TABLES

	<u>Page</u>
Table I	10
Table II	114
Table III	213
Table IV	219
Table V	223

SUBJECT: Cattaraugus Creek Harbor, New York
TO: U. S. Army Engineer District, Buffalo

1. AUTHORITY AND SCOPE

This study was undertaken in accordance with specifications set forth in contract No. DACW49-74-C-0118. The Scope of Work, Paragraph 1, specifies:

(The) purpose of (the) work (is) to provide data on littoral currents and stream currents and the source and amount of sediment transported by each. The data provided is to be used by the Buffalo District Corps of Engineers in their study of the proposed breakwater structures for the Cattaraugus Harbor project and the effects of these structures on both the littoral and stream currents.

Based on the data collected according to the Scope of Work, Paragraph 3(b), we have analyzed five alternative breakwater configurations. The selection of a preferred structure was based on criteria specified in Scope of Work, Paragraph 2(4):

Based on his findings (the contractor should) propose a breakwater configuration that will have the least detrimental effect on the regional environment.

Subsequent to the completion of the above contract in August, 1974, modification P00001 was put into effect, calling for further field work in the fall. The new Scope of Work, Paragraph 7(c), states:

The Contractor will compare the results of the summer and fall studies and draw some conclusions about the effects of the proposed structure on the littoral drift.

2. REPORT OUTLINE

The problems specified above have been analyzed in this study of sediment distribution and process variability within the Cattaraugus Embayment. It is the intent of this approach to determine in detail the littoral process pattern during any individual storm and to outline the consequent long-term sediment dispersal paths. Based on the developed process-response model for the unmodified Cattaraugus Embayment, the report concludes with a prediction of possible sedimentation problems associated with five different breakwater configurations at the creek mouth.

The report consists of five closely related parts:

1. General reconnaissance of the morphology and sediments of the southeast shore of Lake Erie (Chapter 3).
2. Geomorphological history of the Cattaraugus Creek area (Chapters 4 and 5).
3. Active littoral processes and sediment response in the Cattaraugus Embayment (Chapters 6, 7, 8 and 10).
4. Preliminary estimate of the gravel transport rate on Cattaraugus Creek (Chapter 11).
5. Conclusions and a discussion of tentative breakwater design alternatives (Chapters 9 and 12).

A synopsis of the major results and conclusions from both the spring and the fall field studies is provided.

3. RECONNAISSANCE OF THE MORPHOLOGY AND SEDIMENTS OF THE SOUTHEAST SHORELINE OF LAKE ERIE

3.1 Introduction.

Before the geomorphology and sedimentation of the Cattaraugus embayment can be properly assessed, it is necessary to determine how it relates to the rest of the southeastern shoreline of Lake Erie. In order to do this, a regional reconnaissance of the morphology and sediments of the shoreline between Fairport Harbor, Ohio and Wanakah, New York (Fig. 1) was carried out in May, 1974. The purpose of this study was to: (a) determine regional patterns of erosion and sedimentation; (b) briefly examine all major man-made structures in the area; and (c) to describe as succinctly as possible the morphology and sediments of specific sites thought to be representative of the region as a whole.

This regional reconnaissance was accomplished by application of the zonal method developed over the past few years by Hayes and associates of the Coastal Research Division. This method consists of the following steps:

1. A single large physiographic unit is chosen as the area of study, in this instance, the southeastern shoreline of Lake Erie.
2. Study of aerial photographs, maps and charts of the area chosen, as well as of the available literature, precedes the field work.
3. Field work begins by aerial reconnaissance of the entire area. The study area (Figs. 1 and 2) was flown twice, once in April and once in May. The area was photographed in detail during both flights.

Figure 1. Location map showing the area studied during the regional reconnaissance of the southeastern shoreline of Lake Erie. The study covered the area between Fairport Harbor, Ohio, and Wanakah, New York.

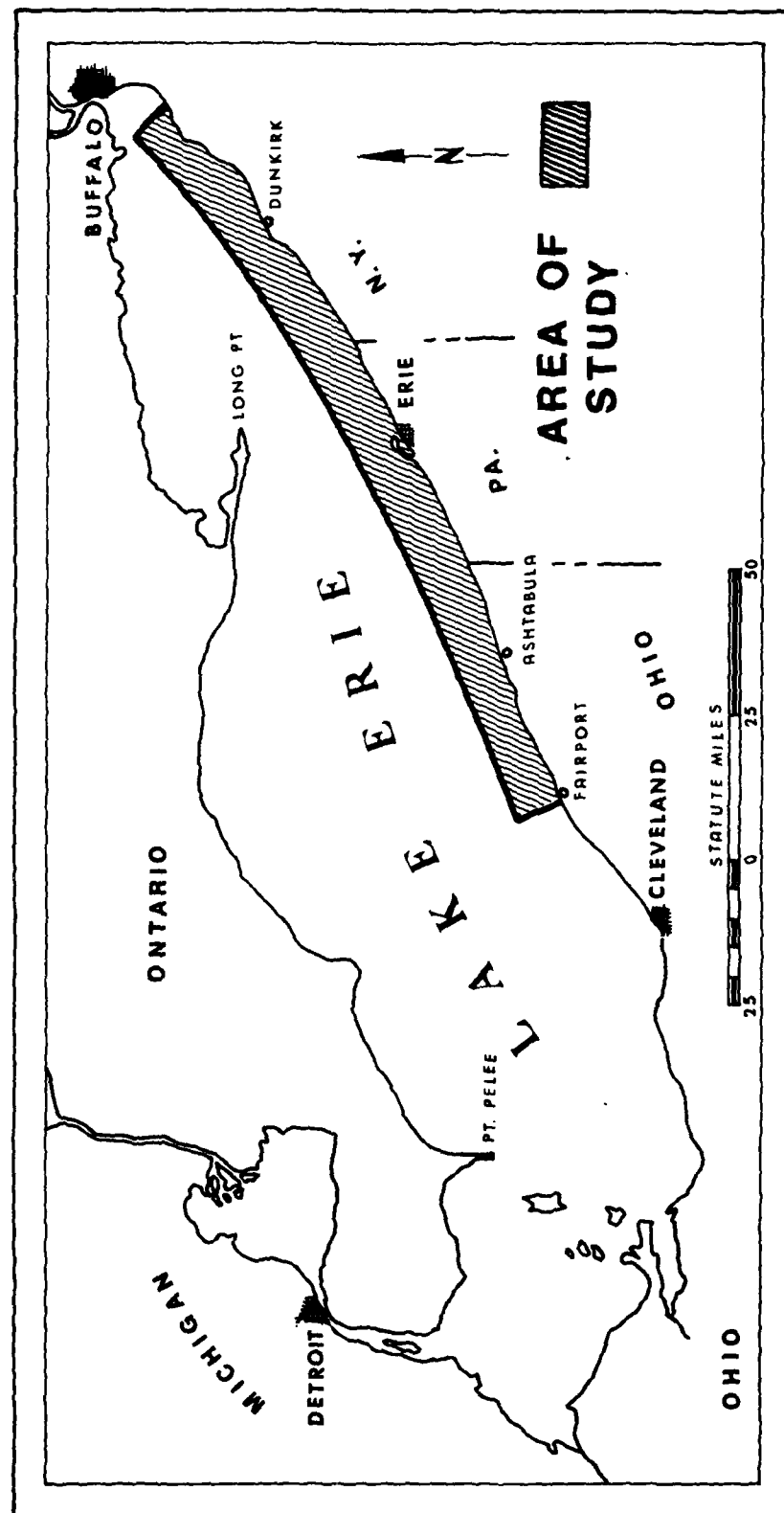


FIGURE 1

Figure 2. Location of shoreline morphological units (A-N) and zonal study sites (1-20) on the southeastern shoreline of Lake Erie. Descriptions of the morphological units are given in Table I.

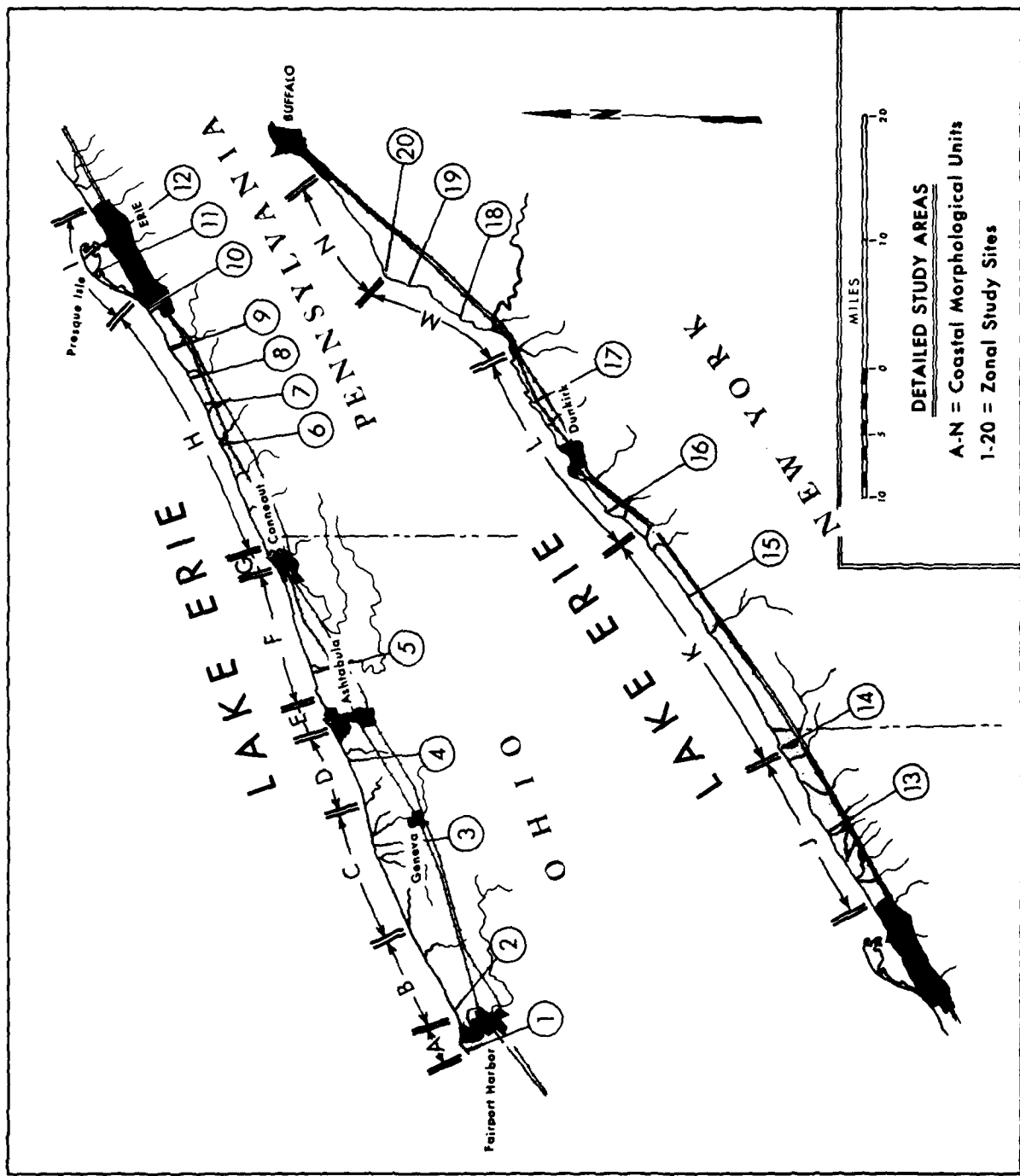


FIGURE 2

4. If desired, a sediment sampling interval is then chosen. In this study, we did not sample the sediments in detail because of lack of time and resources necessary to work up the data in the laboratory.

5. Next, the study area is divided into physiographic subdivisions. These subdivisions are defined on the basis of a change in morphology or in one of the major process parameters. During the second flight, the study area was carefully described (with a tape recorder) and coastal physiographic units were chosen, as well as sites for detailed study, within each major unit. The study area was divided into 14 coastal units, which are located on Figure 2.

6. Within each of the subdivisions, specific sites thought to be representative of that particular type of coastal morphology are chosen for detailed study. There may be several of these sites within each subdivision, depending upon the complexity of the unit. In the study area, 20 of these detailed studies, called zonal studies, were carried out by a 3-man crew.

Each zonal study may include the following:

- a. Construction of a three-dimensional block diagram of the beach zone. In the study area, this was usually accomplished by combining beach profiles with pace-and-compass maps.
- b. Grain-size estimates and photographs of the sediments are made at selected localities.
- c. Detailed topographic surveys and statistical studies of features within the zone.
- d. Detailed photographs to illustrate sediment characteristics and topographic features within the zone, both from the ground and from the air.

e. Detailed sketches are made of the zone. These are important because they force the observer to carefully inspect all aspects of the morphology and sediments within the zone.

The end product of a zonal study is a general summary and map of the morphology of a large coastal region, with some details on the local morphology and sediment dispersal trends. The location of the 14 coastal units and 20 zonal study sites for the study area are given in Figure 2.

3.2. Shoreline units.

3.2a. Introduction. The fourteen coastal units chosen are described in Table I. The boundaries between the units were chosen at points where significant changes in morphology occurred, such as at major harbor structures (e.g. at Ashtabula and Conneaut), or at significant topographic breaks (e.g. southwest border of Presque Isle).

3.2b. Unit A. The Fairport Harbor area, Unit A (Fig. 2), is an improvement project that was authorized in 1835 and has been modified several times since then. It consists of an outer harbor about 360 acres in area, a west breakwater 3878 ft. long, which is connected with the shore, and an east breakwater 6750 ft. long, which is separated from the shore by approximately 2700 ft. of open water. Figure 3A gives an outline map of the harbor area.

A brief ground study, or zonal study, was conducted on the beach west

Table I. Description of major shoreline morphological units (A-N; Fig. 2).

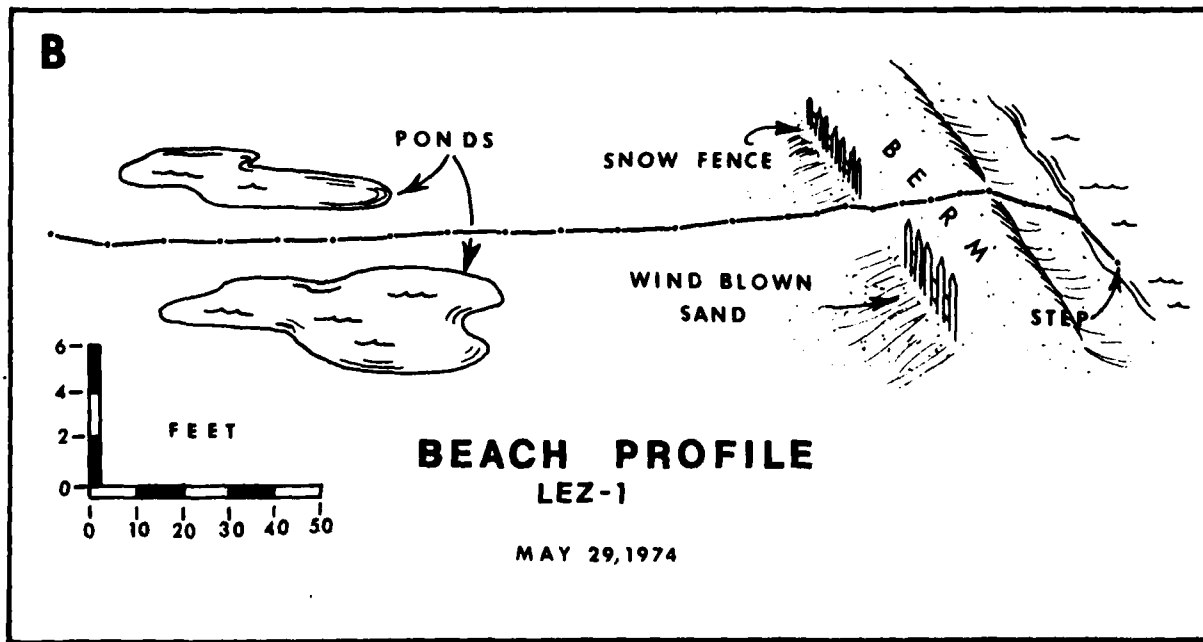
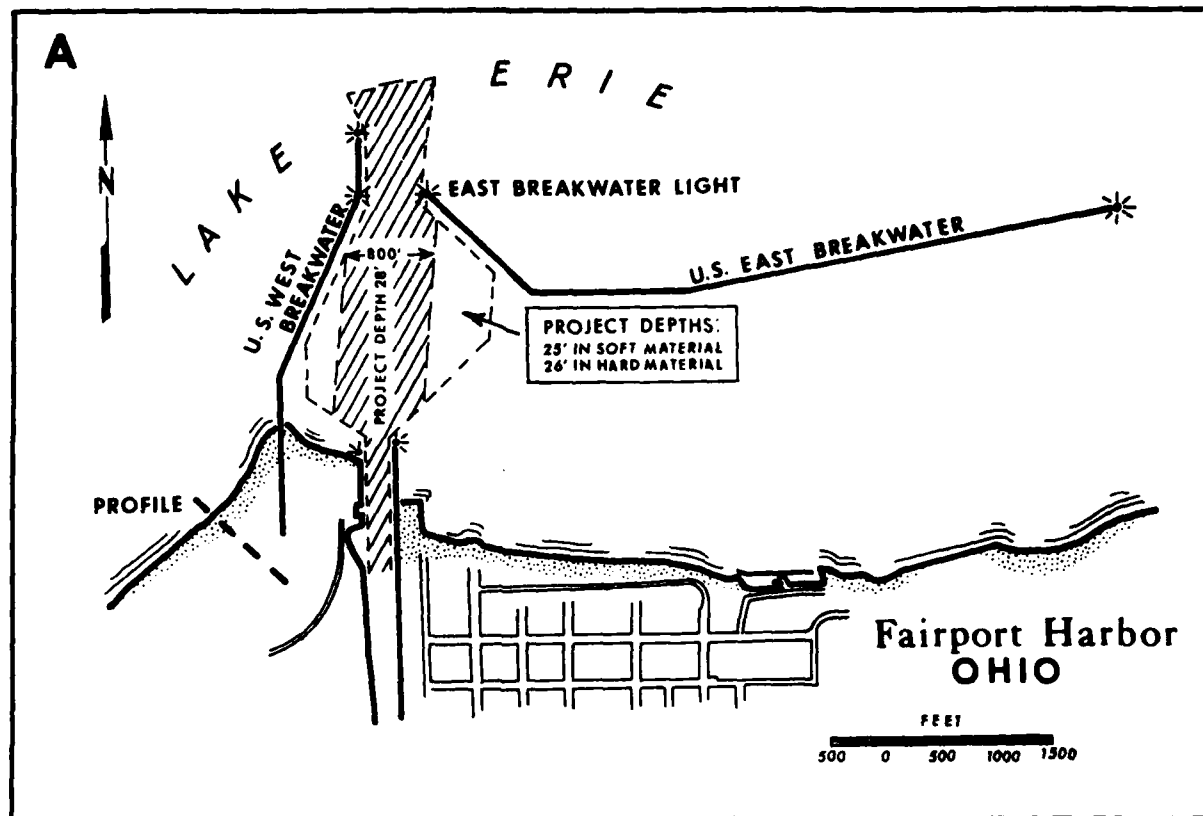
Unit	Location	Description
A	Fairport Harbor, Ohio, area	Major harbor structure consisting of two large breakwaters and dredged area.
B	Eight miles of shoreline northeast of Fairport Harbor, Ohio	Eroding cliffs of intermediate height (50-60 ft.) composed predominantly of fine-grained Pleistocene sediments.
C	Unit B to Indian Creek, Ohio (10.5 miles)	Lowland topography with numerous deltas separated by some cliffs; heterogeneous area; severe erosion.
D	Indian Creek, Ohio, to Ashtabula, Ohio, (6.5 miles)	High eroding cliff composed predominantly of glacial deposits; cliff relatively straight.
E	Ashtabula, Ohio, structure	Major harbor structure consisting of two long breakwaters and dredged area.
F	Ashtabula, Ohio, to Conneaut, Ohio (13 miles)	High eroding cliff composed predominantly of glacial deposits; cliff somewhat irregular.
G	Conneaut, Ohio, structure	Major harbor structure consisting of two long breakwaters and dredged area.
H	Conneaut, Ohio, to Erie, Pa. (21 miles)	Cliffs of variable heights with shale at base; several minor deltas; complex shoreline.
I	Presque Isle, Pa.	Large recurved spit system migrating northeastward.

Table I. (cont'd.)

Unit	Location	Description
J	Erie, Pa., to Twentymile Creek, Pa., (16 miles)	Complex area with numerous deltas separated by cliffs of varying heights; amount of bedrock in cliffs increasing.
K	Twentymile Creek, Pa., to Lake Erie State Park, N.Y. (22 miles)	Cliffs of intermediate height composed predominantly of bedrock; many small river deltas; shoreline relatively straight.
L	Lake Erie State Park, N.Y., to Silver Creek, N.Y. (16 miles)	Cliffs of intermediate height composed entirely of bedrock (shale); shoreline very irregular with orientation of major headlands controlled by joint patterns in bedrock.
M	Silver Creek, N.Y. to Sturgeon Pt., N.Y. (16 miles)	Headlands of intermediate height separating wide, sandy embayments; large streams with heavy sediment input.
N	Sturgeon Pt., N.Y. to Wanakah, N.Y. (8.5 miles)	Cliffs of intermediate height composed of bedrock and glacial sediments; shoreline somewhat irregular.

Figure 3. A. Map of the structure at Fairport Harbor, Ohio. Note location of beach profile given in B.

B. Profile of beach just west of the west breakwater of the Fairport Harbor structure. Profile was measured on 29 May 1974. This wide, predominantly sandy beach has accumulated at this locality as a result of the Fairport Harbor structure trapping sediment in transport in the nearshore zone. The sediment transport direction is predominantly from southwest to northeast in this area.



FIGURES 3A AND B

of the west breakwater. The profile of the beach at that location is given in Figure 3B. The measured beach profile consists of a very wide, high, predominantly sandy berm. A large portion of the beach, principally that area behind the snow fence (shown in Fig. 4), has been manicured with bulldozers to maintain a flat profile. The measured width of the beach between the low dune scarp and the present water level was 357 ft., which makes this one of the widest, sandy beach areas on the southeast shore of Lake Erie. The beach is wide at this position as a result of the attenuation of longshore transport of sediments in a northeasterly direction by the exceptionally long west breakwater of the Fairport structure. It is evident from the aerial photograph in Figure 4 that a large bar occurs offshore (note waves breaking on bar). We also observed ridge-and-runnel systems and beach protuberances at different times at this locality; therefore, this is an area of active sediment transportation and deposition.

3.2c. Unit B. Unit B, an area of eroding cliffs of intermediate height, starts just east of the Fairport Harbor structure and continues eastward for about 8 miles (Fig. 2). The cliffs are composed of glacial material and are frequently scalloped by landslides and slumping, as at zonal site #2, where a road has recently been truncated by a large slump (Fig. 5A,B). The cliff is composed mainly of fine-grained gray clay. The measured height of the cliff at the zonal site is 57 ft.

3.2d. Unit C. Unit C is approximately 10.5 miles in length (Fig. 2) and is dominated by lowland topography that contains numerous small river deltas separated by some erosional cliffs. In general, the area is intensely erosional and much property is being lost. Unit C offers a strong contrast

Figure 4. Wide sandy beach located southwest of Fairport Harbor structure (west breakwater is shown in foreground). Note location of beach profile given in Figure 3B.

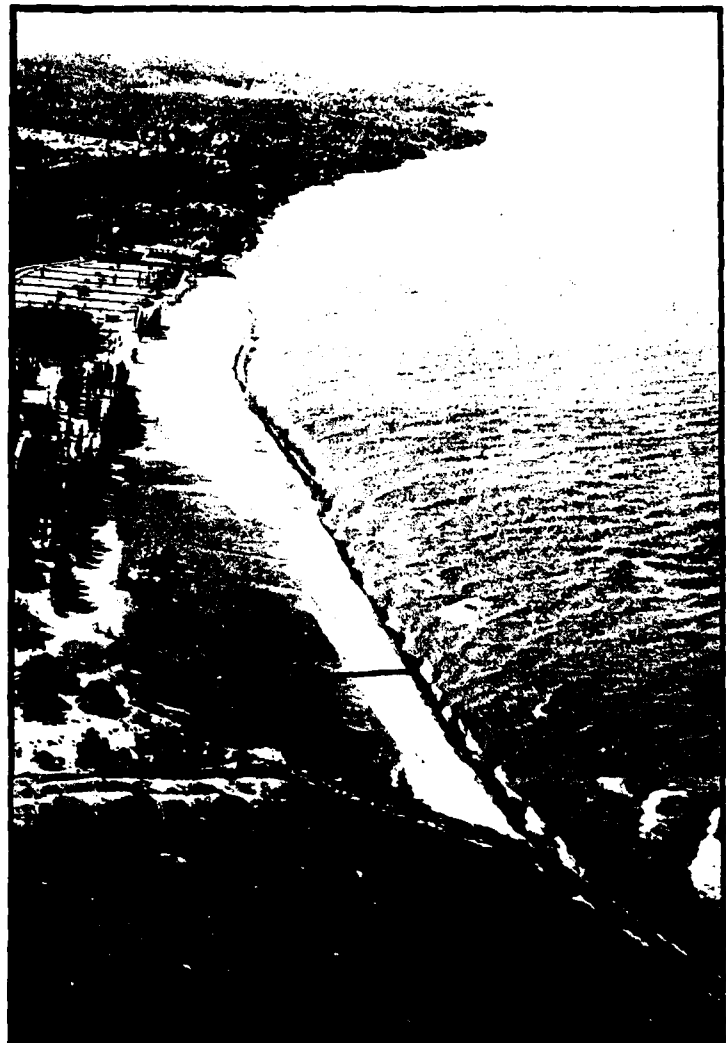
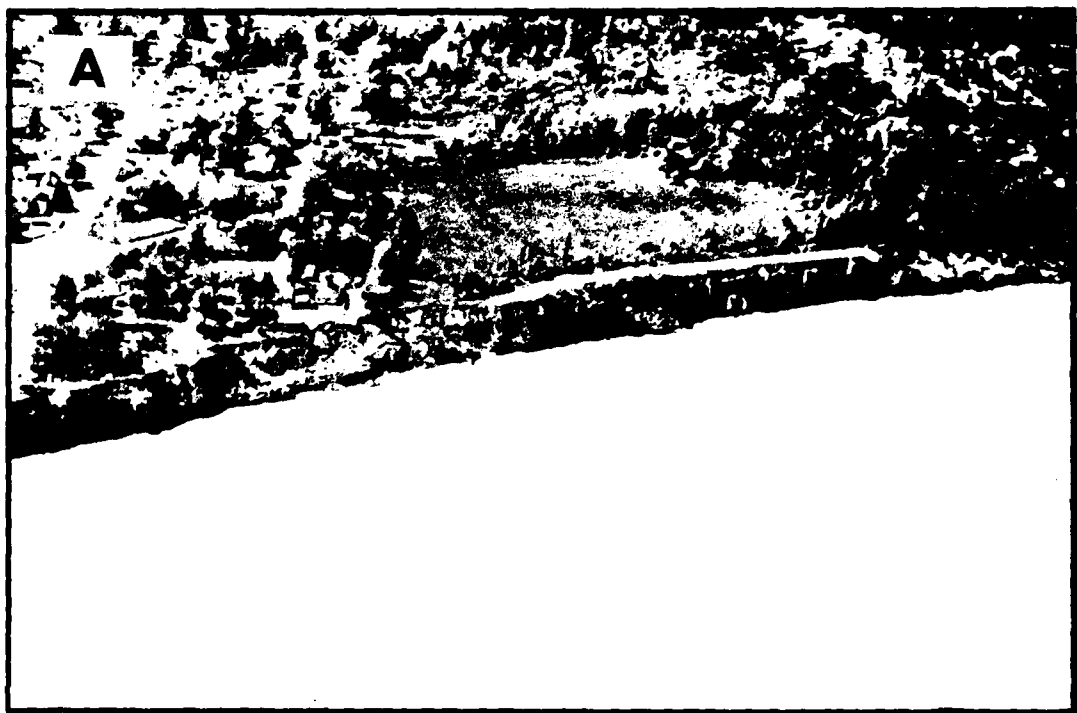


FIGURE 4

Figure 5. A. Eroding cliff at zonal study site #2 (Fig. 2). This site is located approximately 3 miles east of Fairport Harbor, Ohio.

B. Cliff near area shown in aerial view (A). Note intensive slumping of the cliff.



FIGURES 5A AND B

to Unit B, in that it is much more heterogeneous, contains more rivers, and is notably lacking in thick accumulations of glacial material.

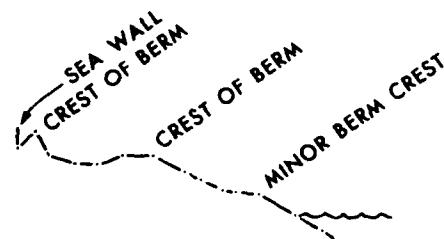
Zonal site #3 is located at Geneva-on-the-Lake, Ohio. It is dominated by a single groin structure 139 ft. in length, which has a large accumulation of sediment on the west side (see sketch map in Fig. 6). The sediment accumulated updrift of the groin is 106 ft. wide at the groin and extends 330 ft. updrift. The accumulation amounts to approximately 4,200 cubic yards of sediment. To the west of this accumulation, a corrugated seawall has been built which has been only partially successful in retarding erosion in that area, and to the east of the structure, severe erosion is presently taking place. In fact, the general area represented by Zonal #3 is one of the most severely eroding portions of the southeastern shoreline of Lake Erie.

Three beach profiles were measured at the zonal site. Two profiles on the updrift side, A & B (Fig. 6), are made up of multiple berms that are composed of a mixture of fine gravel and sand. This area is illustrated by the photograph in Figure 7. The profile downdrift of the groin is narrow, also consists of multiple berms, but is finer-grained, being composed mostly of granule-sized material.

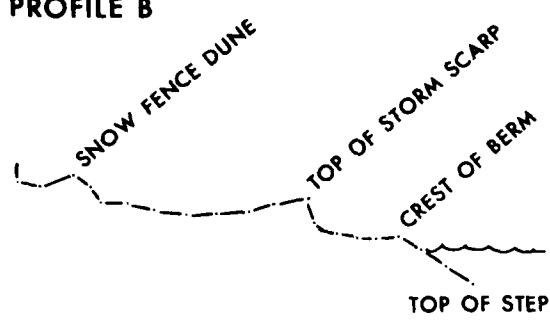
3.2e. Unit D. Unit D., which extends for 6.5 miles between Unit C and Ashtabula, Ohio (Fig. 2), is a high eroding cliff composed predominantly of glacial material. The cliff is relatively straight but shows some slumping and erosional features. The zonal site (#4; Fig. 8) is located at Red Brook, Ohio, which is a small stream cutting through the cliff. It contains small jetty structures, which are illustrated in the aerial

Figure 6. Sketch map (right) and three beach profiles measured at zonal site #3 (Geneva-on-the-lake, Ohio) on 29 May 1974. There is strong nearshore sediment transport from southwest to northeast in this area. Note heavy sediment accumulation on the updrift side of the groin.

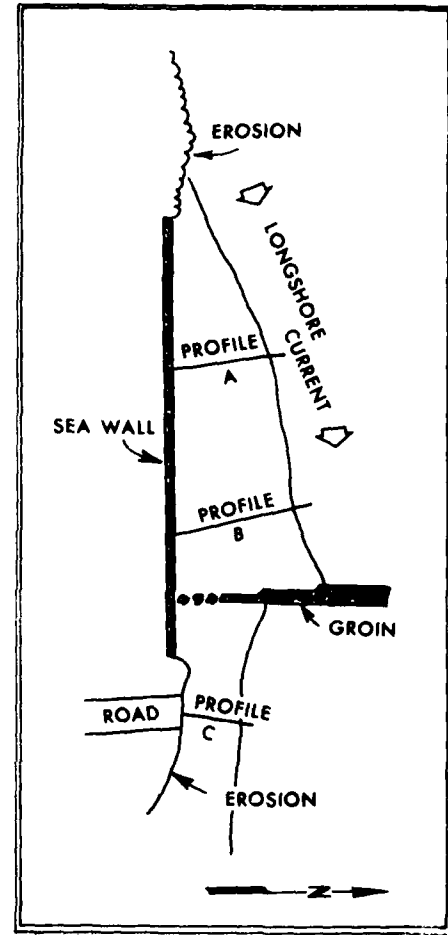
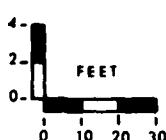
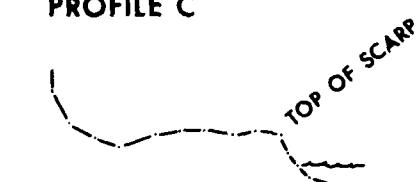
PROFILE A



PROFILE B



PROFILE C



ZONAL 3

GENEVA-ON-THE-LAKE, OHIO

MAY 29, 1974

FIGURE 6

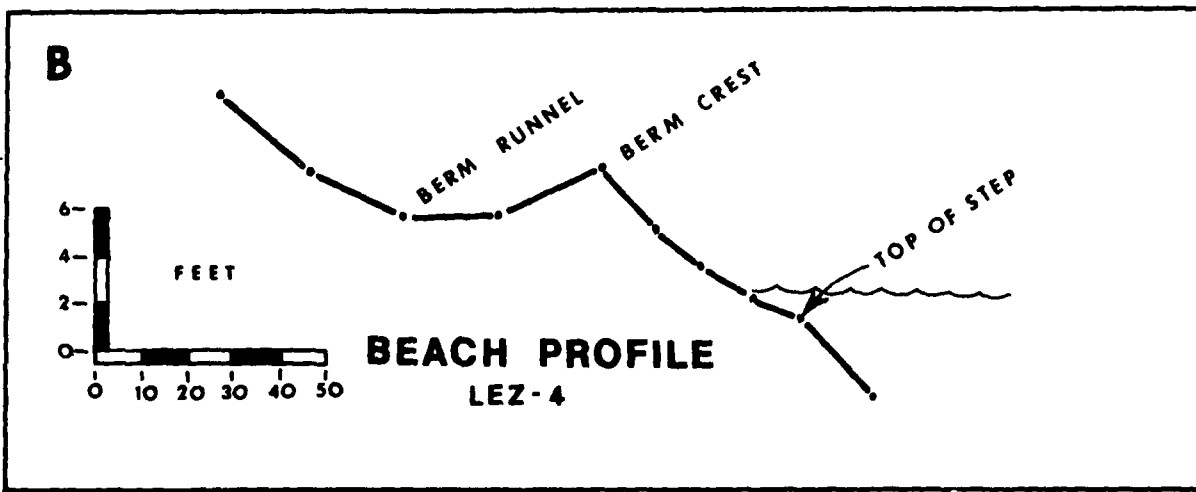
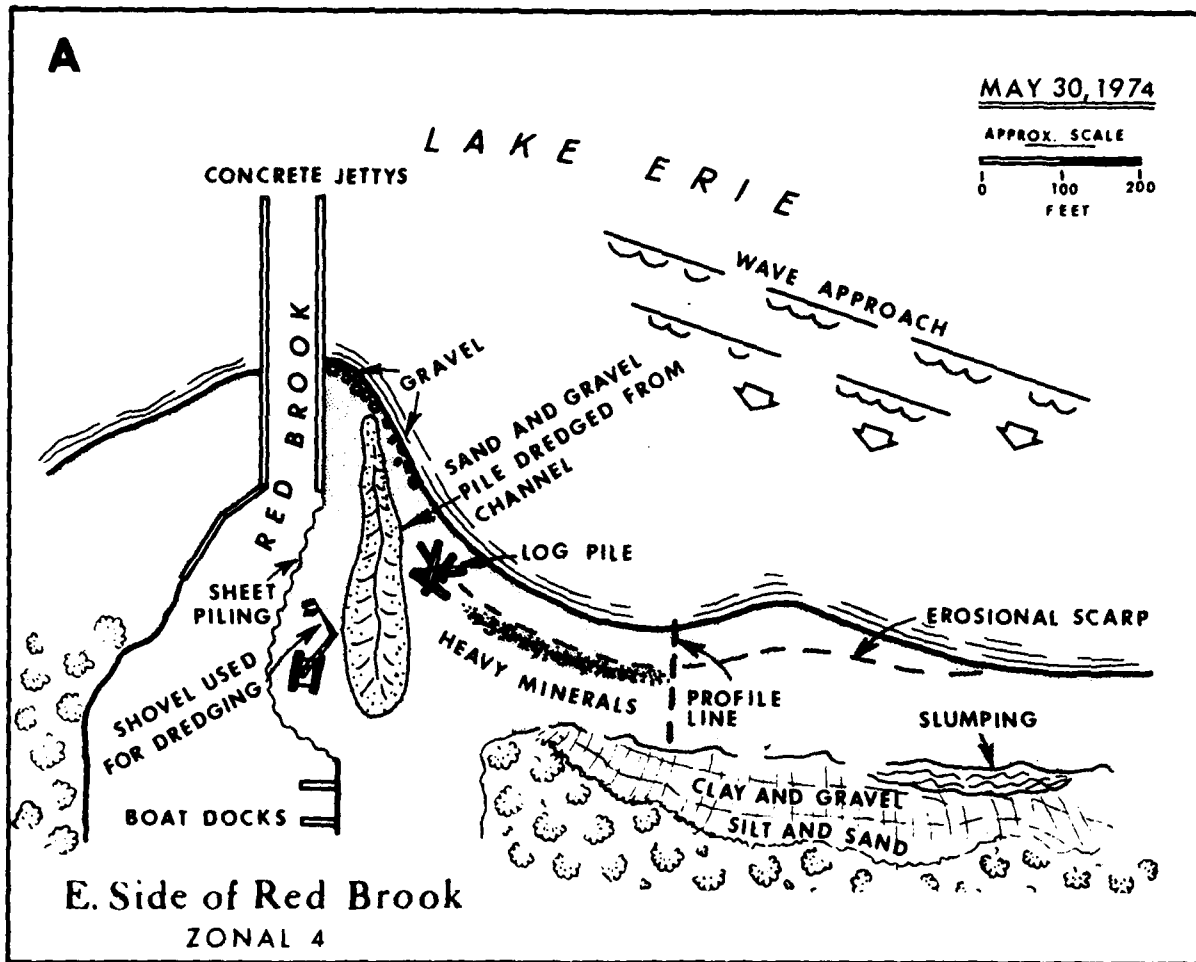
Figure 7. Area updrift of the groin at zonal site #3.
View looks east-northeast. Compare with profile
B in Figure 6.



FIGURE 7

Figure 8. A. Sketch map of zonal site #4 at the mouth of Red Brook, Ohio. Sediment is accumulating on the updrift (southwest) side of the jetties and periodic erosion occurs on the downdrift (northeast) side. Note location of beach profile given in B.

B. Profile of beach approximately 400 feet northeast of the Red Brook jetties. Profile was measured on 30 May 1974.



FIGURES 8A AND B

photograph in Figure 9. The cliff is 20 ft. in height. It is composed primarily of fine clay with pebbles scattered throughout (presumably till). A 2.3 ft. layer of silty sand occurs at the top of the cliff. As indicated by the sketch map (Fig. 8A), the jetties show a wide updrift accumulation of sediment (also see aerial photograph in Fig. 9), and periodic erosion on the downdrift side, although there was a narrow beach in front of the cliff on the date we visited the site (30 May 1974). The profile of the beach in front of the cliff was measured (Fig. 8B). At this location, the profile consists of a single sandy berm with coarse gravel occurring at the step.

The jetties at Zonal #4, like other structures in this general area, strongly demonstrate the rapid rate of sediment transport from southwest to northeast. All structures of this nature show sediment accumulation on the west side and accelerated erosion on the east side.

3.2f. Unit E. The Ashtabula structure (Unit E; Fig. 2) was authorized in 1896 and has been subject to many modifications since that time. It consists of an outer harbor about 185 acres in area, and two long breakwaters, a west breakwater 7891 ft. long and an east breakwater 4342 ft. long. There is noticeable sediment accumulation to the southwest of the west breakwater. With reference to the regional geomorphology, the Ashtabula structure separates two like units, D and F, which both consist of high, eroding till cliffs.

3.2g. Unit F. Unit F extends from the Ashtabula, Ohio, structure to Conneaut, Ohio, a distance of 13 miles (Fig. 2). Unit F is a very homogenous morphological unit, consisting almost entirely of

Figure 9. Jetties at mouth of Red Brook, Ohio. Arrow indicates direction of predominant longshore sediment transport.

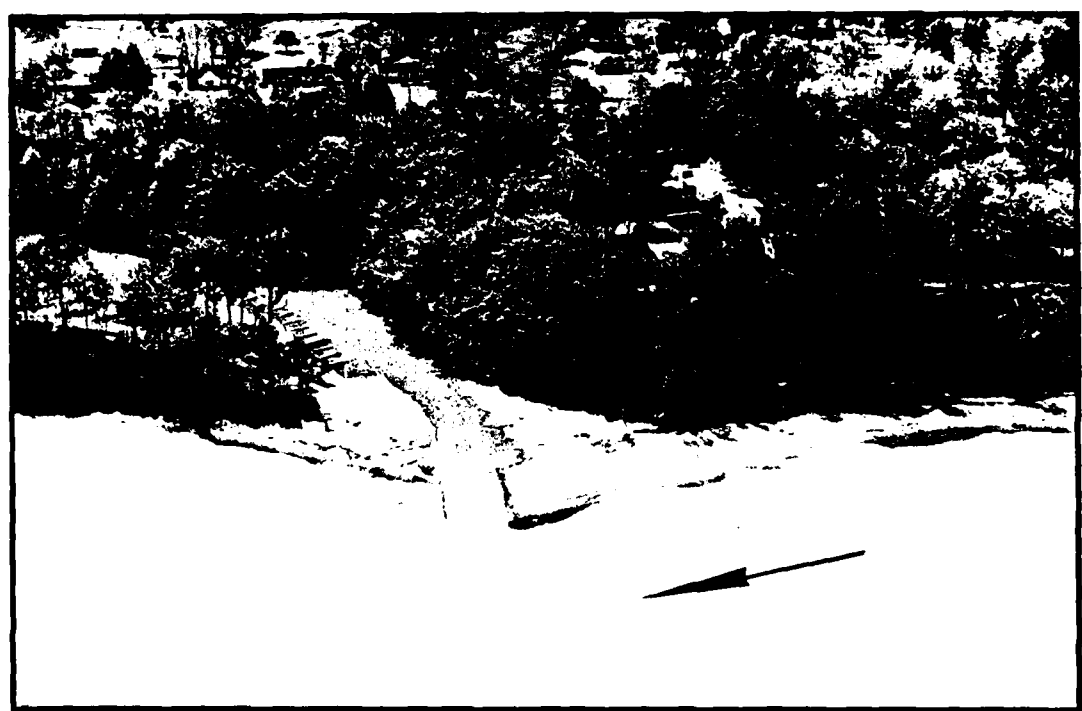


FIGURE 9

an irregular high till cliff which has intensive slumping at some places. At Zonal site #5, the cliff consists of clay that contains scattered pebbles of unknown origin. Figure 10 is a ground view of the cliff. Note the slumping and the occurrence of a gravel beach at the base of the cliff.

3.2h. Unit G. The Conneaut Harbor, Ohio, structure, which was authorized in 1910 and has been altered several times since then, consists of a double breakwater system with a large outer harbor occupying approximately 142 acres. The west breakwater is 5938 ft. long, and the east breakwater is 3675 ft. long. This structure, like the others in the area, shows excessive deposition on the west side. Figure 11 is a map showing the general configuration of the Conneaut Harbor structure.

3.2i. Unit H. This morphological unit extends from Conneaut Harbor, Ohio, to Erie, Pa., a distance of 21 miles (Fig. 2). This is such a variable area that we found it necessary to do five zonal studies (6-10) in order to properly describe it. The unit contains abundant cliffs of variable heights interspersed among several minor deltas. There is strong evidence of longshore sediment transport from southwest to northeast, as indicated by the accumulation of sediments on the southwest sides of the numerous jetties and groins that occur along this section of shoreline. Erosion is severe in many localities.

The first morphological type encountered east of Conneaut is an eroding, scalloped cliff of intermediate height. A number of small deltas occur further to the east. Zonal site #6, at Elk Creek, Pa., is representative of these deltas. The mouth of Elk Creek is flanked by a

Figure 10. Eroding and slumping cliff in Pleistocene sediments at zonal site #5, which is located 4 miles northeast of Ashtabula, Ohio. Photograph taken on 30 May 1974.

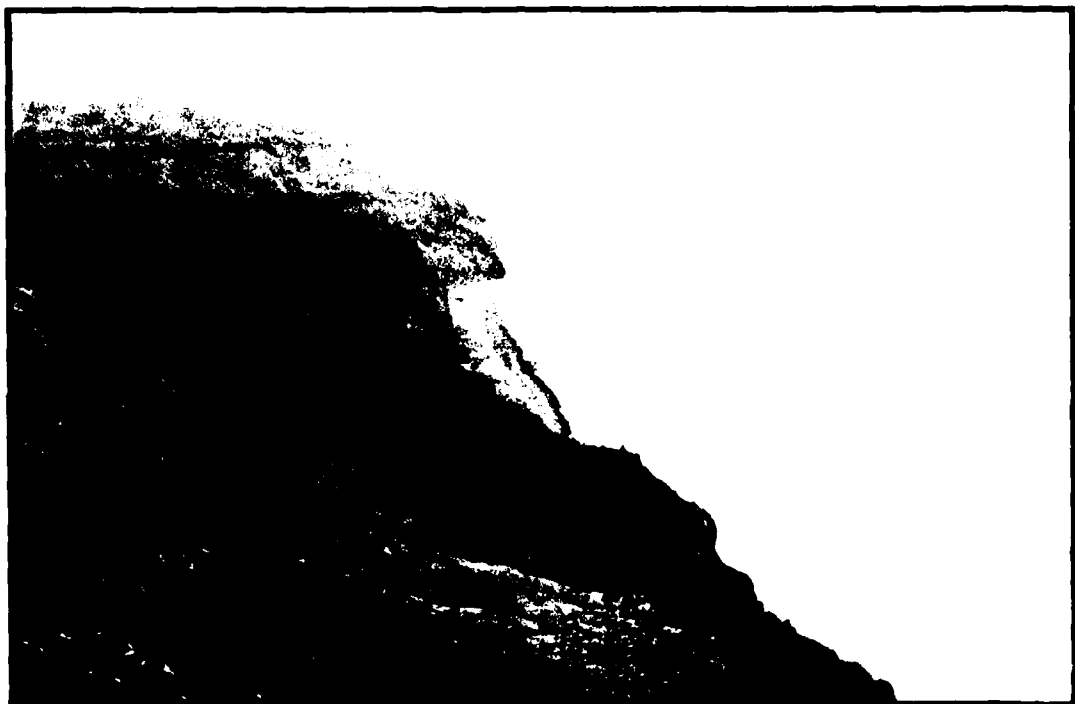


FIGURE 10

Figure 11. Structure at Conneaut Harbor, Ohio.

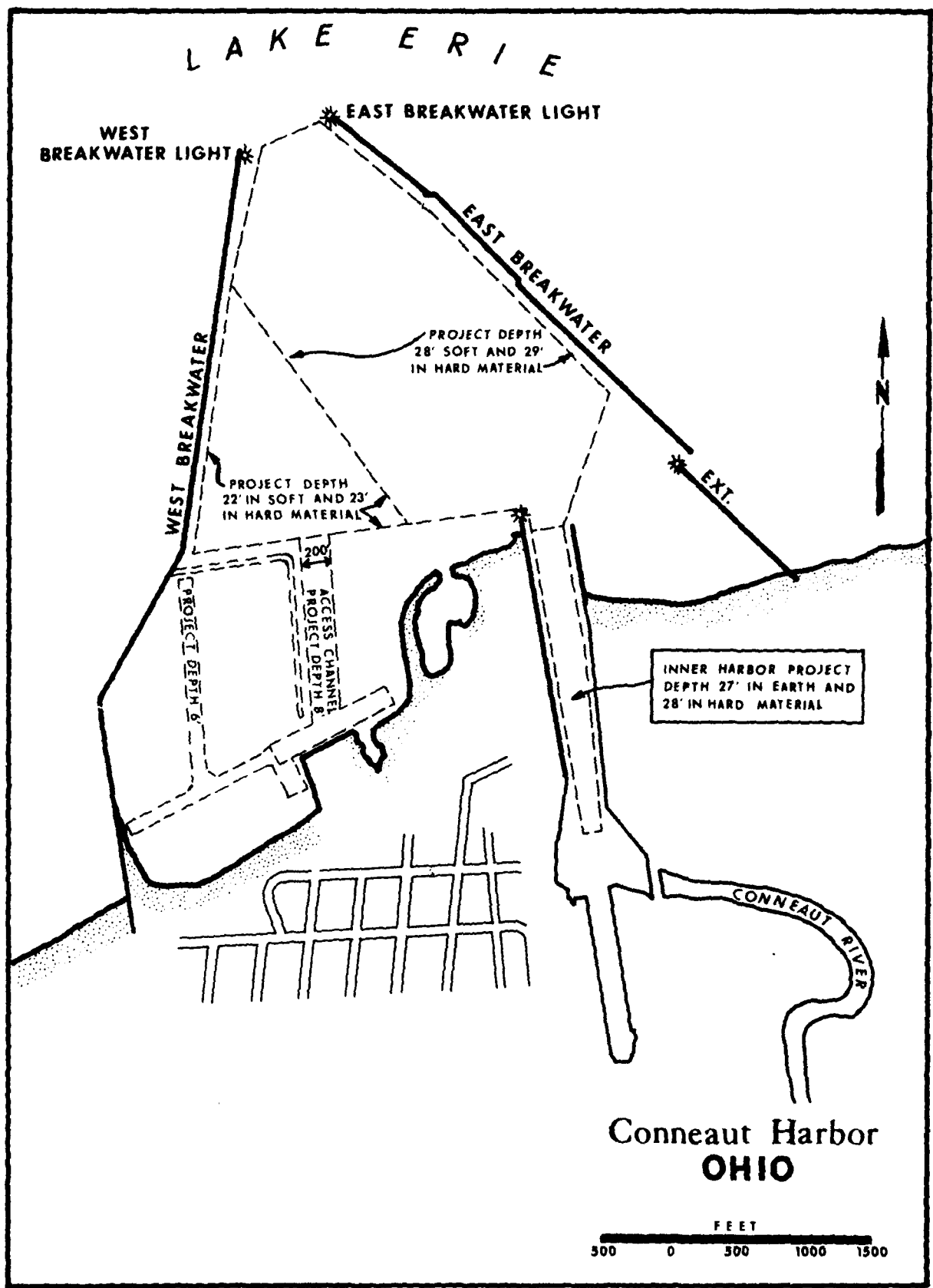


FIGURE II

westerly projecting gravel spit composed of multiple berms and covered by abundant logs and tree limbs. The nature of this spit is illustrated by the aerial photograph in Figure 12. The multiple berms are composed of different grain sizes of gravel beginning with the coarsest material at the highest berm and gradually decreasing in size to the swash line. This grain-size decrease presumably indicates diminishing strength of waves from the peak of the storm, during which time the coarse material was deposited on the crest of the high berm, through the waning stages of the storm, during which time finer-grained material was deposited on the berms of diminishing height. This gradation in grain size is demonstrated by the photographs in Figure 13. At the present time, the main channel of Elk Creek is floored by coarse gravel and the stream itself is considered to be the source of most of the material now accumulating at its mouth. The gravel here, like the gravel in most parts of this section of the Lake Erie shoreline, is composed of sedimentary rock fragments that are flat and discoidal in shape. Many of the gravel particles are composed of relatively fine-grained siltstones.

Proceeding east from Elk Creek, the shoreline once again becomes an eroding cliff which at points exceeds 80 ft. in height. At zonal #7, which is illustrated by the two photographs in Figure 14, the cliff consists of shale at the water line, a unit of coarse-grained till overlying the shale, and a thick clay sequence, presumably lake-bed deposits, overlying that. The nature of the till is illustrated by the photograph in Figure 14B. The till is approximately 5 feet thick; the clay is silty and is blue in color. At this location a groin was emplaced in 1940 which has effectively protected the property just west of the groin. However, the cliffs have

Figure 12. Mouth of Elk Creek, Pa., the site of zonal
#6. The line indicates the location of beach profile
given in Figure 13.

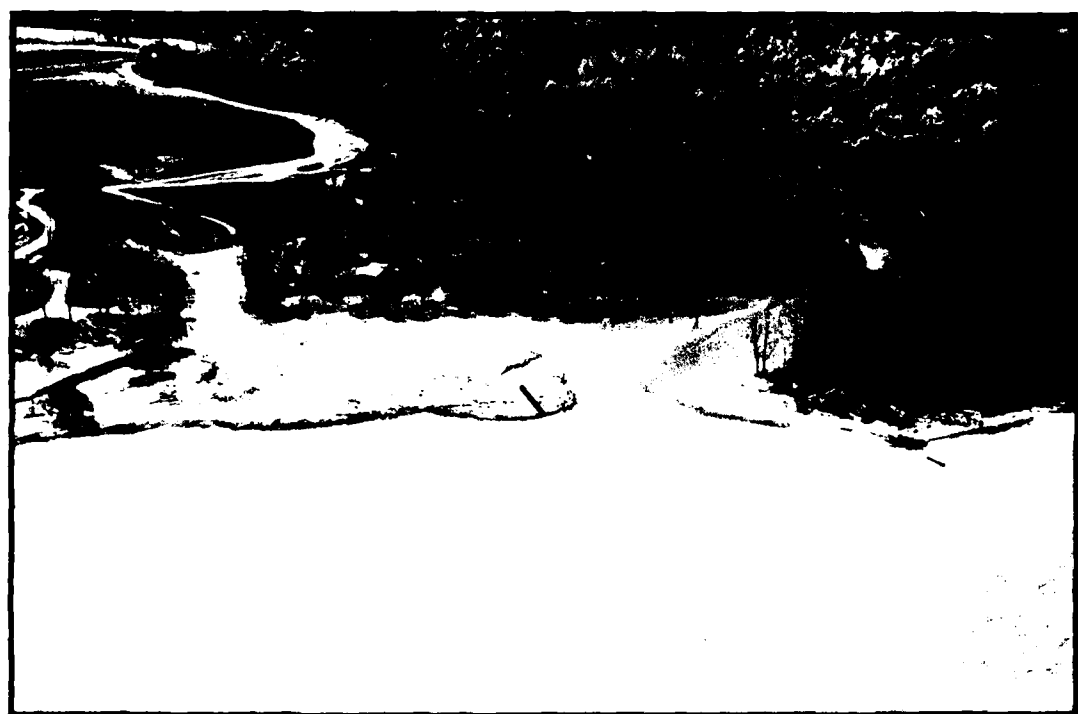
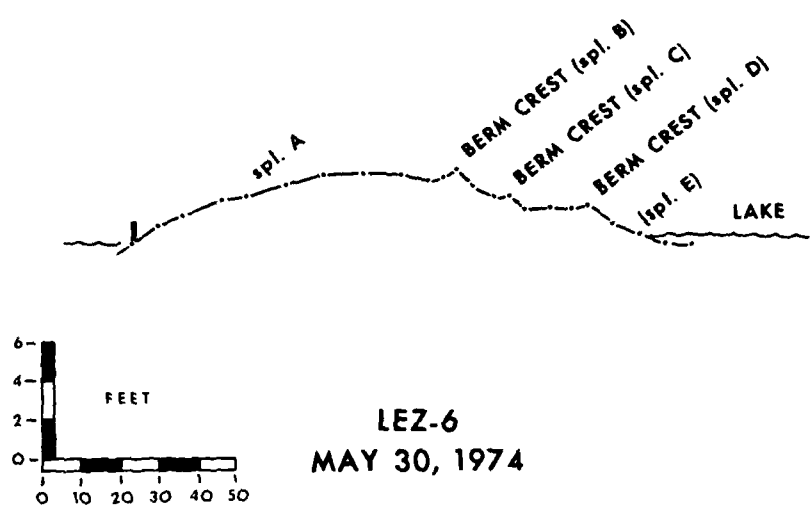


FIGURE 12

Figure 13. Beach profile and sample photographs at zonal site #6 (see location of profile on aerial photograph in Fig. 12). Coarsest material occurs on the highest berm and grain size diminishes gradually toward the swash line.



LEZ-6
MAY 30, 1974



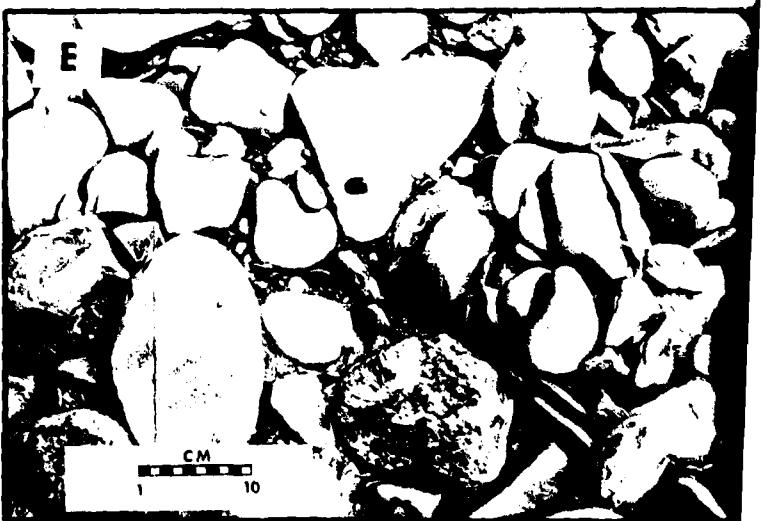
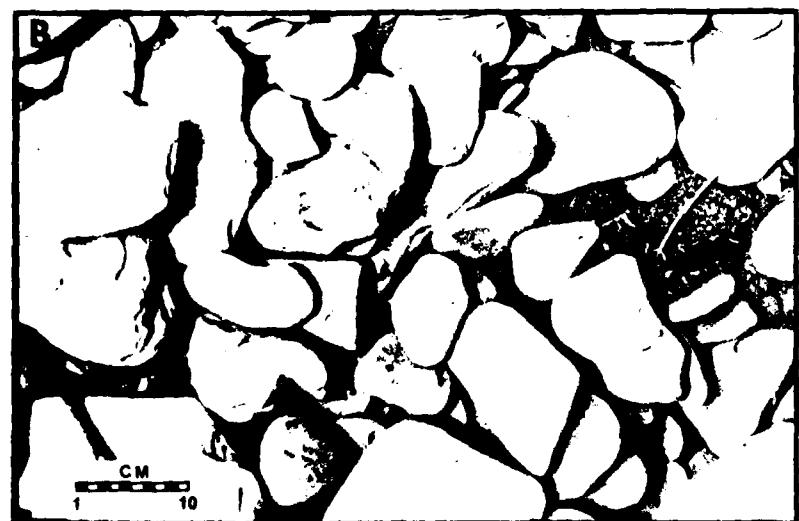
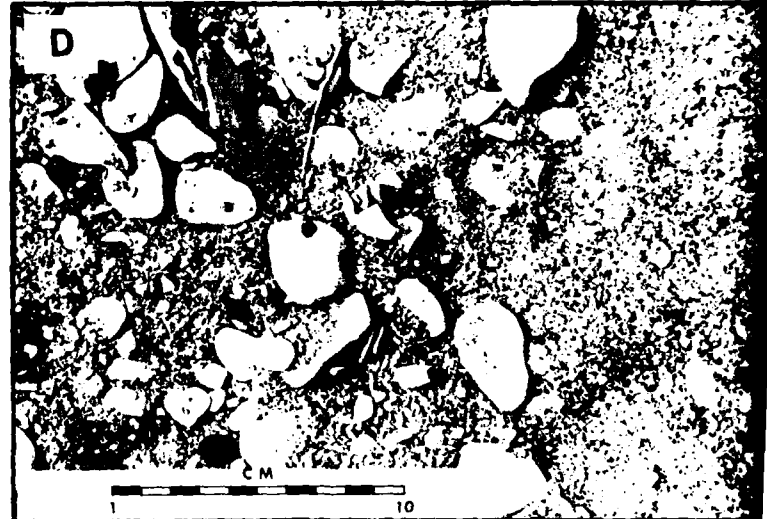
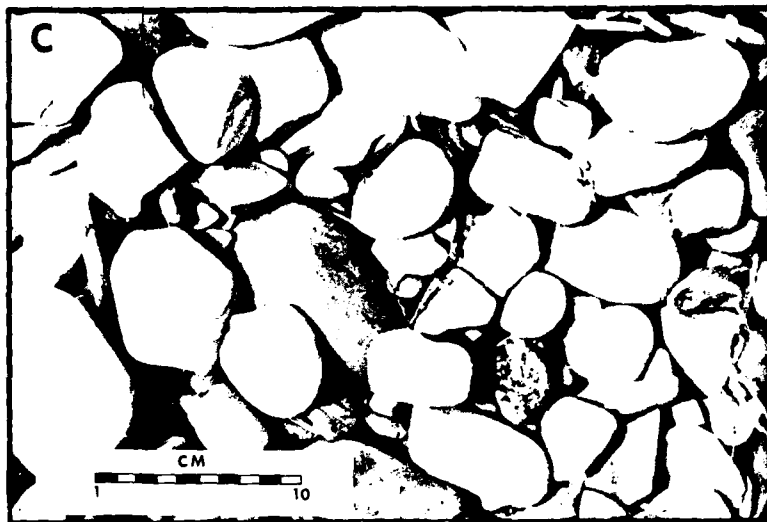
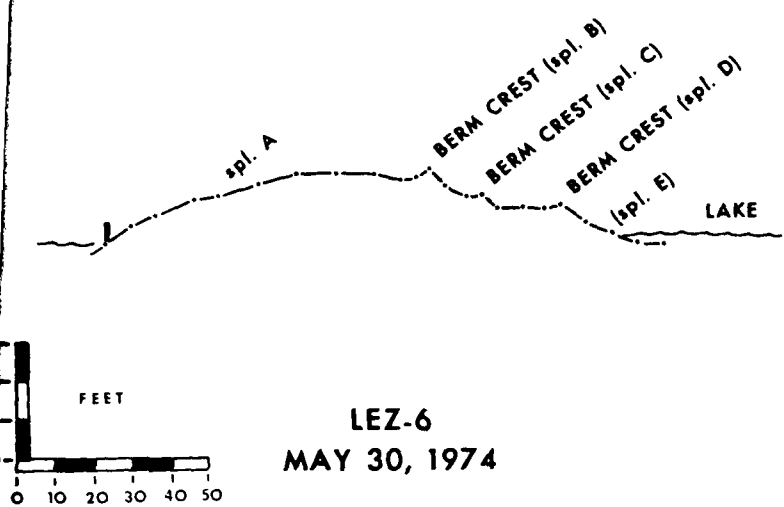


FIGURE 13

Figure 14. A. Zonal site #7, near Fairplain, Pa. The cliff is 70-80 feet high at this location. Note the erosion downdrift of the small groin in the right foreground. Arrow points to locality shown in photograph B.

B. Base of cliff at zonal site #7. Coarse-grained till at base of cliff is approximately 5 ft. thick.



A



B

FIGURES 14A AND B

eroded severely on both sides of the groin since that time. Refer to aerial photograph in Figure 14A. This type of private protective structure is very common along this section of cliffs.

The interval between Zonal sites #7 and #8 continues to be a high eroding cliff. At Zonal #8, the cliff is 78 ft. in height. It consists from top to bottom of 30 ft. of light, yellow-brown coarse silt, which is laminated (possibly loess), overlying 46 ft. of till, which overlies 2 ft. of shale. The till is composed of blue clay with scattered pebble fragments. There is some question as to whether this should be called till; it could be lake deposits containing dropstones. The beach area is the site of several groin structures, which are shown in Figure 15. Two beach profiles were measured (Fig. 15), which show multi-level berms with an erosional scarp on the lakeward side of the high berm. A field sketch of profile B is given in Figure 16, and photographs in Figure 17 demonstrate the nature of both the cliff and the beach area. The beach material is composed of a mixture of sand and gravel with sand predominating. The sediments on the beach were definitely not derived from the cliff, because of great differences in the composition and the absence of coarse gravel in the cliff. A coarse gravel platform is present just lakeward of the step area.

The larger groin shown in the sketch in Figure 16 and the photograph in Figure 17A was extended 4 months before the field work was done on 30 May 1974. This structure has accreted a large volume of sediment on the west side of the groin within that short period of time, further substantiating the occurrence of strong drift from west to east in this area.

Zonal site #9 is located at Walnut Creek, Pa., which has a small jetty

Figure 15. Map of part of the groyne field at zonal site #8,
which is located near the mouth of Trout Run Creek, Pa.
Note large sediment accumulation on west side of groynes.
Inset gives beach profiles at the two localities indicated
on the map.

ZONAL 8
TROUT RUN, PA.

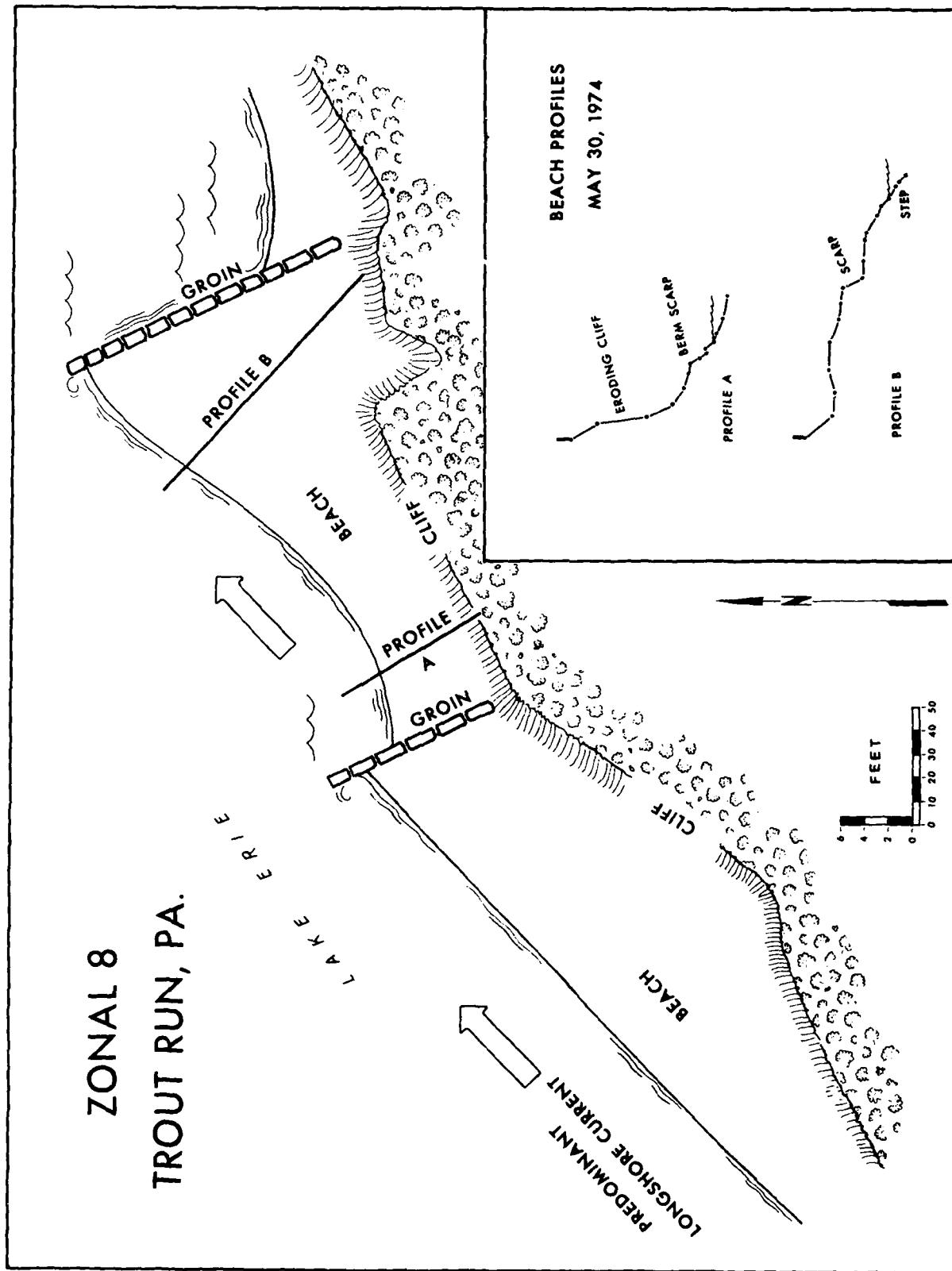


Figure 16. Field sketch of profile B at zonal site #8. Heavy line indicates position of profile, which is plotted in Figure 15. Multi-level berms are formed when the lake is at different levels as a result of wind tides.

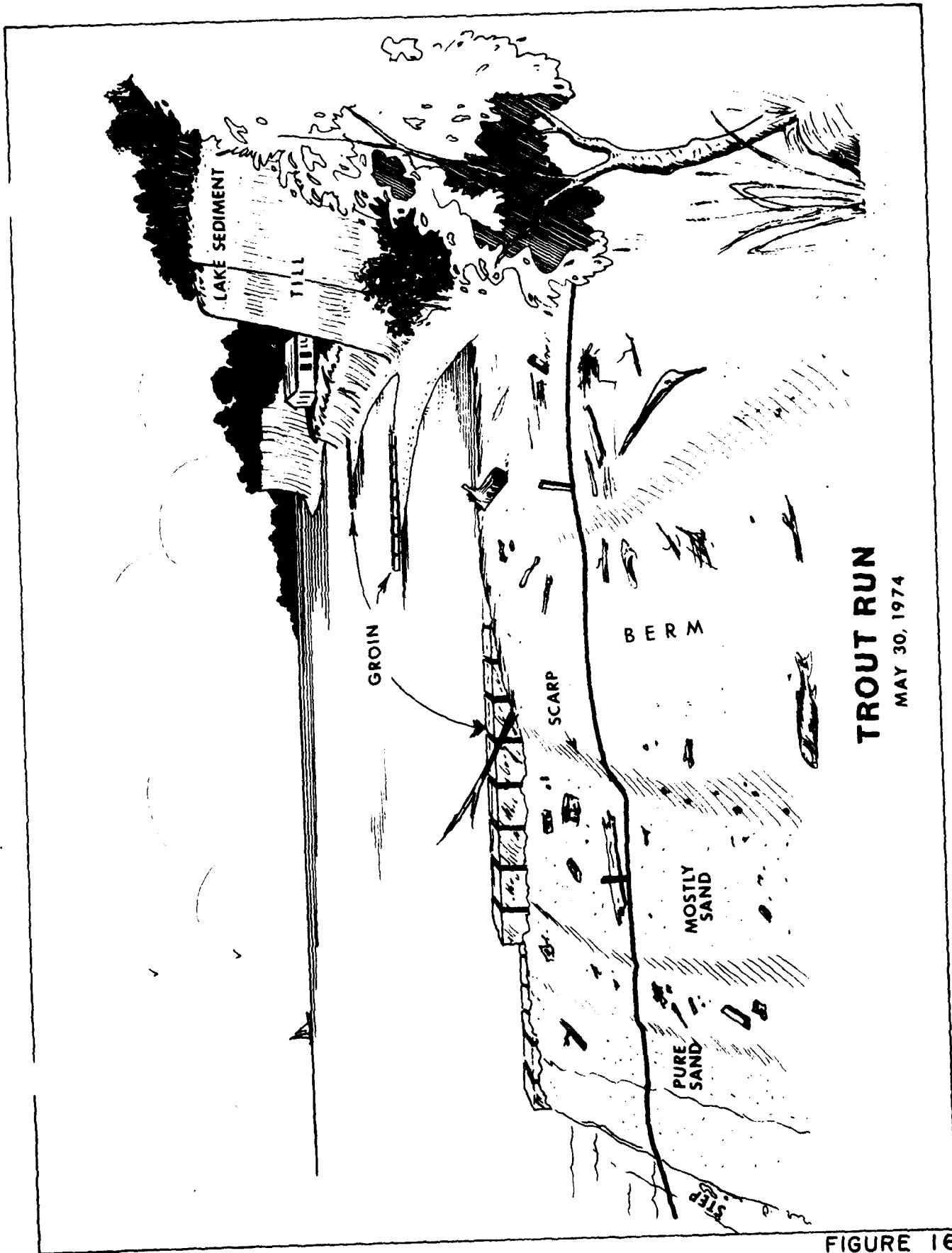
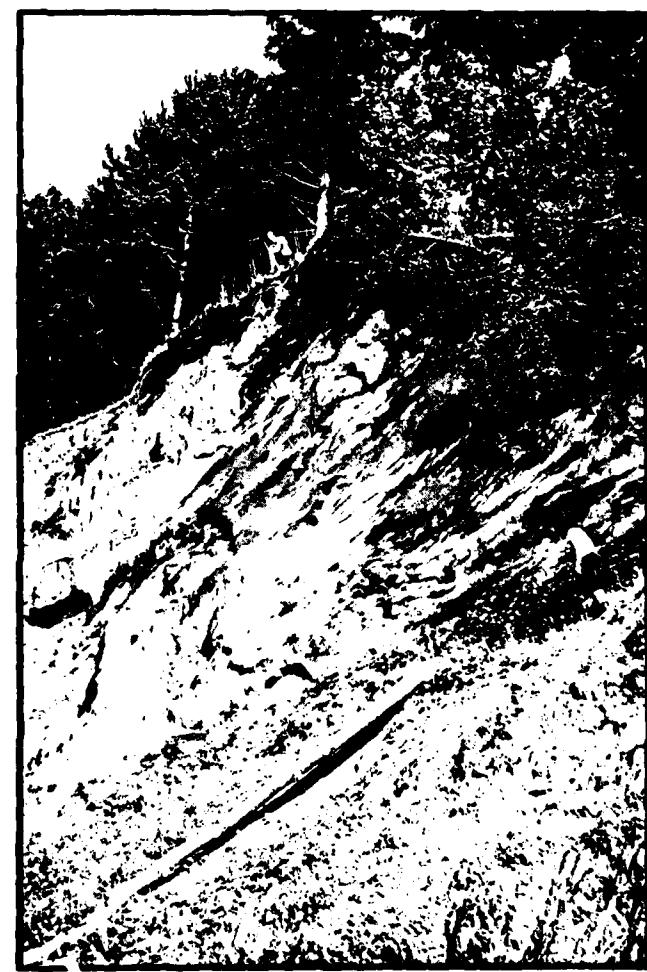


Figure 17. A. Cliff-top view of groin field at zonal site #8, Trout Run, Pa.

B. Eroding beach cliff at zonal site #8. Description of cliff sediments is given in text.



A



B

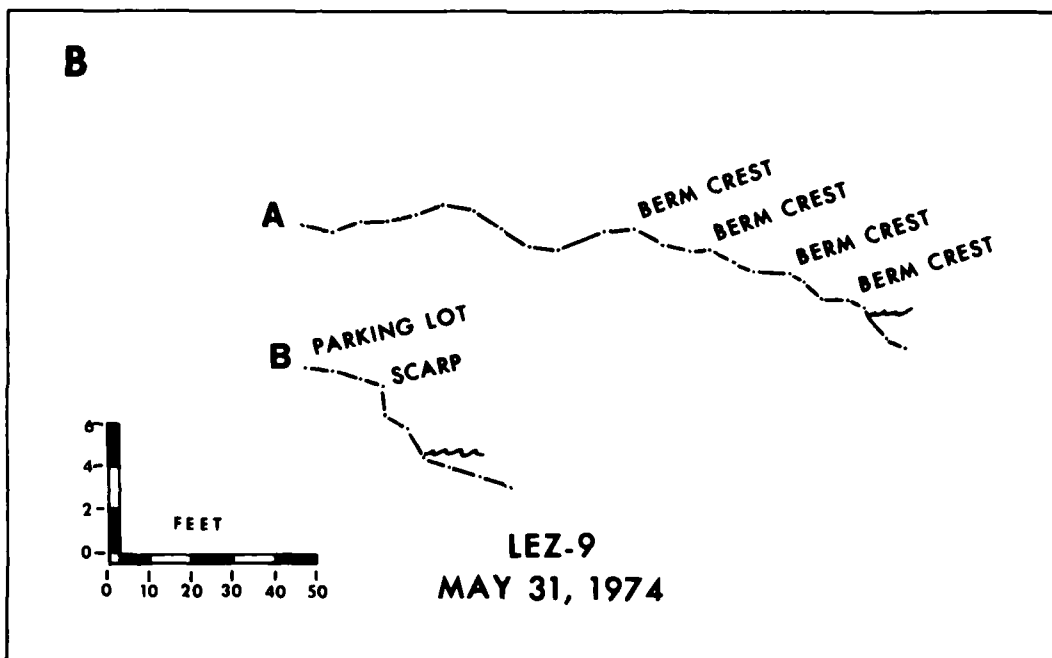
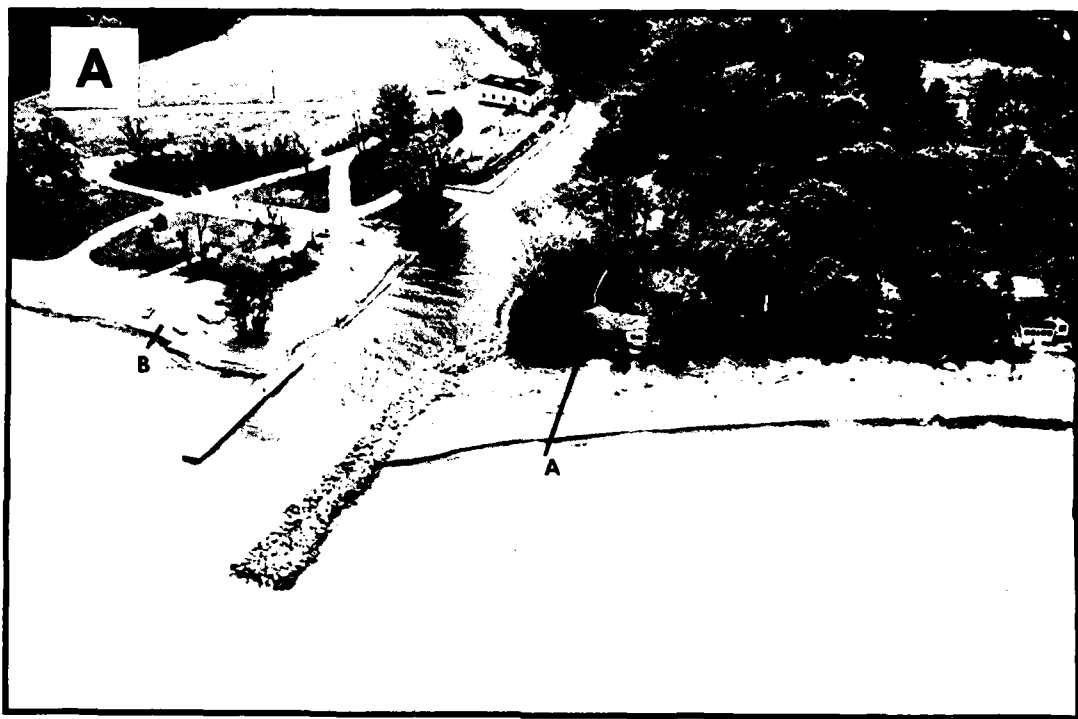
FIGURES 17A AND B

system at its mouth. These jetties produce a classic updrift deposition/downdrift erosion system (see Fig. 18). The offset of the beaches on either side of the jetties was 70 ft. In general, the gravel is finer on the updrift side than on the downdrift side. There has been some mancuring of the beach on the updrift side by bulldozers. Updrift of the jetties, the gravel has been deposited in a series of multiple berms (Figs. 18B and 19A). Downdrift of the jetties, erosion has been intensive. Note the eroding parking lot in the photograph in Figure 19B. Observations of N. Shea, an employee of the Pennsylvania State Fisheries Commission, indicate that 5 acres of land have been lost on the downdrift side since 1960.

Zonal site #10 is the location of the most intensive destruction of property seen along this whole southeastern shore of Lake Erie. Many beach cottages have been totally destroyed during the recent lake-level rise. Evidence of this destruction can be seen in the photographs in Figure 20A,B. Note the large accumulation of trees and logs on the beach. These logs were used as battering tools by storm waves, bashing in the fronts of many of the cottages. Also, the logs have stacked up at some places and have served as natural groins, as shown by the photograph in Figure 20A. This is the only place we visited where the beach cottages had been built on the beach below the crest of the cliff, which is 83 feet high at this locality. This indicates to us that the beach must have been considerably wider at this location when the cottages were built than it is today, inasmuch as the present beach is not significantly different at this locality from most of the other localities visited. See, for example, the beaches at Zonal sites #7 and #8. Since the destruction of the cottages,

Figure 18. A. Jetties at mouth of Walnut Creek, Pa. (zonal site #9). Lines show locations of profiles given in B. Note accretion on the right (southwest) side of jetties and erosion on the left (northeast) side. Ground views of these areas are shown in Figure 19.

B. Beach profiles on updrift side (profile A) and downdrift side (profile B) of the Walnut Creek jetties. Note abundance of gravel berms in profile A.



FIGURES 18A AND B

Figure 19. A. Beach zone just updrift of the Walnut Creek jetties. Note multi-level gravel berms. Compare with profile A in Figure 18B.

B. Beach zone just downdrift of the Walnut Creek jetties. Blocks of the parking lot pavement occur several feet offshore. Compare with profile B in Figure 18B.



FIGURES 19A AND B

Figure 20. A. Intense erosion zone one-half mile west of Presque Isle, Pa. (zonal site #10). The geologist is standing on a gravel berm built up onto the rooftop after the house collapsed. Note natural groin effect of the log jam in the middle distance.

B. Beach zone 200 feet west of the area shown in A.

A



B



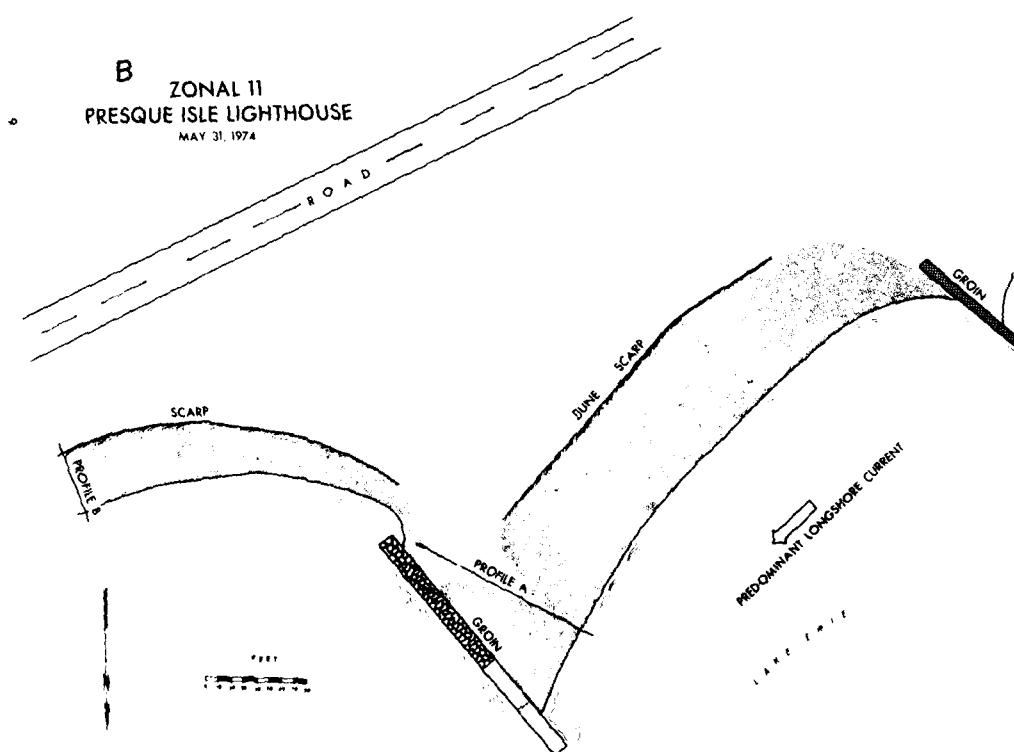
FIGURES 20A AND B

a storm berm of coarse gravel has been deposited in front of them. This berm can be seen in the photograph in Figure 20A. The gravel at this locality, as at most of the other localities along this stretch of shore, consists of discoidal siltstone.

3.2j. Unit I. Presque Isle, Unit I (Fig. 2), is a flying spit composed of a mixture of sand and gravel, which is building progressively northeastward as a series of recurved spits. On Presque Isle, we have chosen two sites as being representative of its general morphology. Zonal site #11 is on the western, or eroding, side of the isle, and zonal site #12 is located on the depositional, or recurve, portion of the isle. Zonal #11 is located in a groin field near the lighthouse on the northwest point of the spit. As shown by the aerial photograph (Fig. 21A), the planimetric map of the area (Fig. 21B), and the measured beach profiles (Fig. 22C), the groins have brought about remarkable changes in erosional and depositional conditions. The offset on the groin located just northeast of the lighthouse is approximately 400 ft. Erosion on the downdrift side has threatened the roadway behind the lighthouse. Notice the eroding scarp with abundant trees falling into the lake in the photograph in Figure 22A. Sediment on the updrift side of the groin is accumulating in a series of multi-level berms and is mostly sand except where gravel has been deposited in the berm runnels (Fig. 22B). This gravel is fine, averaging between .5 and 1.0 cm in diameter. This area has one of the most pronounced groin offsets witnessed in any location by the writers. All of the groins on the west side of Presque Isle show some degree of offset and indicate strong littoral transport of sediment along the spit from the southwest to the northeast.

Figure 21. A. Zonal site #11, Presque Isle, Pa., lighthouse.

B. Map view of zonal site #11. Note large sediment accumulation on up-drift (southwest) side of groins, and intensive erosion on the down-drift side. Beach profiles A and B are given in Figure 22C.

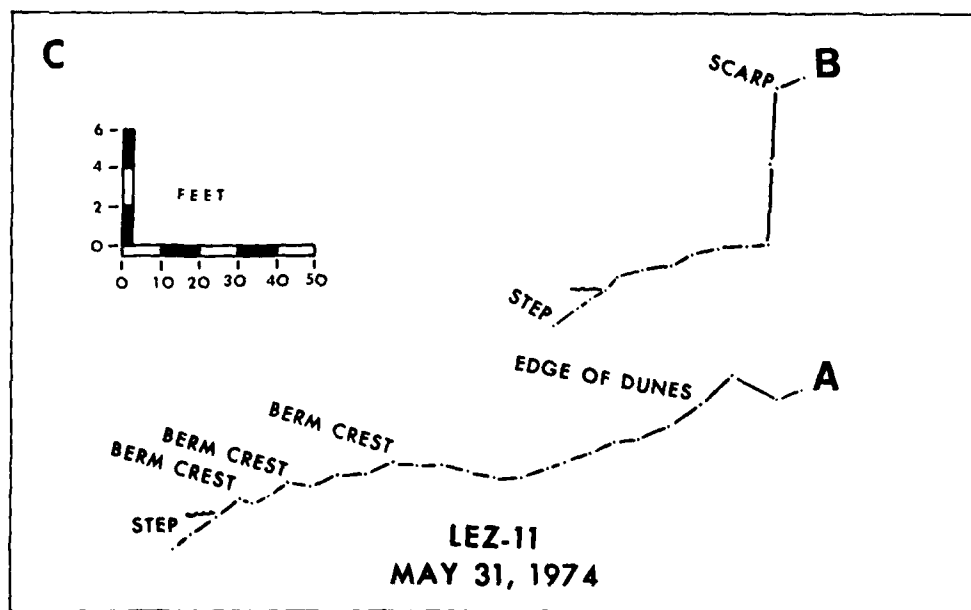


FIGURES 21A AND B

Figure 22. A. Area downdrift of lighthouse groin; zonal site #11. Profile B (see C) is located in foreground.

B. Area updrift of lighthouse groin. Profile A (see C) is located in middle of photograph.

C. Profiles A and B at zonal site #11. See map in Figure 21B for location.



FIGURES 22A, B AND C

Zonal site #12, located on the recurve spit portion of Presque Isle (Fig. 23), is the first natural depositional system between Fairport Harbor and Presque Isle that we studied. All the other depositional areas occurred updrift of man-built structures. The sediment making up the spit is mostly sand and what gravel is present is small and discoidal in shape. The major component of the spit at this location is basically an overwash terrace that is pushed landward during storms (see three-dimensional block diagram in Fig. 24). It is interesting to note that the beach face and nearshore zone on this spit is relatively steep. This is presumably a result of the fact that the spit is building out rapidly into a deeper portion of the lake. Sediment is transported along the face of the spit in the form of a series of beach protuberances, which are illustrated in the aerial photograph in Figure 23.

3.2k. Unit J. Unit J extends for 16 miles from just northeast of Erie, Pa., to approximately 2.5 miles west of the New York border. It is a complex area, being composed of numerous deltas separated by cliffs of varying heights. The amount of bedrock in the cliffs, which is principally siltstone and shale, increases in a northeasterly direction. The cliffs contain chasms and sea caves in the places where the bedrock predominates, and the higher cliffs show considerable slumping and scalloping. Till predominates in the upper portions of the higher cliffs. The delta at Twelvemile Creek, Pa. (Zonal site #13), was visited on 20 May 1974, but no detailed data were collected. It is a small delta and the stream channel is flanked by several higher terraces. The stream itself is transporting gravel, and a coarse

Figure 23. Zonal site #12, the recurved spit area on Presque Isle, Pa. The approximate location of the specific area mapped (see block diagram in Fig. 24) is located between the two lines.

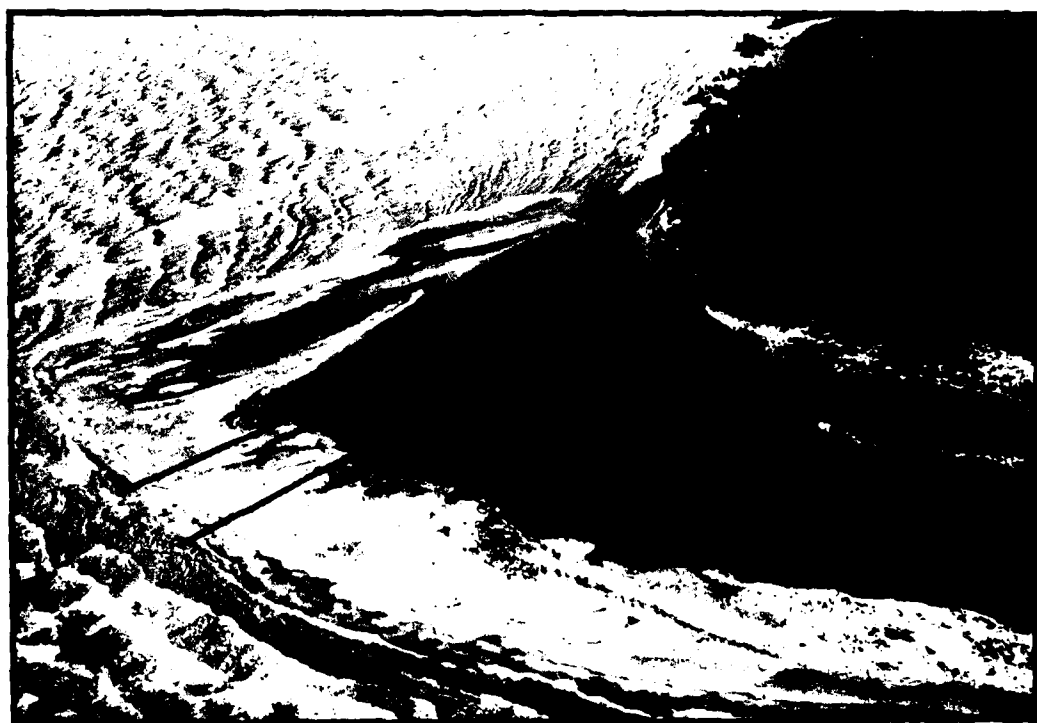


FIGURE 23

Figure 24. Block diagram of recurved spit area of Presque Isle (zonal #12). This feature is principally an overwash terrace that migrates lagoonward during storms.

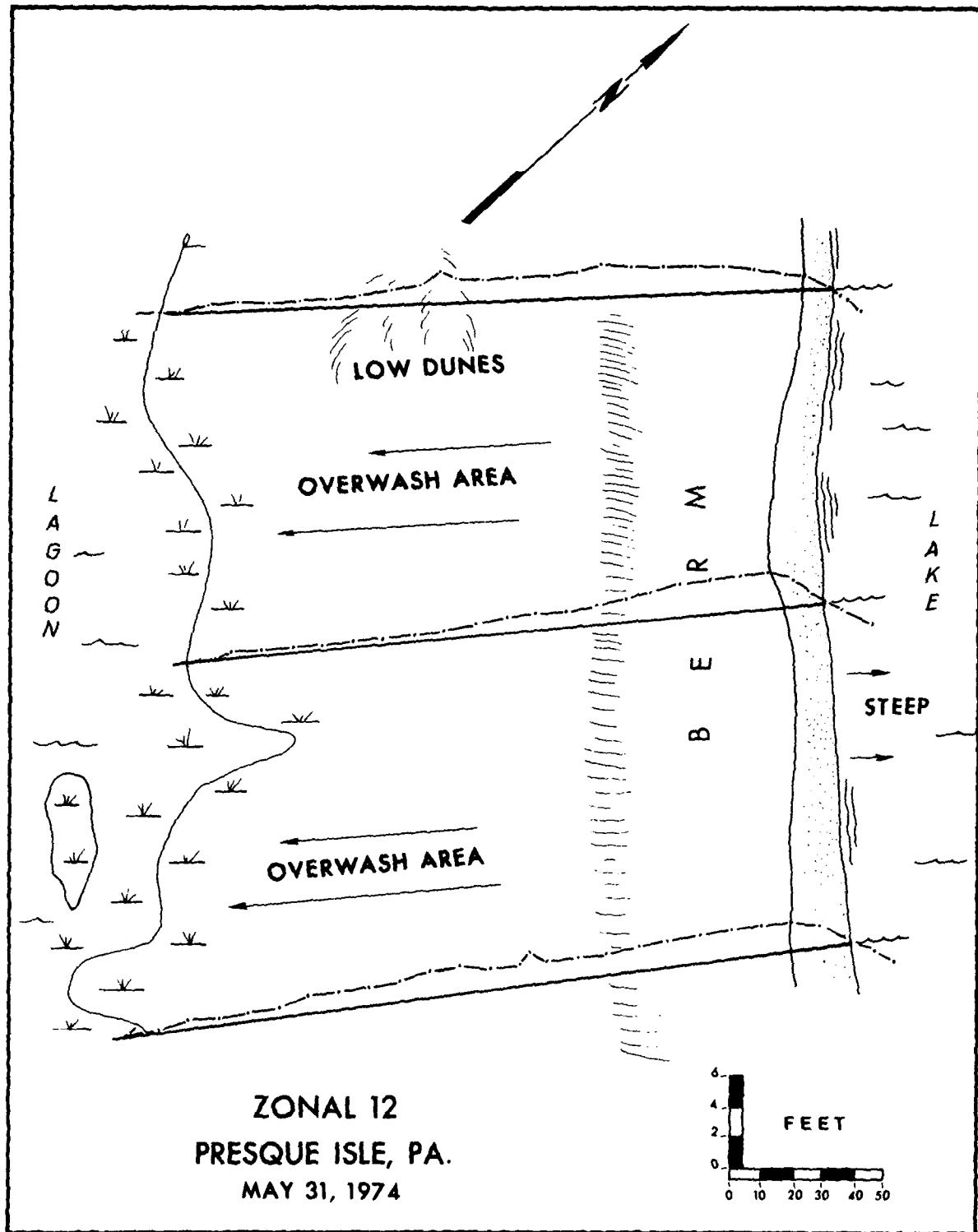


FIGURE 24

gravel bar and gravel beaches are deposited around the margin of the delta. At the time of the visit, a gravel bar was building to the west across the mouth of the stream under the influence of waves approaching from the northeast.

3.21. Unit K. Unit K, which extends 22 miles along the shore between Twentymile Creek, Pa., and Lake Erie State Park, N. Y. (Fig 2), is distinct from Unit J in that it is composed of cliffs of intermediate height that are predominantly bedrock. There are still many small river deltas that dissect the cliff, but the cliff is the dominant feature. The cliff shows pronounced effects of rock jointing and erosion along the joints, although, in general, the shoreline is relatively straight. In many places, waterfalls cascade down the face of the cliff. The two zonals studied were chosen to represent the two dominant morphologies in the area. Zonal site #14 is at the mouth of Twentymile Creek, Pa., whereas Zonal site #15 is in the bedrock cliffs at Blue Water Beach, Pa.

Zonal #14 is dominated by a long gravel spit that overlaps the mouth of Twentymile Creek. The spit projects toward the northeast a distance of 500 ft. According to local residents, the entire spit has been built since 1972. It has been deposited as a series of small recurves projecting in the northeasterly direction. The spit consists of multi-level berms with a high central berm composed of coarse gravel, which had a mean grain size of 33 mm on the date of observation (20 May 1974), and a lower level berm, which had a mean diameter of 21 mm (measurements made at profile B). The decreasing size of the gravel from the high berm to the low berm probably indicates diminishing wave energy following storms, with the high berm being built by major storm waves. The gravel consists

primarily of flat, discoidal siltstone fragments. The nature of the spit is illustrated by the aerial and ground views in Figure 25A,B, by the three-dimensional diagram of Figure 26, and by the gravel photographs in Figure 27. On the night before the date of observation, 20 May 1974, the direction of wave approach shifted from west to east, and a gravel spit began to build in a westerly direction. This indicates that the gravel is very mobile and can be transported readily by Lake Erie waves and built into gravel spits within the matter of a few hours.

Zonal site #15 is located in a bedrock cliff area at Blue Water Beach. The most conspicuous feature in the cliff is the intensive jointing pattern which is illustrated in the photograph in Figure 28. Two primary joint directions were noted, N 60° E and N 10° W. These two joint directions control the orientation of the cliff faces on a local scale. The height of the cliff at this locality is 19.5 ft. The contact between the bedrock and the till occurs at 10.6 ft. above the water level. The bedrock consists of interlayered siltstones and mudrock. This has been an area of considerable erosion over the past few months. According to a local resident, a 75 ft. wide beach composed of sand and gravel was present as recently as the summer of 1973.

At Barcelona, which is near the midpoint of Unit K, a breakwater system was completed in June 1960. The east breakwater is 693 ft. long and is not connected with the shore. The west breakwater, which measures 790 ft., is connected with the shore, and a large amount of sediment has accumulated on the updrift side since it was built.

3.2m. Unit L. Unit L, which extends 16 miles from Lake Erie State

Figure 25. A. Zonal site #14, mouth of Twentymile Creek, Pa. Note long rivermouth spit projecting northeastward across the mouth of the stream. A three-dimensional block diagram of the spit is given in Figure 26.

B. View along rivermouth spit shown in A (looking southwest).



FIGURE 25

Figure 26. Three-dimensional diagram of zonal site #14.
The spit is composed almost entirely of gravel, which
accounts for the steep beach profiles. The spit grew
in a northeastward direction as a series of smaller
recurved gravel spits.

ZONAL 14
TWENTY MILE CREEK, PA.

MAY 20, 1974

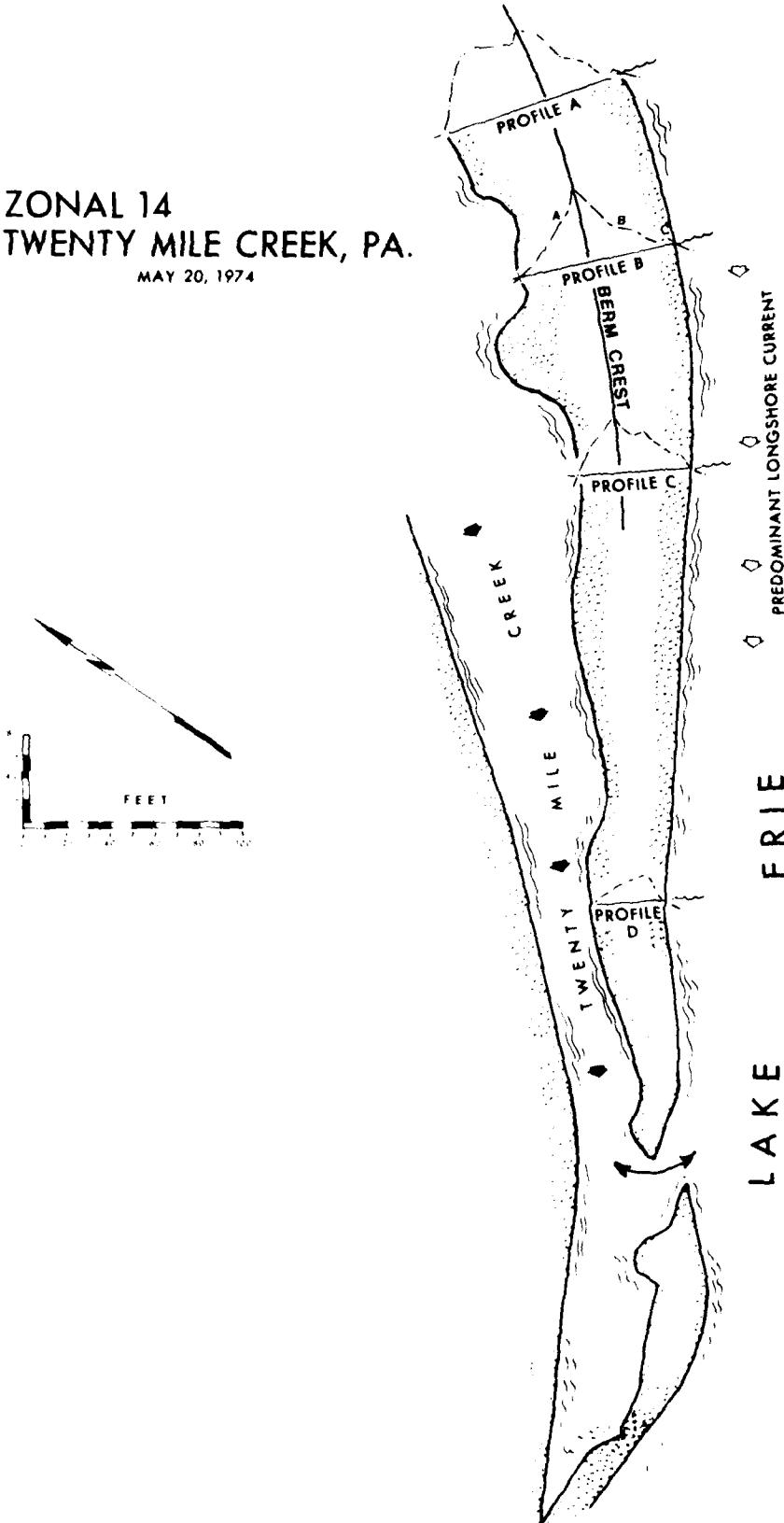
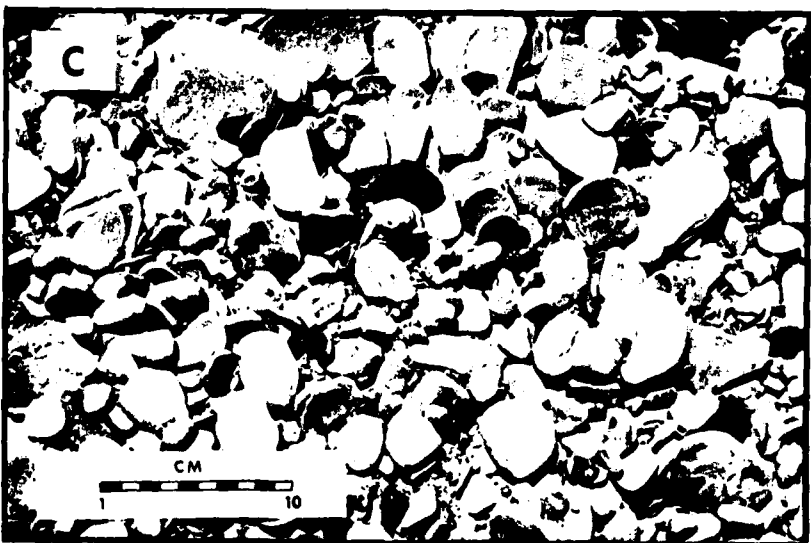
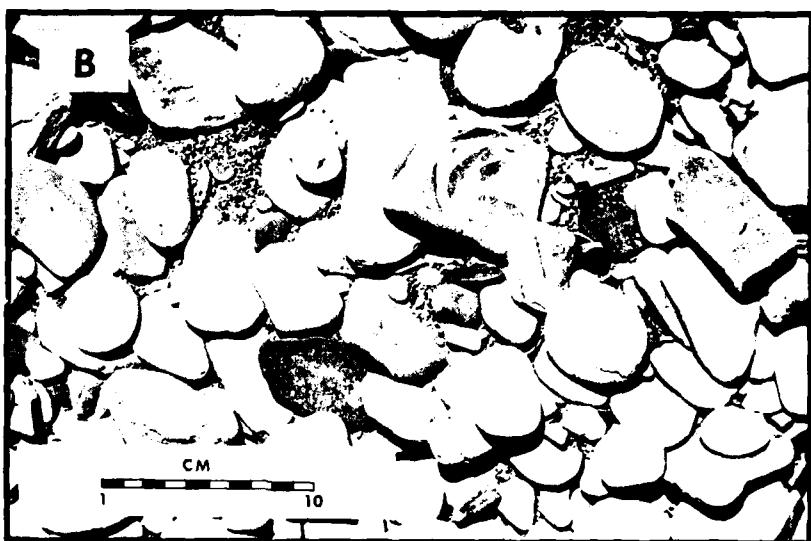
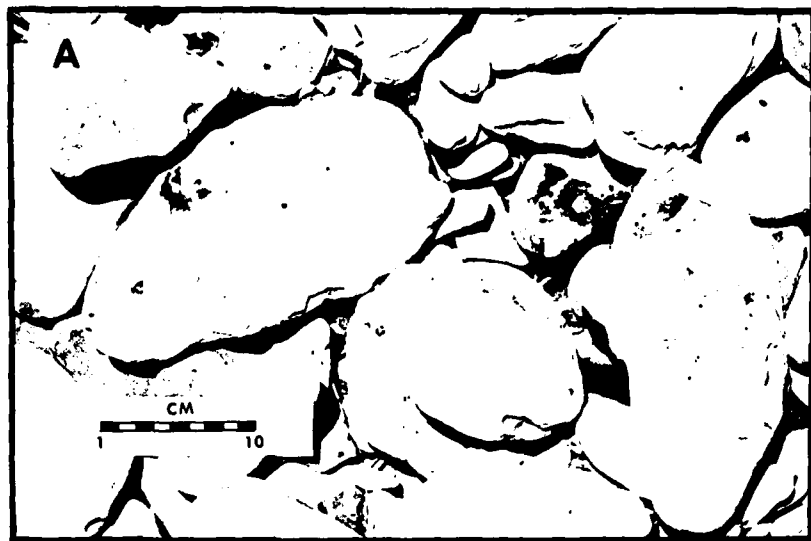


FIGURE 26

Figure 27. Gravel samples A, B, and C on profile B at zonal site #14 (located in Fig. 26). Sample A is located on the high berm and samples B and C are located progressively closer to the swash line.



FIGURES 27A, B AND C

Figure 28. Rock cliff at zonal site #15, Blue Water Beach, N. Y. Note well developed joint pattern in the shale. Two joint trends predominate, N 60° E and N 10° W.



FIGURE 28

Park, N. Y., to Silver Creek, N. Y., is a very distinctive morphological unit composed of headlands that project in a northerly direction away from the general orientation of the shoreline. Ten headlands occur in this area, with the two largest being Van Buren Point and the headland just south of Dunkirk. The cliffs are generally of intermediate height and are composed almost entirely of bedrock. There is a remarkable joint pattern in these cliffs, which appears to control the general configuration of the shoreline. This joint control is illustrated by the photograph and measured joint patterns given in Figure 29A,B.

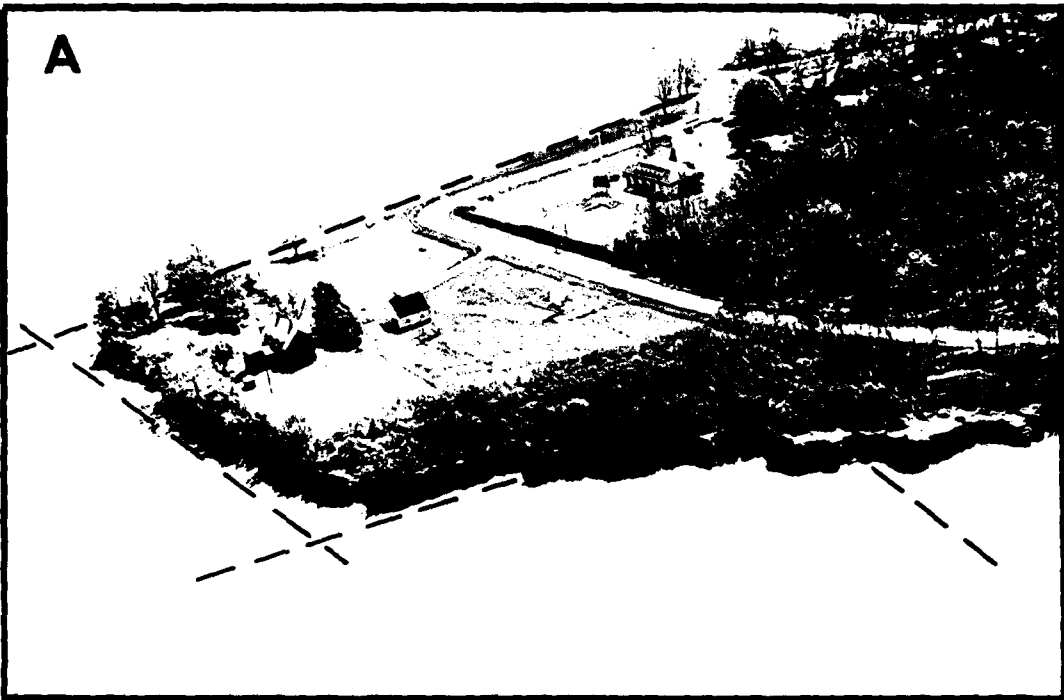
Zonal site #16 is located at Van Buren Point, N. Y. It is an eroding headland and has the classic features of bedrock headlands including a sea stack and sharply eroding cliffs with pocket gravel beaches. These features are illustrated by the two photographs in Figure 30A,B. The rocky headland at Van Buren Point is all shale and is representative of the general area between Van Buren Point and Cattaraugus Creek. Joint control is important with two trends predominating, N 10° W and N 60° E (see Fig. 29). The beach pebbles are over 95% sedimentary rocks with shale and siltstone fragments being most abundant. The gravel particles, which average about 35 mm in mean diameter at this locality, are extremely discoidal. Our observations indicate that erosion is occurring at the rate of at least 3-4 ft. per decade along these cliffs. The two beach profiles measured at this locality consist of multiple berms of gravel which generally grades from coarsest material on the highest berm to finest material at the present water level. The cliff height at profile B is 18 ft.

Zonal site #17 (Fig. 2) is located along a straight stretch of high, inaccessible vertical cliff which measures approximately 75 ft. in height.

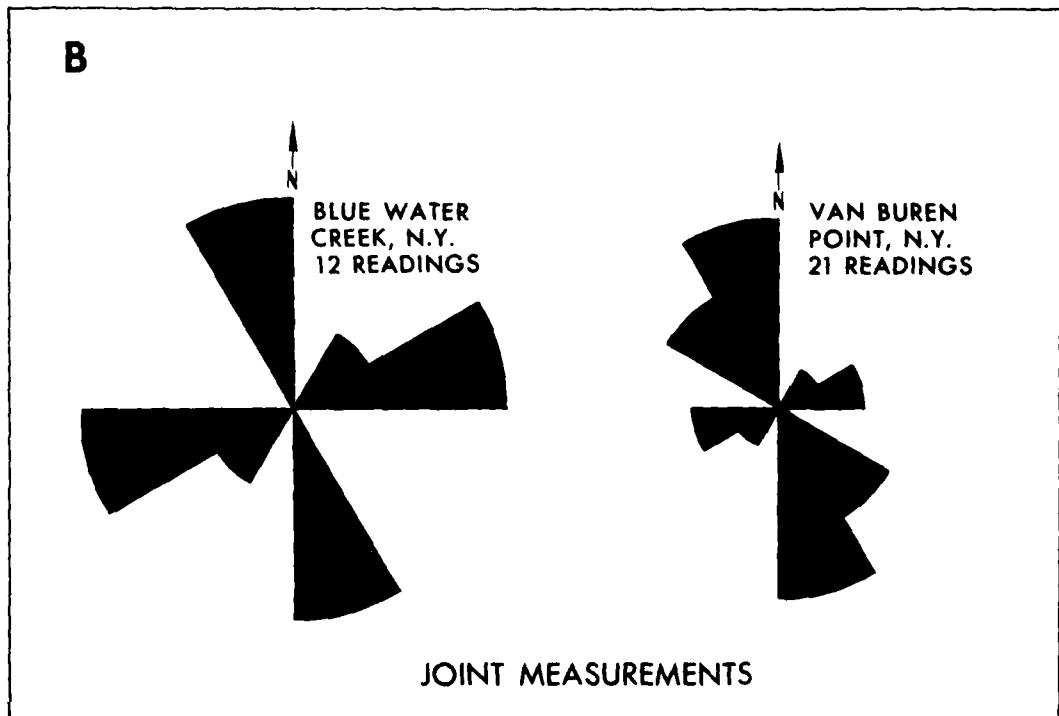
Figure 29. A. Joint-controlled topography on headland just south of Dunkirk, N. Y. (lighthouse is Dunkirk Light). The two shoreline trends, indicated by the dashed lines, conform with the two major joint patterns measured in the shale bedrock (N 10° W and N 60° E; see B).

B. Joint patterns measured at Bluewater Creek and Van Buren Point, N. Y.

A



B

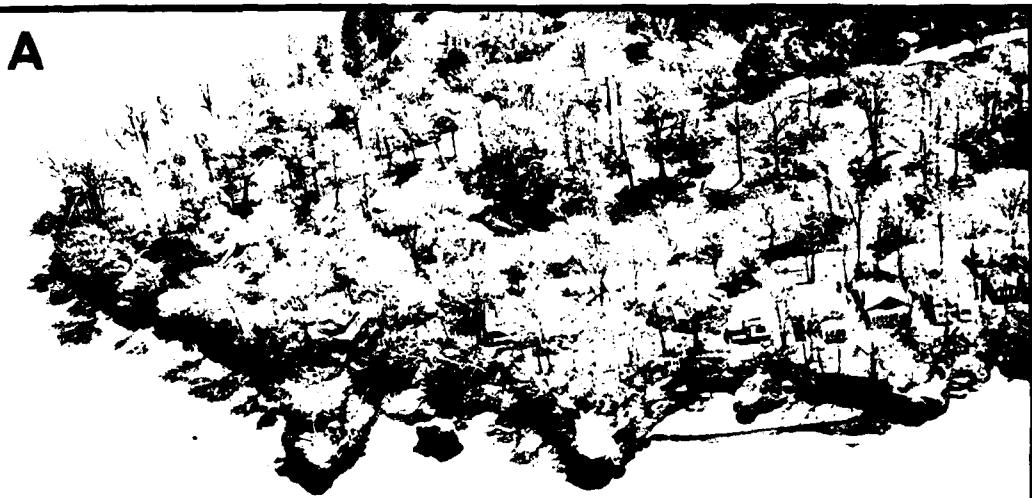


FIGURES 29A AND B

Figure 30. A. Zonal site #16, Van Buren Point, N. Y.

B. Ground view of the area shown in the right-central portion of the aerial photograph. Note joint-controlled patterns in the cliff.

A



B



FIGURE 30

The upper half is mostly shale but the lower half contains abundant siltstone beds 1-2 ft. thick. There is no evidence of beach deposits at the base and the water depth appears to increase rapidly away from the cliff. No joint patterns were evident in the cliff face.

The major man-made structure at Dunkirk Harbor, N. Y., is located approximately 5 miles northeast of the southern border of Unit L. The harbor is a deep draft navigation project which was authorized in 1827 and has been modified many times over the past 150 years. There is a detached breakwater located seaward of the main channel. We did not do field observations here in detail and there is no evidence that this structure has a strong effect on the littoral drift system.

3.2n. Unit M. Unit M extends 16 miles from Silver Creek, N. Y., to Sturgeon Point, N. Y. This unit is distinctly different from Unit L in that it is made up of headlands of intermediate height separating wide embayments that have large streams with a heavy sediment input. Consequently, the area has abundant wide sandy beaches which show excellent spit growth toward the north, and, in places, the development of coastal sand dunes. The main reasons why sandy beaches are so well developed in this area are probably:

1. The occurrence of numerous streams carrying sediment into the area, including the largest stream on the northeast shoreline of Lake Erie, Cattaraugus Creek. The detailed study conducted along the entire stretch of the Cattaraugus Creek embayment makes up the bulk of this report, so it will not be discussed in this section.
2. The orientation of the shoreline, which is almost perpendicular to

the dominant wave approach direction (i.e., waves approaching from the west), which tends to slow down the rate at which sediment is transported out of the area.

Zonal site #18 is located at Evangola State Park, N. Y. The beach is sheltered between two projecting headlands of shale cliffs of intermediate height. The beach averages around 180-200 ft. in width, contains several berms as indicated by the sketch in Figure 31, and has been frequently manicured by the managers of the park. The sediment of the beach is very variable in size, being mostly sand but containing gravel as coarse as 8 in. in diameter. A unique aspect of the gravel at this locality is the occurrence of angular shale fragments created by frost heaving on the rock platform upon which the beach is situated. A small active dune area is located just in front of the seawall, at the back part of the beach. A large zone of driftwood accumulation occurs along the middle portion of the beach. The configuration of the beach is shown by the three-dimensional block diagram in Figure 32 and the general aspect of the beach on the ground is shown by the photograph in Figure 33. This beach is considered typical of the numerous wide sandy beaches that occur along the entire length of Unit M.

Zonal site #19 is the northward projecting spit that overlaps the mouth of Big Sister Creek, N. Y. Two sites were investigated in detail on the spit, which is shown by the aerial photograph in Figure 34A. The first area studied, the end of the spit, is shown in the block diagram in Figure 34B. The spit end is a growing recurve system which is formed basically as a sandy washover terrace. Gravel berms accumulate on the east end of the spit, indicating selective transport of the gravel toward

AD-A102 282

STATE UNIVERSITY OF NEW YORK COLL. AT FREDONIA DEPT 0--ETC F/6 8/8
CATTARAUGUS CREEK HARBOR, NEW YORK GENERAL DESIGN MEMORANDUM, P--ETC(U)
MAR 76

DACW49-74-C-0118

NL

UNCLASSIFIED

2 of 5
49
A102282

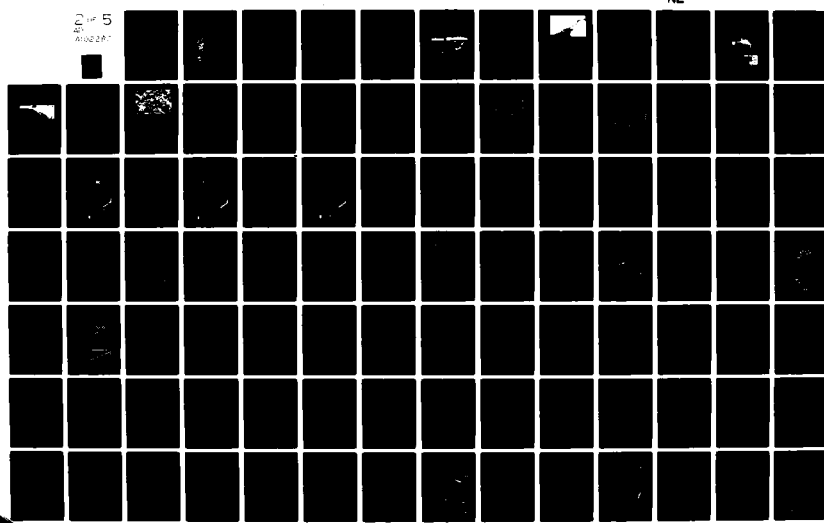


Figure 31. Field sketch of zonal site #18, the beach at Evangola State Park, N. Y. This wide beach, which is predominantly sand with an admixture of gravel, is sheltered between two bedrock headlands.

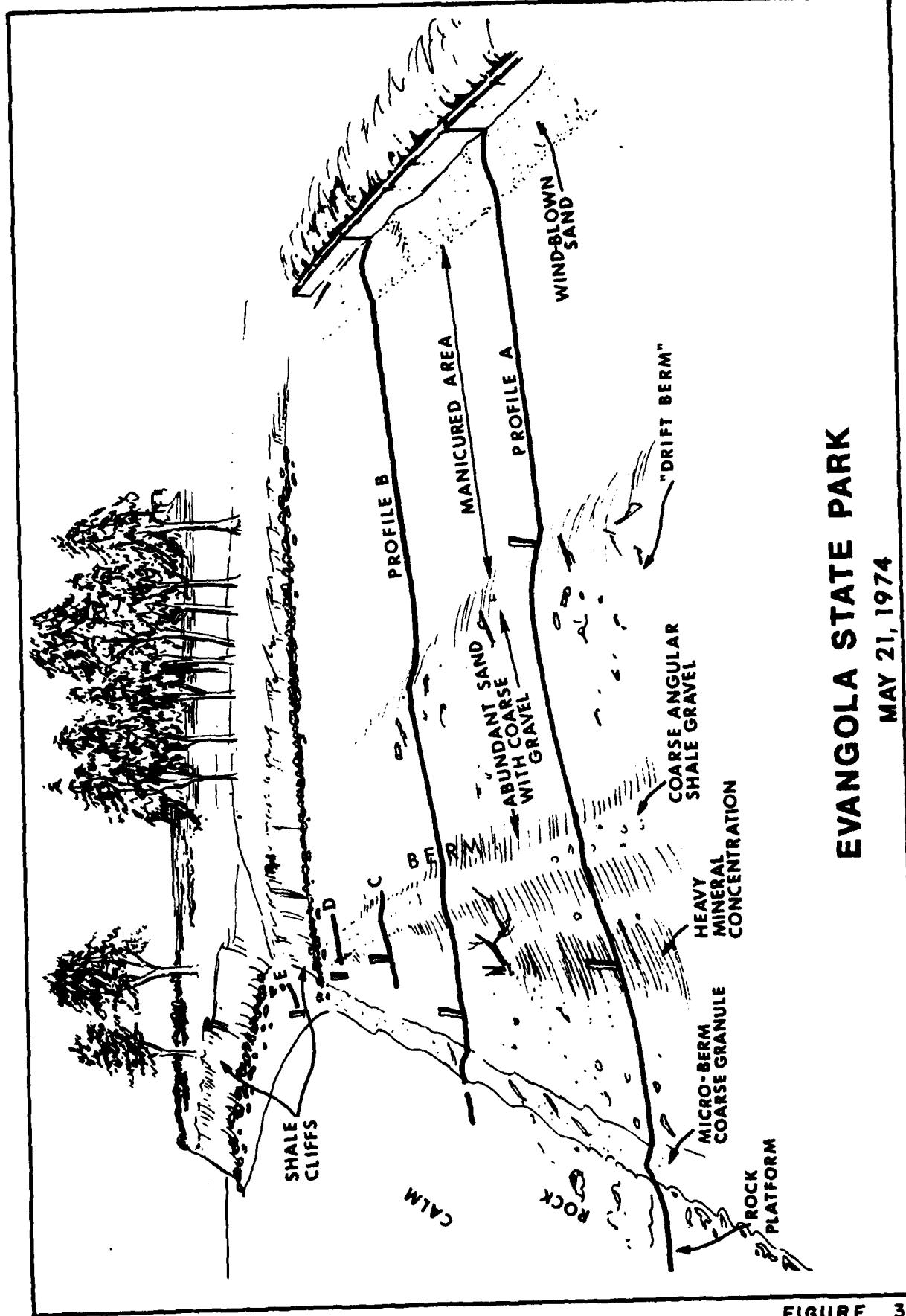


FIGURE 31

EVANGOLA STATE PARK

MAY 21, 1974

Figure 32. Three-dimensional diagram of the beach zone at Evangola State Park. This sandy beach sits on top of a rock platform cut by the waves.

ZONAL 18
EVANGOLA
STATE PARK, N.Y.

MAY 21, 1974

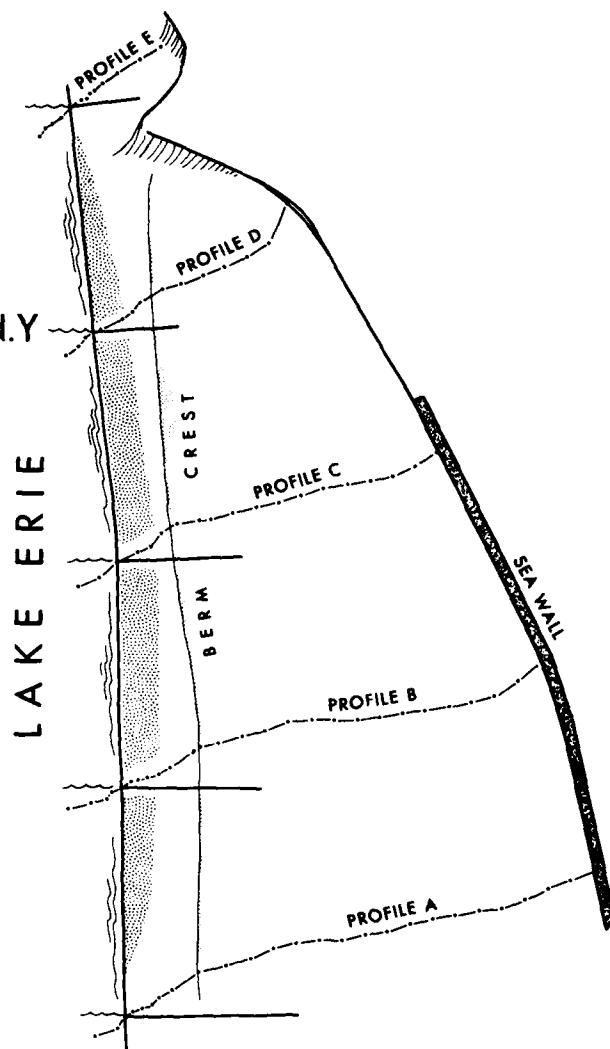


FIGURE 32

Figure 33. The beach at Evangola State Park. View looks southwest. Note cusps developing in new fine-grained gravel berm.

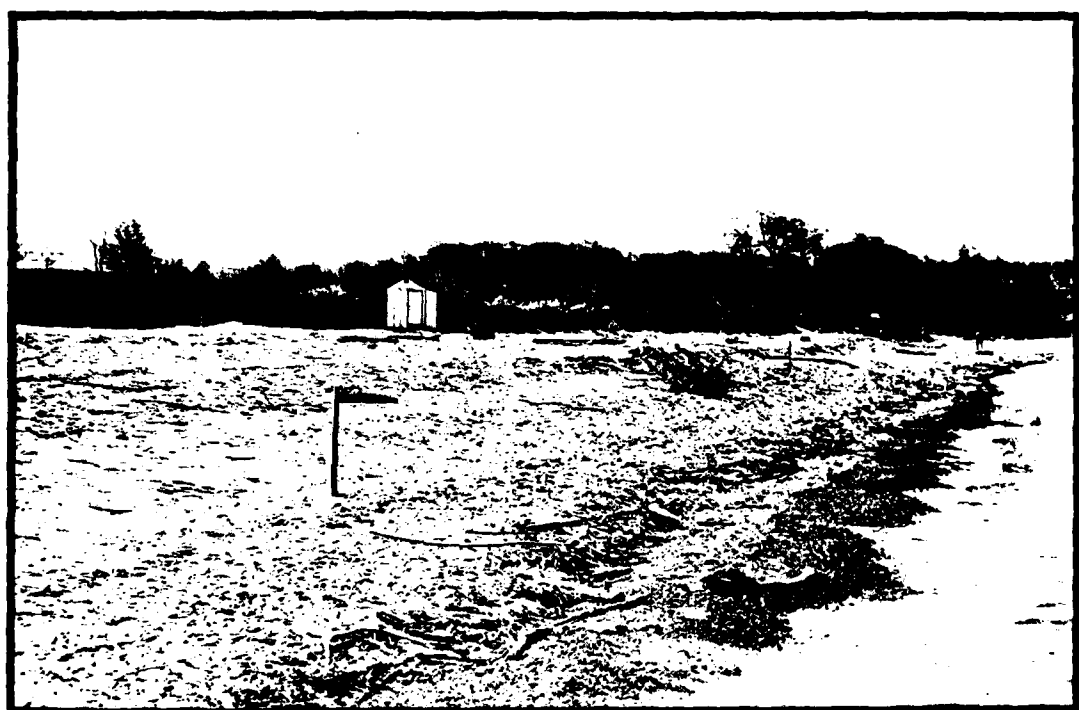
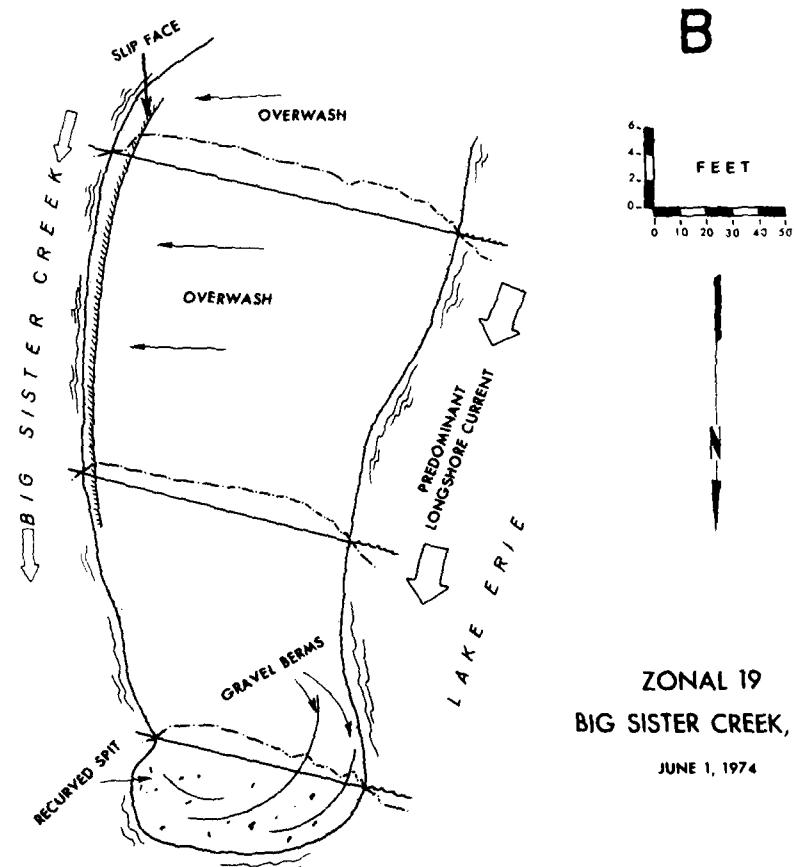


FIGURE 33

Figure 34. A. Zonal site #19, Big Sister Creek, N. Y. (second stream from left). View looks southwest. Note the northeastward projection of the spits, indicating longshore sediment transport in that direction. Arrow A points to spit area mapped and presented in B. Arrow B points to the profile presented in Figure 35A.

B. Spit at the mouth of Big Sister Creek. This entire spit, which is migrating in a northeasterly direction as a series of recurved gravel spits, is overwashed by waves during storms. Note actively accreting slip face on the west side of the spit.



FIGURES 34A AND B

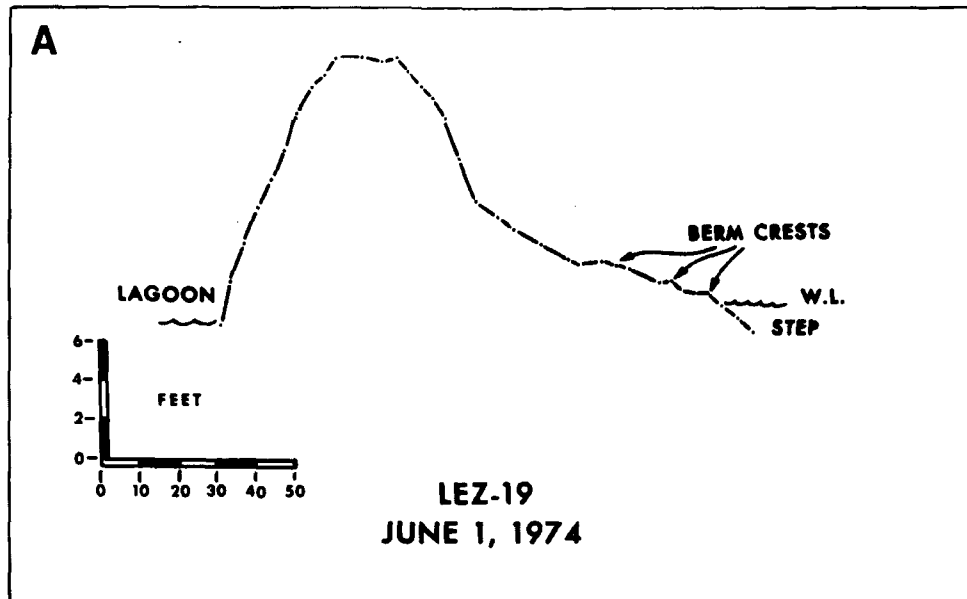
the end of the spit. The surface of the spit is flat and is obviously frequently overwashed by waves during periods of high wind tides. Thus, the spit is building both toward the northeast and landward into Big Sister Creek. The main portion of the spit is capped by high, vegetated eolian dunes. A profile of an active dune area is given in Figure 35A, and photographs illustrating the details of the profile are given in Figure 35B & C. These dunes at Big Sister Creek are the biggest that occur on the northeast shoreline of the lake and rival in size those occurring anywhere on the lake, with the possible exception of those found on Long Point, on the Canadian shore. At the present time, the dunes are eroding, with an erosional scarp occurring along much of the dune area. Heavy mineral layers accumulate in front of the scarp as it retreats during this period of high lake level. There are several other spits overlapping stream mouths in Section M.

Zonal site #20 is located at Sturgeon Point, N. Y. The dominant feature there is a breakwater, the shape and dimensions of which are shown in Figure 36. It is a very effective trap for sediment being transported from both the south and east, consequently the harbor has to be dredged repeatedly if it is to serve as an effective boat basin. To the southwest of the structure, the beach narrows, being composed of a number of berms made up of sedimentary rock fragments overlying a flat rock platform cut by the waves in black shale. At this locality, black shale has become a predominant component in the sediment fraction and it is commonly quite angular, as is illustrated in the photograph in Figure 37A. A general view of the beach along this area is given in Figure 37B. Black

Figure 35. A. Dune and beach profile extending from the lagoon of Big Sister Creek to the lake. The profile is located by arrow B on the aerial photograph of Figure 34A. The peaked central area is an eroding dune ridge.

B. Beach zone of profile shown in A. Note gravel accumulations on berms.

C. Slip face on dune at landward margin of profile given in A. Big Sister Creek can be seen on the right.



FIGURES 35A, B AND C

Figure 36. Structure at Sturgeon Point, N. Y. (zonal site #20). Note heavy sediment accumulation on both sides of the structure.

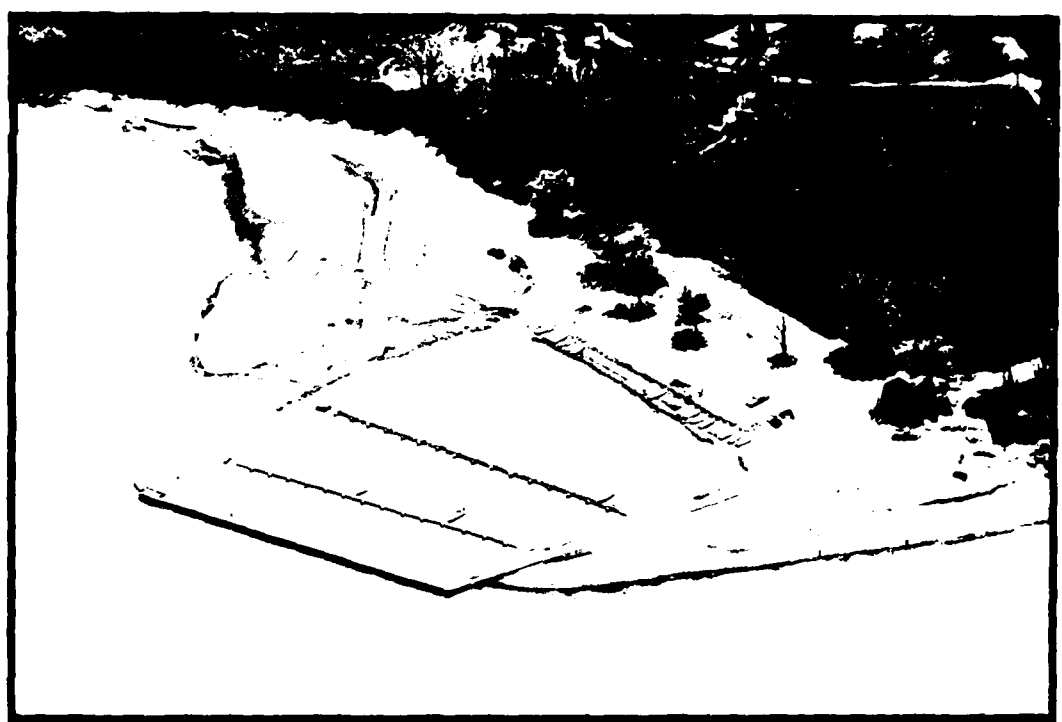


FIGURE 36

Figure 37. A. Gravel on beach a few hundred feet southwest of the structure at Sturgeon Point. Gravel is composed predominantly of black shale, which crops out in the cliff at this locality.

B. View looking southwest at locality A (above). A rock platform in the black shale occurred just below water level at the time the photograph was taken (21 May 1974).

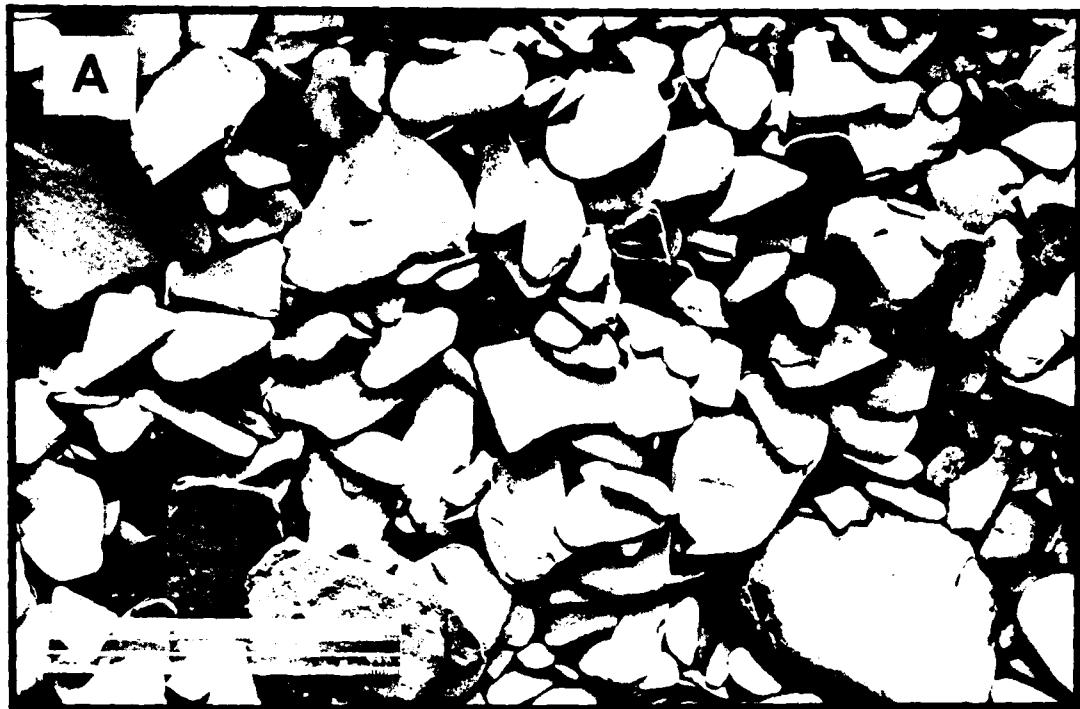


FIGURE 37

shale crops out at the base of the cliff, but the bulk of the cliff, which is approximately 60 ft. high, is made up of unstratified and stratified till.

Unit M is obviously a zone of intense sediment accumulation. It has more sandy beaches than any other part of the southeastern shoreline of Lake Erie. It is the only major sand accumulation zone, with the exception of Presque Isle, in the entire study area.

3.2o. Unit N. At Sturgeon Point there is a sharp break in the orientation of the shoreline, with the shore projecting in an east-northeasterly direction away from the point. Also, there is a corresponding strong change in the morphology of the coast at that point. The bedrock and till cliffs become considerably higher, and there is very little sand accumulation. The cliffs are somewhat irregular, being quite similar to the stretch of shoreline located between Dunkirk and Silver Creek (Unit L). The terminus of Unit N and the terminus of the study area is located at Wanakah, N.Y. Unit N is 8 1/2 miles in length. No zonal study was done in this area, inasmuch as it is so similar to Zonal #17 in Unit L, which was an inaccessible vertical cliff. Parts of Unit N and the rest of the shoreline between Wanakah and Buffalo, N.Y. have been so intensely modified by man that we could not determine details of the origin of the morphology of the coast, therefore we omitted those areas from the reconnaissance study.

3.3 Conclusions.

This reconnaissance study of the morphology and sediments of the southeastern shoreline of Lake Erie has led us to the following general conclusions:

1. The Cattaraugus embayment is somewhat unique in its morphology and sediments in that it occurs in an area that has an exceptionally large sediment supply and accumulation. Wide sandy beaches commonly occur between widely spaced bedrock headlands. This is thought to result from the facts that:
 - a. Cattaraugus Creek and neighboring streams deliver a large amount of sediment to the Lake Erie littoral drift system (discussed in detail later in report); and
 - b. The orientation of the shoreline in the Cattaraugus embayment area is into, or perpendicular to, the dominant wave approach direction (from west). This tends to slow down the rate at which sediments are transported out of the area.
2. The dominant longshore littoral transport in this area is from southwest to northeast. The morphological evidence for this trend is overwhelming, as is indicated by data collected at almost all of the 20 individual zonal study sites.
3. A severe erosion problem exists along most of the southeastern shoreline of Lake Erie. This is presumably the result of the present high stand of the lake. If the lake level does not recede soon, large losses of private and public property will continue.
4. Almost without exception, any man-made structure built in the beach area, such as jetties or groins, has a profound effect upon erosional and depositional conditions of the adjacent shoreline. The usual

pattern is widening of the beach on the southwest side and intensified erosion on the northeast side.

5. The role played by the cliffs in the erosional and depositional history of the shoreline is still uncertain. More detailed studies are needed on the relationship between cliff composition and local conditions.

6. A wide variety of morphological types are found in this area; it makes an excellent field laboratory for the study of coastal processes and geomorphology.

4. GEOMORPHIC HISTORY OF CATTARAUGUS HARBOR AND VICINITY

In the development of the Cattaraugus Embayment, shoreline, stream, and glacial processes acted on a relatively uniform shale bedrock. On a regional scale, glaciers advanced through the area for hundreds of miles to the west and more than forty miles south (Fig. 38). The topography over which the ice advanced controlled the ice flow. The most prominent of these topographic features was the lowland that is now the basin of Lake Erie and the 1000 foot escarpment that now borders it on the south in New York. Ice flow through the escarpment was controlled by pre-glacial stream valleys.

Predominant among these pre-glacial stream valleys in New York was the Ancient Allegheny Valley (Fig. 39). In many places this valley is filled with glacial deposits which have been compacted by thousands of feet of overriding ice. This valley is followed from Gowanda, New York, by the present Cattaraugus Creek. Records of wells drilled through the glacial deposits indicate that the elevation of bedrock is between 200 and 300 feet below sea level. A gravity survey along the beach places the bedrock at the present mouth of Cattaraugus Creek at about 275 feet below the lake (Wilson, 1973). Such deposits often provide reasonable foundation conditions, but the variability of the fill requires detailed on-site investigation. Detailed studies of the glaciation of western New York and extensive bibliographies are contained in Muller (1963, and in press).

The primary evidence of the earlier glaciations is the blockage of the northward course and the establishment of the southward flowing Allegheny-Ohio River system (Fig. 39). The last major continental ice in the area

Figure 38. Simplified glacial map of the eastern part of
Lake Erie.

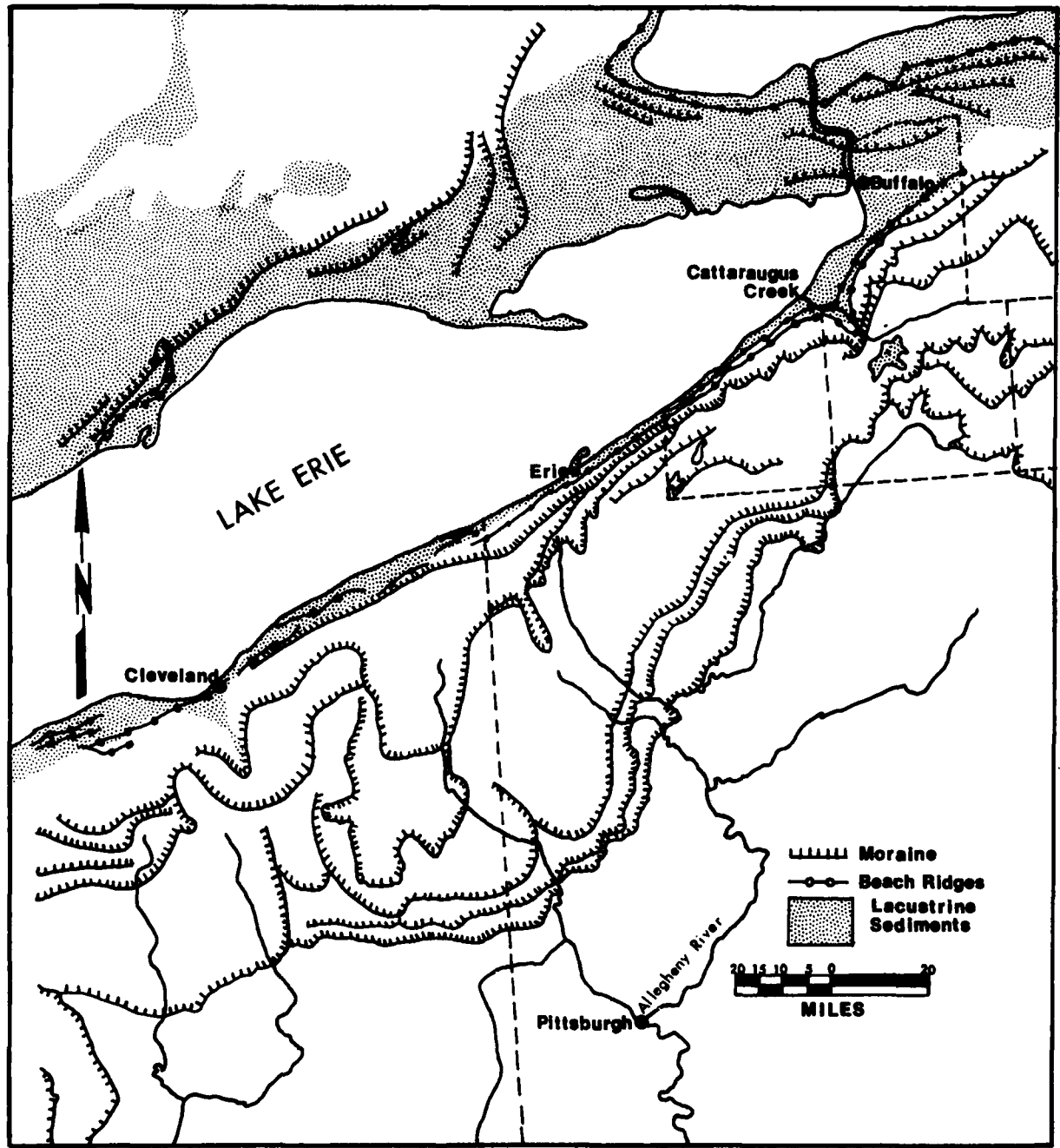


FIGURE 38

Figure 39. Formation of the Allegheny River from preglacial drainage.

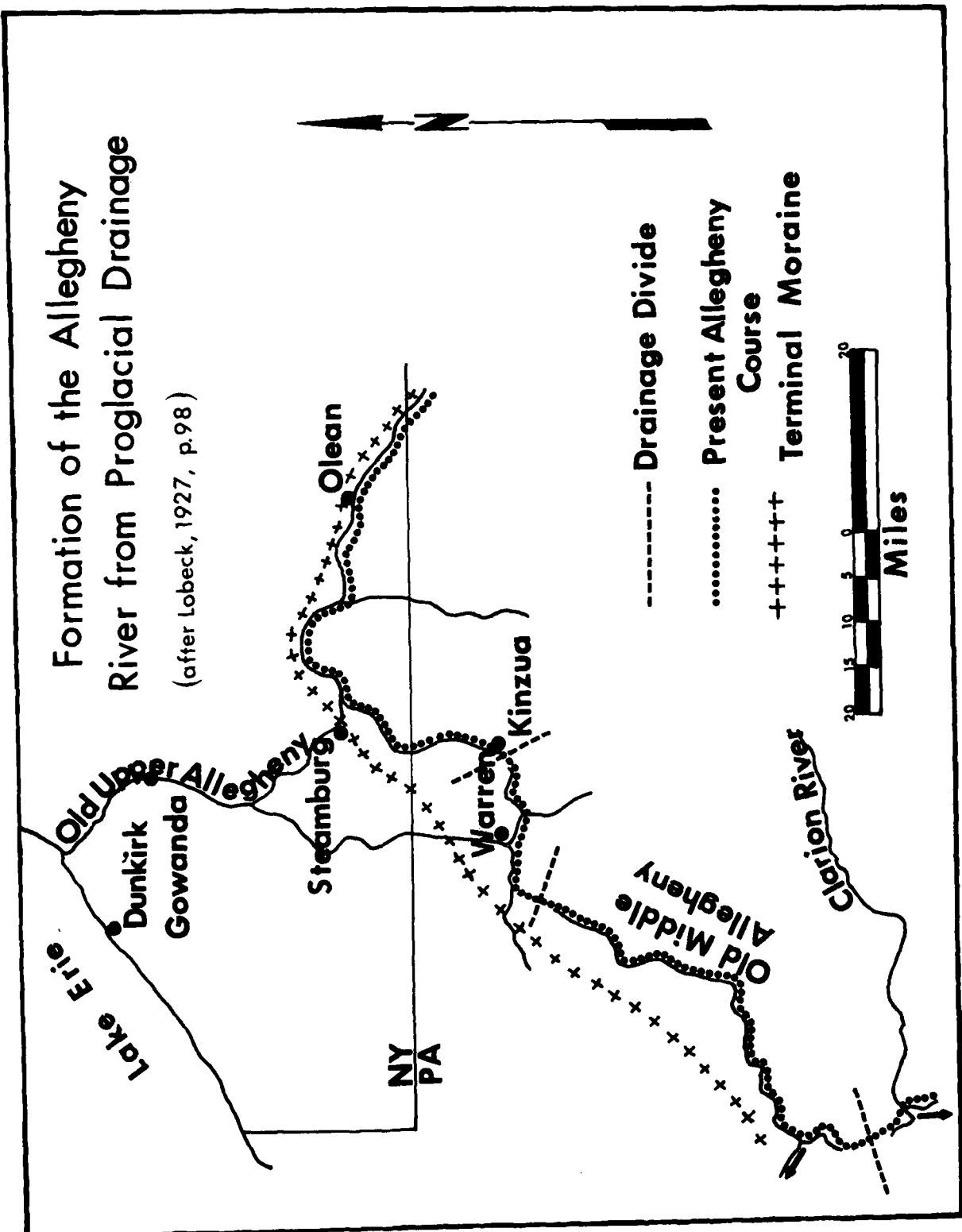


FIGURE 39

left behind a detailed record of its retreat in its moraine deposits (Figs. 38 and 40). A chronology of these events is given in Table II.

The moraines are ridges of unsorted sediment, formed during pauses in the glacier's retreat when the rate of melting was balanced by the rate of ice flow toward the margin. Under these equilibrium conditions the ice front may have remained at the same location for tens to hundreds of years, piling up the sediment that the glacier delivered as a sort of conveyor belt. The moraines in the vicinity of Cattaraugus Creek are shown in Figure 40, and ice positions and drainage development associated with these moraines in Figures 41, 42, and 43.

This glacial material provided the sediment source for beaches and deltas built during periods of high lake levels. These ancient lakes (Figs. 38 and 43) were formed when the outlet over the Niagara Escarpment was blocked and the flow of the Great Lakes basin, swollen by the meltwaters of Canadian glaciers, poured south through such rivers as the Wabash and the Illinois. Each time the retreat of the glacier allowed these ancient lakes to find a lower outlet, a new system of shoreline features was formed.

Unlike the shoreline of the present lake, these shorelines were primarily depositional features with only a few miles of wave-cut bedrock cliffs and many miles of beaches much wider than those of Lake Erie today. Detailed investigations and an extensive bibliography on these ancient lakes and beaches are contained in Calkin (1970). The beach features in the vicinity of Cattaraugus Creek are shown in Figure 40.

The relatively thick cover of unconsolidated glacial materials provides

Figure 40. High-level beaches and moraines of western New York.

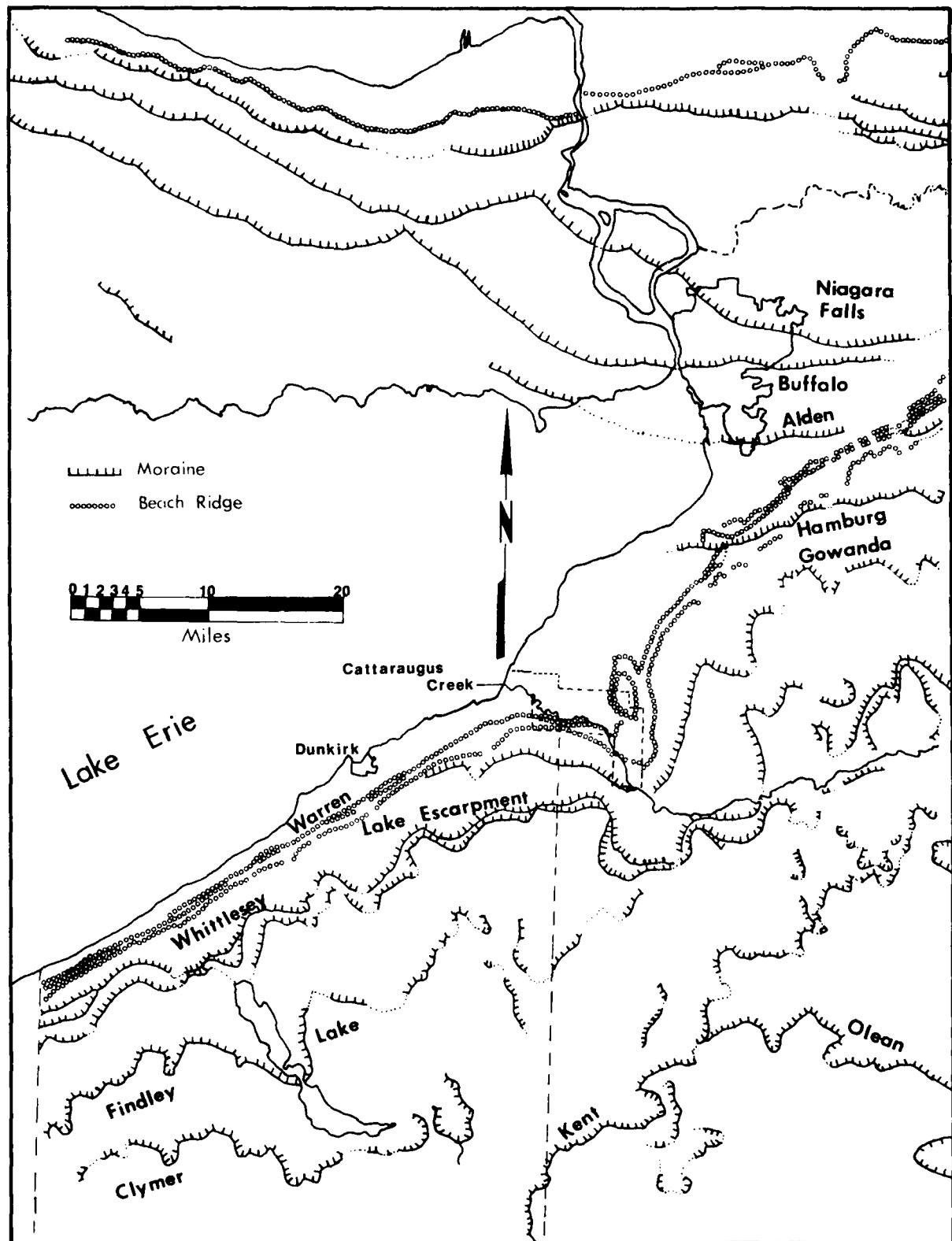


FIGURE 40

Figure 41. Lake escarpment glaciation. Position of ice-margin
and drainage patterns.

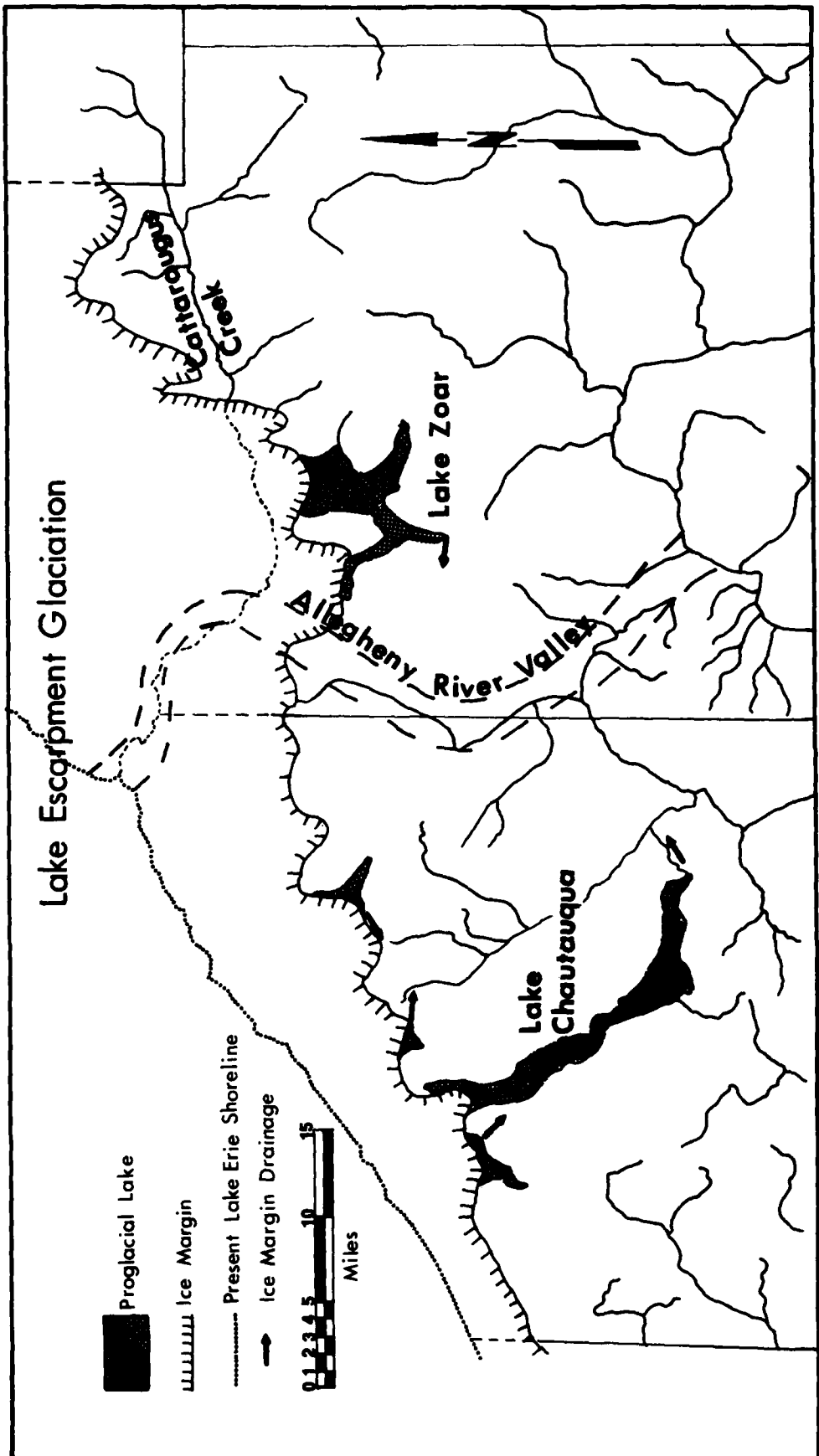


FIGURE 41

Figure 42. Gowanda glaciation. Position of ice-margin and
drainage pattern.

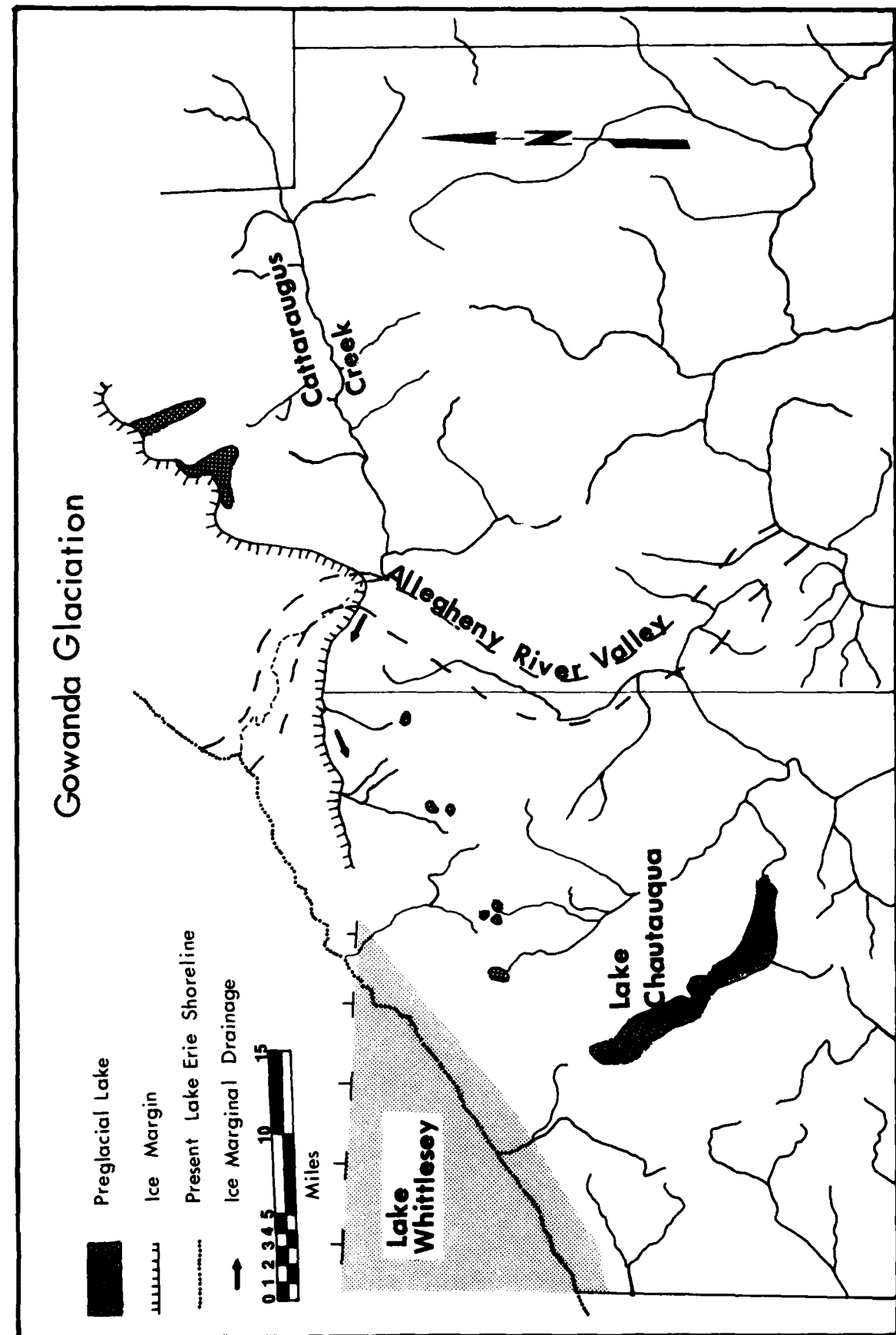


FIGURE 42

Figure 43. Lake Whittlesey and associated drainage.

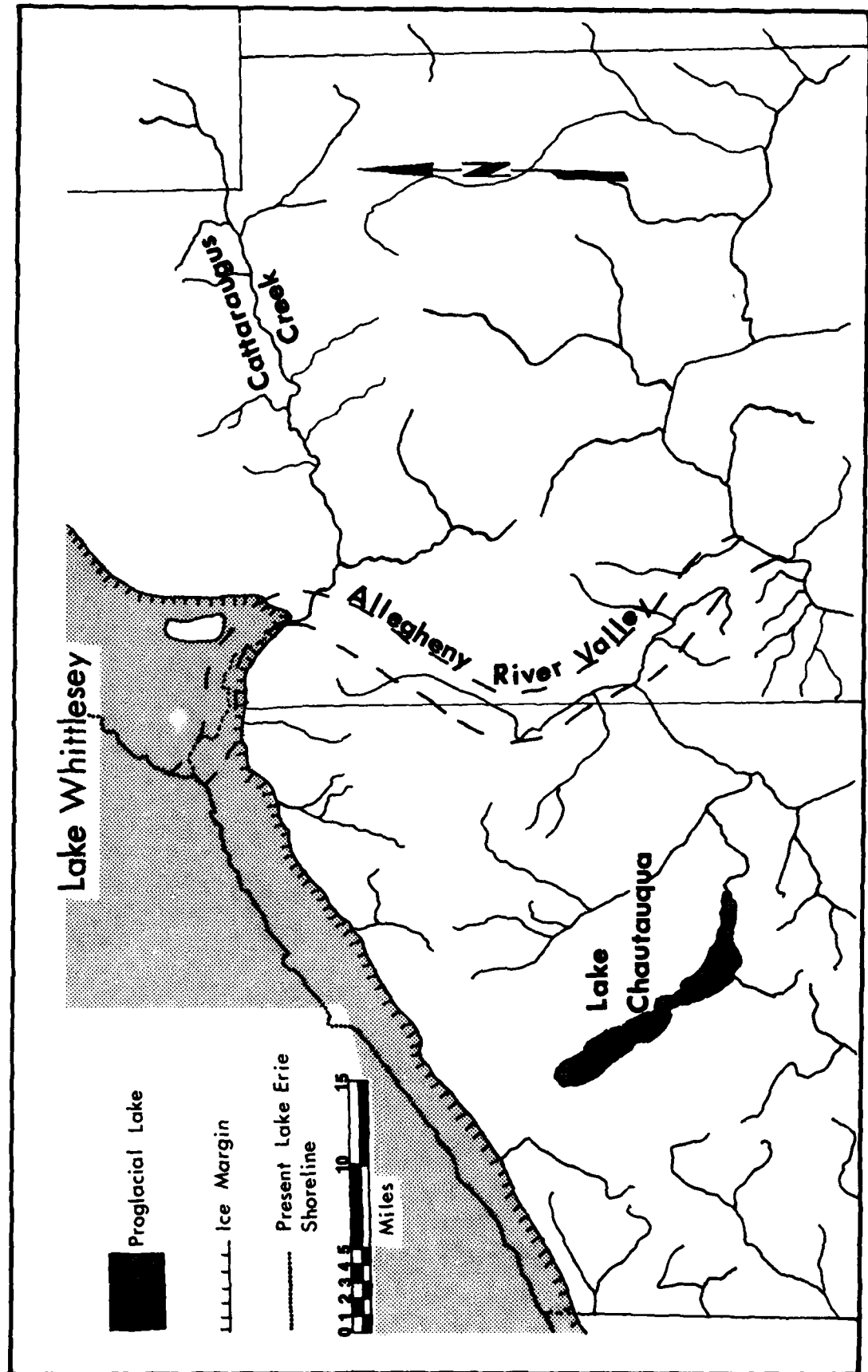


FIGURE 43

TABLE II
Correlation of Late Wisconsin Lakes⁺ and Moraines,
Western New York, from Calkin (1970)

Years B.P.	Glacial Event	Lakes of Erie Basin (*evidenced in N.Y.)	Moraines in N.Y.
-11,000	St. Lawrence ice-free		
	Valders Advance		
	Two Creeks	Iroquois (Ontario basin)	
	Interstade		
-12,000	Rome, N.Y. ice-free	*Early Erie (473?)	
		*Dana (570)	Albion M.
		*Early Algonquin (605)	Barre M.
		*Lundy (620)	
		*Grassmere (640)	Batavia M.
		*Warren III (675)	Niagara Falls M.
		*Wayne (660)	Buffalo M.
		*Warren II (680)	Alden M.
		*Warren I (690)	Marilla M.
	Port Huron Advance	*Whittlesey (738)-?	Hamburg M.
-13,000	Cary/Port Huron	Ypsilanti? (543-373)	Gowanda M.
		III (695)	Lake Escarpment M.
		II (700)	
		Arkona I (710)	
	Cary Advances		Moraines of SW New York (see Muller, 1963)
-14,000			

⁺Elevations of glacial lakes south of respective zero isobases, (after Wayne and Zumberge, 1965).

the present streams, such as Cattaraugus Creek, with a readily available source of both fine and coarse sediment which ultimately is delivered to the lake. Wave erosion of glacial materials exposed along the lake shore contributes a major amount of sediment to the lake, but not near the mouth of Cattaraugus Creek.

Table II indicates that, following the high-level lakes of the Lake Erie Basin, a level considerably lower than the present stage existed for an unknown length of time. In adjusting to the lower lake level, streams cut channels in bedrock or in glacial drift. As the lake level rose to the present level, some of these channels, like Cattaraugus, were backfilled while others remained as estuaries.

Wave erosion has caused the present shoreline of Lake Erie to retreat hundreds to thousands of feet in most places since the lake rose to its present level. Partly as a result of the sediment supplied by Cattaraugus Creek, this segment of the shoreline may be one of the few to have escaped severe wave erosion. Table II suggests that the present lake is no more than 11,000 years old and may be considerably younger than that.

5. HISTORIC CHANGES NEAR THE MOUTH OF CATTARAUGUS CREEK

Air photos and maps provided the basis for a series of maps showing the changes in the configuration of the shoreline and the stream near the mouth of Cattaraugus Creek (Fig. 44,45). The role of stream and shoreline processes is evident on close inspection. Changes in lake level for the period between 1935 and 1969 on the average beach slopes of 1 in 10 (north side of Creek mouth) and 1 in 30 (south side) would result in little or no apparent change in position of the shorelines at the scale of the map.

In general, the interaction of littoral and fluvial currents appears to control the form and position of the deposits at the mouth of the creek. The maps of 1935, 1942, 1958, and 1966 show the south spit to be projecting northwest into the lake, a condition thought to reflect relatively strong fluvial currents in the period prior to the mapping. This contrasts to 1956, 1961, and 1971, when the south spit was found to recurve into the creek mouth, a condition probably caused by sustained wave-power dominance.

The changes between maps reflect the sum of all the changes in the intervening years. Floods may flush out sediments blocking the mouth of the creek only to have them replaced by high wave and current activity at lower stream flow. The seasonal fluctuations in spit morphology are discussed below.

The spit on the north side of the mouth is almost always recurved into the harbor, indicating its dominant control by wave power. The latest air photo, 1971, showed that the creek had broken through the north spit about 300 meters north of the present channel mouth. This breach has been closed

Figure 44. Maps of Cattaraugus Creek mouth and the adjacent shoreline. From 1875 to 1961. See Figure 45 for legend.

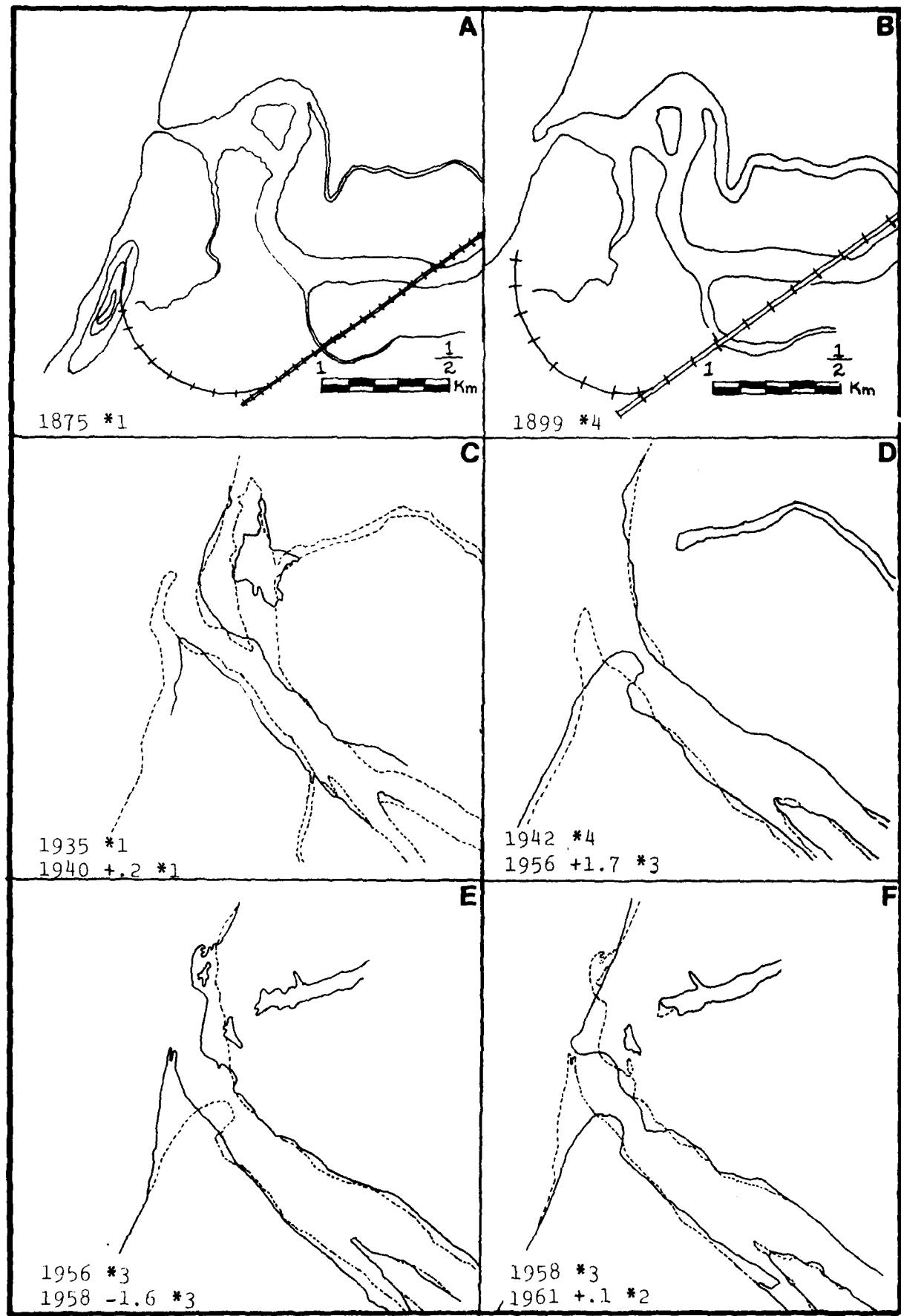


FIGURE 44

Figure 45. Maps of Cattaraugus Creek mouth and the adjacent shoreline. From 1961 to 1971.

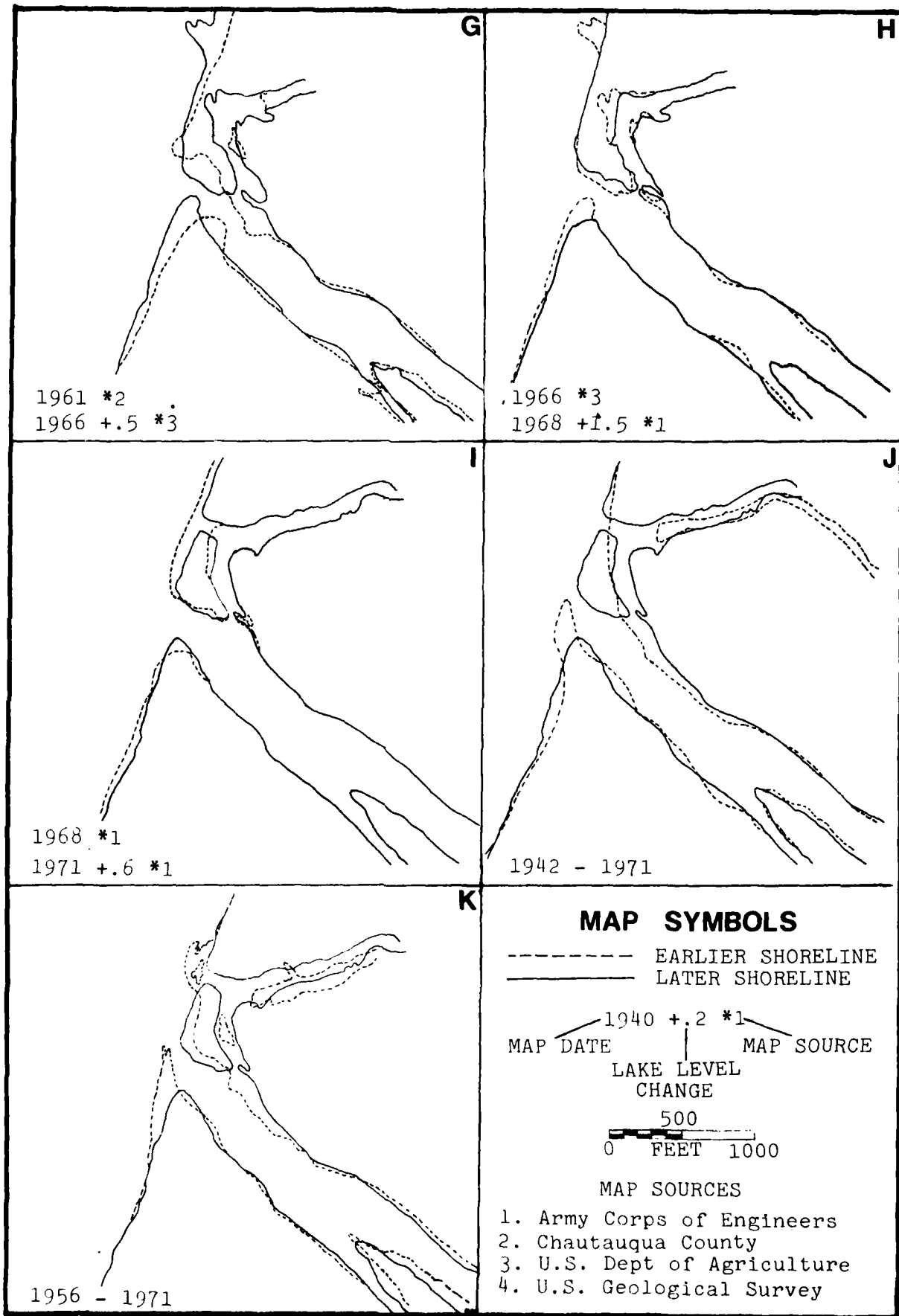


FIGURE 45

by 1974 and probably before that. Such openings may develop when the primary mouth of the stream is blocked by ice from the lake or stream or both. The rapid infilling of the breach demonstrates the high rate of littoral sediment transportation on this stretch of beach.

If the map of 1875 can be believed, there was a sand dune more than 30 feet high on the shore south of the creek. Its removal for use elsewhere was probably the sole purpose of the railroad spur shown on the same map.

The long-term stability of the shoreline and the channel may be inferred from Figures 44 and 45 . A comparison with erosion rates of unconsolidated portions of the Ohio shore, which averaged more than two feet per year over the last one hundred years, indicates that sediment losses from the nearshore of the Cattaraugus Embayment must be replaced. The dominant source of sediment is Cattaraugus Creek.

6. LITTORAL PROCESSES

Typically, Lake Erie is ice covered from early December through March. The lake ice is responsible for frequent spring flooding of the lower 3/4 mile of Cattaraugus Creek because an ice jam at the mouth raises the downstream control level of the river (U. S. Army Engineer District, Buffalo, 1972). This problem will be analyzed in some detail later. The ice prevents any active sediment transportation during the winter months, leaving April through November for field measurements of littoral processes. Data from Saville (1953), representing hindcast wave conditions for the three years 1948-1950, indicate that the stormiest conditions are associated with March ice break-up (Fig. 46). May and November are the months with the highest wave action during the ice free period.

In order to cover both the spring storm activity and the transition into typical summer lake conditions, the field data collection program ran from May 7 through June 13, 1974. A brief field period is planned for November to monitor a typical fall storm.

6.1. North American cyclone patterns.

The most severe weather disturbances affecting the Great Lakes region are the extratropical cyclones. The location of fronts or areas of cyclogenesis depends on the general zonal circulation and location of characteristic air masses. Three principal frontal zones generate cyclones affecting the Great Lakes: 1) the Atlantic polar front, 2) the Pacific arctic front, and 3) the Pacific polar front (Petterssen, 1969, p. 222-223). The Atlantic

Figure 46. Annual variation in wave characteristics. Maximum storm activity occurs in March, generally associated with the break-up of lake ice. May and November have about the same storm frequency. Summer thunderstorms may occasionally create high waves. Wave hindcasting, however, does not adequately reconstruct such local phenomena. Data from Saville (1953).

HOURS PER MONTH WITH WAVE HEIGHT OF 6 FEET AND ABOVE

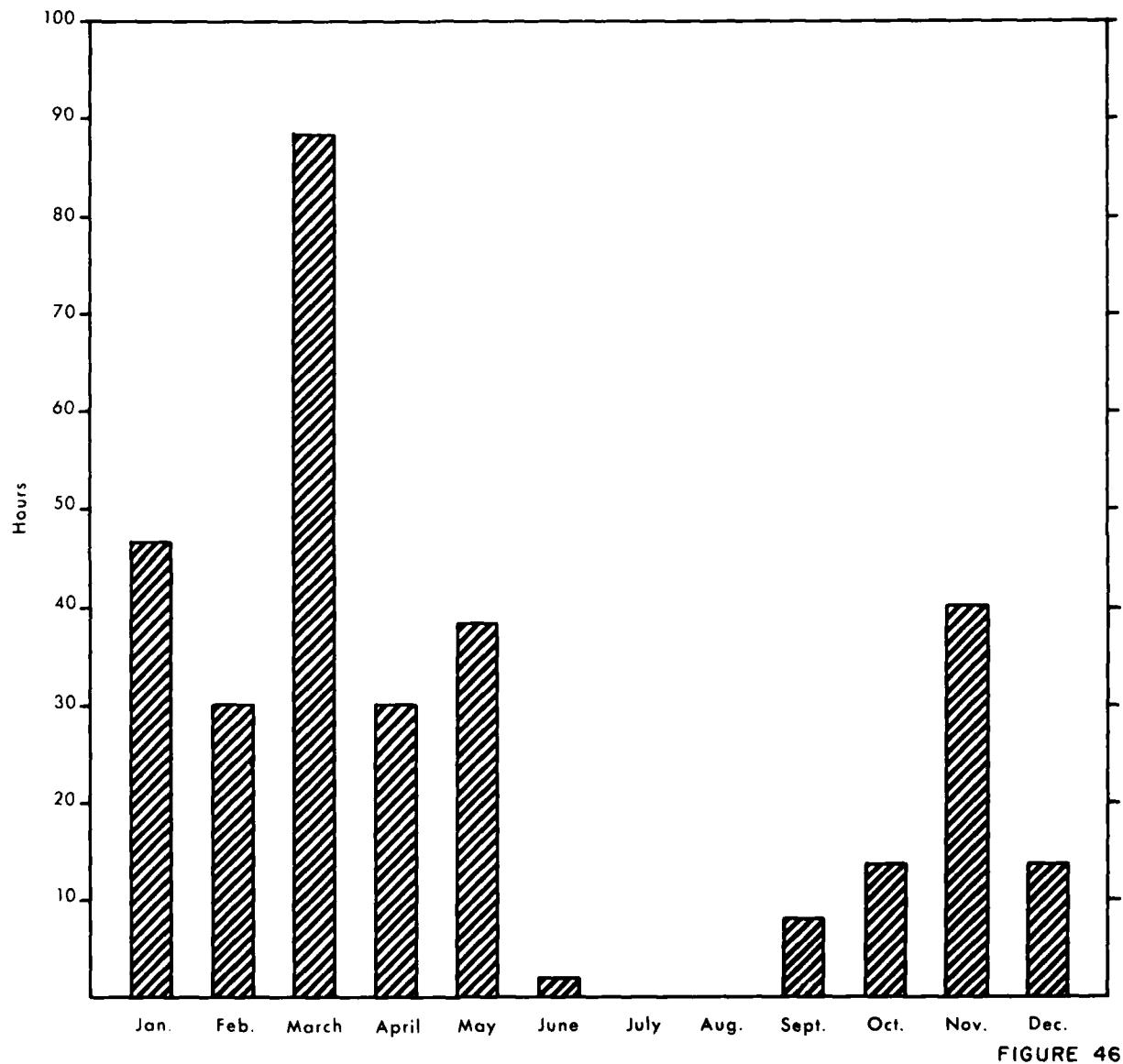


FIGURE 46

polar front is formed by the temperature contrast provided by the difference in air-mass properties between polar continental and tropical maritime sources. Most of the cyclones affecting eastern North America are generated on this front, and some extend west into the Great Lakes region. The Pacific arctic front often extends itself inland, and storms generated to the east of the Canadian Rockies on this front provide the major disturbances in the Lake region (Alberta lows (1), Fig. 47A). Cyclones developed on the Pacific polar front tend to weaken as they cross the Rocky Mountains, but they frequently redevelop on the east side (North Pacific lows (2) and South Pacific-Colorado lows (3), Fig. 47A) and converge towards the Great Lakes. Texas lows ((4), Fig. 47A) are generated in a similar way and frequently travel into the lake region.

Analysis of weather maps (NOAA, Daily Weather Maps, 1974) revealed that of the storms observed on Lake Erie during the field period, three were Alberta lows, one a North Pacific-Colorado low, and one a South Pacific-Texas low (Appendix I tabulates the relevant information). Four of the five observed storms passed to the north of Lake Erie. Consequently, the observed wind direction on the south shore of Lake Erie rotated from south (offshore) through west-southwest (along the axis of the lake) to northwest during the passage of the storm (Fig. 47C). When the low pressure center is close to the lake, the winds over the lake are generally out of the west-southwest, causing the simultaneous occurrence of maximum wind velocity and maximum fetch. The circulation pattern and frontal locations associated with the most severe storm to hit Lake Erie during the observation period are shown in Figure 48. By analyzing the charts for a few days prior to June 9, it is

Figure 47. A. Major North American cyclone tracks. Most eastward moving cyclones, regardless of their western area of generation, are focused on the Great Lakes with the most frequent track being to the north of Lake Erie. Data from Goode's World Atlas (1970) and Petterssen (1969).

B. Generalized cyclonic circulation. The geostrophic wind pattern is controlled by equilibrium between the pressure gradient and the Coriolis force.

C. Variations in wind direction on Lake Erie with passage of a typical cyclone. The change in wind direction from south through west to northwest is caused by the lake experiencing different sectors of the wind field during the cyclone passage.

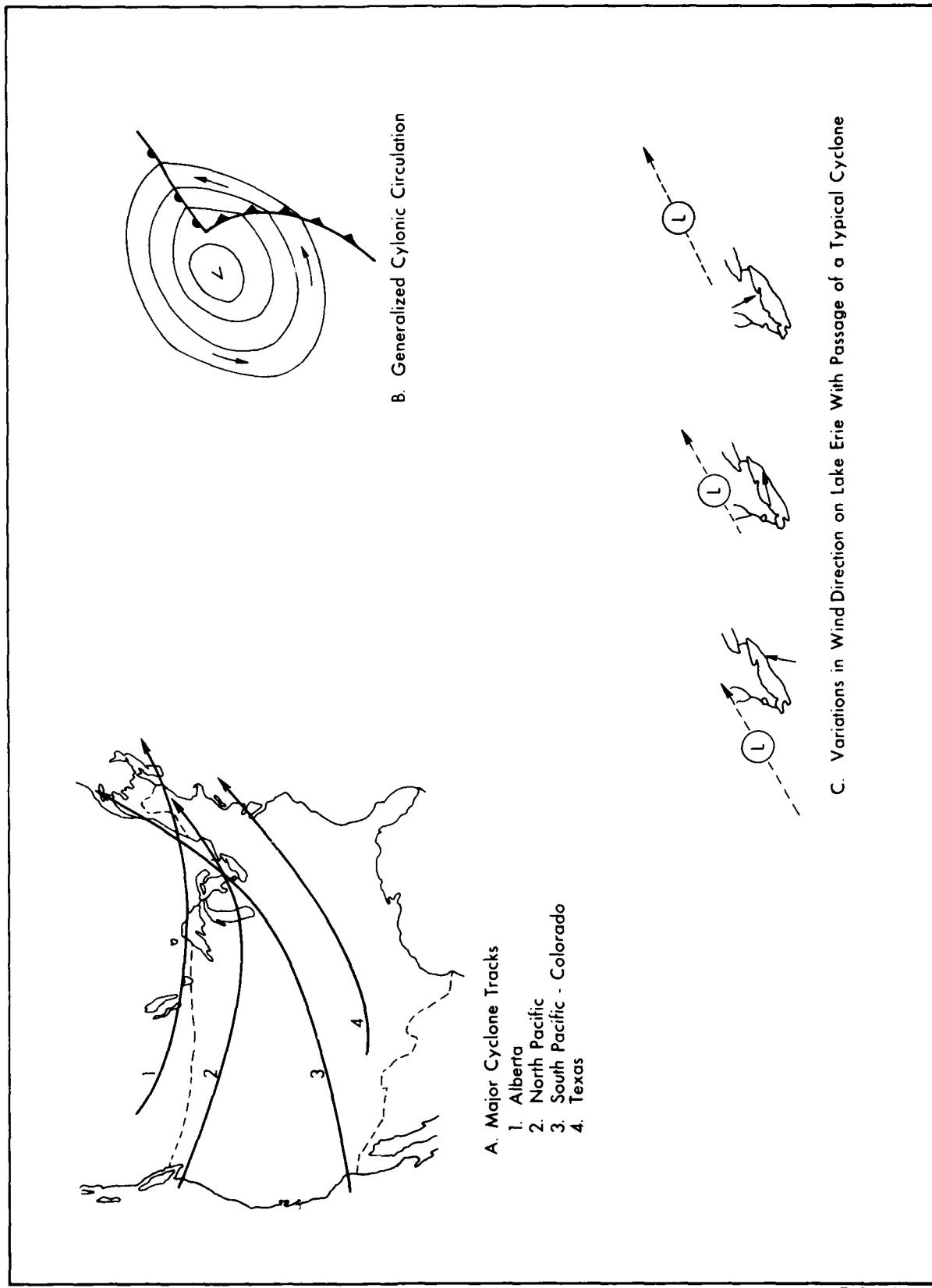


FIGURE 47

Figure 48. Synoptic charts at 24 h intervals for storm of June 9-June 13, 1974. The storm was generated in Texas and crossed the Great Lakes near Sault St. Marie about 2 days later. The wind direction over Lake Erie typically changes from south through west during passage of the storm. Data from NOAA (1974).

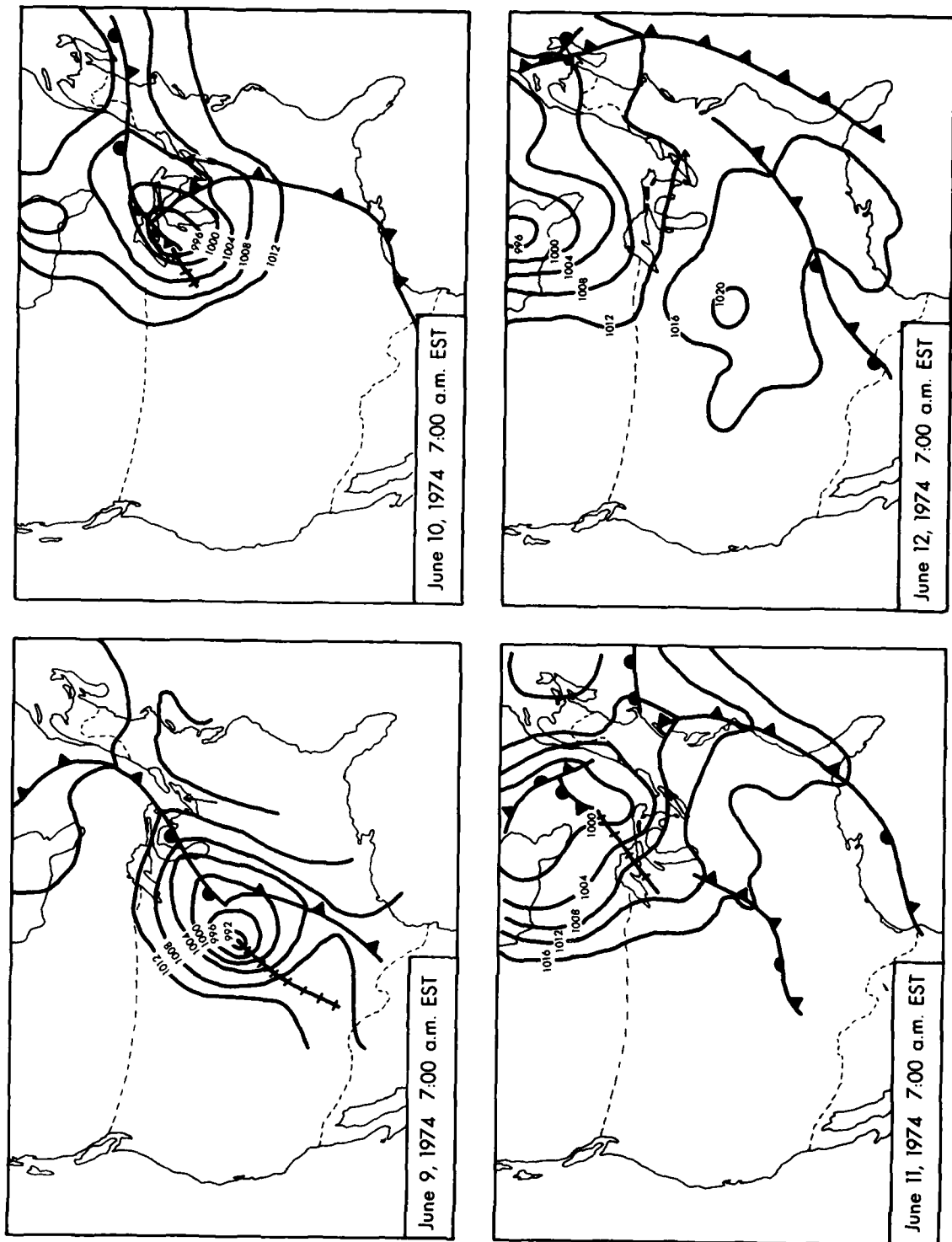


FIGURE 48

→ Wind Direction at Buffalo

seen that the storm is a typical South Pacific-Texas low. A regenerated low formed in north Texas on June 7 and migrated northeastward to cross the Great Lakes near Sault St. Marie on June 10. Maximum wave height was observed on Lake Erie in the early morning hours of June 11 after a night of westerly winds (map, June 10, Fig. 48) with speeds of 15 to 20 knots. During the passage of the storm the wind changed from south (offshore) on June 7 and 8, through south-southwest on June 9 and 10, to west-southwest during the waning stages of the storm.

Anticyclonic circulation around a high pressure center to the north of Lake Erie occurred on May 11 (high over Ontario) and May 19-20 (high over James Bay). Typically, the wind directions are easterly. The wind velocities are low, however, in comparison to the cyclonic circulation, and longshore current velocities remain small.

6.2. Wind and wave statistics.

The analysis of North American synoptic situations indicated a dominance of westerly winds over Lake Erie. The wind observations at Buffalo Airport (Fig. 49) demonstrate that during 27.6 per cent of the year the wind blows from the southwest over an ice free lake, and for an additional 7.9 per cent of the year winds are out of the west. These figures compare to 35.8 per cent of the year with winds out of any other direction and ice free lake. It should be pointed out that wind conditions over the open lake are not identical to those at Buffalo because of the difference in surface friction over land and water. Reduced friction over the lake will increase wind speed and make the wind more nearly geostrophic, i.e. parallel to the isobars. With the low pressure centers passing north of the lake, this

Figure 49. Wind diagram for Buffalo, New York. The diagram demonstrates the dominance of winds blowing along the axis of the lake from the southwest. The winds over the open lake are more nearly geostrophic because of the lower friction over the water. Consequently, a wind diagram for the open lake would have somewhat stronger westerly and northerly components.

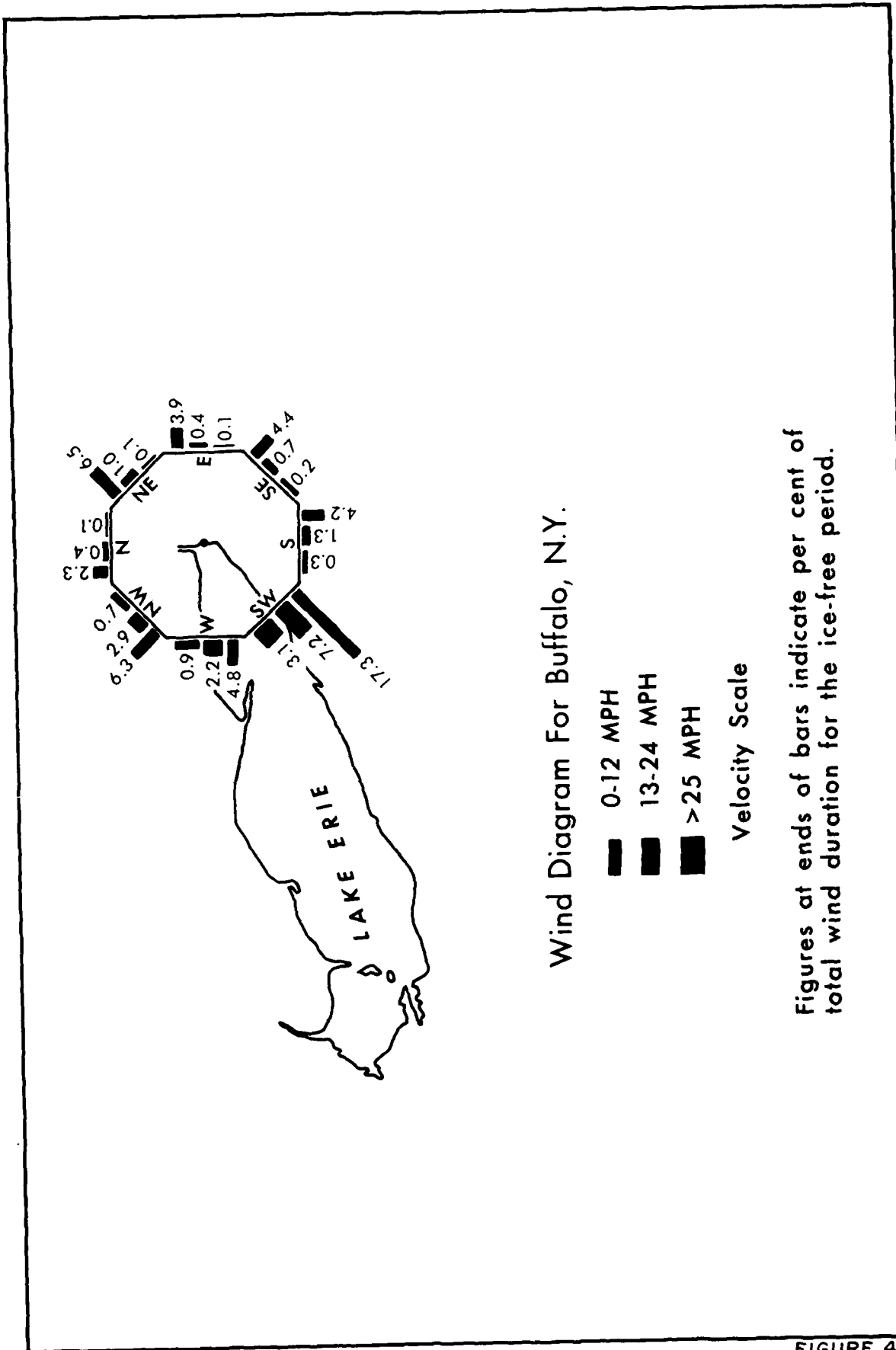


FIGURE 49

implies a stronger northerly component in the lake wind than what is recorded at Buffalo.

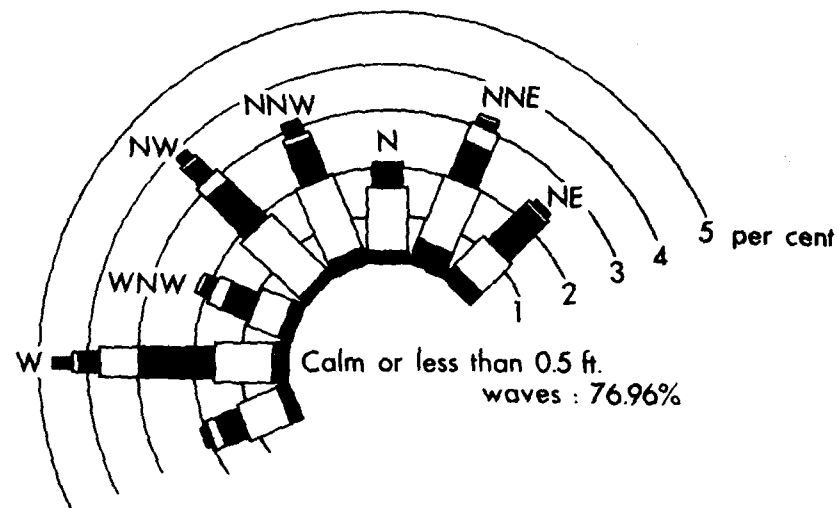
Continuous wave observations of a duration of one year or more are not available for Lake Erie. To evaluate deep water wave approach directions and energies, therefore, one has to resort to wave hindcasting. Of the existing methods, Cole (1967) concluded that the Sverdrup-Munk-Bretschneider wave hindcast method based on surface winds obtained from the geostrophic wind analysis produced the best correlation with observed data on the lakes. Wave hindcasting has been performed for three of the Great Lakes, including Lake Erie (Saville, 1953). Rather than using the geostrophic wind analysis, however, Saville used the recorded surface winds at coastal stations. The additional inaccuracy this introduces into the computations cannot be evaluated. It is the belief of these authors that Saville's approach may underestimate the northerly component in his wave diagrams (Fig. 50) for reasons stated above. The implications will be discussed further below.

Saville hindcast wave conditions for Monroe, Cleveland, Erie, and Buffalo. Wave and wave energy diagrams for Erie and Buffalo are presented in Figures 50 and 51 respectively. The location of Buffalo at the eastern end of the lake effectively eliminates fetch from any directions but southwest through west. At Erie, on the contrary, substantial fetch exists in all directions from west-southwest through northeast. It is further observed that a fair correlation exists between fetch length and relative annual wave energy from that direction. Westerly waves dominate, however,

Figure 50. Wave diagrams for Erie, Pa., and Buffalo, N. Y. The frequency of waves from each direction is related to the relative fetch length. Erie, therefore, experiences waves from almost a 180 degree sector, whereas Buffalo has significant waves from a sector of about 60 degrees. The highest waves at Erie (76 feet) come out of the west. Data from Saville (1953).

WAVE DIAGRAMS

ERIE, PA.



BUFFALO, N.Y.

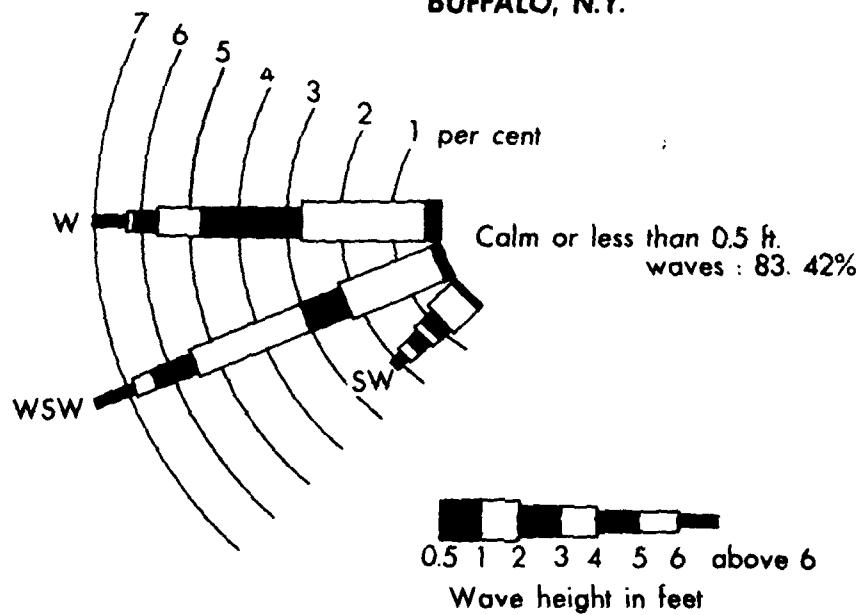


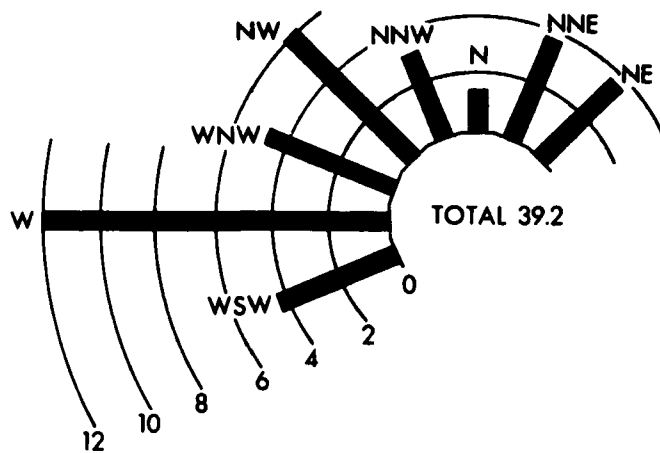
FIGURE 50

Figure 51. Wave energy diagrams for Erie, Pa., and Buffalo, N. Y. Wave energy flux from each direction correlates well with fetch length. Therefore, for any location on the Lake Erie shoreline between Erie and Buffalo an approximate wave energy diagram can be found by constructing a fetch diagram for that location (see Fig. 53B). Data from Saville (1953).

WAVE ENERGY

in 10^8 $\frac{\text{ft. lb.}}{\text{ft. yr.}}$

ERIE, PA.



BUFFALO, N.Y.

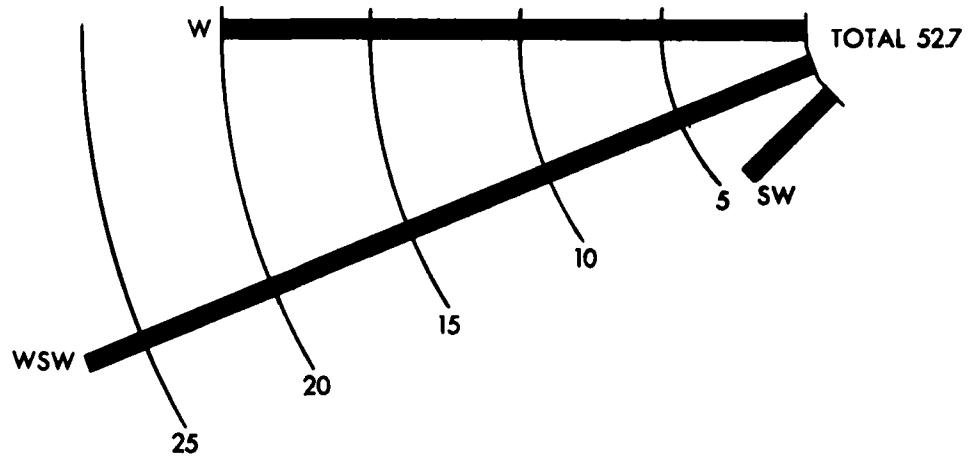


FIGURE 51

more than proportional to their associated fetch length, because of the nature of the cyclone migrations described above.

A wave diagram can be derived for the Cattaraugus Embayment by interpolation of the data in Figures 50 and 51 (Saville, 1953, p. 3). The accuracy of the resultant diagram is unknown. Therefore, only a qualitative interpolation will be attempted. The Cattaraugus Embayment is likely to receive annual wave energies from the west-southwest and west intermediate in value between those at Erie and Buffalo. The northwest fetch is about half of that at Erie, the north fetch about the same, and the northeast fetch is reduced to about one-third. With these approximate interpolations one finds that about 75 per cent of the total deep water wave energy flux approaches the Cattaraugus Embayment from the west and west-southwest. Of the remaining 25 per cent about 10 per cent enters the embayment from west-northwest and northwest and therefore approaches normal to a major segment of the Cattaraugus beach. Only about 15 per cent of the wave energy flux arrives from the north or northeast at an angle sufficient to cause substantial southward oriented littoral currents. The fetch diagram in Figure 53B approximates the wave energy distribution discussed above.

6.3. Littoral processes at Sunset Bay.

Despite the relatively short time coverage of our sampling program, the synoptic situations and consequent wave conditions encountered seem to give a fair representation of year round conditions, with the possible exception of some major fall or early spring storms.

Data on longshore current velocity, angle of breaker crest relative to

shore, period and height of breaker, and wind speed and direction were obtained at 12 hour intervals at Station Cat. 3 (see Fig. 53C for location). Station Cat. 3 was judged "characteristic" of the beach south of Cattaraugus Creek for moderate wave energy conditions like the ones observed in May and June of 1974. For high wave energy conditions the site is sheltered by shoals in the southern part of the embayment and off the Silver Creek headland. The data are summarized in Figure 52 and tabulated in Appendix II.

During passage of Alberta lows to the north of Lake Erie, the longshore currents are consistently to the north. The speed of the current correlates more closely with the breaker angle than with the breaker height. A typical example is provided by lake conditions on May 15 and 16. The storm was generated by a cyclone migrating from Wisconsin to James Bay. On the morning of May 15, the longshore current was moving to the north at a speed of 1.7 fps at a wave height of 1.7 feet and a breaker angle relative to shore of 18° . A slight drop in both wave height and breaker angle occurred during the day, reducing the evening current velocity to about 1.4 fps. During the passage of the May 9 storm, the current velocity reached only 1.4 fps for a wave height of 3.3 feet. Because of the increased refraction these higher waves reached the shore at a 5 degree angle, causing the lower current velocity. An even better example is provided by the June 11-13 storm. Wave height decreased from 3.3 feet to 1.2 feet in 24 hours. This was accompanied by an increase in breaker angle from 0 to 12 degrees and an increase in current velocity from 0.2 to 0.9 fps. Wind speed and direction were approximately constant during this time. High longshore current velocities seem

Figure 52. Process parameters at Cattaraugus Beach, Cat. 3, May 7-June 13, 1974. Longshore current velocity is closely correlated with breaker angle, period, and height. Maximum wave energies are encountered during periods of persistent westerly or southwesterly winds. The wind reported here was measured at the same site on the beach where the other process measurements were obtained. Water level was recorded at a staff gage at Keene Marina, about 500 feet upstream of the mouth of Cattaraugus Creek.

**PROCESS PARAMETERS AT CATTARAUGUS BEACH, CAT 3
MAY 7 - JUNE 13, 1974**

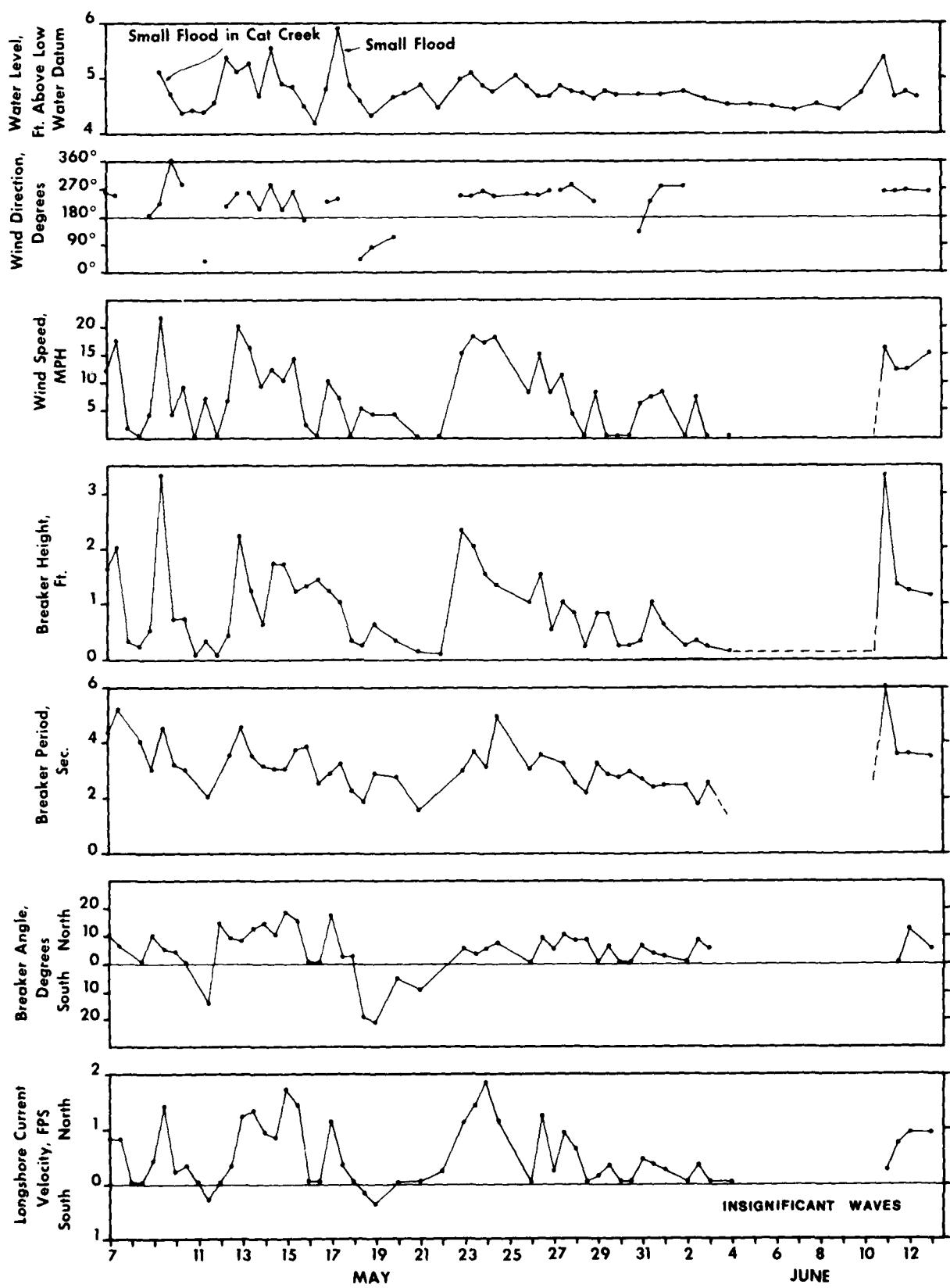


FIGURE 52

to be associated with moderate waves approaching the shore at a steep angle and a period of 3 to 4 seconds. Southerly longshore currents occur, as on May 19 and 20, associated with anticyclonic circulation around a high pressure system north of the lake. Rarely, however, is the anticyclonic circulation strong enough to generate any major waves. Cyclones passing to the south of the lake will also generate southerly currents in the Cattaraugus Embayment, but these cyclones are rare, and none occurred during the field period.

With the passage of a cyclone north of the lake the wind generally rotates from south through west to north, e.g. storm of May 8-9 or June 10-12. Quite frequently, the most intense winds during a storm passage blow parallel to the lake axis, i.e. out of the west-southwest or west. The shear stresses at the air-water interface cause a downwind rise in water surface elevation. Because the deep water return flow is ineffective in the shallow Lake Erie (average depth 50 feet), even moderate storms can produce wind tides of many feet at the eastern end of the lake. Hunt (1959) calculates that 25 mph southwesterly winds may generate a 2 to 3 foot lake level rise at Buffalo (the exact value depends on atmospheric stability). A near maximum difference in recorded water levels between Buffalo and Toledo of 13.2 feet occurred during gale force winds on November 3, 1955. NOAA's Lake Survey Center (1973) has published water level diagrams for recent major storms. These show that a seiche of a period of 12-18 hours and a duration of 2-3 days generally follows a major wind tide. The wind tides in the Cattaraugus Embayment are expected to be similar to the ones at Buffalo (Hunt, 1959, Fig. 10, p. 29).

The wind tides observed in the Cattaraugus Embayment during the field

period were not high, and some coincided with flood discharges in Cattaraugus Creek. This made it difficult to determine the exact wind tide because the staff gage is located in the river channel. The high water levels observed in the period May 13 through May 17 (Fig. 52), however, are primarily wind tides. The 12 hour fluctuations in stage probably reflect lake seiches. The .8 foot rise in water level during the strong June 11 storm is solely a wind tide, as the creek discharge did not increase at all.

The existence of significant tides on Lake Erie creates conditions similar to many oceanic shorelines where astronomical tides of a similar range are operative. These short-term fluctuations in water level superimposed on seasonal and long-term water level variations add to the complexity of the harbor entrance sedimentation patterns as discussed below. Furthermore, high wind tides, often coincident with high discharges in Cattaraugus Creek, will raise the downstream control of the river and increase the hazards of flooding in the Sunset Bay area.

6.4. Wave refraction.

The deep water waves approaching the Cattaraugus Embayment refract with a pattern of change dependent upon bottom topography. Wave refraction computations performed by the U. S. Army Engineer District, Buffalo (1966, Plates D-1 and D-2), demonstrate that 7 second waves approaching from the west start refracting at about 50 feet of depth, i.e. 2 miles offshore, and approach the shoreline almost perpendicularly. The shoal extending lakeward between profiles Cat. 2 and Cat. 3 (Fig. 53C) was found to cause a concentration of wave energy flux at about Cat. 3. The wave orthogonals are also in this

Figure 53. A. Location map of the Cattaraugus Embayment.

B. Fetch diagram. Bar lengths are proportional to the fetch length in that direction. Linear scale in arbitrary units.

C. Wave refraction diagram. 4 second waves out of the west-southwest, typical of the conditions responsible for a majority of the sediment transport, were chosen for study. The refraction diagram is constructed by methods outlined in CERC Tech. Rept. No. 4 (1966). Bathymetry is from USGS 15' quadrangle map, with 6 foot contour.

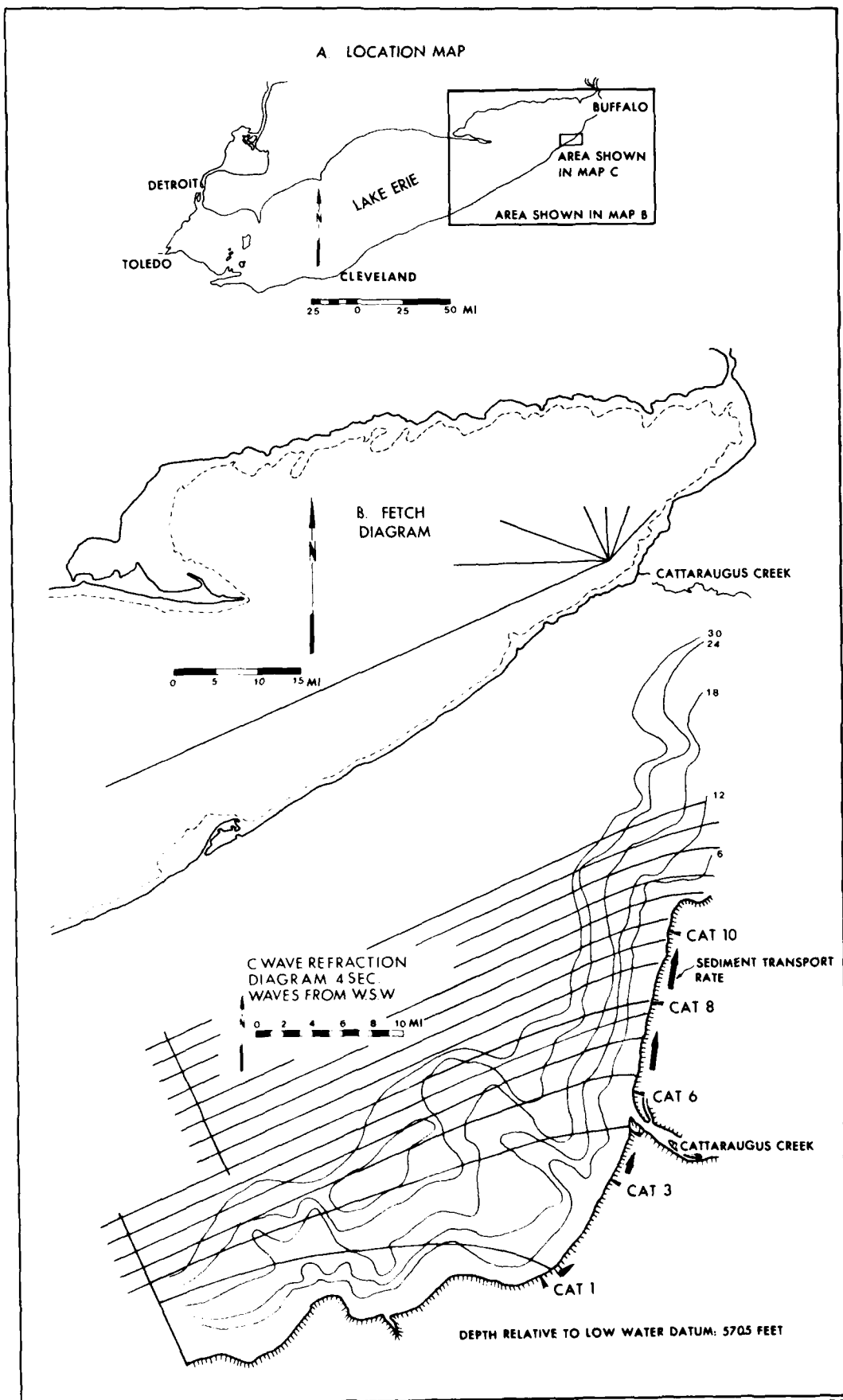


FIGURE 53

case approximately normal to the shore.

Waves of 7 second period or more out of the west, however, account for only a small percentage of the total annual wave energy flux. Furthermore, their high refraction coefficients make these waves relatively inefficient in longshore sediment transportation. Most efficient are probably the 3 to 5 second waves which occur for a much higher percentage of time and approach the shoreface at a steeper angle because they are subject to less refraction.

To determine a typical pattern of process variability and sediment transportation within the Cattaraugus Embayment, wave refraction was performed on 4 second waves approaching the embayment from the dominant direction, west-southwest. The surface wave rays were traced in accordance with the method outlined in Coastal Engineering Research Center, Technical Report No. 4 (1966, p. 65-67).

Significant wave refraction begins at a depth approximately equal to half of the wavelength. Consequently, the 30 foot contour was chosen for beginning refraction in this study. The principal result of this wave refraction study (Fig. 53C) is the uneven distribution of wave energies along the shoreline of the Cattaraugus Embayment. The steep lake bottom slope off the northern beach causes a relatively small wave refraction, whereas the extensive shoals off Silver Creek cause high divergence of the wave energy flux approaching the southern section of the shoreline. The angle between the arriving wave rays and a line orthogonal to the beach is high at Cat. 8 through Cat. 10 and near Cat. 1, in the former case because of relatively little refraction, in the latter because of the westerly curvature of the beach. At the central section of the embayment, the waves are expected to approach shore

almost perpendicularly. The rate of littoral sediment transportation is a function of the product of the wave energy flux and the approach angle. The wave refraction diagram, therefore, predicts that for a moderate storm from the west-southwest a relatively high transport rate exists at the northernmost beach, a low rate at the central section, and an intermediate rate in the Hanford Bay area. The relative length of the solid arrows in Figure 53 intends to portray this pattern.

A wave refraction pattern for a northeasterly storm has not been determined yet, but the process variability within the embayment is expected to be much less because the Silver Creek shoals will play no significant role.

6.5. Observed process variability in the embayment.

Data on longshore current velocity, angle of breaker crest relative to shore, and period and height of the breaker were obtained on a daily basis at six stations representing the entire embayment. The data are tabulated in Appendix II, and the station locations are shown in Figures 53C and 54.

For the three westerly storms studied in detail, May 14, May 24, and June 11, a repetitive pattern is observed (Fig. 54). The angle of wave incidence is relatively high (10-15 degrees) at Cat. 1 and from Cat. 8 to Cat. 10. At Cat. 3, 5, and 6 the waves approach almost perpendicularly to shore. Invariably, the waves are higher on the northern beach than on the southern. An unexpectedly high value was observed at Cat. 6 on June 11.

The consequent variability in longshore current velocity follows closely the general pattern of sediment transport rates outlined in paragraph 6.4. The highest current velocities are observed at the northernmost part of the beach, low current velocities are observed near the creek mouth, and intermediate

Figure 54. Process variability in the Cattaraugus Embayment. For each of the six stations monitored three process parameters are shown. Wave height is proportional to the length of the onshore arrow, angle of approach is the angle between the orthogonal to the shoreline and the wave ray, and longshore current velocity is proportional to the length of the arrow parallel to shore. Three southwesterly storms and one northeasterly storm are shown.

- A. May 13, 1974. Southwest storm.
- B. May 19, 1974. Northeast storm.
- C. May 24, 1974. Southwest storm.
- D. June 11, 1974. Southwest storm.

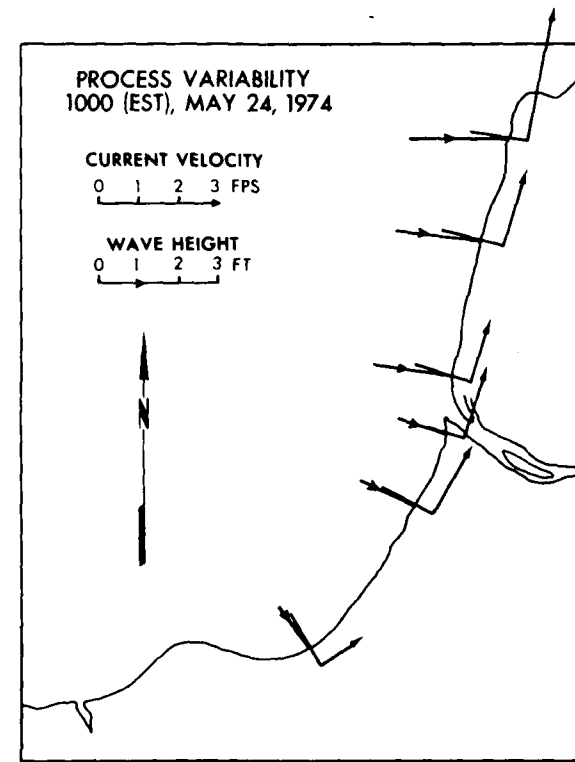
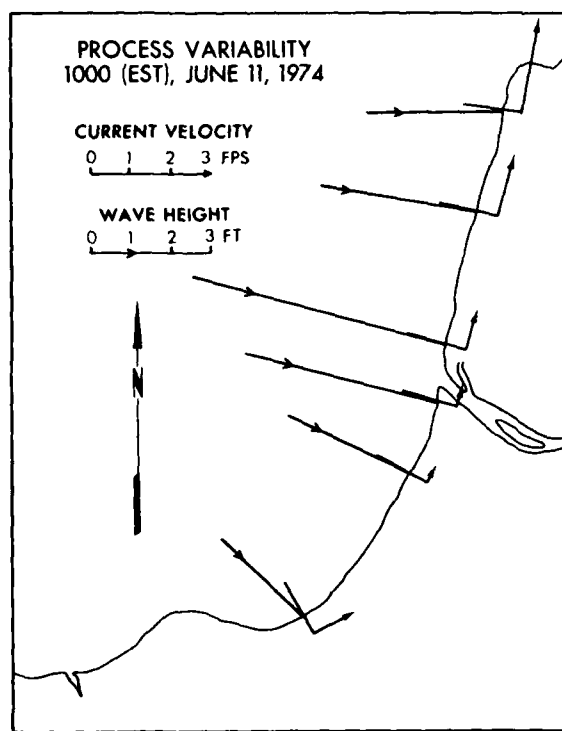
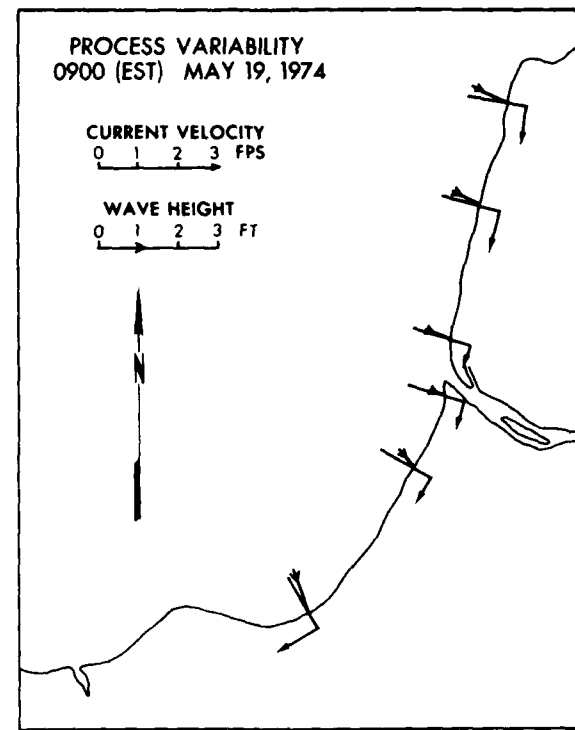
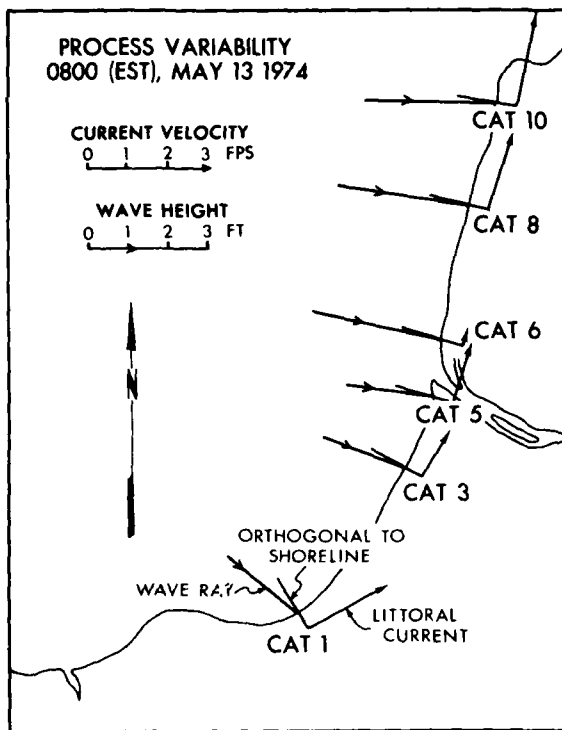


FIGURE 54

velocities are observed in Hanford Bay (Cat. 1). In the application of these data in the structure design (paragraph 10) it will be assumed that, to a first approximation, the rate of sediment transportation is related directly to the longshore current velocity, as has been suggested (Komar, 1971).

Although it is possible at this stage to proceed with a quantitative estimation of volume rate of littoral sediment transportation, this has not been performed. It is our firm belief that the relatively poor state-of-the-art of sediment load computations is likely to produce results that might be orders of magnitude wrong. Consequently, a numerical value of sediment transport rates might introduce bias into the assessment of factors relevant in the structure design.

Surface suspended sediment samples were obtained during the storm of June 11, 1974. The determined sediment concentrations are listed in Appendix VII.

No significant flood was observed in Cattaraugus Creek during the field period. Data which would be meaningful in a quantitative estimate of fluvial sediment supply, therefore, were not available. Suspended sediments were sampled with a depth-integrated sampler (DH-48) during a moderate flood in May, 1974. The data are presented in Appendix VII B, for comparison with the surf zone sediment concentration data.

7. SEDIMENT SOURCES AND DISPERSAL PATTERNS

7.1. Sediment sources.

Potential sources for the sediment on the beach or in the nearshore of the Cattaraugus Embayment include: 1) Cattaraugus Creek, 2) Silver Creek headland and pocket beaches beyond, 3) Lotus Point and pocket beaches beyond, and 4) offshore sources. To evaluate, independently of the collected process data, the relative importance of each of these sources, the characteristic lithologies of each of the sources were compared to the lithologic composition of the beach gravels.

1) The Cattaraugus Creek drainage basin includes late Devonian and younger shales, siltstones, and sandstones (Tesmer, 1963). From Versailles to upstream of Gowanda the river has cut a gorge, many hundred feet deep, into the Gowanda Shale (Plate 1). This shale is adequately represented on channel bars in the gorge. Because of its loose consistency, however, it does not survive long distance transport. The point bars immediately downstream of the gorge (Plate 2), therefore, are characterized by a very high percentage of siltstone, derived from thin silt beds within the Gowanda Shale, and red sandstone, possibly from outcrops of the Medina Sandstone. Granite and other crystalline rock fragments, as well as quartzite and some chert, are derived both from till units and ancient beaches representing post-Wisconsinan high stands of Lake Erie (Hough, 1958). These components contribute about 80 per cent siltstone and sandstone, 10 to 15 per cent crystalline rocks, and a few per cent dark shale to the gravel bed material of the stream.

Sampling of the lower reaches of Cattaraugus Creek, between the last point bar at the U. S. 20 bridge and the lake, was done only on a reconnaissance basis, with about 20 samples obtained. This sampling demonstrated that gravel of the size and composition typical of the upstream point bars exists on the bottom throughout the lower channel. The gravel was buried by a few inches of mud during summer slack water in the river. Floods of a few thousand cfs, however, are probably capable of moving this material. It is concluded that Cattaraugus Creek is a prime contributor of siltstone, sandstone, and crystalline rock fragments to the embayment and its beaches.

2) The upland drainage basin of Silver and Walnut creeks, draining into Silver Creek Bay, is much smaller than the Cattaraugus Creek watershed. There are two other important differences. First, Silver and Walnut creeks are cut deeply into the Hanover Shale (Tesmer, 1963) practically all the way to their mouth, in contrast to Cattaraugus Creek, which flows through a broad alluvial valley. Second, the creeks cut through the highly resistant Pipe Creek member of the Hanover Shale, a black shale unit which can survive long distances of littoral or fluvial transportation. In contrast to the mouth of Cattaraugus, therefore, the mouth of Silver Creek and the adjoining pocket beach are dominated by shale, predominantly dark shale (Appendix III, Fig. 55B). The Pipe Creek Shale also outcrops all along the Silver Creek headland west of Cat. 1. From the top of the 20-30 foot vertical shale cliff, about 10 feet of till contributes various crystalline rock fragments, quartzite, and chert into the littoral drift system of the Cattaraugus Embayment.

3) The shale cliffs of Lotus Point are lower and much less extensive than

Figure 55. A. Lithological variations in Cattaraugus Beach gravel. Data based on pebble counting of the active berm and high-level storm berms at each sample station. The lithologies are grouped in categories representative of the sources.

B. Characteristic lithologies of the source materials. Silver Creek headland and the embayment supply black resistant shale derived from the Pipe Creek member of the Hanover Shale. Cattaraugus Creek supplies predominantly siltstone and sandstone, and till-units and high-level beaches supply crystalline rock fragments.

LITHOLOGICAL COMPOSITION OF GRAVEL
ON CATTARAUGUS BEACHES

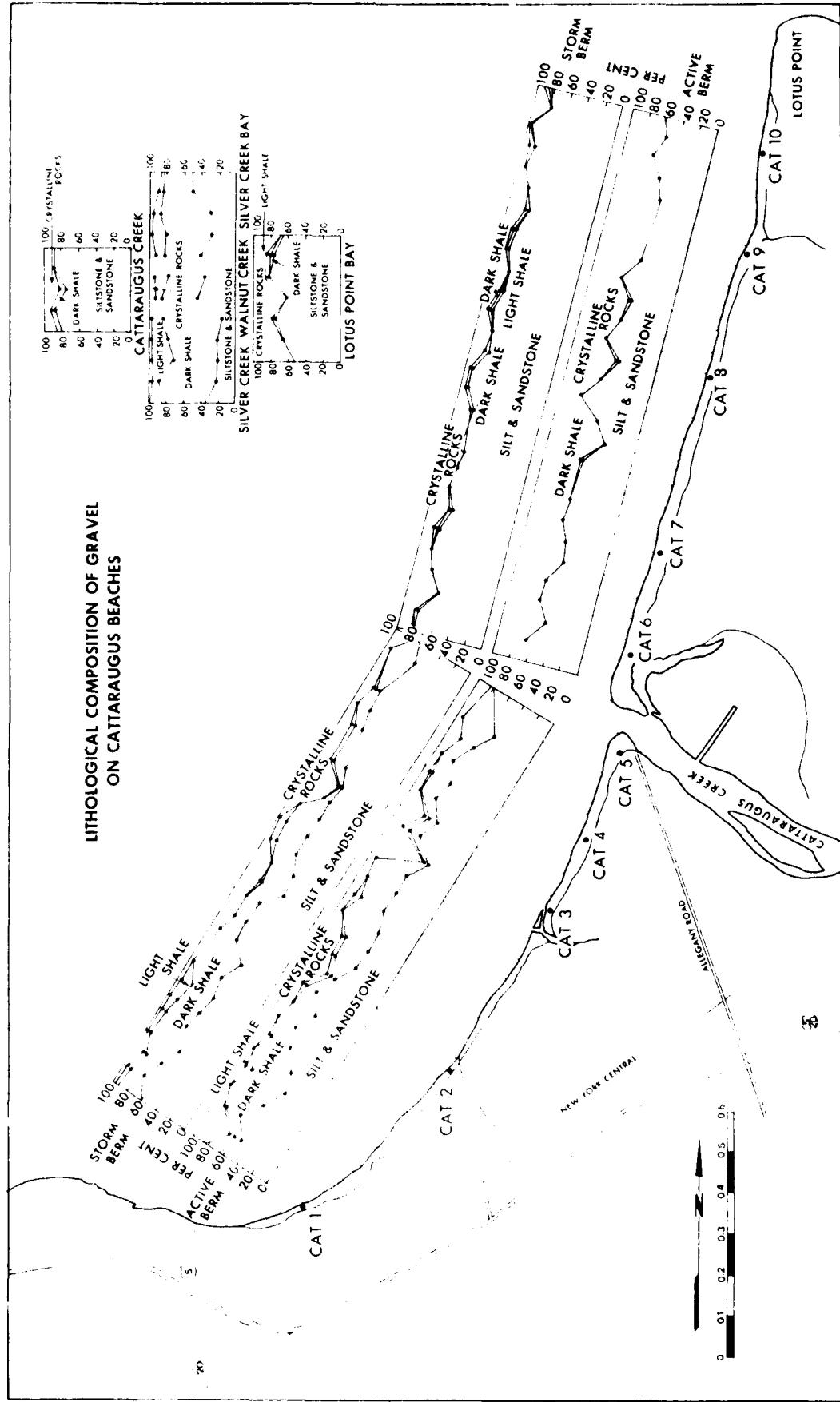


FIGURE 55

the Silver Creek headland. Furthermore, the dark and resistant Pipe Creek member of the Hanover Shale is not exposed at this locality because of the southerly dip of the strata. Consequently, Lotus Point plays an insignificant role in the overall sediment budget of this section of the lake shore.

A shallow (0.5-2 ft deep) gravel bench follows the base of the Lotus Point cliffs all around the headland. Currents of up to 2-3 fps moving north and east around the headland were measured during westerly storms generating 3-4 foot waves at the cliff base. Clearly, this current is fully capable of moving gravel from the northernmost beach of the Cattaraugus Embayment around the point and into Lotus Bay. It is to be expected that the pocket beaches at Lotus Point (Plate 3) and Lotus Bay have the lithologies typical of the north Cattaraugus beach, i.e. 60-80 per cent siltstone and sandstone, 15-40 per cent crystalline rocks and a minor fraction of shale, both dark and light.

4) The contribution from offshore sources is difficult to assess, but it is expected to be small for the following reasons. The only gravel deposit in the embayment is just off the mouth of Cattaraugus Creek (Fig. 57A) and is clearly fluvially supplied. Second, the generally fining offshore sequence from coarse (or medium) sand into lake muds seems not to favor any significant landward sediment transport. Third, there is no observed gravel lithology or sand minerals on Cattaraugus beach which cannot be accounted for by the sources already discussed.

With this knowledge of source materials and locations, the sediment distribution on the Cattaraugus beach and in the embayment should now tell the general pattern of sediment dispersal.

7.2. Beach sediments.

Lithology and texture of the beach sediments were analyzed with the hope of detecting trends that would lead to discovery of dominant transport patterns. The lithological variations in the Cattaraugus beach gravels are tabulated in Appendix III and graphically displayed in Figure 55A. The texture of the beach sediments together with an explanation of the methods used in sampling and computation are listed in Appendix IV and graphically displayed in Figure 56.

The lithological composition of the berm active on the day of sampling or of a high level storm berm was based on a determination of the lithology of each clast which fell exactly on each 20 centimeter mark on a 10 meter long tape laid parallel to the berm crest. Thus, 50 clasts at each berm were sampled at 55 sample stations spaced about 250 feet apart along the entire beach.

The lithological pattern on the Cattaraugus beach shows an interesting relationship to the lithologies of the creek derived material and the lithologies of the western source areas, Silver Creek and Silver Creek headland. The percentage of dark shale at the southern portion of Cattaraugus beach, about 40 per cent, is just a little higher than at the northernmost part of Silver Creek beach, where black shale accounts for 30 to 40 per cent of the gravel. This black shale decreases in significance northward to less than 5 per cent at Cat. 5. Two interesting minima exist at the southern beach. At about Cat. 2 and Cat. 3, the black shale percentage drops to less than five. The crystalline rock category reaches maxima at the same two locations. The

Figure 56. Texture variations in Cattaraugus Beach gravels. The gravel percentage refers to the areal coverage of gravel measured along a narrow strip from the step to the seawall or dune ridge. Typical gravel size measures the size of the most dominant fraction (primary mode) within each homogenous zone on the beach. See Appendix IV for details.

TEXTURE VARIATIONS OF CATTARAUGUS BEACHES

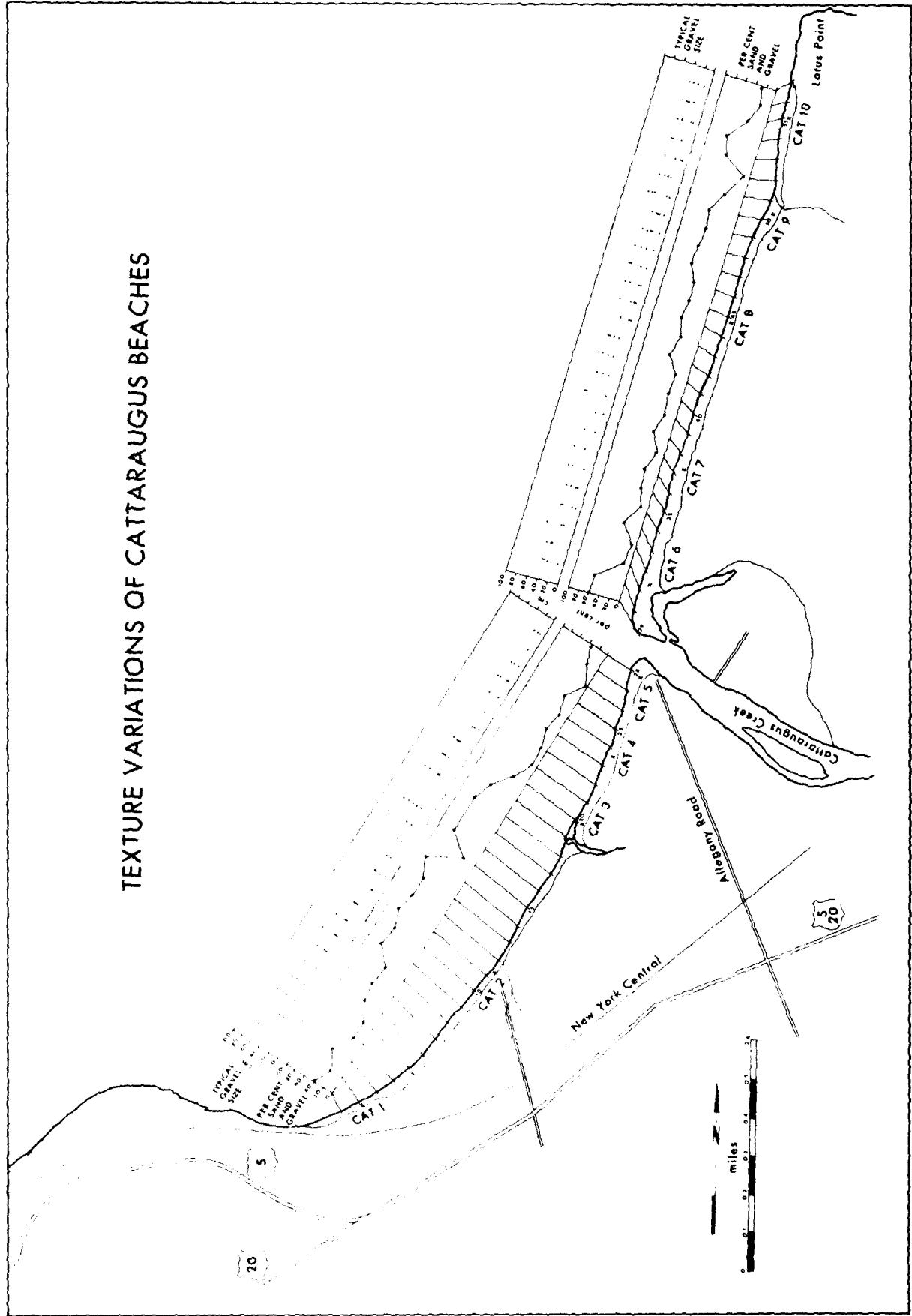


FIGURE 56

siltstone plus sandstone fraction is high all along the beach and reaches its most dominant proportion, about 80 per cent, near the mouth of Cattaraugus Creek.

On the section of beach north of Cattaraugus Creek, the black shale is all but gone, the sandstone plus siltstone fraction remains as high as to the south, and the crystalline rock fraction is very dominant, accounting for 40 to 60 per cent of the total gravel population.

The high level storm berm shows the same general pattern, but the siltstone plus sandstone fraction remains higher throughout. The storm berms sampled undoubtedly represent different time units at different sample stations. Therefore, whether one samples a time unit, as in the case of the active storm berm, or time-transgressive units, as in the case of the multiple storm berms, the pattern remains essentially the same. The sediment, accordingly, represents the long-term average of the processes which have brought it to its sample location. Correlation between the transport patterns derived by process measurements and by lithologic analysis, therefore, provides the best test of the long-term representativeness of the obtained process data.

The sediment patterns described above strongly suggest a dominant transport northward from the Silver Creek headland towards Cattaraugus Creek and further northward towards and past Lotus Point into Lotus Bay. Apparently, shale fragments of gravel size do not pass the creek mouth, but sand undoubtedly does. Cattaraugus Creek is an important source of materials for both the northern and southern beaches, although the largest amount of fluvial sediment feeds the northern beaches. During occasional reversals in transport

direction, fluvial material is brought south and ultimately reaches Hanford Bay (Cat. 1). Because of the sheltered location for storms from the west, this area tends to be one of net shoreline accretion. There is no evidence that Lotus Point adds any sediment to the system. During periods of southerly transport, however, local redistribution of sediment on the north beach occurs, causing a net southward displacement of the entire sediment population. Under natural conditions with unrestricted wave impact on the entire north beach, this displacement is quickly reversed during the next westerly storm. The net displacement has to be northward, because there is no northerly sediment source!

The evidence contained in the textural composition of the beach sediments (Fig. 56) is more difficult to interpret. The texture at any one station is a function of the typical wave energies at the station, the distance of transport of the different sediment fractions, and the resistance of each fraction to mechanical attrition. To separate out one of these factors and try to interpret its variability from the aggregate data is difficult. However, some observations seem to be valid. The gravel percentage is relatively low at Cat. 1, increases to a high of 80 per cent at Cat. 2, stays high to about Cat. 3, and then decreases rapidly to the mouth of Cattaraugus Creek. The northern beach shows less dramatic variation in gravel percentage. It is relatively low from Cat. 6 to almost Cat. 8, then remains relatively constant at 40 to 50 per cent to Lotus Point, with the exception of the drop to 10 per cent at the wide beach associated with the creek north of Cat. 9.

The most obvious correlation with gravel percentage is beach width.

The narrow beaches are found between Cat. 2 and Cat. 3 and relatively narrow beaches at about Cat. 8 (Plate 4). At some of these locations the beach face terminates directly at a seawall. With no back beach present, there is no room for sand storage. The narrow beaches consist solely of gravel berms.

Basically, the factor just discussed is the wave energy. The pattern resulting from another important factor, distance from source, is superimposed on the wave energy pattern. The only clearly recognizable trend here is the low gravel percentage between Cat. 3 and the mouth of Cattaraugus Creek, reflecting the high sand supply to this segment of the beach.

7.3 Nearshore sediments.

Bottom sediments were sampled by a modified Petite Ponar grab sampler¹ at about ten locations on the extension of each beach profile line between the swash zone and the 20-foot contour. A theodolite, positioned at the adjacent beach profile location, determined the boat position at each sample station. The samples obtained were bagged, numbered and subjected to granulometric analysis at the University of South Carolina sedimentation laboratory. The sand fraction was analyzed in a settling tube (Anan, 1972). The less than 62 μ fraction was wet-sieved off the original sample and subsequently subjected to pipette analysis (Folk, 1968).

The resultant size distribution pattern is shown in Figure 57A. An inset map of the embayment bathymetry is included for reference (Fig. 57B).

¹The modified grab retains all fine materials within the sample during transport through the water column.

Figure 57. A. Distribution of sediment sizes in the nearshore of the Cattaraugus Embayment. Bottom sediment samples were collected by a Petite Ponar grab sampler along the extension of each beach profile at ten evenly spaced sites between the shore and the 20 foot depth contour. The textural composition was subsequently determined in the laboratory by settling tube and pipette analysis of the sediments.

B. Bathymetry of the Cattaraugus Embayment. Data from USGS 7.5" sheet, Silver Creek Quadrangle.

A. NEARSHORE SEDIMENT DISTRIBUTION
JUNE 1974

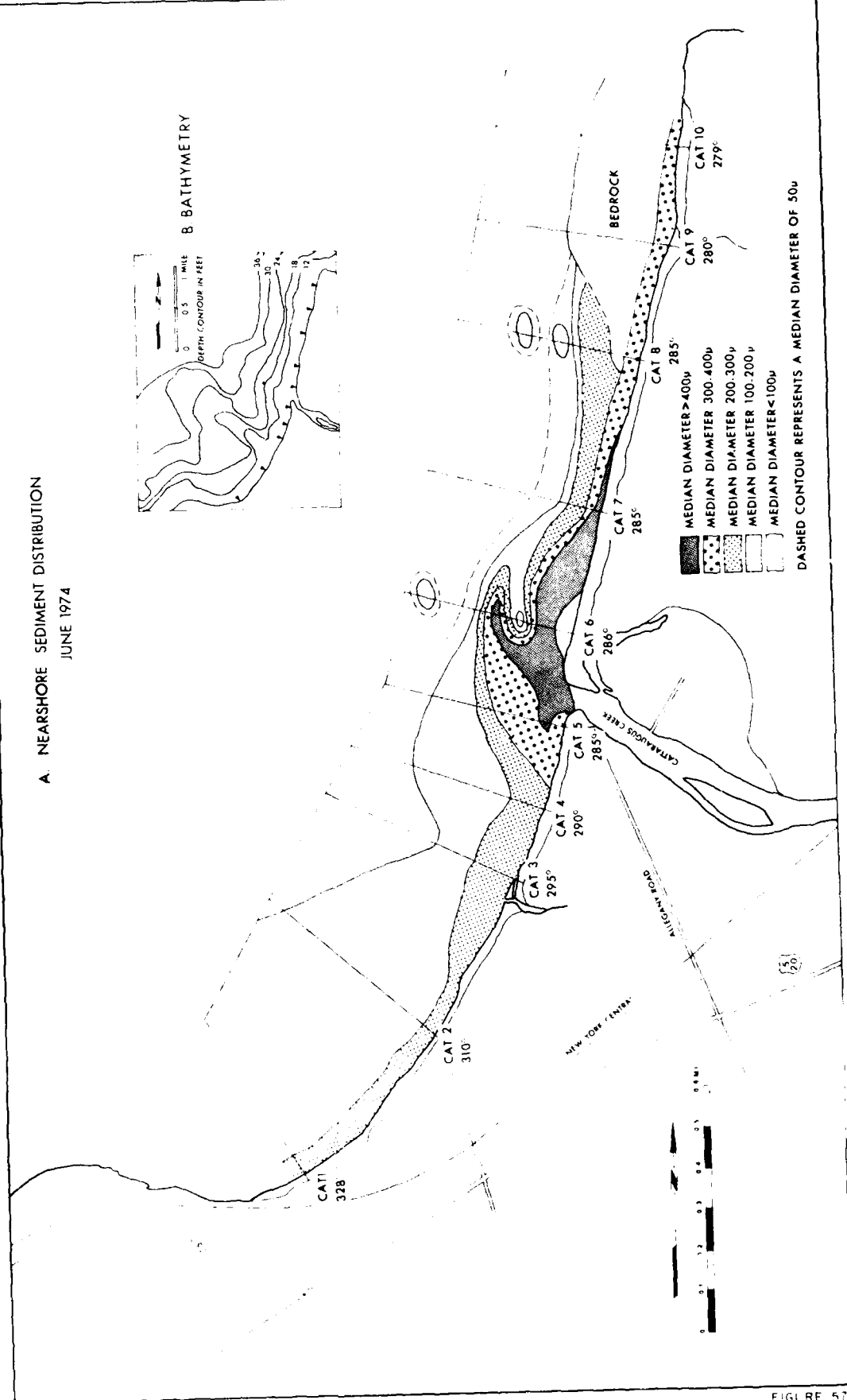
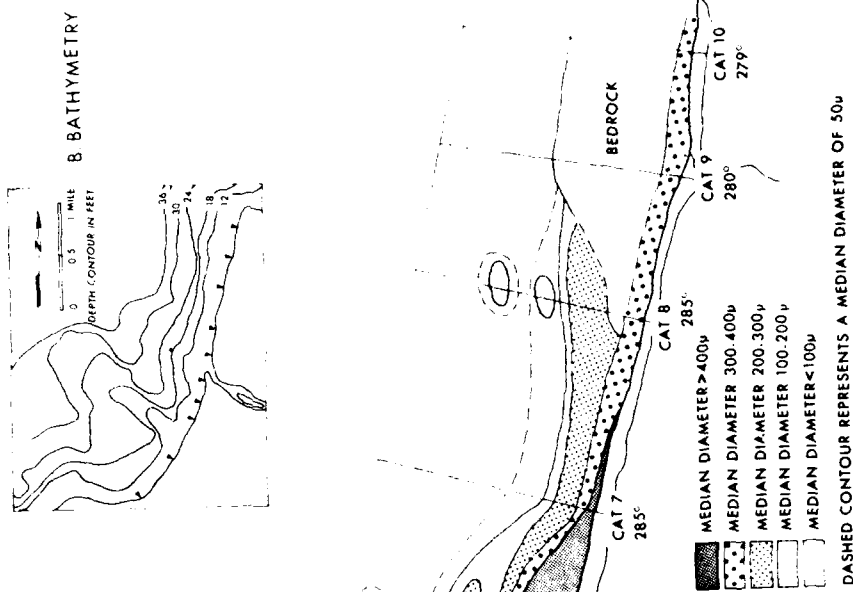


FIGURE 57

The overall trend is a fining offshore sequence from medium sand near shore to lake muds with a median diameter in the coarse silt range characterizing the bottom at the 20 foot depth contour. Great variations in this generalized pattern can be observed. A coarse sediment bulge, deflected to the north, characterizes the lake shore near the mouth of Cattaraugus Creek. Part of this bulge is a major gravel bar trending northwest or north across the creek mouth as a continuation of the southern beach. The nature of this bar will be analyzed in detail in a subsequent section.

At the time of sampling low river discharge and low wave energies had prevailed for about two weeks. Fine grained sediments, generally transported further offshore, had, therefore, been deposited on the lakeward side of the "delta" front. These fines probably form a continuum into the zone of similarly sized materials extending northward parallel to the shore.

The steep gradient of the northern lake bottom is associated with a much more rapidly fining offshore sequence than the flat bottom of the southern embayment.

The distribution pattern of the nearshore sand is somewhat easier to interpret than the beach gravel pattern. Wave energy and directions of the wave generated currents are the controlling factors. Kinetic wave energy, to a first approximation, is a function of water depth. Low wave energies and consequent finer sediment accumulations are associated with the deeper parts of the embayment. Note, for example, the close correlation between the 100: size contour and the 18 foot depth contour (Figs. 57 A and B).

The deflection of the coarse sediment bulge demonstrates the net northward

flux of wave energies capable of transport of gravel and coarse sand. Sand is also transported southward, as the Cattaraugus Creek must have been the ultimate source of the sand in Hanford Bay. The sand must be transported southward close to shore and spread out onto the shallow platform of Hanford Bay, because no sand transport is possible across the steep, north facing escarpment extending lakeward between Cat. 2 and Cat. 3.

8. COASTAL MORPHOLOGY

8.1. Beach profiles.

The shoreline morphology is a direct function of 1) wave energy distribution, 2) nature and quantity of sediment supply, and 3) littoral processes of sediment transportation. In the preceding paragraphs these factors have all been analyzed in some detail. Here we present shoreline morphological data that demonstrate the response of a natural unmodified beach to the dominant littoral processes.

Three sets of morphological data were collected during the field period: 1) beach profiles, for monitoring of changes in beach width, steepness, and micromorphology; 2) maps of the active spit at the south bank of Cattaraugus Creek, for determination of shape and rate of growth; and 3) maps of sediment waves on the northern beach, to delineate their pattern of movement, if any.

Ten profile stations were established along Cattaraugus beach. The profiles were measured bi-weekly except during the first week of June, when wave action remained insignificant for a week. The profiles were measured by a procedure established by Emery (1961). All the recorded profiles are presented in Appendix VI. Profile locations, labeled Cat. 1 through Cat. 10, are shown on most of the preceding maps.

The most noticeable trend in beach character is the drastic steepening of profiles just north of Cattaraugus Creek. Figure 58A shows the profiles at Cat. 5 and Cat. 6 superimposed for May 10 and during the storm on June 11. More typical for the north and south beaches, respectively, are profiles Cat. 7 and Cat. 3, superimposed for the same two days in Figure 58B. Plates 5 and 6 show ground photographs of the two profiles during and after the June 11 storm.

Figure 58. A. Beach profiles Cat. 5 and Cat. 6 superimposed for May 10 and June 11.

B. Beach profiles Cat. 3 and Cat. 7 superimposed for May 10 and June 11.

In both figures the profiles are adjusted to the same water level for easy comparison of steepness. The steep profiles of the northern beach as compared to the southern are apparent, as is the abrupt steepening of the northern beach during the June 11 storm.

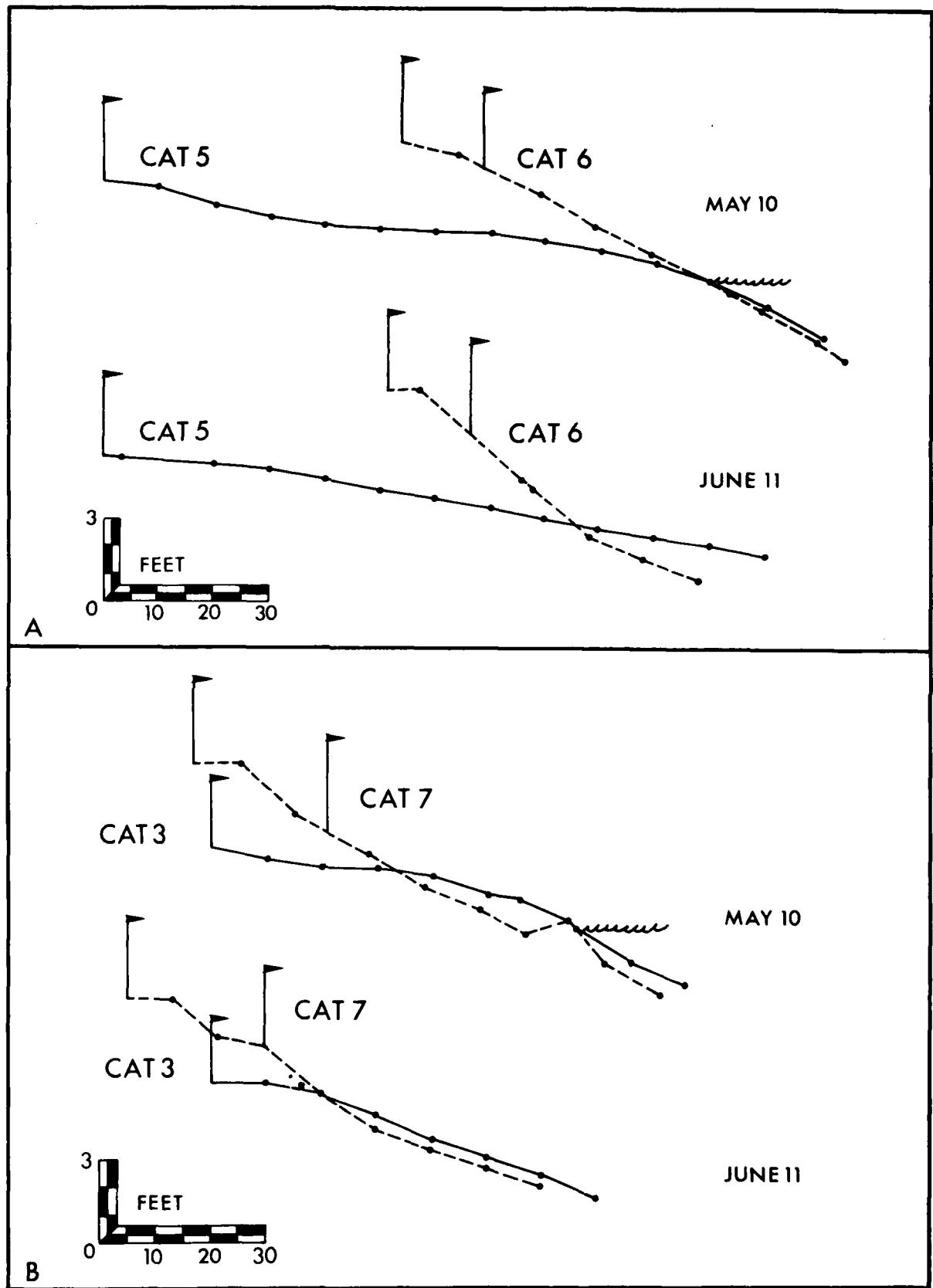
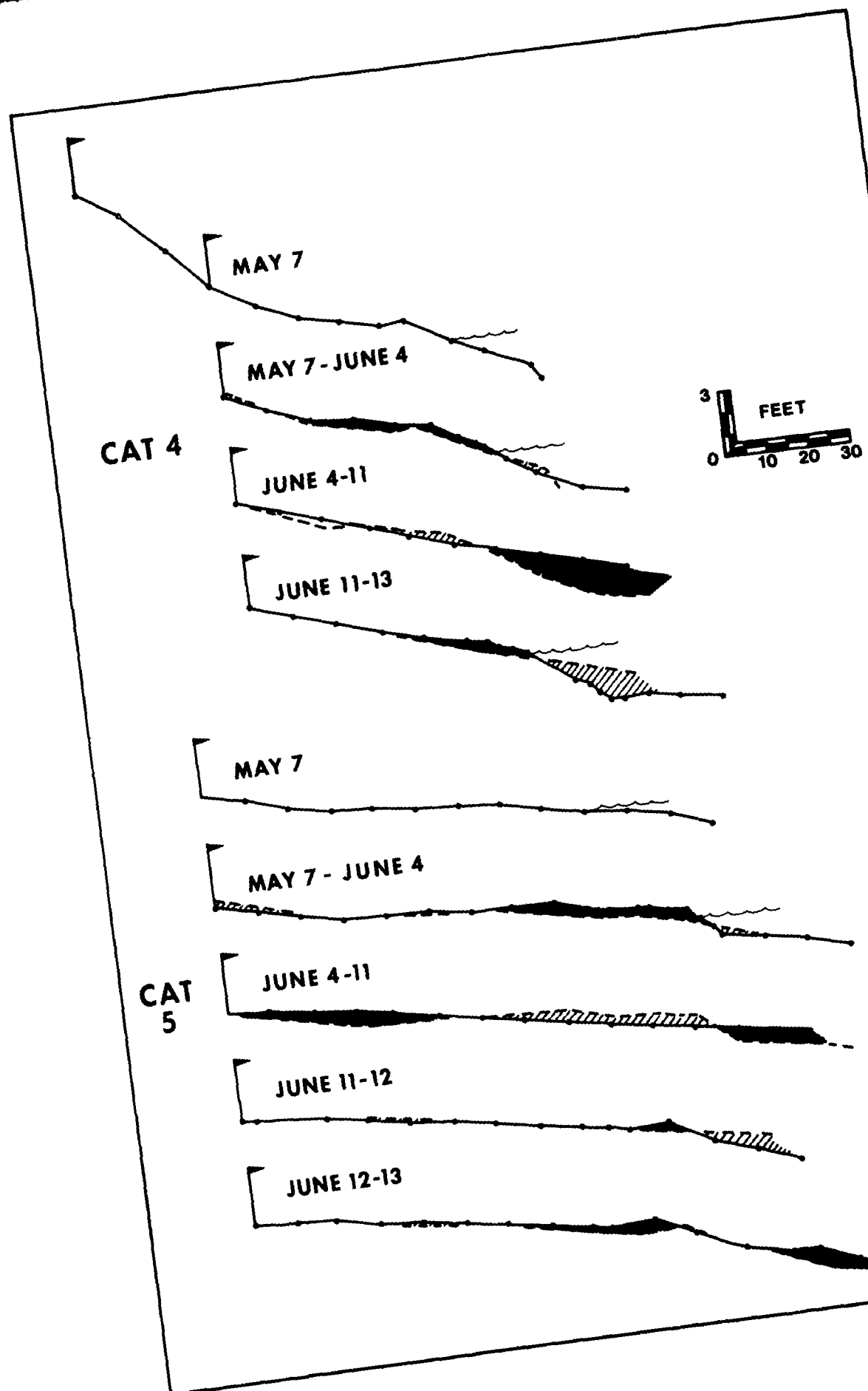


FIGURE 58A AND B

The higher wave energies affecting the northern beach because of the steeper lake bottom profile are thought to be the prime factor causing this difference. Two of the beach profiles, Cat. 4 and Cat. 5, demonstrate significant lateral accretion during the field period (Fig. 59). Upon a close examination of the beach profiles, supplemented by observations while in the field (Plates 7 and 8), this lateral accretion was found to result from the landward migration of nearshore sand bars during constructional wave conditions. During destructive wave conditions the accreted berm is eroded, and the sand is temporarily stored in the nearshore.

The theory has been suggested (Dyhr-Nielsen and Sørensen, 1970) that waves breaking on the nearshore sloping plane will generate secondary bottom currents directed towards the breaker line. This will have an accumulating effect on the sediment particles, moving them towards the breaker line where they build up a bar. Offshore of the bar the current is directed landward; inshore it is directed seaward. The bar height is controlled by maintenance of an equilibrium between the amount of sand transported upward by bottom currents and the amount of sand returned in suspension at the bar crest. "Constructional" waves are those that pass the bar without breaking, causing a net shoreward current. This onshore current erodes the bar crest and provides the beach with material for accretion. The close interaction between sediment transportation and deposition on the nearshore bar system and the beach has been recognized both on oceanic shores (Hayes, 1972) and the shorelines of the Great Lakes (Bajorunas and Duane, 1968; Davis, et al., 1972). The fact that shallow water sand bars exist just south of the mouth of

Figure 59. Beach profiles Cat. 4 and Cat. 5 on May 7, June 11, June 12, and June 13. Each profile has the preceding one superimposed. The dark pattern shows deposition and the light pattern shows the erosion which has taken place in the time interval. Note the characteristic pattern of beach profile change associated with the storm of June 11: deposition on the back beach, erosion of the gravel berms, deposition and progradation at the step.



Cattaraugus Creek might create additional shoaling problems between the planned harbor breakwaters, both because of the potential lakeward displacement of the bar(s) as a consequence of the erected breakwaters and the high rate of littoral suspended sediment transportation over the bar crest. The severity of the problem will be discussed in the comprehensive structure analysis below.

The dramatic change in beach profile during a moderate storm, like the one observed on June 11, illustrates the very transient nature of the micromorphology of the beach. Because long-term changes are composed of a convergent sequence of almost instantaneous fluctuations, a proper understanding of the dynamics of destruction of a beach during a storm and its post-storm recovery is essential. Figure 59 shows the alterations at Cat. 4 and Cat. 5 during and after the storm. Figure 60 shows similar changes at the steep Cat. 6 profile and the gently sloping Wide Beach at Cat. 10.

The typical pattern of change during the early erosive phase of the storm consists of 1) erosion of the berms with 2) subsequent deposition of the gravel on the lakeward side of the step, causing its progradation, and 3) the deposition of some variable amount of sand on the back beach. The net effect is to smooth the entire beach profile by eroding the central portion (berms) and depositing sediment at the lakeward and landward portions. Gravel is totally removed from the beach face because of the vigorous upper flow regime conditions within the extensive swash zone (Fahnestock and Haushild, 1962).

The swell, which characterizes the waning stages of a storm, typically is constructional. Because of the relatively high waves, often superimposed on a substantial wind tide, the first set of recovery berms is generally

Figure 60. Beach profiles Cat. 6 and Cat. 10 on May 10, June 4, June 11, June 12, and June 13. The pattern of erosion and deposition is similar to the previous figure. Note the enormous erosion at Cat. 6 from May 10 through June 11.

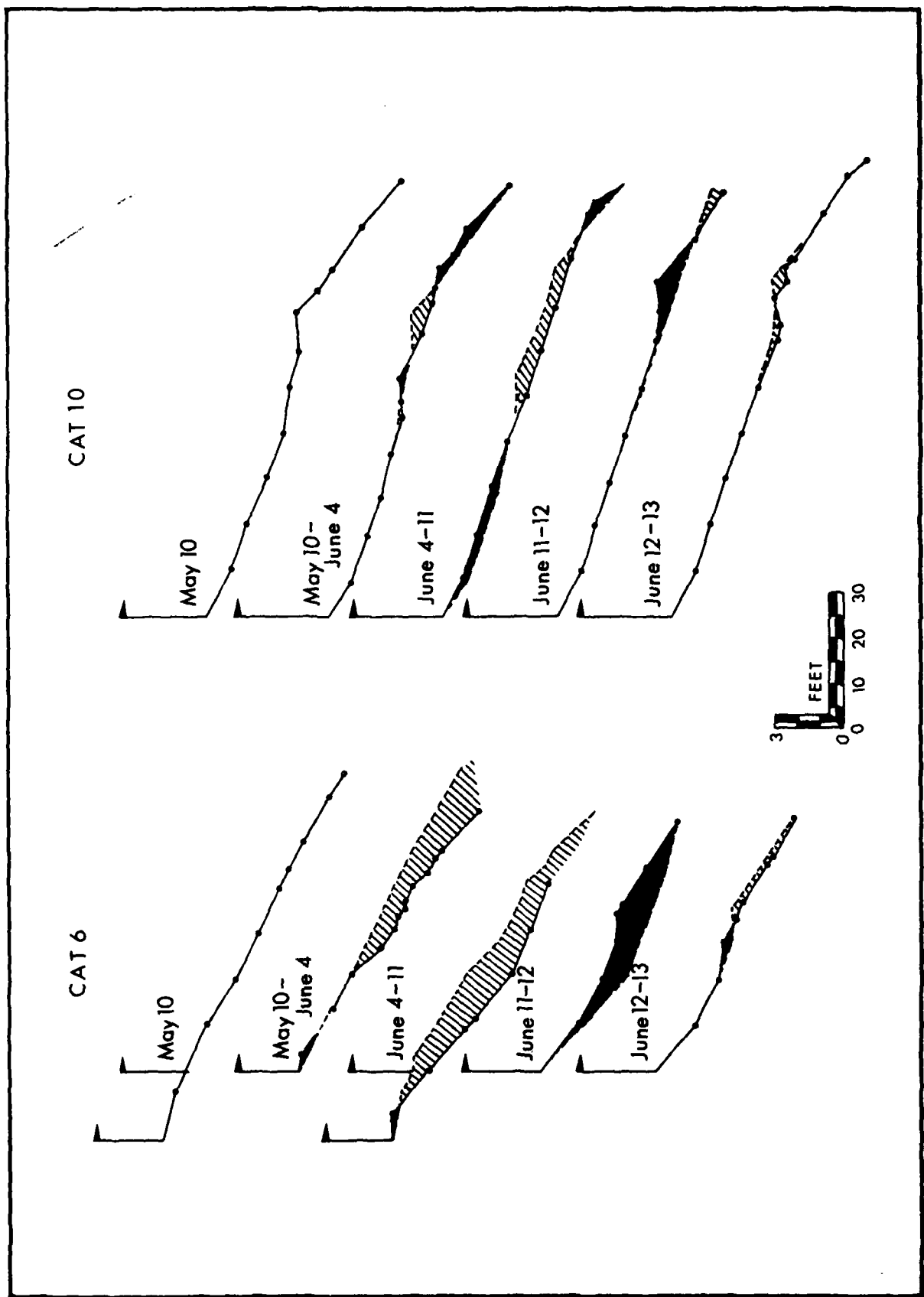


FIGURE 60

formed high on the beach face, with additional berms forming lower down in response to falling lake level and reduced wave height. Note, for example, at Cat. 3, Cat. 8, and Cat. 10, how the initial berms forming on June 12 were replaced by high level and low level (active) berms on June 13 (Appendix VI).

8.2. River mouth spits.

Figures 61 and 62 show the changes in spit morphology between May 10 and June 6, 1974. The changes in the Brant spit (north side of creek) were minor except for the alteration of some low level gravel berms. Because the zone of drift reversal is located between the creek and Cat. 6 during southwesterly storms (Fig. 53C), sediment supply to the Brant spit was very limited during the observation period.

The Hanover spit (south side of creek) shows rapid morphological changes in response to a changing wave power / stream power ratio. The most noticeable trend from May 10 to June 6 is a growth in spit size, while its alignment remains essentially that of the south bank of the creek. This is thought to reflect the prevalence of constructive wave conditions coinciding with low summer discharge in Cattaraugus Creek, i.e. a dominance of constructive wave power.

The location of a spit slip face is a reliable indicator of short-term sediment transport patterns. The presence of a slip face on the channel side of the Hanover spit on three of the four maps (May 10 and 28, June 6), therefore, demonstrates a net sediment flux from south to north across the spit. This transport pattern shows that littoral sediment transportation is primarily responsible for the development of this spit. On May 18, a few days after

Figure 61. Planimetric maps of the Hanover spit (south side of Cattaraugus Creek). The maps, made by theodolite from a land base on the left bank, show the significant features on the subaqueous portion of the spit, the crest, the slip faces, and the outline of the bar margin. Note the change in slip face location from the lake side to the channel side between May 18 and June 6.

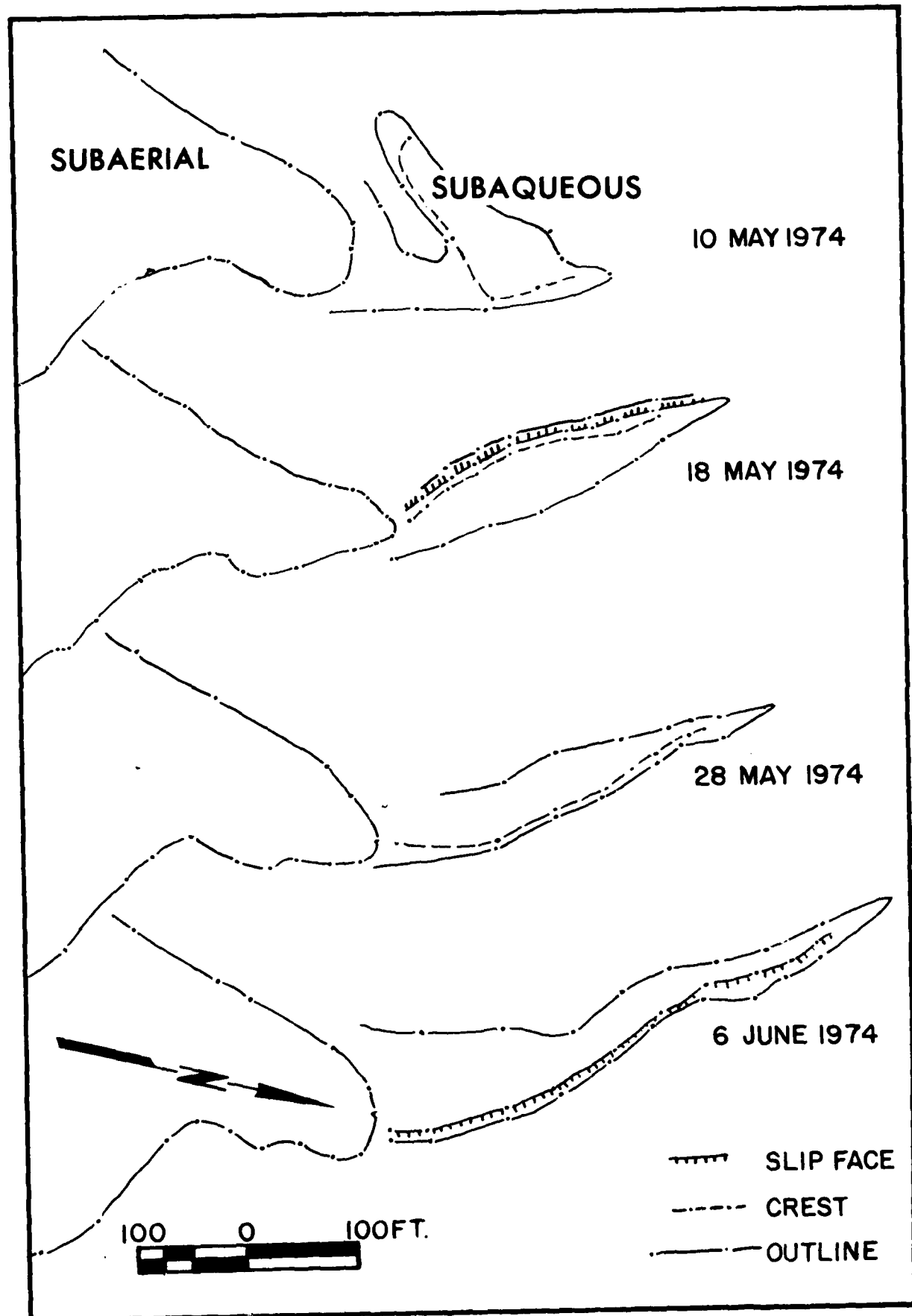


FIGURE 61

AD-A102 282 STATE UNIVERSITY OF NEW YORK COLL AT FREDONIA DEPT 0--ETC F/6 8/8
CATTARAUGUS CREEK HARBOR, NEW YORK GENERAL DESIGN MEMORANDUM, P--ETC(U)
MAR 76 DACW49-74-C-0118

UNCLASSIFIED

NL

3 in 5
AD 3412787

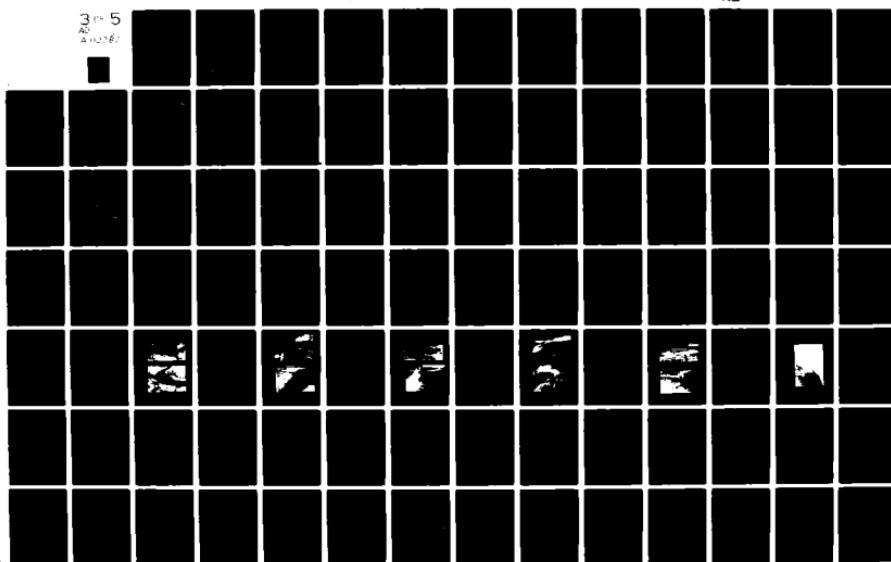


Figure 62. Planimetric maps of both the Brant and the Hanover spits. The Brant spit is all subaerial and shows insignificant change during the time period of observation.

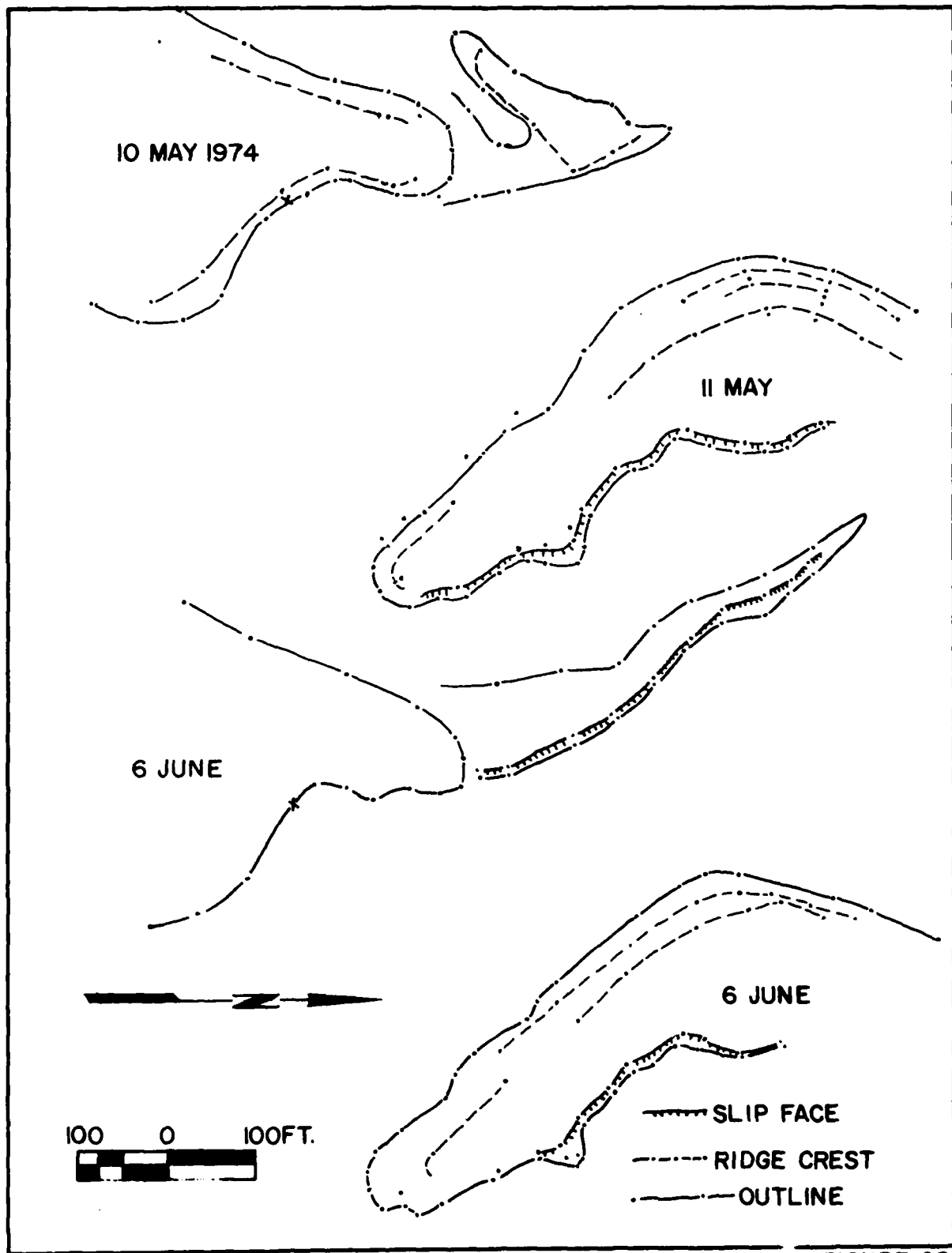


FIGURE 62

a moderate flood in Cattaraugus Creek (see process data in Fig. 52), the spit slip face was found on the lake side, attesting to the temporary reversal in net sediment flux as a consequence of increased stream power.

The significance of this sediment transport pattern in the engineering analysis of structure design will be apparent in the discussions presented in paragraph 10.

8.3. Protuberances.

Aerial photographs of the Cattaraugus beach show a series of more or less sinusoidal sand waves of an amplitude of 20 to 30 feet and a wave length of 500 to 1000 feet (Plate 4). As it has been noticed elsewhere that these sand waves, often called protuberances, may move along the beach face as distinct entities, it was decided to monitor the behavior of one of the Cattaraugus features by repetitive topographic mapping.

A major protuberance, located between Cat. 6 and Cat. 7 (Fig. 63) was chosen. The three dimensional map of this sediment accumulation was constructed by running 10 closely spaced beach profiles, covering the beach face from the updrift to the downdrift embayments flanking the protuberance. The protuberance was mapped twice, on May 15 (Fig. 63) and on May 27 (Fig. 64). The feature was found not to move laterally in this short time interval. Redoing of this map at the end of the summer and again after a few fall storms, however, may prove it to be less stationary than indicated by these preliminary results. Because of its location just downdrift of the planned northeast breakwater, its behavior pattern can yield significant information about possible detrimental effects of the planned structure on this segment of the beach.

Figure 63. Map of protuberance between Cat. 6 and Cat. 7 on May 15, 1974. The map was constructed by measuring ten closely spaced beach profiles. The berms generally follow the sinusoidal outline of the sand wave but are commonly better developed in the embayments than near the center of the protuberance.

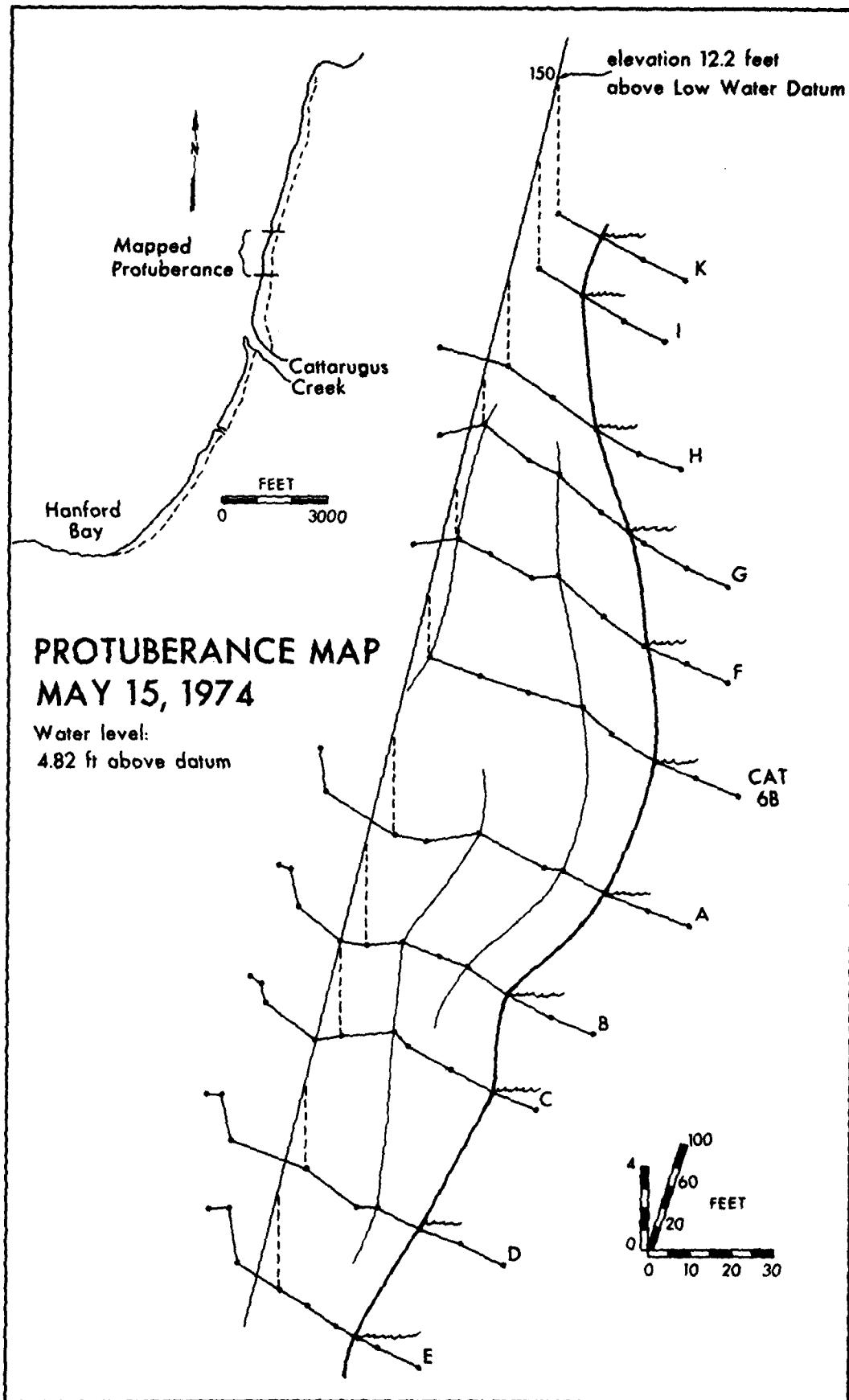


FIGURE 63

Figure 64. Map of protuberance between Cat. 6 and Cat. 7 on May 27, 1974. By comparing with the previous figure, the lakeward progradation of the protuberance can be clearly seen. The accretion has taken place by multiple berm growth, particularly in the embayments. No lateral movements of the form can be detected.

PROTUBERANCE MAP
MAY 27, 1974

Water level:
4.85 ft. above datum

elevation 12.2 feet
above Low Water Datum

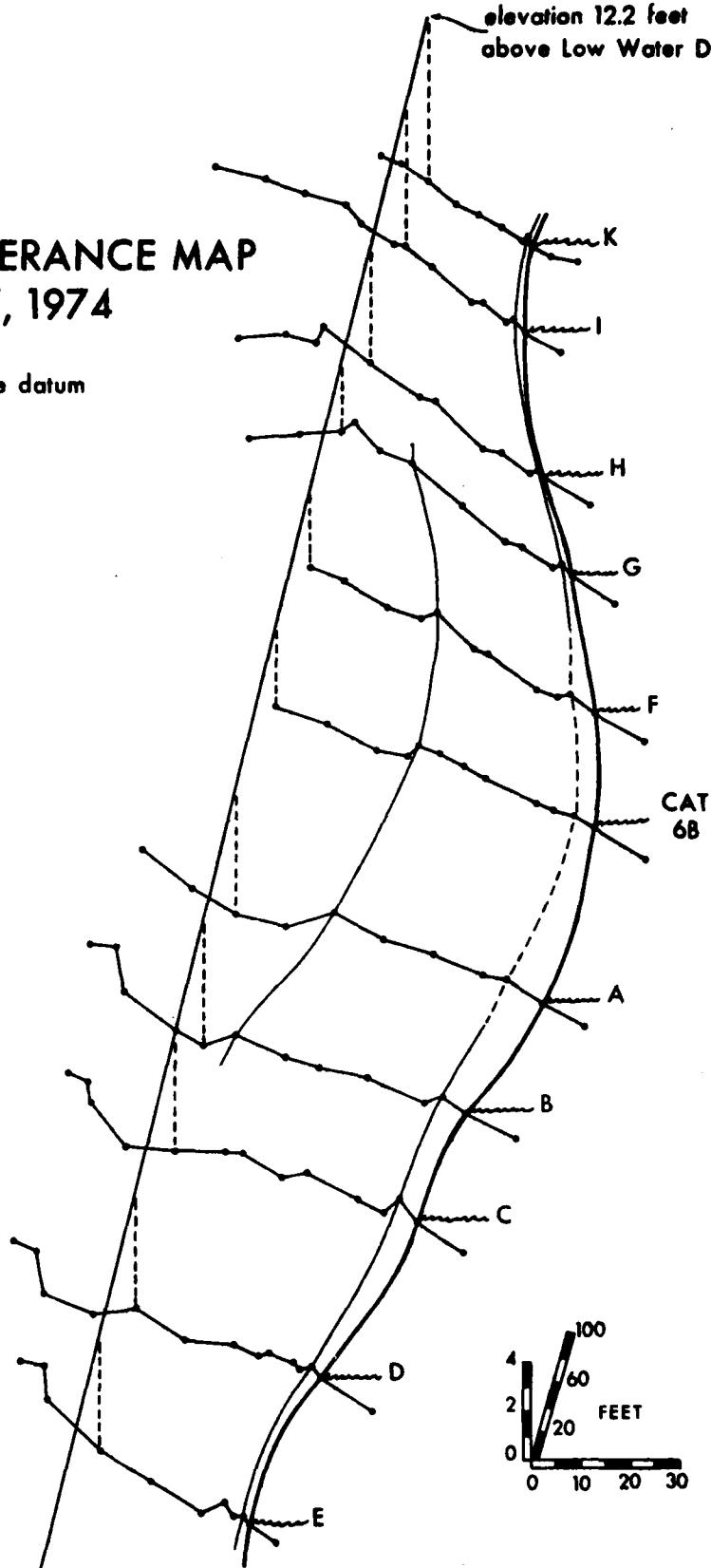


FIGURE 64

9. BREAKWATER DESIGN ALTERNATIVES

Selection of the most suitable design for the structure proposed for the mouth of Cattaraugus Creek has to be based on a thorough analysis of at least three factors:

- 1) the pattern of sediment transportation and deposition within the area which will be affected by the structure,
- 2) the pattern of winter and spring ice formation and associated flooding,
- 3) the effect of the structure on lake conditions within the marina it is built to protect.

Other environmental, technical, socio-economic, and political factors have to be considered in a comprehensive engineering analysis of the project. This, however, is far beyond the authority of this investigation.

Although the data collected for the purpose of this study pertain exclusively to factor 1 above, we feel that recommending a structure based solely on its impact on sedimentation would be unsatisfactory. The constraints set by factors 2 and 3 must also be properly evaluated.

Figure 65 shows five alternative designs discussed in this analysis. 1 and 2 are asymmetric arrowhead breakwaters. 1 is equivalent to the one proposed in the 1966 report on the Cattaraugus Harbor project, 2 is the same structure but turned to have a west breakwater facing the dominant wave approach direction. Structures 3 through 5 are significantly different from the previously proposed structures. Their associated merits and problems will be discussed below.

Figure 65. Alternative structure designs. Conceptual models of five different breakwater designs. The effects of the five structures on littoral and fluvial currents and sediment transportation, lake and river ice jamming, and wave conditions in the harbor are discussed in paragraph 10 of the text.

1. Arrowhead breakwaters, opening to the southwest.
2. Arrowhead breakwaters, opening to the north.
3. Straight arrowhead breakwater.
4. Parallel piers with a detached breakwater.
5. Parallel piers of uneven length.

ALTERNATIVE STRUCTURE DESIGNS

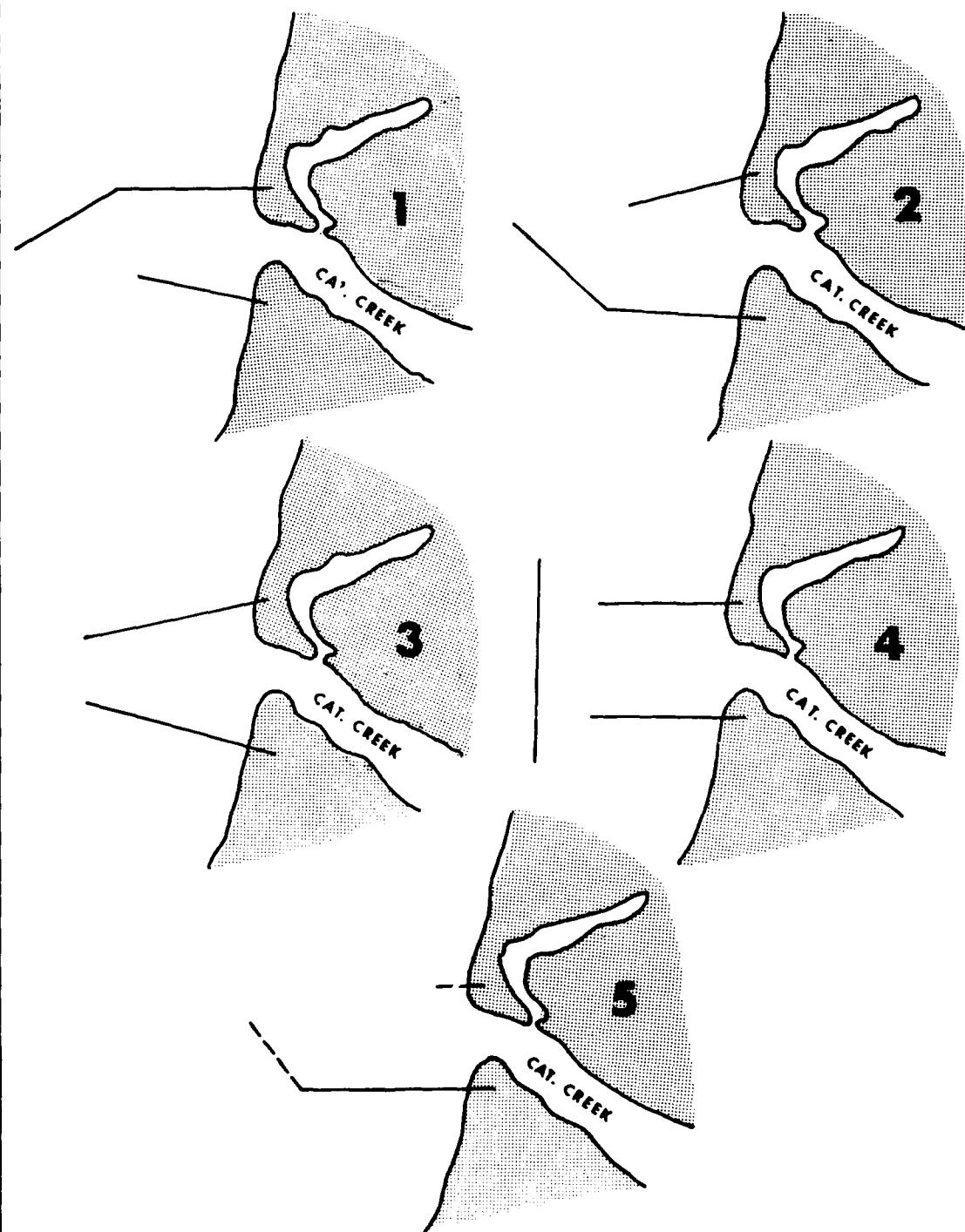


FIGURE 65

In the following sections the effects of each design will be analyzed for specific processes.

9.1. Changes in the updrift beaches.

The dominant transport direction is from the southwest to the northeast. At any one location the rate of transport is likely to be reduced the more northerly the beach face is turned because the longshore component of the wave energy flux will be reduced as the beach becomes more nearly orthogonal to the dominant wave approach direction. Therefore, the updrift sediment accumulation observed at almost every structure seen along the shoreline of lakes Erie and Ontario (paragraph 3) is likely to attain an ultimate shoreline orientation about perpendicular to the dominant local wave approach. With the dominant wave approach direction at the mouth of Cattaraugus Creek being almost orthogonal to the present shoreline, one should not expect a dramatic change in shoreline orientation. The updrift accumulation will affect a wide stretch of beach and a long time will be required before the wider beach will cause any serious increase in sediment transport rates past the south jetty and into the harbor.

Any structure, therefore, is likely to benefit the southern beaches. In order to continue to resupply these beaches, however, it is imperative that fluvial sediment still can reach them. The jetties, therefore, should not terminate in water too deep for removal of materials at their end by wave and wind-generated current action.

9.2. Changes in downdrift beaches.

As suggested by previously reported observations, beach erosion down-

drift of a structure, of whatever kind, seems to be an inevitable consequence of the interruption of continuity in the littoral drift system. With no sediment source downdrift of the structure, erosion probably is inevitable. With a sediment source associated with the structure, however, the design should attempt to permit reintroduction of sediment into the longshore transport system. If the source is significant enough, equilibrium transport rates could be reestablished without cost to the downdrift beaches.

Cattaraugus Creek is the only major source of sediment in the embayment. Therefore, by providing for fluvial sediment supply to the downdrift beaches, their erosion can be minimized if not eliminated. These considerations request that fluvial sediment have free path to the north as under natural conditions, a requirement that would favor parallel piers of uneven length (design 5, Fig. 65) or, to a lesser degree, arrowhead breakwaters with opening to the north (design 2). Furthermore, the breakwaters should not terminate in water too deep for effective littoral transport of sand.

9.3. Harbor shoaling due to littoral drift.

Because the net sediment flux is towards the north, any structure with a shorter breakwater on the south side than on the north side is likely to have severe problems with shoaling at the harbor entrance. This seems not to favor the arrowhead breakwaters with opening to the southwest (design 1, Fig. 65) as well as, possibly, the parallel piers with a detached breakwater (design 4, Fig. 65), although the situation here is less clear. Because of wave refraction around the detached breakwater, sediment transported northward between the termini of the jetties and the detached breakwater might accumulate at the jetty mouth.

The most desirable structures in terms of harbor shoaling might be the arrowhead breakwaters with opening to the north (design 2, Fig. 65) and the parallel piers of uneven length (design 5, Fig. 65). In both of these cases, fluvial sediment will have free path to the north and the littoral drift, bypassing the south jetty, is likely also to bypass the northern jetty.

The circulation pattern in lee of such structures, however, is fairly complex and an accurate prediction is impossible. Saylor (1966), studying the currents at Little Lake Harbor in Lake Superior, found that a lee side eddy developed behind an asymmetric arrowhead breakwater during strong westerly wind-driven currents (Fig. 66). This circulation pattern will result in the scour of a relatively deep channel near the southwest breakwater and the possible accumulation of sediment in the middle of the harbor entrance.

9.4. Harbor shoaling due to fluvial sediment supply.

During moderate and low discharge in Cattaraugus Creek, some fluvial sediment will undoubtedly be deposited in the harbor. There is reason to believe, however, that during floods the current velocities are sufficiently high to provide adequate flushing action in the harbor to avoid the formation of a major channel mouth bar. During floods in the present unmodified channel, gravel and sand are transported right through to the open lake, and there is no reason to expect this to change by the addition of the jetties. Designs 2 and 5 might develop a fluvial sediment deposit in the harbor basin to the north of the southern breakwater. This material would partly replenish the northern beach, but it could also be caught in the reverse circulation shown in Figure 66 and be redeposited in the entrance channel to the harbor.

Figure 66. Current pattern near entrance to Little Lake Harbor (Lake Superior) during strong westerly wind with outflow from the harbor. From Saylor (1966).

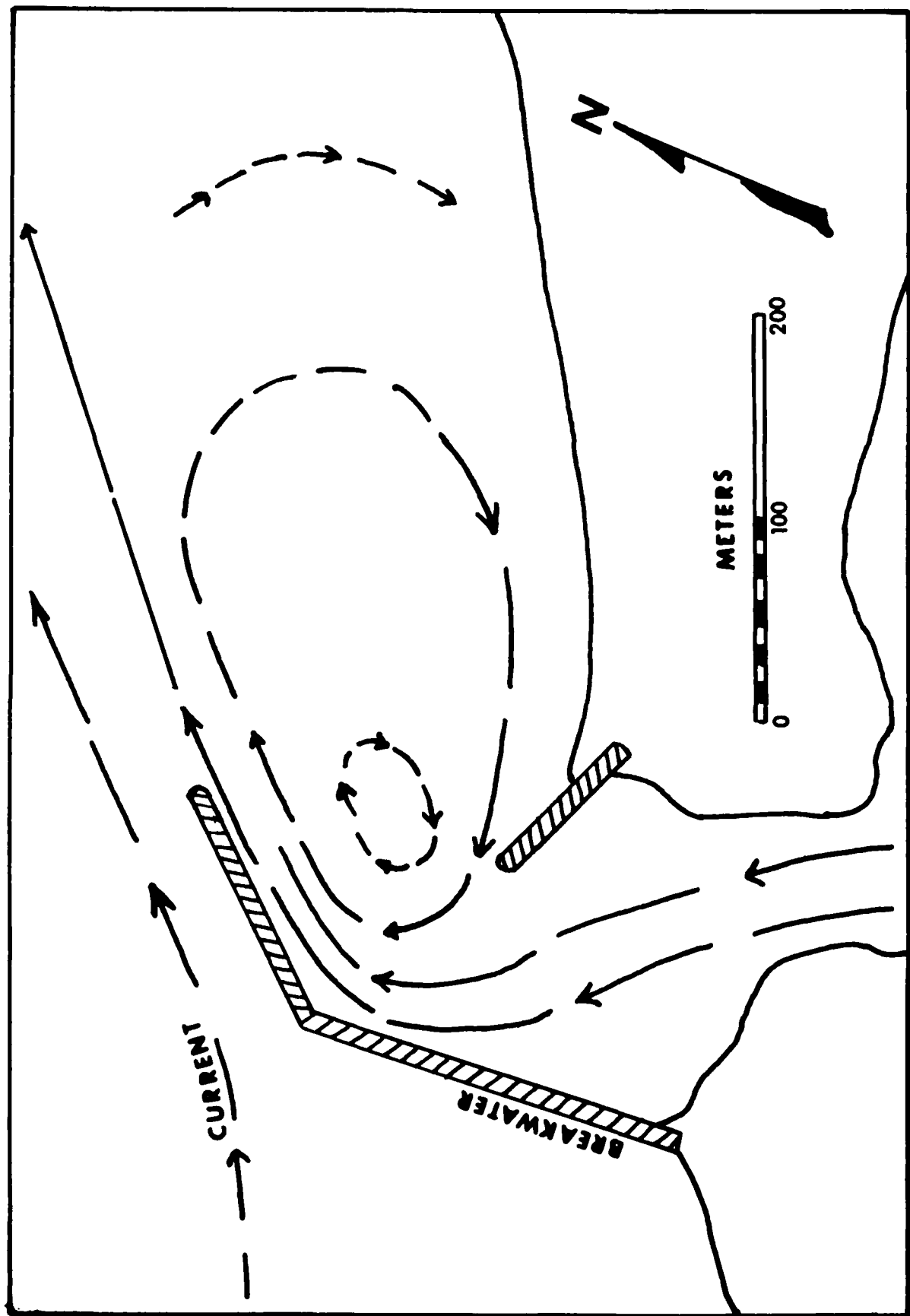


FIGURE 66

9.5. Ice jams and related flood problems.

The most severe flooding of the Sunset Bay area is caused by ice jamming of the creek mouth during periods of high discharge. The jam can be caused by three different ice conditions and the impact of a structure on the ice problem will depend on these conditions.

If solid ice extends from the shore lakeward to beyond the end of the breakwaters at the time of high discharge in Cattaraugus Creek, the flooding is going to be severe irrespective of structure design. Designs 1 through 4, however, are likely to aggravate the situation more than design 5, because the two impermeable breakwaters will have a leveeing effect on the water and raise the downstream control. Creek water flowing onto the lake ice under unmodified conditions is known to build its own "ice-levees," but these are low and somewhat permeable and have relatively little effect on raising the water level in the channel.

Drift ice in the lake tends to be wind rowed parallel to shore in embayments like Cattaraugus during strong westerly winds. An arrowhead breakwater might be effective in providing an unobstructed outlet for the creek water through this ice jam.

Frequently, the creek itself blocks its mouth by ice brought downstream during the flood. This ice is held back by the channel mouth sand spit and jams the creek further upstream. It has been observed to fill the channel completely from the mouth to the New York Central railroad bridge.

Although any of the proposed structure designs probably will eliminate the sand spit problem, it is questionable whether the relatively narrow opening between the arrowhead breakwaters will prove adequate for a rapid discharge of

river ice. Parallel breakwaters of unequal length (design 5, Fig. 65) may be the best for this ice condition; an arrowhead breakwater with opening to the north (design 2, Fig. 65), away from the main wave approach direction, may be an acceptable second alternative.

9.6. Wave conditions in the harbor entrance.

For safety, easy maneuverability, and minimum damage to mooring facilities in the marina it is imperative that the breakwaters are designed to receive as little wave energy as possible and to quickly dissipate whatever does arrive at the entrance channel. The entrance should face away from the dominant storm wave approach direction, and multiple wave reflection between the breakwaters should be minimized.

Design 2, and to a lesser degree 4 and 5, are protected from westerly storm waves. The landward divergence of breakwaters with arrowhead design will quickly dissipate any incoming wave energy, as will the parallel breakwaters of uneven length because there is almost no northern breakwater to cause multiple reflection. Designs 1 and 3 might be the least desirable ones in terms of their effect on wave conditions in the harbor entrance.

9.7. Tentative recommendations.

Paragraph 4(2) of the Scope of Work specifies: "Based on his findings (the contractor should) propose a breakwater configuration that will have the least detrimental effect on the regional environment." In the preceding paragraphs, the possible environmental impact of 5 alternative structures has been discussed. It is premature to make any final recommendations based on

these analyses. Tentatively, however, it seems that design 5 (Fig. 65), parallel breakwaters of uneven length, has a number of valuable attributes. Design 2, arrowhead breakwaters with opening to the north, might also be acceptable. The remaining three designs seem to be generally less desirable unless some presently overlooked factor should count heavily in their favor.

The alternatives discussed in the previous paragraphs should be thoroughly tested in the movable bed model constructed at the U. S. Waterways Experiment Station at Vicksburg, Miss. If the natural sedimentation processes presently observed in the Cattaraugus Embayment can be adequately reproduced in the model, one should also be able to predict, with some degree of confidence, the post-construction sedimentation patterns.

10. SEASONAL CHANGES IN SHORELINE AND RIVER MOUTH FORM

10.1. Introduction.

Beach profiles established in May, 1974, (Fig. 55) were rerun several times between September 15th and October 29th. This did provide better data for an assessment of typical fall trends than a single one-week field survey would have done. The fall field work also included mapping of the changes in the form of the creek mouth, aerial photography, and sampling of sediment in Cattaraugus Creek for an estimation of gravel transport rates.

10.2. Beach morphology.

Still water level in Lake Erie dropped 1.4 ft (from 4.6' above L.W.D. in May to 3.2' above L.W.D. in October) during the summer and fall of 1974 (Lake Survey Center, 1974). This caused the exposure of a wider beach and a larger subaerial spit area. In addition to these apparent morphologic changes, substantial beach accretion and spit growth occurred.

As shown in section 8.1, there is a distinct morphological difference between the beach south of and north of Cattaraugus Creek. The steep beach profiles of Cat. 6 and Cat. 7 were attributed to high wave energy characteristically affecting that area during west and southwest storms (Figs. 53C and 54). Comparing the beach profile of Cat. 6 for June 13th and October 26th (Fig. 67A) reveals a substantial net accretion over that time period, changing the beach from a concave profile on June 13th to convex with multiple large gravel berms on October 26th. The truncated beach profile on September 15th, however, indicates that accretion has not been a continuous process through the summer. At least

Figure 67. A. Beach profiles at Cat. 6. The stake marking the profile location in spring disappeared over the summer and was replaced by a new marker at approximately the same location on September 15th. The spring and fall profiles, however, are not directly comparable. Note the steep beach at Cat. 6 at all times and the large accretion between September 15 and October 26, 1974.

B. Beach profiles at Cat. 5 superimposed for June 13 and October 26, 1975. Dot pattern indicates accretion; cross-hatched pattern indicates erosion. The profiles demonstrate net accretion with little change in morphology or beach face slope over the summer.

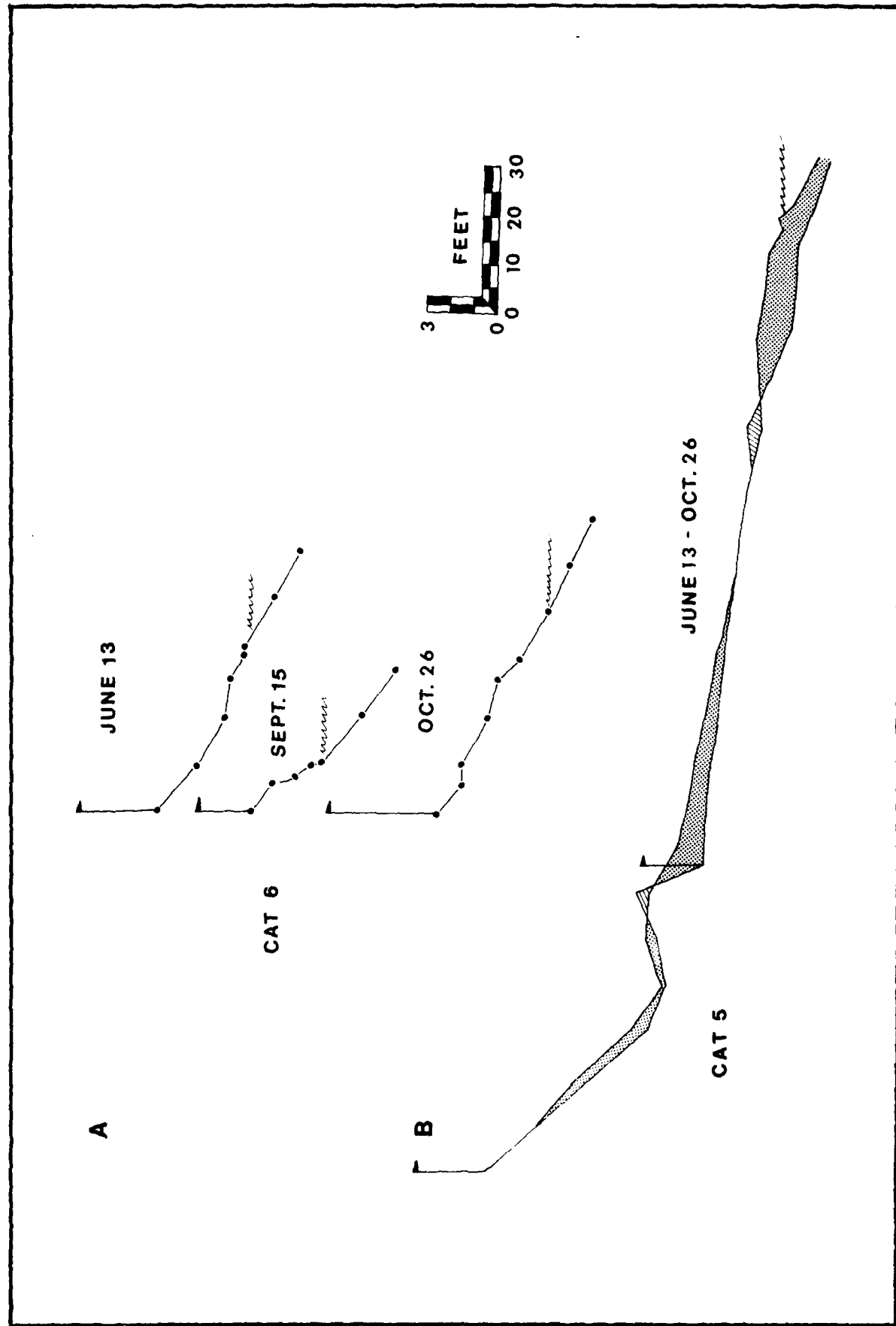


FIGURE 67

one, probably multiple, erosional events have interrupted the long-term accretional trend. Fluctuations in beach slope are large, ranging from 1 in 3 on September 15th to 1 in 8 on October 29th.

The rather flat profile of Cat. 5 displays much less change over the same time period (Fig. 67B). The smaller wave energies and finer grained sediments result in a flat, less active beach without significant gravel berm developments. Changes in beach slope are small, ranging from 1 in 35 on September 15th to 1 in 25 on October 29th. Similar slope values and profile variations also characterize the rest of the beach immediately south of the creek, and are typical also for Wide Beach, located between profiles Cat. 9 and Cat. 10.

The characteristics of the fall beaches are not significantly different from those of the spring and early summer. The beach face at Cat. 6 remains steep and is subject to rapid erosion and deposition in response to high wave energies. The beach at Cat. 5 appears relatively stable in the short run, an observation which probably can be attributed to its more sheltered location.

10.3 Seasonal changes in spit morphology.

Figures 61 and 62 feature the major changes in the Hanover spit morphology observed during the spring field season. These are: (1) a gradual growth in spit size, and (2) a change in slip face location from the lake side to the creek side of the spit. The orientation remained essentially unchanged with the spit lined up with the south channel bank. Plate 10 shows the subaerial configuration on June 13th, 1974.

Figure 68 presents plane table maps of the subaerial configuration of the Hanover spit in late October, 1974. Submerged bars, where

Figure 68. Changes in the configuration of Cattaraugus Creek mouth in late October, 1974. Maps were prepared by plane table. Prior to October 19th the creek discharged to the north along the beach at A. Breaching of the spit by a small flood in the creek just prior to the mapping on October 19th provided a more direct outlet for river water and led to the attachment of the spit to the beach at A.

Further growth of the Hanover spit (B) between the 19th and the 29th began a new cycle of creek mouth deflection to the north.

The increase in subaerial spit size is dominantly brought about by onshore migration of bars ultimately welding onto the beach face. The "runnel" observed on October 29th is a topographic low separating a newly formed bar from the beach face.

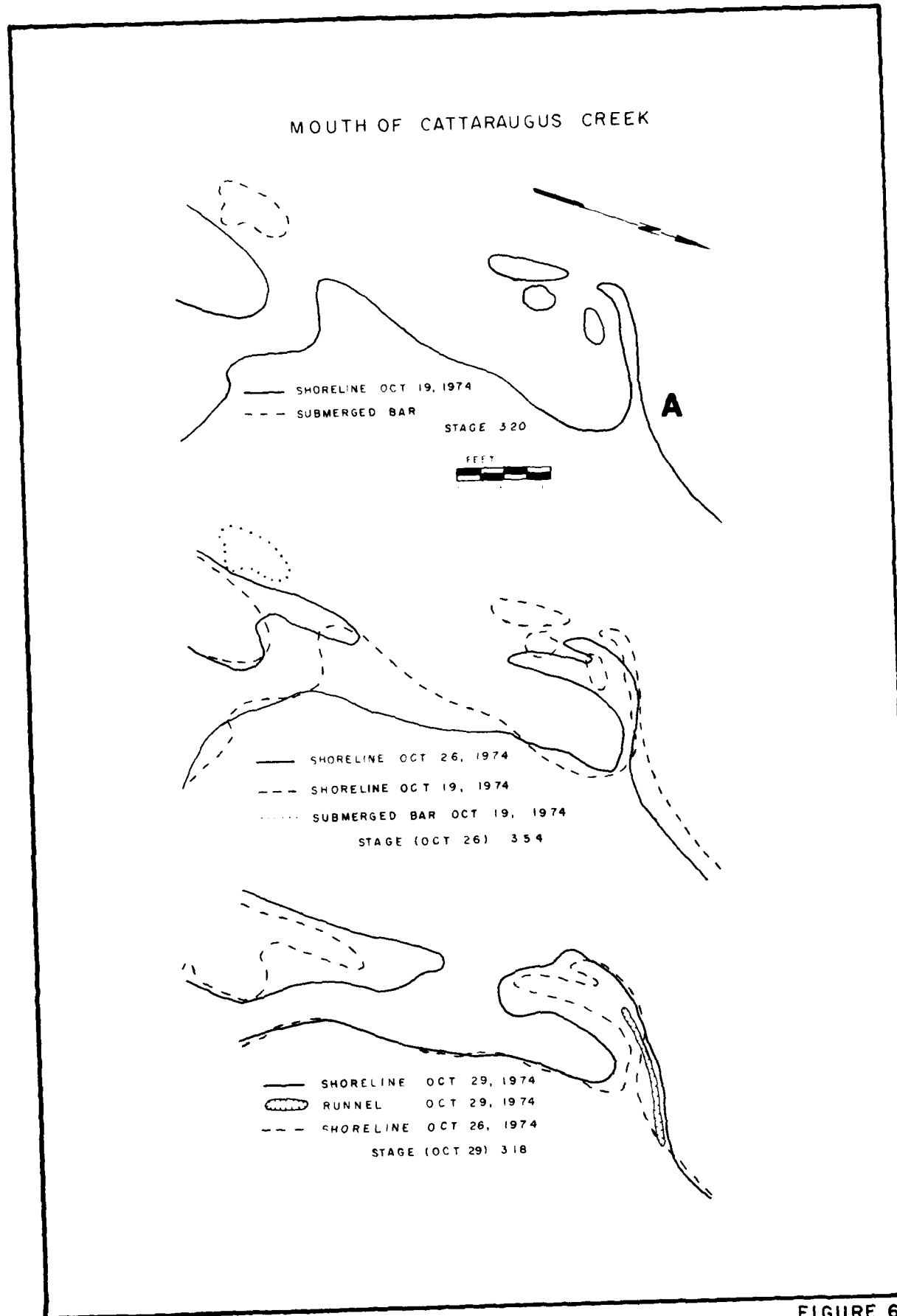


FIGURE 68

noticeable, are sketched. An oblique, low-altitude aerial photo of the fall spit complex is shown in Plate 11. The water level at the Keene Marina staff gauge on October 19th was 3.20 ft above L.W.D. as compared to 4.45 ft on June 6th, the date of the last spring season map.

Prior to October 19th, Cattaraugus Creek discharged to the north along the beach at A (Fig. 68) with its west bank made up of the Hanover spit. A minor flood a few days prior to the October 19th mapping breached this spit and provided a more direct route for the creek into the lake. The north end of the recurved spit was consequently attached to the Brant side beach.

During the mapping period both sides of the spit were enlarged, probably by the migrations of nearshore bars onto the existing beach face. As before, net sediment transport to the north prevailed. The narrow depression on the lake side of the Brant spit (Fig. 68, Oct. 29) indicates that a bar is in the process of becoming attached to the beach face.

The sequence of events just described presents a mechanism for transfer of coarse-grained littoral sediment from the Hanover to the Brant side of the creek. In addition to sediment transfer by spit growth and breaching, coarse-grained material may also move across the creek mouth by a combination of offshore fluvial transport and onshore wave induced bar migration.

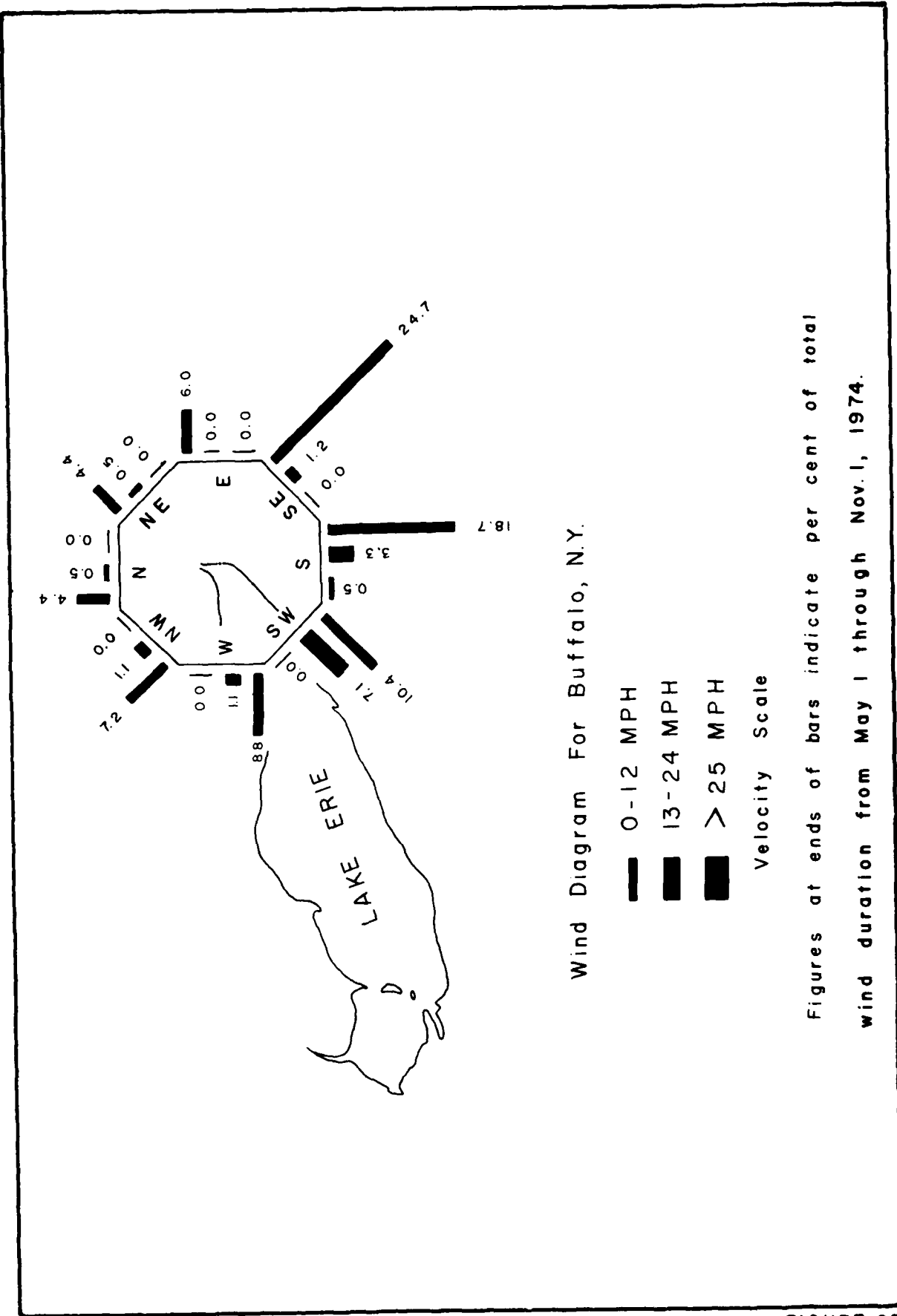
10.4. Lake Erie wind patterns

A detailed analysis of the weather patterns on Lake Erie was presented in section 6. Included here is only a brief discussion of the

wind variability at Buffalo airport for the summer and fall of 1974 as it compares to the climatic average. Figure 69 presents a wind diagram for observations between May 1 and November 1, 1974, i.e., including both the spring and fall field observation periods. For winds with onshore components at the Cattaraugus Embayment the distribution during the study period was almost identical to the climatic average for the entire ice-free period (compare Figs. 69 and 49). Light off-shore winds from the southeast and south, however, were much more frequent than they are on the annual average. This, in part, is due to the infrequent cyclonic activity in the Great Lakes region during summer and the general control of the lake region circulation by a massive Bermuda high.

A comparison of Figures 69 and 49 amply demonstrates that the process variability and sediment response in the Cattaraugus Embayment monitored for 6 weeks in the spring and a short time in the fall of 1974 are representative for the entire ice-free period for 1974 or most years.

Figure 69. Wind diagram for Buffalo, New York, from May 1 to November 1, 1974. The format of the diagram follows that of Figure 49. The figure demonstrates that the distribution of onshore winds during the study period, at the southeast coast of Lake Erie, is very similar to the climatic average presented in Figure 49. The summer and fall of 1974 experienced a higher than normal percentage of offshore winds.



11. GRAVEL TRANSPORT ON CATTARAUGUS CREEK

11.1. Introduction.

In order to estimate the maintenance costs of the proposed turning basin to be dredged near the mouth of Cattaraugus Creek (Corps of Engineers, 1966) the rate of fluvial bed material transport in the lower creek has to be determined. Because of the short time available for data collection, it was decided to estimate flood-associated transportation rates from existing equations of sedimentation engineering, based on data on channel and sediment characteristics collected during low water on October 28th and 29th, 1974. The conclusions reached should be regarded as preliminary; field work during high discharge in the spring of 1975 will be done to arrive at a more reliable prediction.

11.2 Hydraulic computations.

Four different straight reaches between Irving and Gowanda were chosen for field measurements and subsequent bedload computations (Fig. 70). For each reach two or three channel cross sections were surveyed (Fig. 71) and the intermediate axes of two hundred clasts were measured for an estimate of typical bed material size-frequency distributions (Fig. 72). Slopes of the channel bottom and the low-water surface were also recorded. All field surveys were made using plane-table and alidade. Table III summarizes the slope measurements made in the field as well as predicted water surface slopes for standard project floods and intermediate regional floods (Corps of Engineers, 1969, plates 12 and 16) and the local slope derived from the longitudinal stream profile. Table III indicates that the local slope derived from the river profile corresponds much better to the predicted large flood

Figure 70. Map of lower Cattaraugus Creek, Erie and Chautauqua Counties, New York. Hydraulic and sedimentary parameters of four relatively straight reaches of the channel (solid black) were measured in this attempt to determine gravel transport rates of the stream.

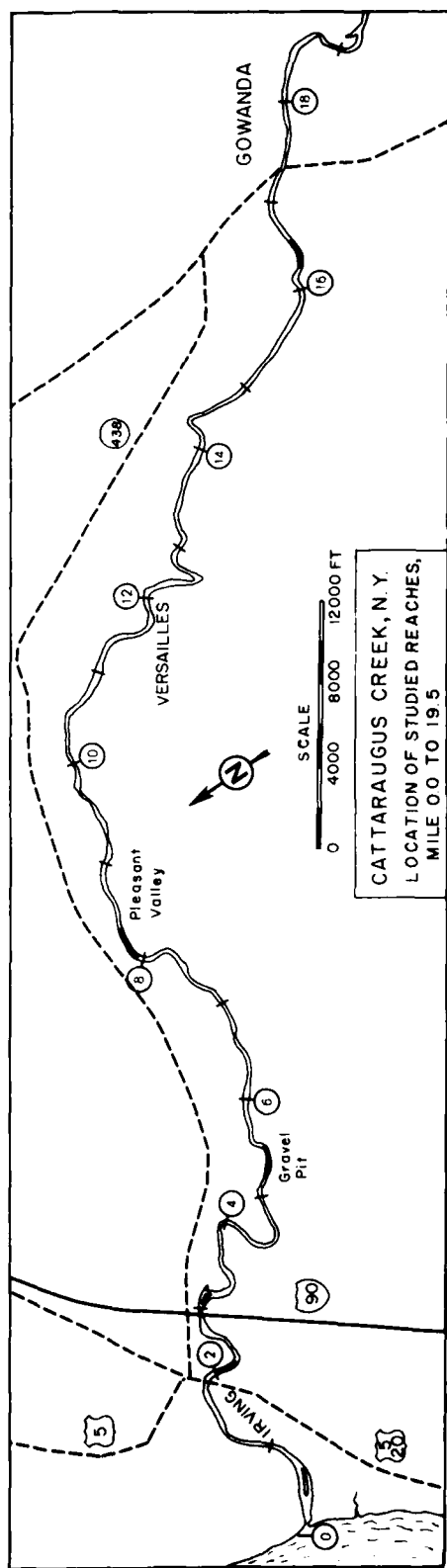


FIGURE 70

Figure 71. Cross sections of studied reaches at Cattaraugus Creek. Measurements were made by plane table and alidade. Vertical datum (0 ft) corresponds to water surface elevation on October 28 and 29, 1974. The hydraulic geometry was determined by planimetry of the drafted cross sections.

CATTARAUGUS CREEK, N.Y.

SELECTED CROSS SECTIONS BETWEEN
IRVING and GOWANDA

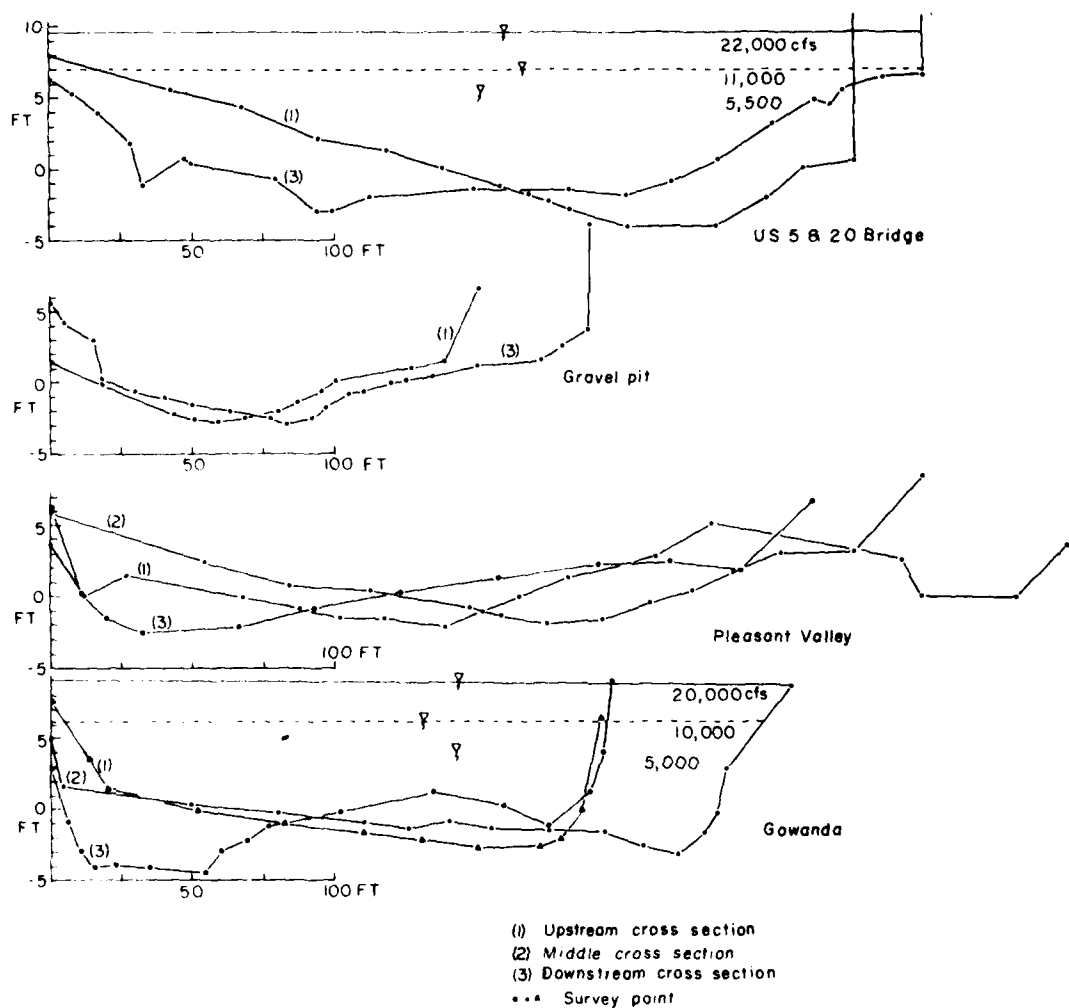


FIGURE 71

Figure 72. Size-frequency distribution of typical point bar gravel (only clasts larger than .8 cm or -3ϕ were measured) on Cattaraugus Creek. For each bar, 200 clasts spaced 20 cm apart along transects perpendicular to the inferred flow direction at the center of the bar were measured.

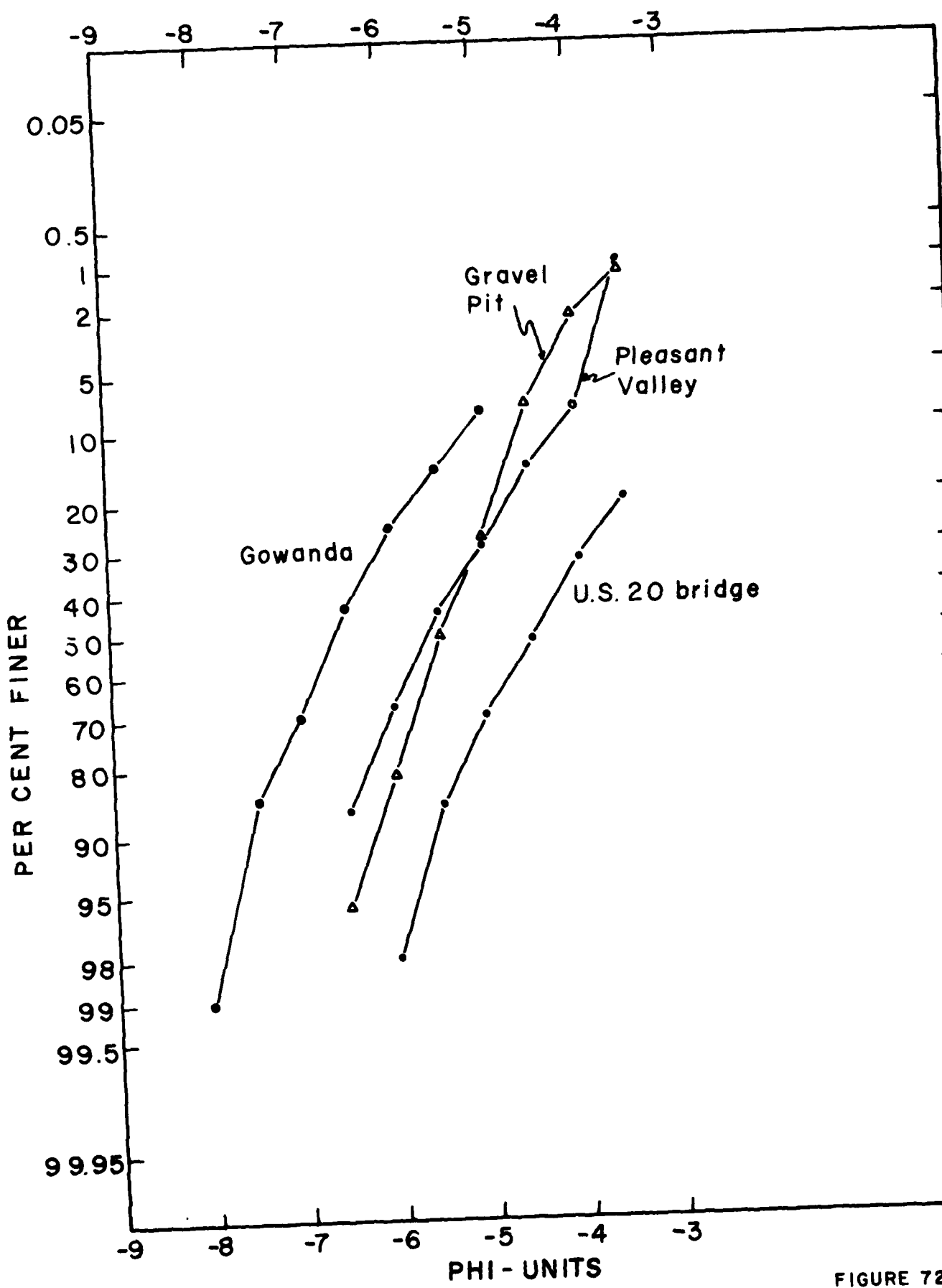


FIGURE 72

TABLE III
Measured and predicted slopes for
selected reaches of Cattaraugus Creek, New York.

<u>Reach</u>	<u>Flow Condition</u>	<u>Slope</u>
Gowanda River Mile 16.3-16.5	Creek bottom*	$2.84 \cdot 10^{-3}$
	Standard project flood*	$2.40 \cdot 10^{-3}$
	Intermediate regional flood*	$2.52 \cdot 10^{-3}$
	Low water surface, Oct. 1974	$7.93 \cdot 10^{-3}$
	Longitudinal stream profile	$1.95 \cdot 10^{-3}$
Pleasant Valley River Mile 8.0-8.2	Low water surface, Oct. 1974	$0.92 \cdot 10^{-3}$
	Longitudinal stream profile	$1.24 \cdot 10^{-3}$
Gravel Pit River Mile 5.2-5.4	Low water surface, Oct. 1974	$0.64 \cdot 10^{-3}$
	Longitudinal stream profile	$1.55 \cdot 10^{-3}$
U.S. 20 Bridge River Mile 2.0-2.2	Creek bottom*	$1.97 \cdot 10^{-3}$
	Standard project flood*	$.32 \cdot 10^{-3}$
	Intermediate regional flood*	$.76 \cdot 10^{-3}$
	Low water surface, Oct. 1974	0
	Longitudinal stream profile	$.645 \cdot 10^{-3}$

*Data from Corps of Engineers (1968, plates 12 and 16).

slopes than does the low water surface profile measured in October. Consequently, the slope of the longitudinal river profile was used in all hydraulic computations.

Stage-discharge curves for the Gowanda and the U.S. 20 and 5 bridge sites (Fig. 73) were derived from historical flood records presented in the "Flood Plain Information" report (Corps of Engineers, 1968). Stage-discharge data were combined with the measured cross-sections at these two locations to compute flow area, wetted perimeter and hydraulic depth for these selected discharges (Table IV). Chosen discharges were 20,000; 10,000 and 5,000 cfs at Gowanda. A linear increase in discharge with downstream distance was assumed amounting to 10 per cent at Irving. Calculations were not attempted for discharges above 20,000 cfs at Gowanda because of the unknown hydraulics associated with substantial overbank flow.

Hydraulic depths for the two intermediate reaches (Pleasant Valley and Gravel Pit) had to be determined indirectly. The Manning's roughness coefficient, n , was computed for the study reaches at Gowanda and Irving from data already presented on flow area, hydraulic radius and energy slope (Fig. 74 and Table IV). Subsequently, n was estimated for the other two reaches based on the assumption that the friction is linearly related to the median diameter of the bed material in the absence of bedforms or large scale obstructions to the flow. The hydraulic depths corresponding to the three design discharges were then determined from the Manning's equation (Chow, 1959, p.128):

$$Q = \frac{1.49}{n} A \cdot R^{2/3} \cdot S^{1/2} \quad (1)$$

Figure 73. Stage-discharge curves constructed from
flood data presented by Corps of Engineers
(1968, Table 4).

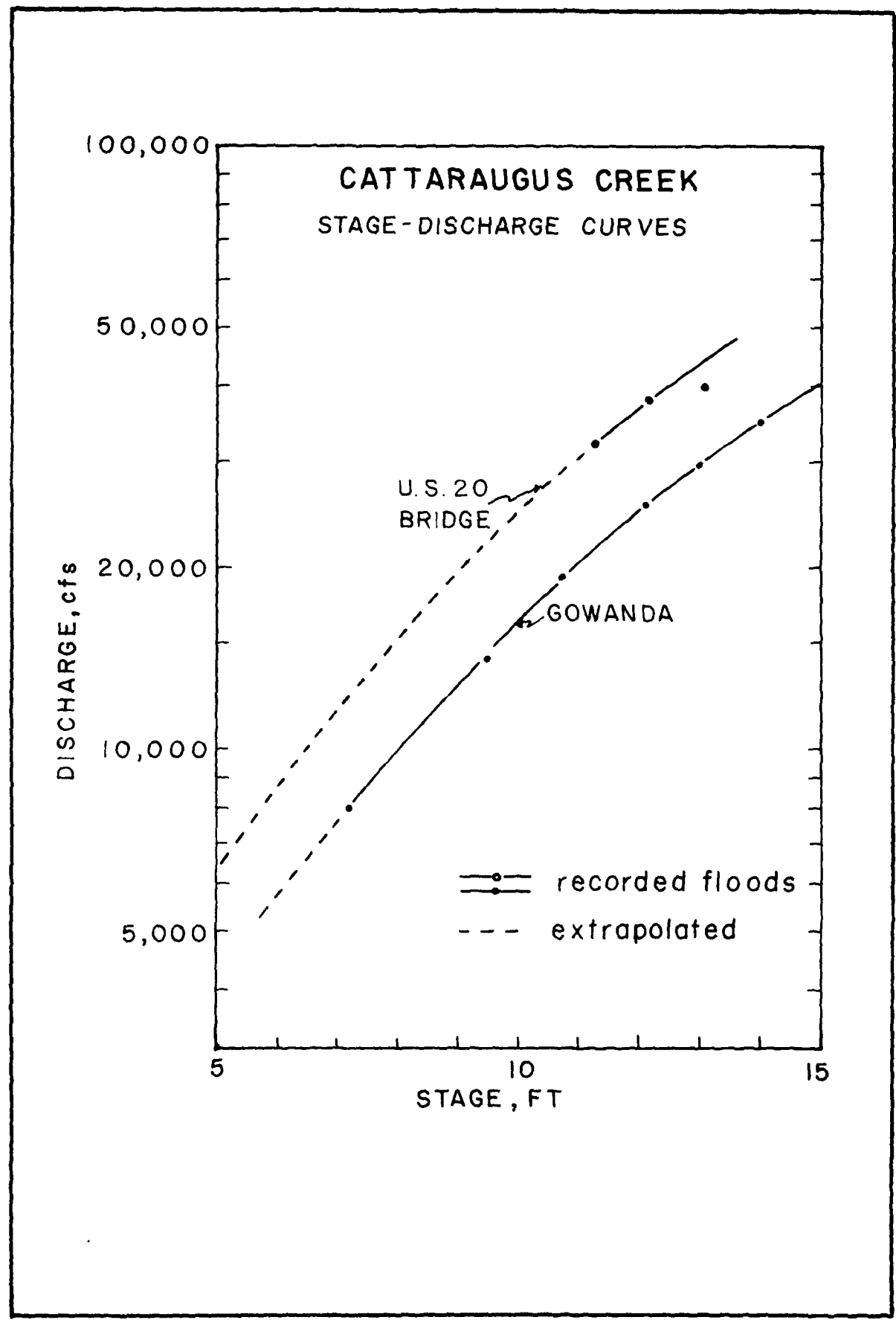


FIGURE 73

Figure 74. Summary of computed hydraulic and sedimentary parameters for the lower Cattaraugus Creek. The longitudinal profile was determined from topographic map data. The local slope at each study reach was derived from the longitudinal profile. Median gravel size refers to the 50th percentile at the size-frequency curves of Figure 72. Mean current velocities for three chosen discharges were computed either from known cross sectional areas (at Gowanda and the U. S. 20 bridge site) or by means of the Manning equation. Bedload discharge is computed according to Einstein's (1950) equations.

Note the high sediment transport rate at the Gravel Pit reach, associated with a local increase in slope.

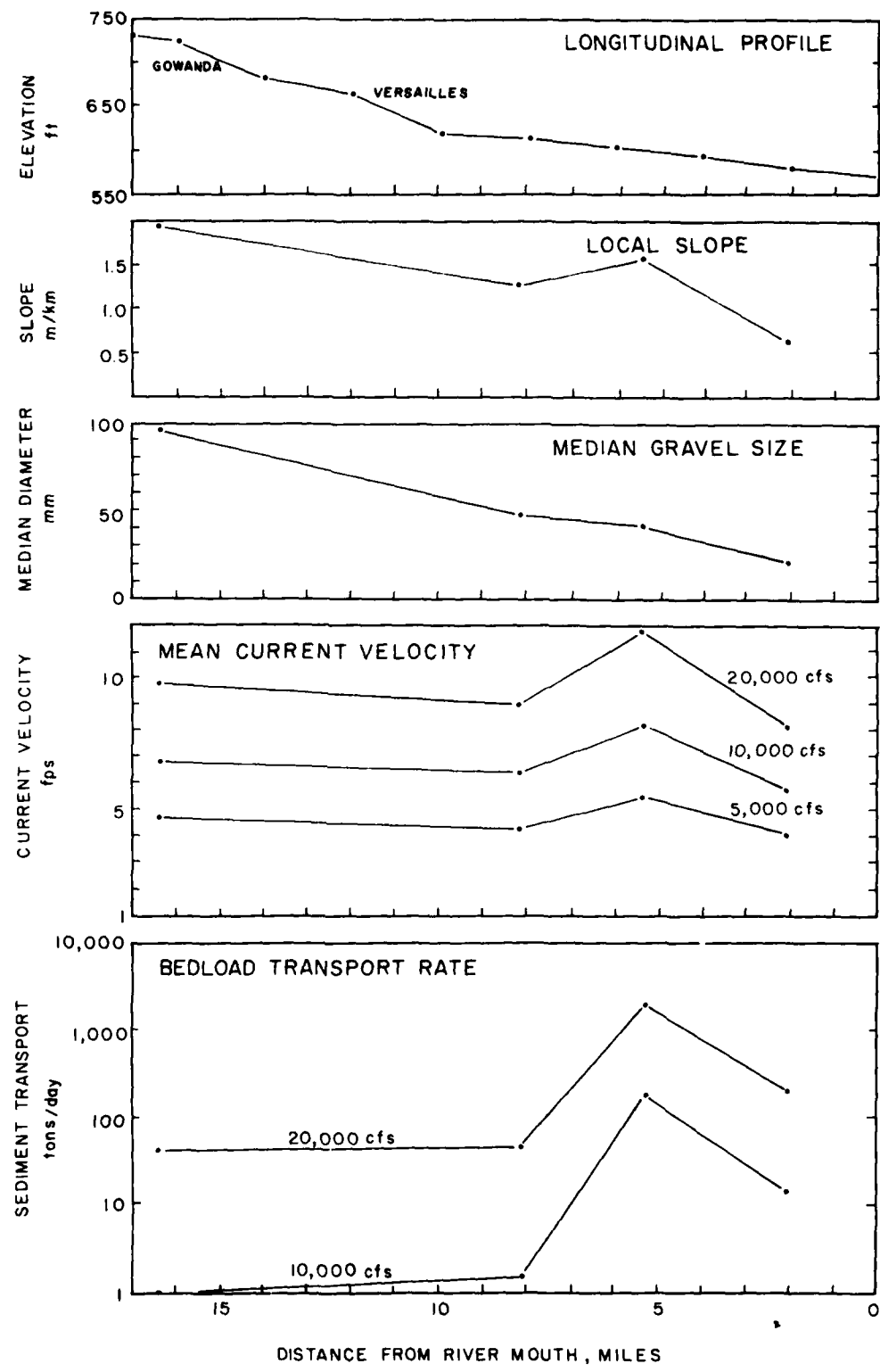


FIGURE 74

Table IV. Sedimentary and hydraulic parameters for Cattaraugus Creek, New York.

Reach	Discharge Q_w , cfs	Sediment sizes, mm			Slope S	Flow Area A , ft^2	Hydraulic Radius R , ft	Mean Current Velocity V , fps	Friction Factor n
Cowanda River Mile 16.3-16.5	20,000 10,000 5,000	76.1	97	119	194	$1.95 \cdot 10^{-3}$	2040 1441 1046	9.23 6.80 5.03	.0296 .0343 .0406
Pleasant Valley River Mile 8.0-8.2	21,000 10,500 5,250	35.5	48.5	59.7	100	$1.24 \cdot 10^{-3}$	2328 1625 1218	7.76 5.91 4.43	.0228 .0265 .0328
Gravel Pit River Mile 5.2-5.4	21,400 10,700 5,350	35.5	43.7	51.9	73.5	$1.55 \cdot 10^{-3}$	1799 1303 976	9.57 6.93 5.19	.0222 .0260 .0321
U.S. 20 Bridge River Mile 2.0-2.2	22,000 11,000 5,500	16.5	21.8	28.8	48.5	$.645 \cdot 10^{-3}$	2677 1882 1438	8.92 6.72 5.14	.0199 .0231 .0295

where Q = water discharge, A = flow area, R = hydraulic depth and S = slope. Measured sediment sizes, local slopes and all computed hydraulic parameters are summarized in Table IV. All computations are performed on a Hewlett-Packard 65 mini-computer.

Because the sediment discharges estimated below rely on these hydraulic computations, it is worth attempting to assess their accuracy. Flow computations are restricted to discharges of 20,000 cfs or less to eliminate the uncertainties associated with substantial overbank flow. The hydraulic radii and flow areas computed for the Pleasant Valley and Gravel Pit reaches, therefore, are considered accurate to within ± 0.5 ft. The computed range and variation in R with discharge correspond well with values determined from observed stage-discharge relationships at Gowanda and the U.S. 20 bridge. The computed mean current velocities and roughness coefficients also fall within the ranges considered normal for this kind of a stream (Chow, 1959, pp. 109-114). The indicated increase in friction factor with a decrease in discharge is an expected response to increased relative roughness.

The most uncertain factor in these computations remains the flood-associated local energy slope. To improve the computations this parameter should be measured during floods.

11.3 Sediment discharge computations.

Based on previous experience (Nummedal, 1974) and general recommendations of hydraulic engineering (Shen, 1971), Einstein's (1950) procedure for estimation of bed material transport rates was selected because the composition of the bed material is such that most of the transportation of this material is expected to take place as bedload.

Basically, Einstein (1950) provides a relationship between a dimensionless expression for the intensity of flow, ψ , and another dimensionless expression for the intensity of bed material transport, Φ . These quantities are defined as:

$$\psi = \frac{\rho_s - \rho}{\rho} \cdot \frac{D}{S \cdot R} \quad (2)$$

and

$$\Phi = \frac{g_s}{\rho_s} \sqrt{\frac{\rho}{\rho_s - \rho} \cdot \frac{1}{gD^3}} \quad (3)$$

where the symbols are defined as follows:

ρ_s = density of sediment particles

ρ = density of water

D = sediment diameter, D_{50} (Table IV) was used in the computations

S = slope

R = hydraulic radius

g = acceleration of gravity

g_s = weight rate of sediment transport

The intensity of flow, ψ , is completely determined for each flow condition by the parameters of Table IV. For relatively low rates of sediment transport, ψ can be related to Φ by a simple analytical function (Graf, 1971, p. 145):

$$0.465 \Phi = e^{-0.391\psi} \quad (4)$$

Equation 4 is valid for $\Phi < 0.4$. For higher rates of sediment transport a graphical relation between ψ and Φ exists (Einstein, 1950, Fig. 9; Graf, 1971, Fig. 7.13). Equation 4 was used for all computations in this study. Table V presents the results.

The median clast size of the total sample was used in computation, giving a rather crude approximation to the real rate of transport for the poorly sorted, often bimodal, sediment population that exists on Cattaraugus Creek. More accurate computations should be performed for each individual size fraction, subsequent to the collection of more precise hydraulic data.

11.4. Discussion

Table V demonstrates that the gravel transport rate on Cattaraugus Creek is moderate. The most intense transport seems to occur at the Gravel Pit reach where the local slope is a maximum. In terms of volume the transport rate there is about 1240 m^3 per day for a discharge of 21,400 cfs. According to the flood frequency diagram presented in Figure 75, such a flood has a recurrence interval of about 3 years, with a peak discharge lasting for two to three days. Therefore, a 21,400 cfs flood may move some $2500-3500 \text{ m}^3$ of coarse gravel in the Gravel Pit section every third year. As the transport rate is found to decrease downstream (Table V) it is unknown at present how much of this actually reaches the area of the proposed dredged turning basin.

TABLE V.

Sediment transport parameters for Cattaraugus Creek, New York.

Reach	Discharge cfs	Flow Intensity Ψ	Intensity of Bedload Transport, Φ	Bedload Transport Rate G_s tons/day
Gowanda	20,000	29.16	$2.40 \cdot 10^{-5}$	45.2
	10,000	39.50	$4.28 \cdot 10^{-7}$.77
	5,000	53.50	$1.77 \cdot 10^{-9}$.003
Pleasant Valley	21,000	27.27	$5.03 \cdot 10^{-5}$	45.5
	10,500	35.80	$1.79 \cdot 10^{-6}$	1.48
	5,250	47.76	$1.67 \cdot 10^{-8}$.014
Gravel Pit	21,400	15.94	$4.22 \cdot 10^{-3}$	2042
	10,700	22.01	$3.93 \cdot 10^{-4}$	190
	5,350	29.39	$2.20 \cdot 10^{-5}$	10.7
U.S. 20 Bridge	22,000	20.50	$7.10 \cdot 10^{-4}$	193
	11,000	27.21	$5.15 \cdot 10^{-5}$	13.1
	5,500	35.57	$1.96 \cdot 10^{-6}$.49

Figure 75. Flow frequency diagrams of Cattaraugus Creek at Gowanda and the mouth. Data from Corps of Engineers, U. S. Army, Buffalo District (1974, personal communication).

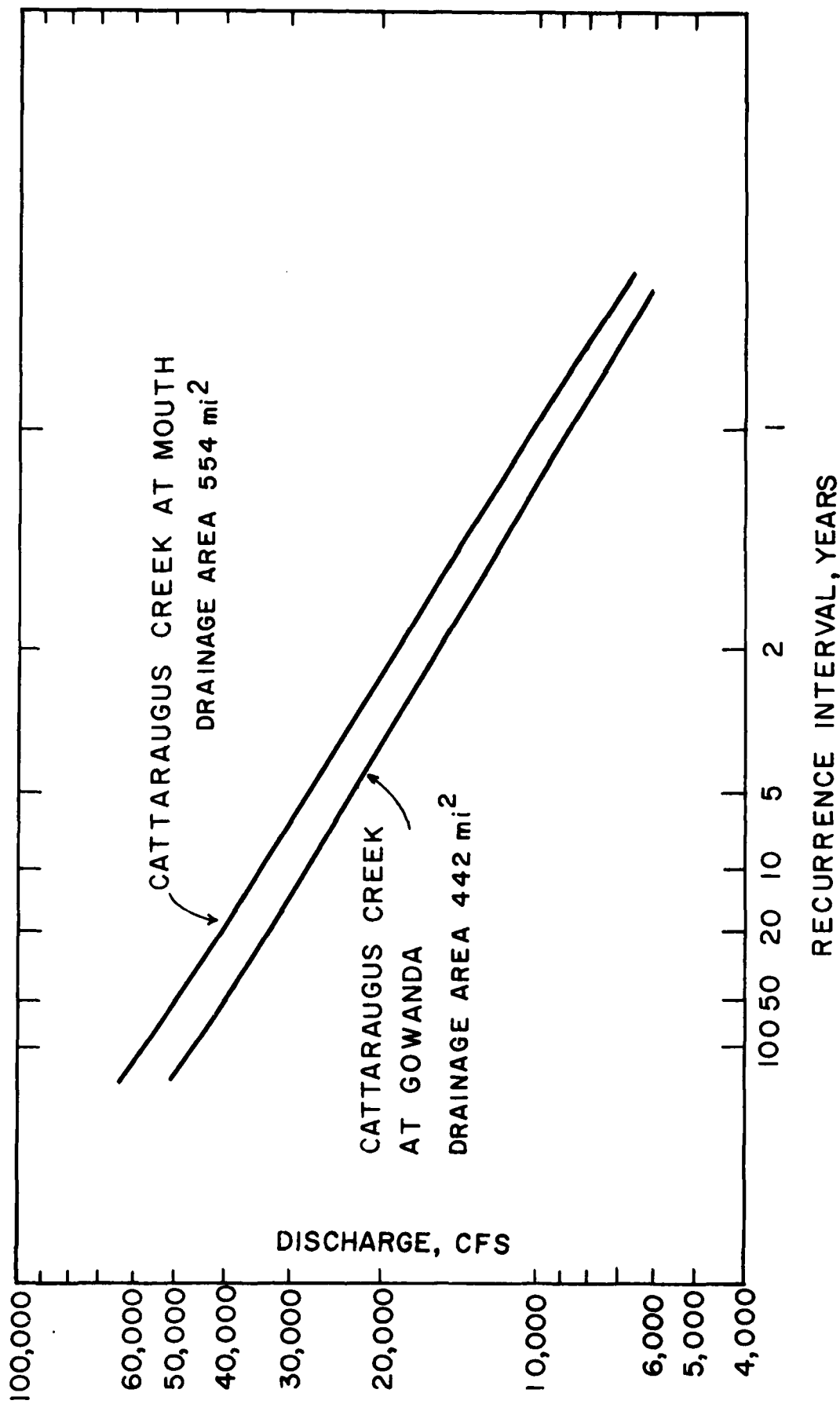


FIGURE 75

12. CONCLUSIONS

The objectives of this study were to 1) determine the pattern of sediment transportation and deposition by littoral and fluvial currents and 2) to propose a breakwater configuration that will have the least detrimental effects on the adjacent beaches.

Objective 1 is accomplished by a detailed analysis of littoral processes, sediment sources and distribution patterns, and shoreline morphology presented in the preceding paragraphs. Objective 2 is met in paragraph 9. The aspects of the sedimentary process-response model derived from the preceding analysis which are of most importance in the breakwater design are:

- 1) Net sediment flux along the southeast shore of Lake Erie, including the Cattaraugus Embayment, is from the west to the east. Sediment accumulations associated with both man made and natural features from Cleveland to Buffalo support this transport pattern. The volume of sediment in the littoral transport depends on the deep water wave energy distribution, the orientation of the shoreline, the nearshore bathymetry, and the conditions of the sediment source. Consequently, the sediment load is highly variable along the lake shore. To establish a meaningful numerical value for the littoral sediment load would require a much more extensive program than what was possible under the provision of this contract.
- 2) Specifically, within the Cattaraugus Embayment the variations in the sediment dispersal pattern reflect the location of the primary sediment source and the nearshore wave climate. Details of this follow.

3) Cattaraugus Creek, entering the lake at the center of the embayment, is the dominant source of sand and gravel. Some coarse grained sediment may be supplied to Cattaraugus beach from the Silver Creek headland and the pocket beaches beyond. No significant amount is contributed from Lotus Point.

4) Gravel lithology, beach gravel/sand ratio, and textural distribution of nearshore sand support the contention that the net coarse sediment flux within the Cattaraugus Embayment is from south to north.

5) Wave hindcast data show this transport pattern to be in complete accord with the prevailing wave conditions on the lake. Both wind generated current transportation and wave dominated sediment movement in the surf zone will cause a net mass flux to the north.

6) Characteristically, during southwesterly storms the littoral current velocities within the embayment are moderate at the southernmost segment of the beach, drop to a minimum near the creek mouth because the waves approach this segment almost perpendicularly to the beach, and increase further northward to reach a maximum near Lotus Point. This is very nearly also the pattern of variation in sediment transport rates.

7) Intermittent reversals in sediment transport direction can occur, however, as evidenced from the extensive sand deposits in the nearshore of Hanford Bay and the recurved spit on the north side of Cattaraugus Creek. Because the Hanford Bay area is subject to very small wave energies during southwesterly storms, sand brought down there during northwesterly storms is likely to remain.

8) A northward oriented spit forms at the mouth of Cattaraugus Creek as an extension of the beach at periods of low fluvial discharge.

Being controlled by the ratio of wave to stream power, the spit becomes enlarged and aligned transverse to the river channel during periods of low fluvial discharge. During periods of high discharge the spit is reoriented lakeward and may also be reduced in size.

9) Shallow water nearshore bars are found to exist, at least intermittently. During periods of constructional wave conditions these bars migrate onshore and weld onto the beach face.

10) During major storms beach berms are eroded and most of the sand and gravel transported lakeward. This leads to a lakeward progradation of the beach step and, possibly, to an increase in the volume of the nearshore bar system. During constructional wave conditions this sequence of events is reversed.

11) Wave conditions and sediment transport patterns in the fall of 1974 correspond well to those observed in the spring. Conclusions 1 through 10, therefore, are strengthened by the fall data. Wind data for 1974 further indicate that process-observations in the spring and fall of 1974 are representative for long-term average conditions on Lake Erie.

12) Two mechanisms for transport of coarse sediment across the mouth of Cattaraugus Creek have been identified: (1) spit growth across the mouth during low fluvial discharge followed by breaching of the spit during increased flow, and (2) offshore sediment movement during periods of high creek discharge followed by onshore wave induced bar migration.

13) A preliminary estimate of the rate of gravel (clasts > 8 mm) transport on the lower reaches of Cattaraugus Creek was made. For a

discharge of 22,000 cfs at the bridge of U.S. highways 20 and 5, the stream delivers about 120 m^3 per day. A 22,000 cfs flood has a recurrence interval of about 3 years and the peak discharge may last for 2 to 3 days. Therefore, an average annual gravel transport rate would be about 120 m^3 . This preliminary estimate ignores the < 8mm fraction and also ignores the role of smaller floods of greater frequency which would make the total sediment transport rate substantially higher.

REFERENCES

Anan, F. S., 1972, Hydraulic equivalent sediment analyzer (HESA): Coastal Research Center, Univ. of Massachusetts, Tech. Rept. No. 3-CRC, 38 p.

Bajorunas, L. and Duane, D. B., 1968, Shifting offshore bars and harbor shoaling: U. S. Lake Survey, Corps of Engineers, Misc. Paper 68-1, 11 p.

Calkin, P. E., 1970, Stand lines and chronology of the glacial Great Lakes in northwestern New York: Ohio Jour. Science, v. 70, p. 78-96.

Chow, V. T., 1959, Open-channel hydraulics, McGraw-Hill, New York, 680 p.

Coastal Engineering Research Center, 1966, Shore protection planning and design: Tech. Rept. No. 4, 401 p., plus appendix.

Cole, A. L., 1967, An evaluation of wind analysis and wave hindcasting methods as applied to the Great Lakes: Proc., 10th Conf. on Great Lakes Research, p. 186-196.

Corps of Engineers, U. S. Army, 1966, Interim report on Cattaraugus Creek Harbor, New York, 34 p. plus appendix.

Corps of Engineers, U. S. Army, 1968, Flood plain information, Cattaraugus Creek and Thatcher Brook, Irving, Sunset Bay and Gowanda, New York, 68 p.

Davis, R. A., Jr., Fox, W. T., Hayes, M.O., and Boothroyd, J. C., 1972, Comparison of ridge and runnel systems in tidal and non-tidal environments: Jour. Sedimentary Petrology, v. 42, p. 413-421.

Dyhr-Nielsen, M. and Sorensen, T., Some sand transport phenomena on coasts with bars: Proc., 12th Conf. on Coastal Engineering, Washington, D. C., p. 855-865.

Einstein, H. A., 1950, The bed-load function for sediment transportation in open channel flow: U. S. Dept. of Agriculture, Tech. Bull. No. 1026, 71 p.

Emery, K. O., 1961, A simple method of measuring beach profiles: Limnology and Oceanography, v. 6, p. 90-93.

Fahnstock, R. K. and Haushild, W. L., 1962, Flume studies of the transport of pebbles and cobbles on a sand bed: Geol. Soc. America, Bull., v. 73, p. 1431-1436.

Folk, R. L., 1968, Petrology of sedimentary rocks: Hemphill's, Austin, Texas, 170 p.

Graf, W. H., 1971, Hydraulics of sediment transport, McGraw Hill, New York, 513 p.

Hough, J. L., 1958, Geology of the Great Lakes: University of Illinois Press, Urbana, 313 p.

Hunt, I. A., Jr., 1959, Winds, wind set-ups and seiches on Lake Erie: U. S. Lake Survey, Corps of Engineers, Research Rept. No. 1-2, 59 p.

Komar, P. D., 1971, The mechanics of sand transport on beaches: Jour. Geophys. Research, v. 76, p. 713-721.

Lake Survey Center, 1974, Monthly bulletin of lake levels.

Muller, E. H., 1963, Geology of Chautauqua County, New York, Part II, Pleistocene geology: New York State Museum Bull. No. 392, 60 p.

_____, (in press) The surficial geology of the Niagara sheet, Geologic map of New York: New York State Museum.

National Oceanic and Atmospheric Administration, Daily Weather Maps, 1974.

NOAA-National Ocean Survey, Lake Survey Center: Water level records on the Great Lakes, 1973.

Nummedal, D., 1974, A methodology of paleohydraulics: Ph.D. Dissertation, University of Illinois, Urbana, Illinois, 310 p.

Petterssen, S., 1969, Introduction to Meteorology: 3rd ed., McGraw-Hill, New York, 333 p.

Saville, T., 1953, Wave and lake level statistics for Lake Erie: Beach Erosion Board, Tech. Memo. No. 37, 24 p.

Saylor, J. H. 1966a, Modification of nearshore currents by coastal structures: U. S. Lake Survey, Corps of Engineers, Misc. Paper 66-1, 14 p.

_____, 1966b, Currents at Little Lake harbor, Lake Superior: U. S. Lake Survey, Corps of Engineers, Research Rept. No. 1-1.

Shen, H. W., 1971, Total sediment load, Ch. 13: in River Mechanics, Shen, H. W. (ed.), Ft. Collins, Colorado, 1322 p.

Tesmer, I. H., 1963, Geology of Chautauqua County, New York, Part I, Bedrock geology: New York State Museum Bull. No. 391, 65 p.

U. S. Army Engineer District, Buffalo, 1972, Report of flood 1-7 March, 1972, western New York, 31 p.

Wilson, M. P., 1973, Gravity studies in the vicinity of Walnut Creek, southwestern New York: State University of New York at Fredonia, M. S. Thesis.

PLATES

Plate 1. Aerial view of a section of Cattaraugus Creek upstream of Gowanda. The channel is incised into predominantly shales of upper Devonian age.
Photo: June 13, 1974.

Plate 2. Aerial view of a Cattaraugus Creek gravel point bar. The dominant lithologies are siltstone, red sandstone, limestone, and a few crystalline rock fragments. Typical gravel size on the point bar in the picture is 5 centimeters. Photo: June 13, 1974.

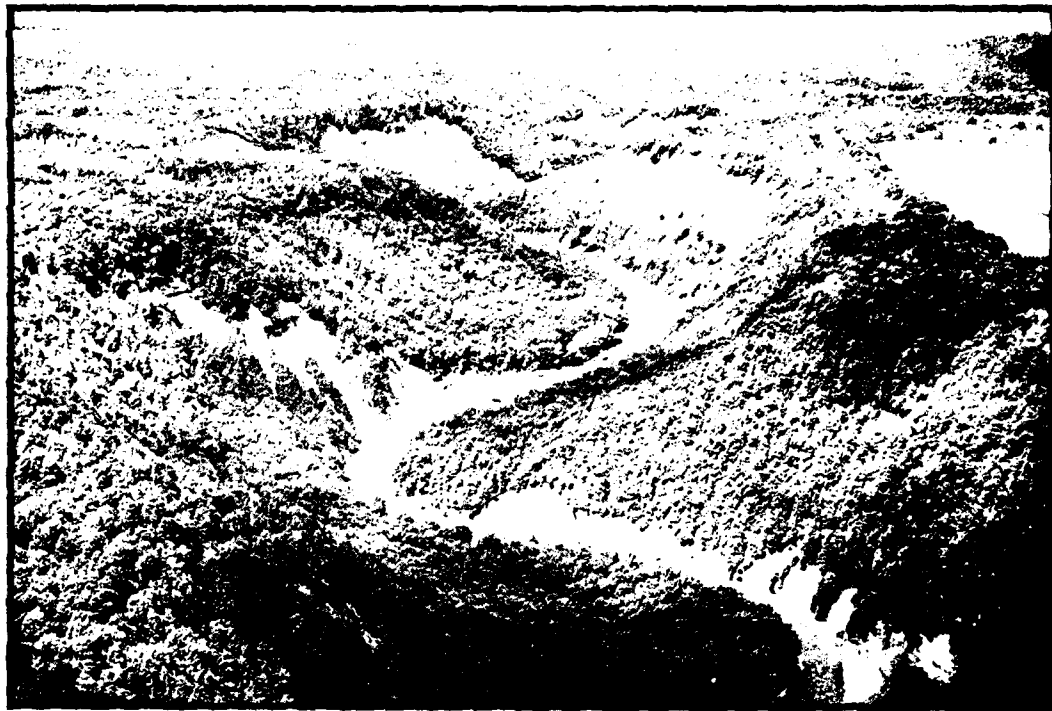


PLATE 1



PLATE 2

PLATES 1 AND 2

Plate 3. Wide beach. View northward from profile location Cat. 10 towards Lotus Point. Despite the proximity of the shale headland the lithological composition of the gravel at Cat. 10 is the same as that much further to the south. Note the multiple gravel berms. Photo: May 23, 1974.

Plate 4. Oblique aerial photograph of the Cattaraugus Embayment from 1000 feet. View towards the south. Note the waves breaking over the offshore sand bars and the spit on the south side of Cattaraugus Creek. The protuberance between Cat. 6 and Cat. 7 (Fig. 63) is clearly visible. Rip currents carry sediment lakeward. Photo: May 4, 1974.



PLATE 3



PLATE 4

PLATES 3 AND 4

Plate 5. Beach face at Cat. 6 during storm. The berm is eroded and the gravel deposited at the step which has prograded lakeward during the storm. The breakers are 4 to 6 feet high. Photo: June 11, 1974.

Plate 6. Beach face at Cat. 6. A wide gravel berm becoming more sandy as it grades into the back beach is typical of the constructional beaches in the Cattaraugus Embayment. The change from the previous photo was accomplished in less than 24 hours.
Photo: June 12, 1974.



PLATE 5



PLATE 6

PLATES 5 AND 6

Plate 7. View towards the north of the beach at profile location Cat. 5. Note multiple gravel berms and the sandy swash zone. Waves are breaking over the sub-aqueous spit at the upper left of the photo.

Photo: June 12, 1974.

Plate 8. View towards the south of the beach at profile location Cat. 5. Note the wide berm in the foreground which was welded onto the beach face by a ridge migrating landward during the waning stages of the storm. Photo: June 12, 1974.



PLATE 7

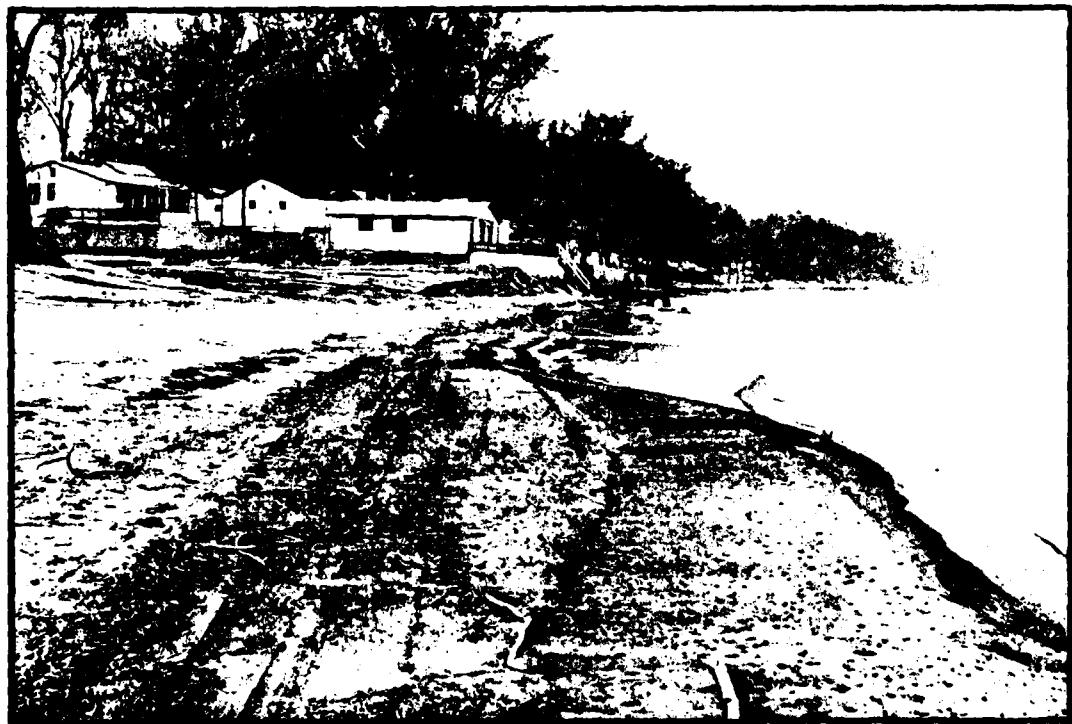


PLATE 8

PLATES 7 AND 8

Plate 9. View of the mouth of Cattaraugus Creek during a storm. Note the washover zone on the gentle south beach and the run-up on the steep northern beach. The waves approach almost perpendicular to the shore because of the large refraction. Photo: June 11, 1974.

Plate 10. Aerial photo of the mouth of Cattaraugus Creek right after a storm. Note the washover terrace forming at the neck of the north side recurved spit. View towards the south from about 500 feet. Photo: June 13, 1974.



PLATE 10

PLATES 9 AND 10

Plate 11. Oblique aerial view of the mouth of Cattaraugus Creek on October 26th, 1974. Water level about 3.5 feet above low water datum. View towards to south. A large recurved spit had been built northward across the channel mouth in response to southwesterly storm waves and low fluvial discharge prior to October 19th. During a minor flood just prior to October 19th the spit was breached giving rise to the two subaerial spit segments observed in this photo.

Compare to Figure 68 and Plate 10.



PLATE II

APPENDICES

Appendix I. Weather data for Buffalo, May 7 - June 13, 1974.

Appendix II. Littoral processes in the Cattaraugus Embayment, May 7 - June 13, 1974.

Appendix III. Lithological composition of Cattaraugus beach and source materials.

Appendix IV. Texture of Cattaraugus beach sediments.

Appendix V. Cattaraugus Creek stage readings at the Keene Marina staff gage.

Appendix VI. Recorded profiles of the Cattaraugus beach.

Appendix VII. A. Concentration of suspended sediment in surface samples from the breaker zone obtained during the storm of June 11, 1974.

B. Concentration of suspended sediment in Cattaraugus Creek at the Buffalo Rd. Bridge.

Appendix VIII. Texture parameters for nearshore sand in the Cattaraugus Embayment.

Appendix IX. Textural composition of the Cattaraugus Beach sand fraction.

APPENDIX I

Weather data for Buffalo. May 7th - June 13th, 1974. Data from NOAA Daily Weather Maps. All observations of 0700 EST.

<u>Date</u>	<u>Wind</u>		<u>Circulation</u>
	Dir. (Az.)	Speed (knots)	(Type of circulation affecting Lake Erie and location of the associated pressure center).
May 7	WSW	10	Anticyclonic
May 8	-	0	Anticyclonic
May 9	SSW	15	Cyclonic
May 10	NW	5	Cyclonic
May 11	SE	5	Anticyclonic
May 12	S	10	Cyclonic
May 13	W	15	Cyclonic
May 14	S	5	Cyclonic
May 15	S	10	Cyclonic
May 16	ESE	5	Anticyclonic
May 17	SW	15	Cyclonic
May 18	W	5	Straight Isobars
May 19	E	15	Anticyclonic
May 20	NE	5	Anticyclonic
May 21	-	0	Straight Isobars
May 22	SW	5	Cyclonic
May 23	SW	10	Cyclonic
May 24	SW	20	Cyclonic
May 25	W	10	Cyclonic
May 26	W	10	Cyclonic
May 27	SW	5	Cyclonic
May 28	SW	5	Cyclonic
May 29	SW	10	Cyclonic
May 30	NE	5	Cyclonic
May 31	SE	10	Cyclonic
June 1	N	5	Anticyclonic
June 2	S	5	Anticyclonic
June 3	SW	5	Anticyclonic
June 4	SSW	5	Anticyclonic
June 5	S	5	Anticyclonic
June 6	S	5	Straight Isobars
June 7	S	10	Straight Isobars
June 8	S	10	Straight Isobars
June 9	SSW	5	Cyclonic
June 10	SSW	15	Cyclonic
June 11	WSW	20	Cyclonic
June 12	SSW	10	Cyclonic
June 13	SSW	10	Straight Isobars

APPENDIX II

Littoral Processes in the Cattaraugus Embayment,
May 7 - June 13, 1974

Station Cat. 1

Date	Time (h)EST	Height (ft)	Waves			Longshore current (fps)	Wind	
			Period (sec)	Breaker angle rel. to shore	Dir. (az.)		Speed (mph)	
May 7	0835	2.0	4.3	10°N	1.6	270°	12	
May 8	0730	0.4	5.0	6°N	0	var.	0-4	
May 9	0800	0.4	3.5	12°N	0.05 S	--	0	
May 10	0813	0.7	3.0	2°N	0	5°	5-7	
May 11	0805	0.1	--	--	0	var.	0-4	
May 12	0850	0.3	1.5	38°N	0.6	250°	8-10	
May 13	0825	2.3	5.2	20°N	2.1	260°	15	
May 14	0745	0.3	3.3	15°N	0	--	0	
May 15	0900	0.8	3.3	18°N	1.5	235°	0-8	
May 16	0830	0.2	4.3	0°	0	--	0	
May 17	0910	0.9	2.5	18°N	1.1	237°	10	
May 18	0805	0.2	2.8	6°N	0	255°	5	
May 19	0815	1.1	3.0	10°S	0.9 S	58°	8	
May 20	0830	0.3	2.7	8°S	0.3 S	27°	5	
May 21	1350	0.1	1.5	--	0	--	0	
May 22	0907	0.2	1.9	10°	0.1	260°	5	
May 23	0925	1.0	2.8	4°	0.6	255°	5	
May 24	1000	1.2	2.9	7°	1.1	263°	15	
May 25	--	--	--	--	--	--	--	
May 26	0810	0.8	2.9	4°	0.6	243°	5	
May 27	0820	0.5	2.4	8°	0.2	265°	7	
May 28	0925	0.4	2.0	15°	0.6	280°	8	
May 29	0822	0.5	3.2	5°	0.3	--	0	
May 30	0825	0.1	1.8	0°	0	--	0	
May 31	1005	0.3	2.8	3°	0.1	var.	0-3	
June 1	0825	0.5	2.1	6°	0.3	274°	8	
June 2	0835	0.1	1.8	--	0	var.	2	
June 3	0825	>0.1	1.5	12°	0	--	0	
June 4	0820	0.1	2.5	0°	0	--	0	
June 5-10		No observations, waves negligible.						
June 11	1010	2.6	5.5	15°	1.0	255°	16	
June 12	0905	0.7	3.3	10°	0.8	255	12	
June 13	1345	0.7	2.5	10°	1.0	275°	15	

Station Cat. 3

Date	Time (h)EST	Height (ft)	Waves			Longshore current (fps)	Wind	
			Period (sec)	Breaker angle rel. to shore	Dir. (az.)		Speed (mph)	
May 7	0805	1.6	4.3	10°	0.8	265°	12	
	1700	2.0	5.2	6°	0.8	245°	15-20	
May 8	0710	0.3	--	--°	0	var.	0-3	
	1700	0.2	4.0	0°	0	--	0	
May 9	0735	0.5	3.0	10°	0.4	180°	0-8	
	1605	3.3	4.5	5°	1.4	226°	18-25	
May 10	0745	0.7	3.2	4°	0.2	0°	4	
	1620	0.7	3.0	0°	0.3	285°	9	
May 11	0750	<0.1	--	--	0	--	0	
	1605	0.3	2.0	15°S	0.3 S	35°	5-9	
May 12	0840	<0.1	--	14°	0	--	0	
	1700	0.4	3.5	9°	0.3	215°	5-8	
May 13	0800	2.2	4.5	8°	1.2	250°	20	
	1525	1.2	3.5	12°	1.3	250°	16	
May 14	0825	0.6	3.1	14°	0.9	205°	6-12	
	1710	1.7	3.0	10°	0.8	280°	12	
May 15	0835	1.7	3.0	18°	1.7	204°	10	
	1800	1.2	3.7	15°	1.4	255°	14	
May 16	0810	0.3	3.8	0°	0	162°	0-4	
	2015	0.4	2.5	0°	0	--	0	
May 17	0815	1.2	2.8	17°	1.1	230°	10	
	1630	1.0	3.0	2°	0.3	240°	7	
May 18	0735	0.3	2.2	2°	0	--	0	
	1915	0.2	1.8	20°S	0.2 S	40°	5	
May 19	0755	0.6	2.8	22°S	0.4 S	75°	4	
No evening observations, May 19-May 22.								
May 20	0805	0.3	2.7	6°S	--	110°	4	
May 21	1240	0.1	1.5	10°S	0	--	0	
May 22	0830	<0.1	--	--	0.2	--	0	
May 23	0855	2.3	2.9	5°	1.1	242°	15	
	1700	2.0	3.6	3°	1.4	242°	18	
May 24	0910	1.5	3.1	5°	1.8	257°	17	
	1750	1.3	4.9	7°	1.1	242°	18	
May 25	No observations.							
May 26	0745	1.0	3.0	0°	0	245°	8	
	1730	1.5	3.5	9°	1.2	244°	15	
May 27	0810	0.5	--	5°	0.2	260°	8	
	1730	1.0	3.2	10°	0.9	260°	11	
May 28	0845	0.8	2.5	8°	0.6	278°	4	
	2110	0.2	2.1	8°	0	--	0	

Station Cat. 3 (cont.)

Date	Time (h)EST	Height (ft)	Waves Period (sec)	Breaker angle rel. to shore	Longshore current (fps)	Wind	
						Dir. (az.)	Speed (mph)
May 29	0800	0.8	3.2	0°	0.1	234°	8
	1845	0.8	2.8	6°	0.3	--	0
May 30	0845	0.2	2.7	0°	0	--	0
	1930	0.2	2.9	0°	0	--	0
May 31	0930	0.3	2.6	6°	0.4	130°	6
	1830	1.0	2.3	3°	0.3	225°	7
June 1	0800	0.6	2.4	2°	0.2	273°	8
		No evening observations.					
June 2	0815	0.2	2.4	0°	0	--	0
	1615	0.3	1.7	8°	0.3	275°	7
June 3	0810	0.2	2.5	5°	0	--	0
		No evening observations.					
June 4	0900	0.1	--	--	0	--	0
		No evening observations.					
June 5-10		No observations.					
June 11	0925	3.3	6.0	--	0.2	255°	16
	1730	1.3	3.5	0°	0.7	252°	12
June 12	0835	1.2	3.5	12°	0.9	260°	12
		No evening observations.					
June 13	1250	1.0	3.4	5°	0.9	258°	15

Station Cat. 5

Date	Time (h)EST	Height (ft)	Waves		Longshore current (fps)	Wind	
			Period (sec)	Breaker angle rel. to shore		Dir. (az.)	Speed (mph)
May 7	0725	1.3	4.0	3°	0.5	270°	18
May 8	0655	0.5	3.5	3°	0.1	--	0
May 9	0715	0.6	3.0	5°	0.4	170°	0-8
May 10	0825	1.0	4.0	0°	0.3	325°	7
May 11	0735	0.1	2.5	--	0	105°	3-4
May 12	0730	<0.1	--	--	0	--	0
May 13	0800	2.2	4.5	8°	1.2	250°	20
May 14	0900	0.9	2.6	6°	1.5	208°	12-22
May 15	0820	1.3	3.0	17°	2.2	201°	24
May 16	0750	0.7	3.9	1°	0.3	165°	0-4
May 17	0725	0.8	2.5	10°	1.0	215°	10
May 18	0725	0.4	2.5	0°	0	--	0
May 19	0735	0.3	3.2	8°S	0.5 S	70°	8
May 20	0745	0.2	4.0	13°S	0.2 S	100°	6
May 21	1200	0.1	2.0	15°S	0.1 S	--	0
May 22	0815	<0.1	--	--	0.1	var.	2
May 23	0820	1.3	3.2	12°	1.5	240°	18
May 24	0810	1.2	3.1	0	1.6	235°	20
May 25	No observations.						
May 26	0730	0.8	2.8	5°S	1.2 S	238°	10
May 27	0750	0.3	2.2	0°	0.2	275°	5
May 28	0800	0.7	2.6	0°	0.5	245°	9
May 29	0745	0.8	3.4	0°	0.5	245°	8
May 30	0855	0.2	3.2	4°S	0.1 S	270°	3
May 31	0830	0.4	1.5	8°	0.6	190°	5
June 1	0750	0.5	2.3	0°	0.1	270°	7
June 2	0755	0.1	3.3	--	0	--	0
June 3	0800	0.1	1.8	--	0	--	0
June 4	0925	0.2	2.5	--	0	--	0
June 5-10	No observations, waves negligible.						
June 11	0840	5.0	7.0	--	0.5	250°	25
June 12	0805	1.0	3.4	0°	0.9	252°	12
June 13	1200	0.5	3.6	0°	0.6	250	9

Station Cat. 6

Date	Time (h) EST	Height (ft)	Waves			Longshore current (fps)	Wind	
			Period (sec)	Breaker angle rel. to shore	Dir. (az.)		Speed (mph)	
May 7	0945	2.3	5.0	0°	--	265°	14	
May 8	0805	0.4	5.3	0°	0.1	--	0	
May 9	0840	1.0	3.5	4°	0.7	192°	4-8	
May 10	0930	0.7	3.5	12°S	0.6 S	335°	10-12	
May 11	0905	0.1	--	0°	0	--	0	
May 12	0834	0.5	1.6	5°	0.4	210°	5-8	
May 13	0900	3.3	5.2	5°	var.	262°	18	
May 14	0945	0.7	3.1	10°	0.8	190°	10	
May 15	0940	2.3	3.6	12°	1.7	234°	20	
May 16	0900	0.3	4.0	0°	0.1	--	0	
May 17	1005	1.7	--	14°	1.2	235°	15	
May 18	0830	0.3	3.0	2°	0	260°	5	
May 19	0850	0.7	3.5	2°S	0.5 S	55°	10	
May 20	0910	0.4	3.0	4°S	0.2 S	112°	10	
May 21	0900	0.1	--	4°S	0.1 S	var.	4	
May 22	0942	0.1	--	0°	0.3	255°	5	
May 23	1000	2.0	3.5	8°	1.2	240°	8	
May 24	1105	2.0	3.6	10°	1.5	260°	20	
May 25	No observations.							
May 26	0830	1.5	3.0	6°S	0.7 S	265°	8	
May 27	0900	0.6	2.5	2°S	0.1 S	280°	9	
May 28	1005	1.0	2.1	0°	0.5	278°	7	
May 29	0902	0.3	3.0	2°	0.4	245°	8	
May 30	1005	0.4	2.9	5°	0.1 S	330°	4	
May 31	1050	1.2	3.1	3°	1.2	207°	12	
June 1	0900	0.8	2.1	0°	0.1	280°	7	
June 2	0907	<0.1	--	--	0.1 S	320°	5	
June 3	0850	0.3	2.5	0°	0.1	225°	7	
June 4	1055	0.1	2.4	0°	0.1	--	0	
June 5-10	No observations, waves negligible.							
June 11	1103	6.7	6.5	--	0.9	275°	20	
June 12	1005	2.7	3.5	10°	0.9	250°	14	
June 13	1425	2.0	3.4	5°	0.8	250°	14	

Station Cat. 8

Date	Time (h)EST	Height (ft)	Waves			Longshore current (fps)	Wind	
			Period (sec)	Breaker angle rel. to shore	Dir. (az.)		Speed (mph)	
May 7	1025	2.3	5.0	5°	1.3	270°	14	
May 8	0825	0.6	4.5	5°	0.2	--	0	
May 9	0910	1.0	3.0	18°	1.0	195°	0-8	
May 10	1005	0.8	3.0	0°	0.3 S	330°	5-6	
May 11	0855	0.1	3.5	0°	0	--	0	
May 12	0850	0.5	1.6	9°	0.6	235°	8	
May 13	0930	3.3	6.1	7°	2.0	255°	14	
May 14	1020	1.7	3.3	11°	1.6	200°	12	
May 15	0955	2.5	4.0	15°	1.8	235°	16	
May 16	0920	0.3	4.3	0°	0.3 S	10°	10	
May 17	1035	1.5	4.3	7°	1.2	230°	8	
May 18	0900	<0.1	3.2	4°	0.1	240°	4	
May 19	0915	0.7	3.1	14° S	0.9 S	30°	10	
May 20	0940	0.4	3.5	11° S	0.3 S	--	0	
May 21	0750	0.1	--	--	0	--	0	
May 22	1002	0.2	1.6	6°	0.3	190°	4	
May 23	1025	1.8	3.7	9°	1.3	220°	8	
May 24	1200	2.2	4.2	8°	1.8	240°	16	
May 25	No observations.							
May 26	0855	1.2	3.1	0°	0	240°	10	
May 27	0930	0.5	2.5	3° S	0.1 S	315°	6	
May 28	1040	0.7	2.0	7°	0.4	270°	5	
May 29	0920	1.2	3.4	6°	0.6	242°	7	
May 30	0945	0.3	2.6	6°	0	--	0	
May 31	1130	1.2	3.3	6°	1.4	190°	12	
June 1	0920	0.7	2.0	0°	0.2	270°	7	
June 2	0930	0.2	2.6	--	0.1 S	335°	5	
June 3	0905	0.3	3.5	0°	0.2	225°	3	
June 4	1023	0.1	2.6	0°	0	--	0	
June 5-10	No observations, waves insignificant.							
June 11	1145	4.0	6.0	5°	1.5	225°	14	
June 12	1050	2.0	3.3	10°	1.4	245°	12	
June 13	1545	1.3	3.5	10°	0.9	250°	9	

Station Cat. 10

Date	Time (h)EST	Height (ft)	Waves			Longshore current (fps)	Wind	
			Period (sec.)	Breaker angle rel. to shore	Dir. (az.)		Speed (mph)	
May 7	1100	2.0	5.0	5°	1.4	265°	14	
May 8	0843	0.6	5.0	0°	0.3	--	0	
May 9	0935	1.2	3.0	15°	0.7	195°	0-8	
May 10	1100	0.8	3.5	2°S	0.3 S	348°	5-6	
May 11	0845	0.1	3.5	0°	0	--	0	
May 12	0915	0.5	2.0	5°	1.2	235°	8-10	
May 13	1000	3.3	5.4	9°	2.5	240°	14	
May 14	1100	1.8	3.1	13°	2.0	192°	16	
May 15	1010	2.8	4.1	13°	2.6	210°	10	
May 16	0940	0.8	4.3	0°	0.4 S	6°	6-8	
May 17	1100	2.0	4.0	23°	1.7	220°	14	
May 18	0945	0.3	3.5	3°	0.1	--	0	
May 19	0935	0.9	3.8	15°S	0.9 S	12°	4	
May 20	1005	0.3	3.5	14°S	0.3 S	55°	3	
May 21	1040	0.1	--	5°S	0.2 S	--	0	
May 22	1020	0.5	1.5	13°	0.4	193°	4	
May 23	1045	2.8	3.7	20°	2.8	225°	12	
May 24	1225	2.5	4.1	10°	3.3	245°	15	
May 25	No observations.							
May 26	0915	1.3	3.1	0°	0	240°	9	
May 27	0950	0.5	2.5	4°S	0	310°	5	
May 28	1105	0.7	2.5	0°	0.3	325°	4	
May 29	0940	1.3	2.8	8°	0.8	235°	8	
May 30	0930	0.3	3.2	0°	0	270°	3	
May 31	1225	1.0	2.9	8°	0.9	185°	10	
June 1	0945	0.8	2.3	4°	0.2	265°	7	
June 2	0950	0.2	1.8	20°S	0.3 S	340°	4	
June 3	0920	0.2	2.7	2°	0.2	230°	4	
June 4	0950	0.1	2.5	0°	0	--	0	
June 5-10	No observations, waves insignificant.							
June 11	1217	3.3	6.0	10°	2.3	240°	16	
June 12	1115	3.3	3.5	7°	2.1	230°	12	
June 13	1615	1.3	3.6	10°	1.6	205°	11	

APPENDIX III

Lithological Composition of Cattaraugus Beach and Source Materials.

Cattaraugus Beach Active Berm

Sample Station	Siltstone and Sandstone (%)	Dark Shale (%)	Light Shale (%)	Crystalline Rocks and Chert (%)
1	80	4	0	16
2	no gravel	-	-	-
3	50	44	0	6
4	64	18	0	18
5	76	16	0	8
6	64	26	2	8
7	70	18	2	10
8	54	10	6	30
9	64	14	8	14
10	38	4	0	58
11	52	42	0	6
12	52	36	2	10
13	54	30	8	8
14	44	48	2	6
15	44	30	4	22
16	46	28	4	22
17	60	2	8	30
18	70	14	4	12
19	56	30	0	14
20	68	24	0	8
21	60	26	2	12
22	44	50	2	4
23	38	46	8	8
24	50	46	0	4
25	68	18	2	12
26	50	8	8	34
27	66	20	2	12
28	no gravel	-	-	-
29	66	0	0	34
30	50	0	0	50
31	62	0	0	38
32	62	0	0	38
33	48	0	0	52
34	52	0	0	48
35	62	0	0	38
36	60	0	0	40
37	no gravel	-	-	-
38	58	2	0	40
39	38	0	0	62
40	52	0	0	48
41	78	0	0	22
42	60	0	0	40
43	46	2	0	52
44	66	0	0	34
45	56	0	0	44
46	48	2	0	50
47	66	0	0	34
48	50	0	0	50
49	no gravel	-	-	-
50	no gravel	-	-	-
51	44	0	0	56
52	52	0	0	48
53	64	0	0	36
54	56	0	0	44
55	62	0	0	38

Cattaraugus Beach High Level Storm Berm

Sample Station	Siltstone and Sandstone (%)	Dark Shale (%)	Light Shale (%)	Crystalline Rocks and Chert (%)
1	68	6	0	26
2	60	34	0	6
3	no storm berm	-	-	-
4	78	6	2	14
5	76	18	0	6
6	72	10	4	14
7	constructional activity	-	-	-
8	66	16	2	16
9	56	2	2	40
10	64	6	2	28
11	64	30	2	4
12	66	26	6	2
13	62	26	6	6
14	52	28	0	20
15	48	30	2	20
16	68	18	0	14
17	70	12	2	16
18	68	22	0	10
19	46	54	0	0
20	58	38	0	4
21	54	28	14	4
22	58	30	10	2
23	62	30	6	2
24	54	40	4	2
25	64	22	2	12
26	74	18	2	6
27	62	32	2	4
28	82	0	2	16
29	82	2	0	16
30	64	0	0	36
31	78	0	0	22
32	86	0	0	14
33	84	2	2	12
34	74	4	0	22
35	84	0	0	16
36	84	0	0	16
37	80	4	0	16
38	82	0	0	18
39	80	2	0	18
40	94	2	0	4
41	94	2	0	4
42	80	4	0	16
43	82	0	0	18
44	90	2	2	6
45	80	2	4	14
46	80	0	0	20
47	88	2	0	10
48	84	2	4	10
49	76	0	4	20
50	82	0	0	18
51	92	0	0	8
52	86	0	6	8
53	96	2	0	2
54	78	0	0	22
55	84	4	4	8

Sample Station	Siltstone and Sandstone (%)	Dark Shale (%)	Light Shale (%)	Crystalline Rocks and Chert (%)
Lotus Point and Bay				
1	54	0	0	46
2	66	0	0	34
3	76	2	0	22
4	62	0	0	38
5	84	0	4	12
6	78	4	2	16
7	64	2	0	34
Silver Creek Point Bars				
1	34	50	14	2
2	22	66	8	4
3	20	52	26	2
4	20	58	20	2
5	16	68	14	2
Walnut Creek Point Bars				
1	44	42	6	8
2	36	42	16	6
Silver Creek Bay				
1	40	42	10	8
2	28	52	18	2
3	28	60	8	4
4	50	34	6	10
5	50	36	2	12
Cattaraugus Creek Point Bars				
1	80	0	8	12
2	88	0	0	12
3	75	7	0	18
4	87	4	0	9
5	80	5	0	15

APPENDIX IV

Texture of Cattaraugus Beach Sediments

Method. The texture was determined at 57 sample stations evenly spaced along the beach. At each station the beach was divided into texturally homogenous zones from the step to the dune ridge or seawall. For each zone the following parameters were determined: width of zone, w_i ; percent gravel, p_i ; typical gravel size, d_i ; and typical sand size, s_i .

If the number of homogenous zones is n , the total gravel percentage for the beach at any one station (P) is computed from

$$P = \frac{\sum_{i=1}^n w_i p_i}{\sum_{i=1}^n w_i} 100$$

South Beach

Sample Station	No. of Zones	Size Range (cm)	Gravel Range in Per Cent	Sand Size Range, ϕ	Total Gravel Percentage
1	4	1-5	5-100	.50-.75	43
2	5	3-7	3-95	.75	24
3	3	3-4	15-100	1.50	43
4	4	3-7	2-95	.50-1.25	21
5	5	3-6	3-50	.50-1.75	21
6	4	3-5	5-50	.75-1.5	40
7	5	3-5	2-80	.25-1.25	46
8	5	3-5	5-80	.50-1.25	41
9	5	3-5	10-100	-.25-1.25	72
10	5	3	2-95	0-1.75	67
11	3	2-4	2-100	-1.0-(-.25)	81
12	4	1-3	20-100	-1.0-(-.75)	70
13	2	2-3	10-100	1.0	70
14	3	3-5	2-100	.5	89
15	3	2-7	5-100	1.0	26
16	5	2-6	30-100	.25-1.25	70
17	Seawall - no beach				
18	5	3-6	15-100	.50-.75	67
19	5	3-4	20-100	1.25	54
20	4	3-4	15-95	1.25-1.75	28
21	3	2	2-40	1.25-2.00	10
22	2	2	30-100	1.75	12
23	2	3	30-100	1.25-1.75	24
24	5	3-4	5-100	1.25-1.50	18
25	3	2	5-85	1.50-2.25	29
26	2	1-2	5-100	.75-1.50	3
27	4	1-2	2-100	.75-1.75	23
28	2	2-3	30-40	.75-1.00	36

North Beach

Sample Station	No. of Zones	Gravel Size Range (cm)	Range in Per Cent	Sand Size Range, ϕ	Total Gravel Percentage
29	4	3-5	40-100	.00-.75	60
30	4	3-4	5-90	.75-1.00	58
31	4	3-4	9-100	.25-1.25	12
32	4	2-5	2-100	.50-.75	6
33	4	.5-3	2-100	.75-1.25	30
34	4	2-3	2-40	.75-1.00	8
35	3	3-4	10-100	.75-1.00	17
36	3	2-4	8-100	.50-.75	21
37	3	3-4	5-100	.75-1.25	9
38	3	.5-6	5-100	.75-1.00	26
39	3	1-5	5-100	.50-1.25	17
40	3	2-4	15-80	.75-1.00	22
41	4	2-5	5-60	1.00-.75	19
42	4	2-4	10-90	.75	41
43	3	1-3	5-50	-.25-1.00	33
44	6	1-5	2-95	.50-1.00	39
45	4	1-3	2-95	.25-1.00	35
46	5	1-4	10-100	.75-1.00	35
47	4	.5-4	5-100	.00-.75	49
48	6	.5-4	20-95	.50-1.25	46
49	6	1-3	2-100	.50-1.00	44
50	5	1-5	20-100	.50-1.00	52
51	4	2-4	10-100	.50-1.00	35
52	5	1-4	2-30	.50-1.00	8
53	5	2-4	2-95	.75-1.00	52
54	4	1-4	30-75	.75	64
55	5	1-4	5-95	.50-1.00	34
56	5	1-4	2-100	.75-1.00	20
57	5	3-10	2-95	.50-1.00	26

APPENDIX V

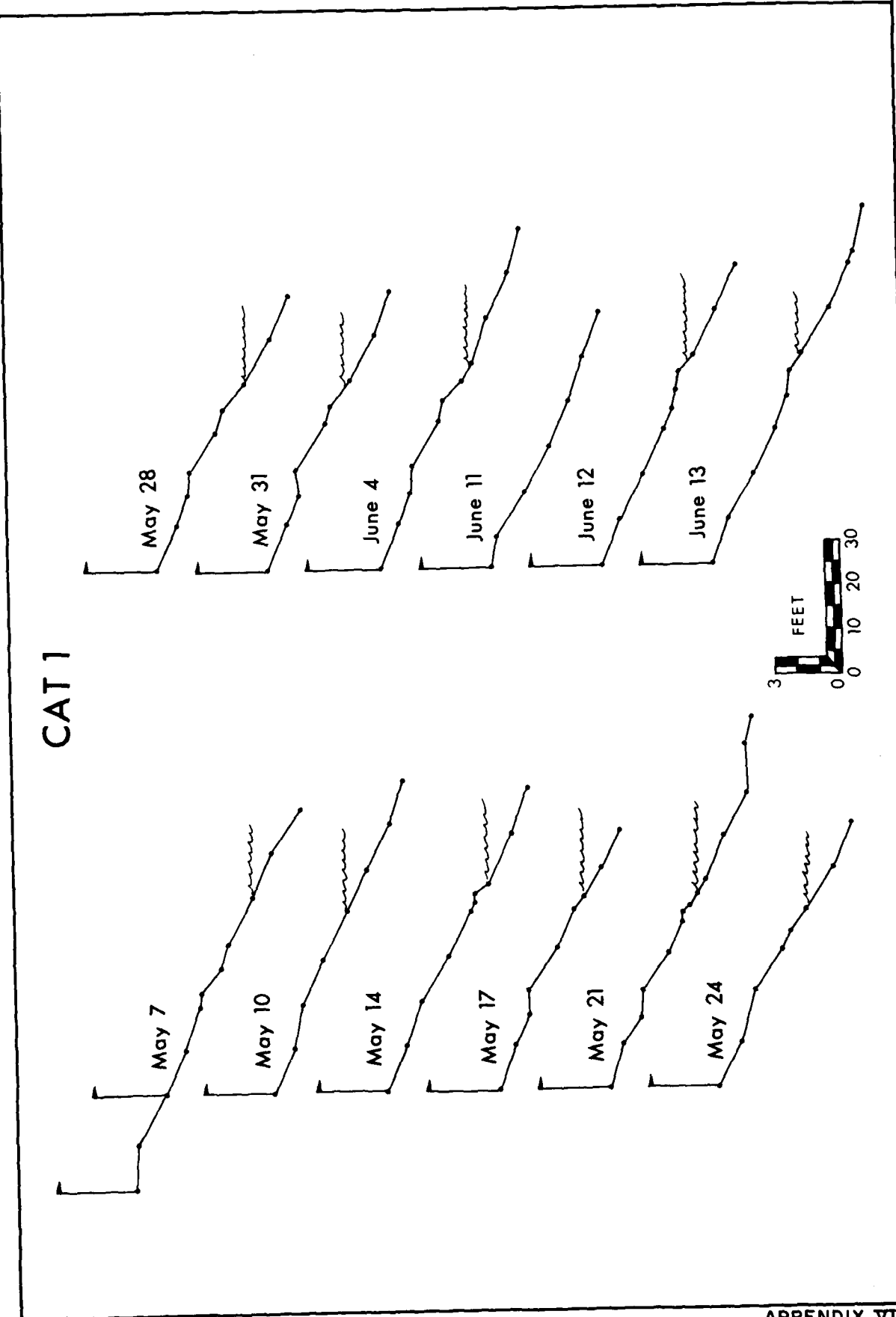
Cattaraugus Creek Stage Readings at the Keene Marina Staff Gage

Date	Time	Stage	Creek Discharge
May 9	1700	5.10	moderate flood
May 10	0805	4.70	moderate flood
May 10	1700	4.34	moderate flood
May 11	0830	4.40	low discharge
May 11	1345	4.38	low discharge
May 12	0830	4.54	low discharge
May 12	1800	5.36	moderate flood
May 13	0815	5.10	moderate flood
May 13	1625	5.26	moderate flood
May 14	0835	4.68	moderate flood
May 14	1240	4.78	waning flood
May 14	1810	5.52	waning flood
May 15	0915	4.88	waning flood
May 15	1910	4.82	moderate flood
May 16	0845	4.48	moderate flood
May 16	2115	4.18	moderate flood
May 17	0820	4.78	increasing flood
May 17	1500	5.68	flood peak
May 17	1730	5.88	flood peak
May 17	1930	5.58	flood peak
May 18	0825	4.86	waning flood
May 18	1610	4.56	waning flood
May 19	0830	4.30	low discharge
May 20	0815	4.64	low discharge
May 20	2245	4.70	low discharge
May 21	1400	4.86	low discharge
May 22	0915	4.45	low discharge
May 23	1205	4.98	low discharge
May 23	1850	5.10	low discharge
May 24	0910	4.85	low discharge
May 24	1845	4.75	low discharge
May 25	1830	5.05	low discharge
May 26	0830	4.85	low discharge
May 27	0850	4.65	low discharge
May 27	1815	4.85	low discharge
May 28	0900	4.72	low discharge
May 28	1400	4.60	low discharge
May 28	2200	4.70	low discharge

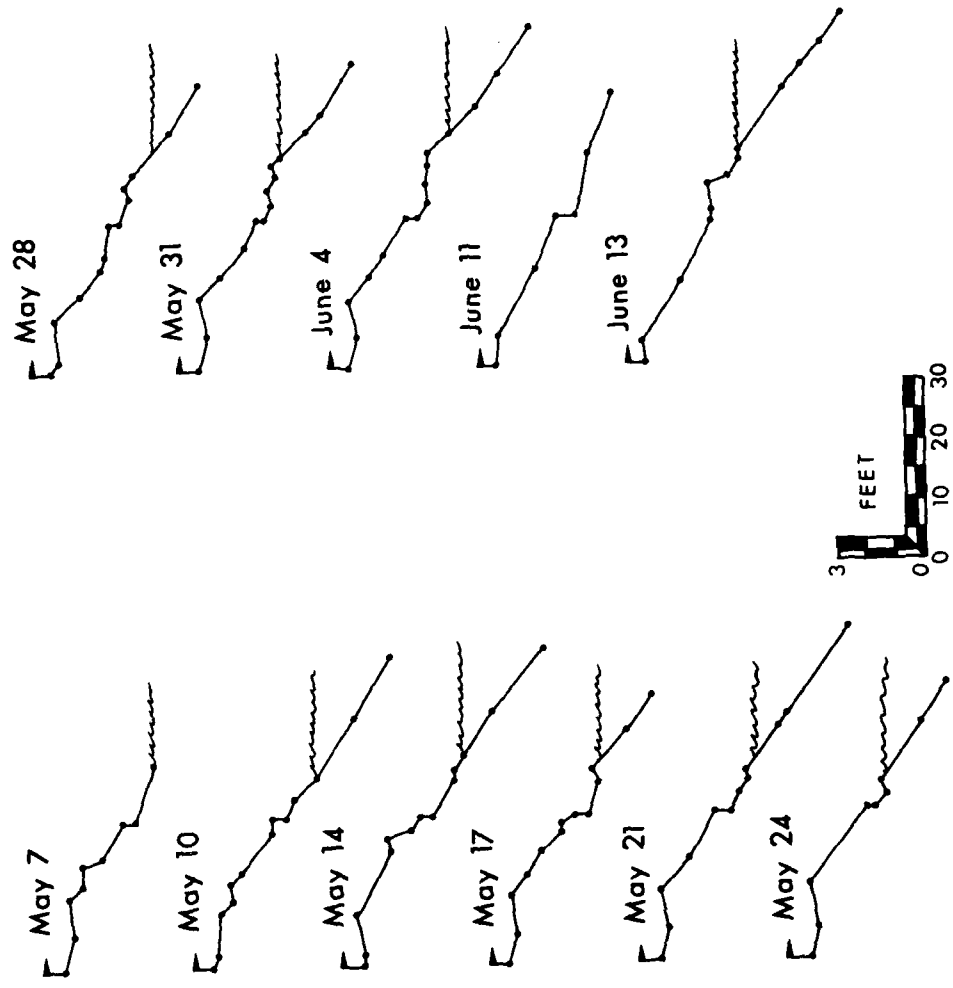
Date	Time	Stage	Creek Discharge
May 29	0830	4.60	low discharge
May 29	0745	4.75	low discharge
May 30	1005	4.68	low discharge
May 31	0930	4.68	low discharge
June 1	0845	4.68	low discharge
June 2	0830	4.72	low discharge
June 3	0900	4.60	low discharge
June 4	1015	4.50	low discharge
June 5	1030	4.50	low discharge
June 6	0835	4.45	low discharge
June 7	1100	4.40	low discharge
June 8	1300	4.50	low discharge
June 9	1230	4.40	low discharge
June 10	1100	4.70	low discharge
June 11	0930	5.35	low discharge
June 11	1820	4.65	low discharge
June 12	0900	4.72	low discharge
June 12	2130	4.64	low discharge

APPENDIX VI
Recorded Profiles of the Cattaraugus Beach

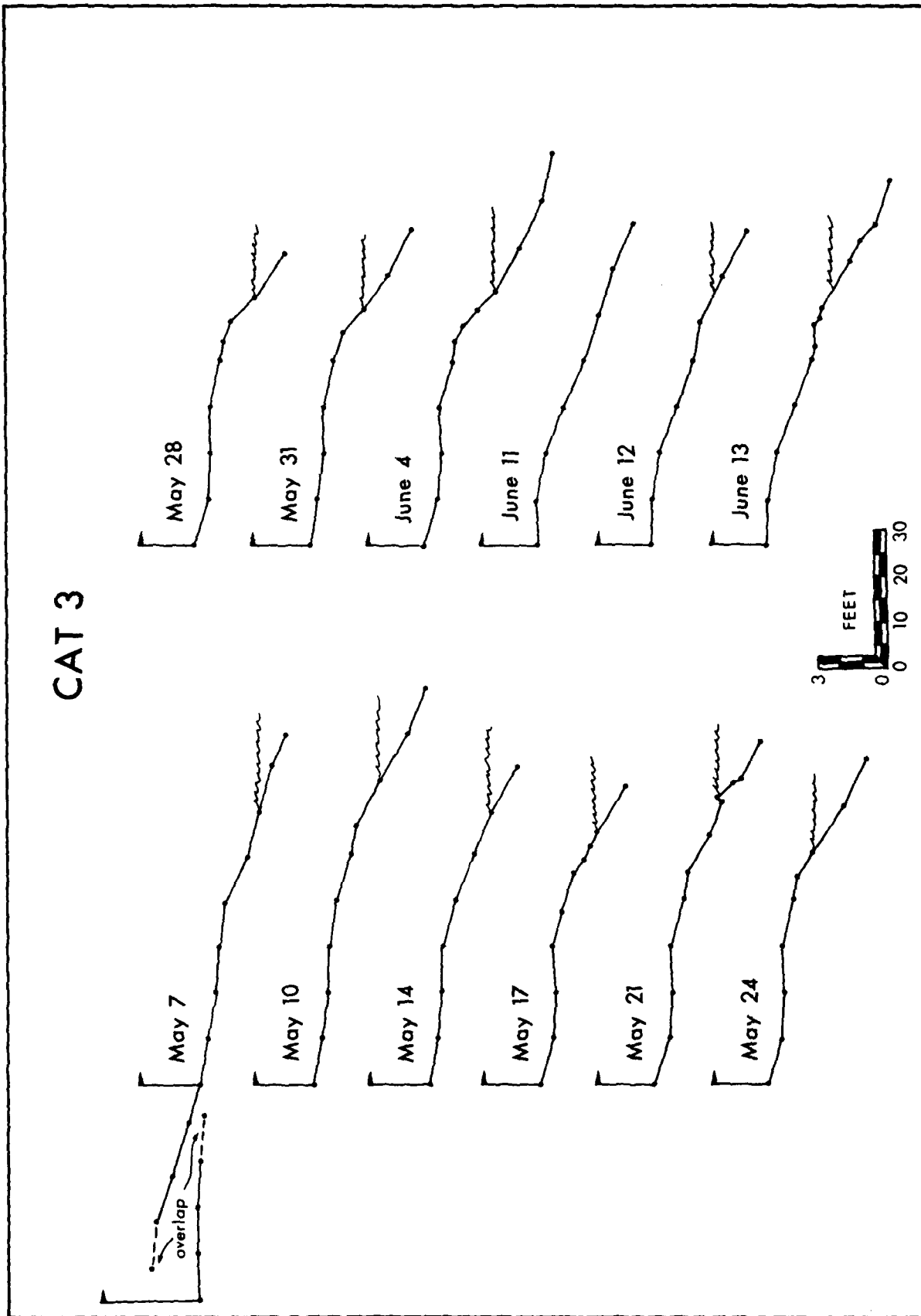
CAT 1



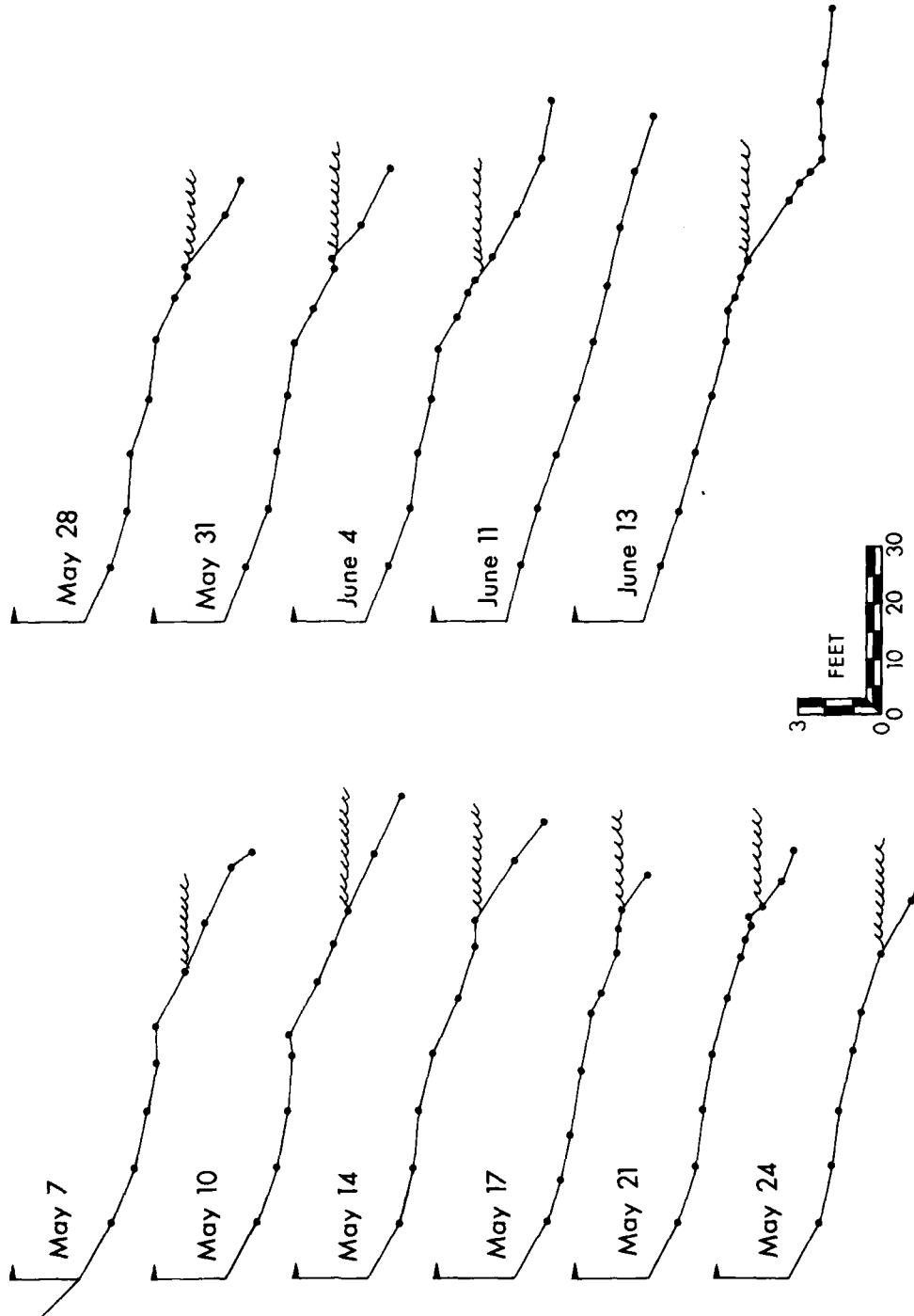
CAT 2



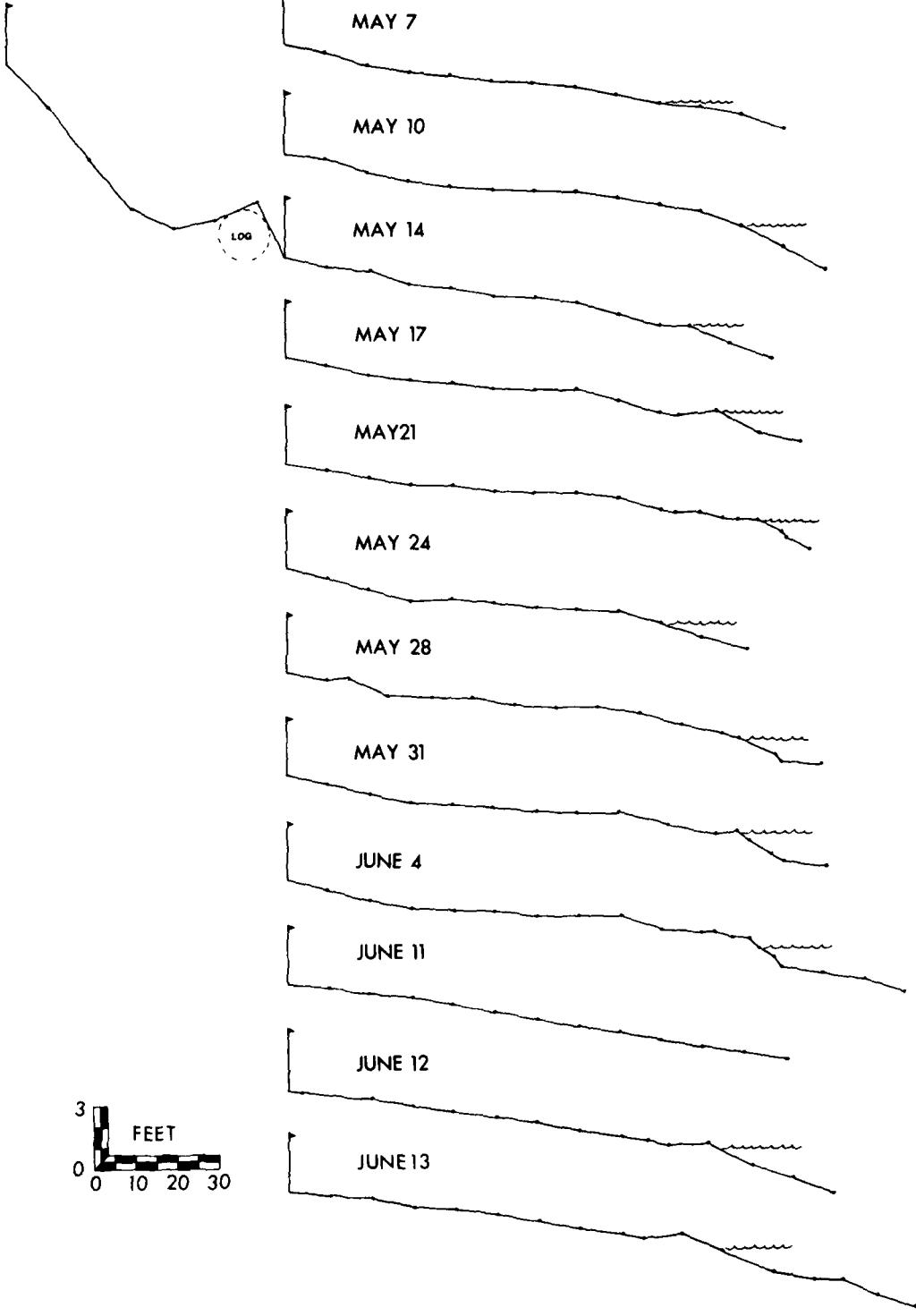
CAT 3



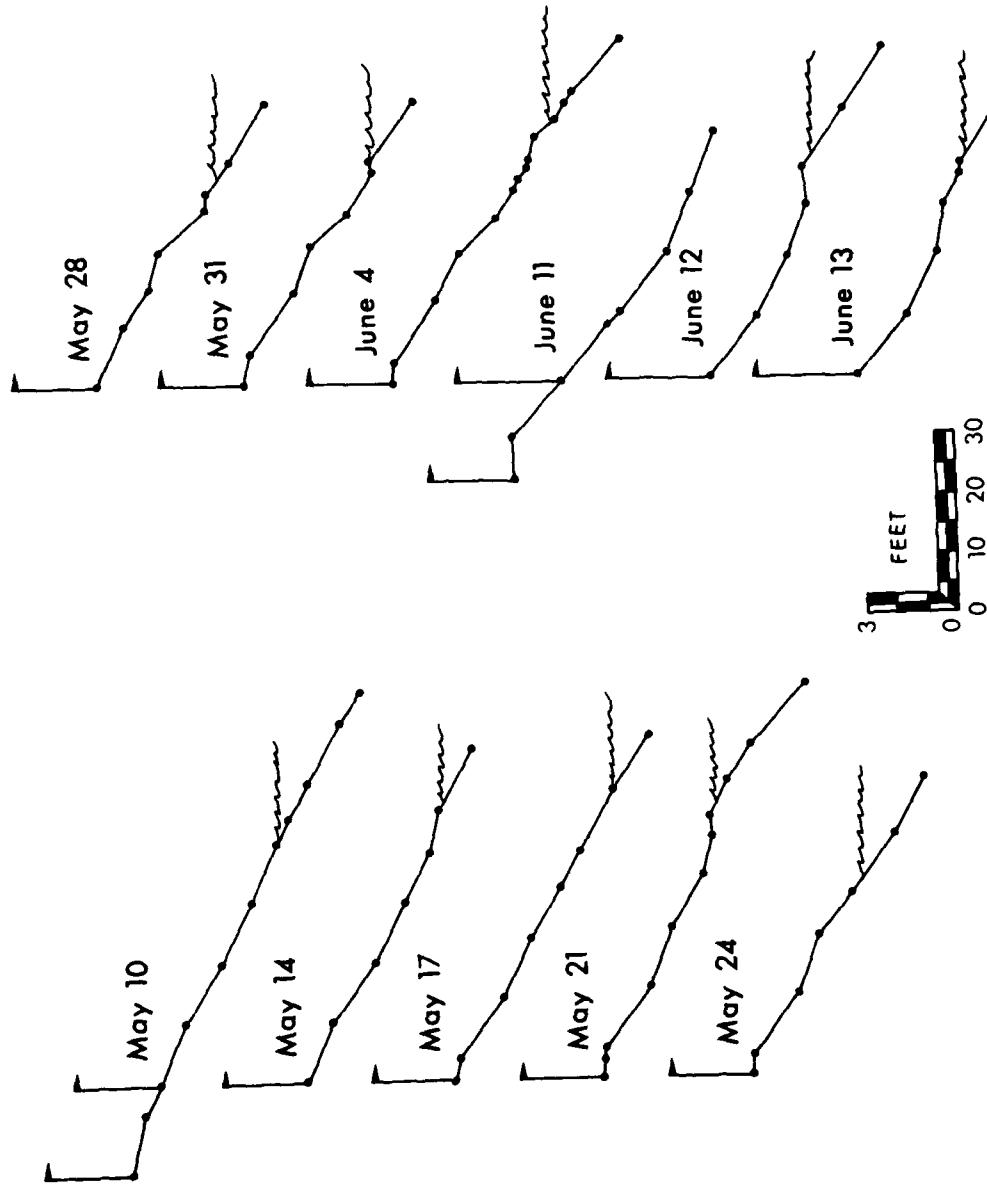
CAT 4



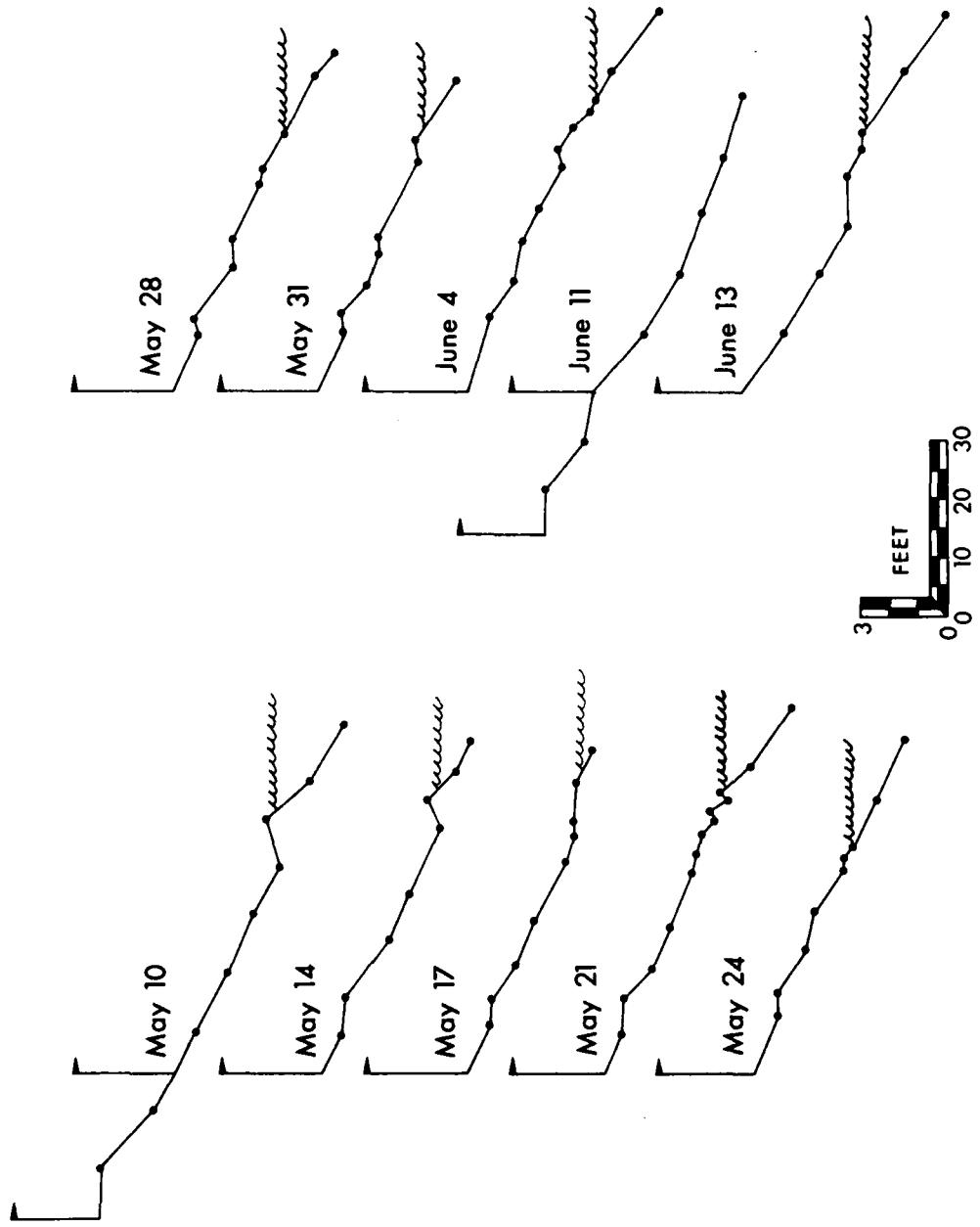
CAT 5



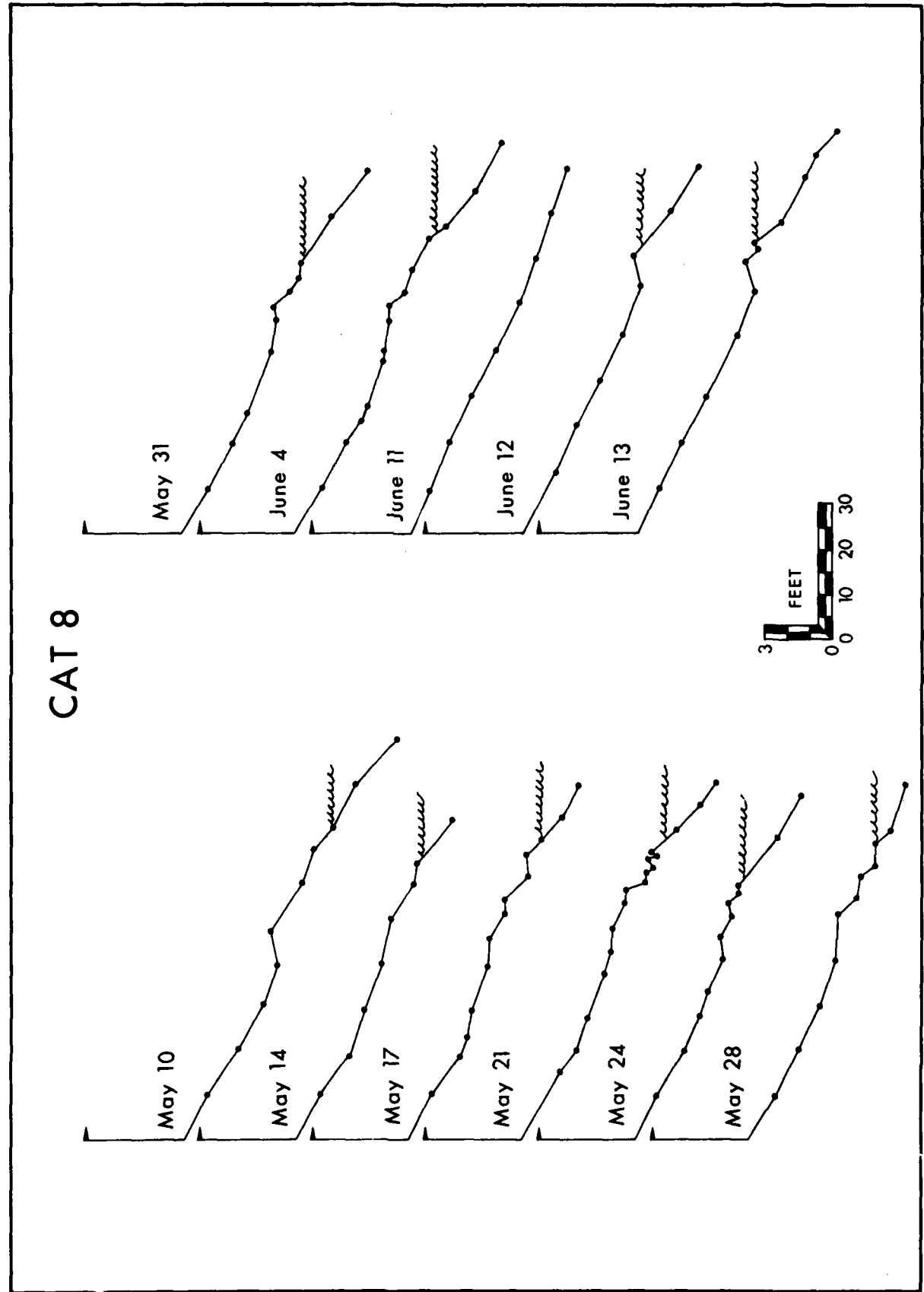
CAT 6



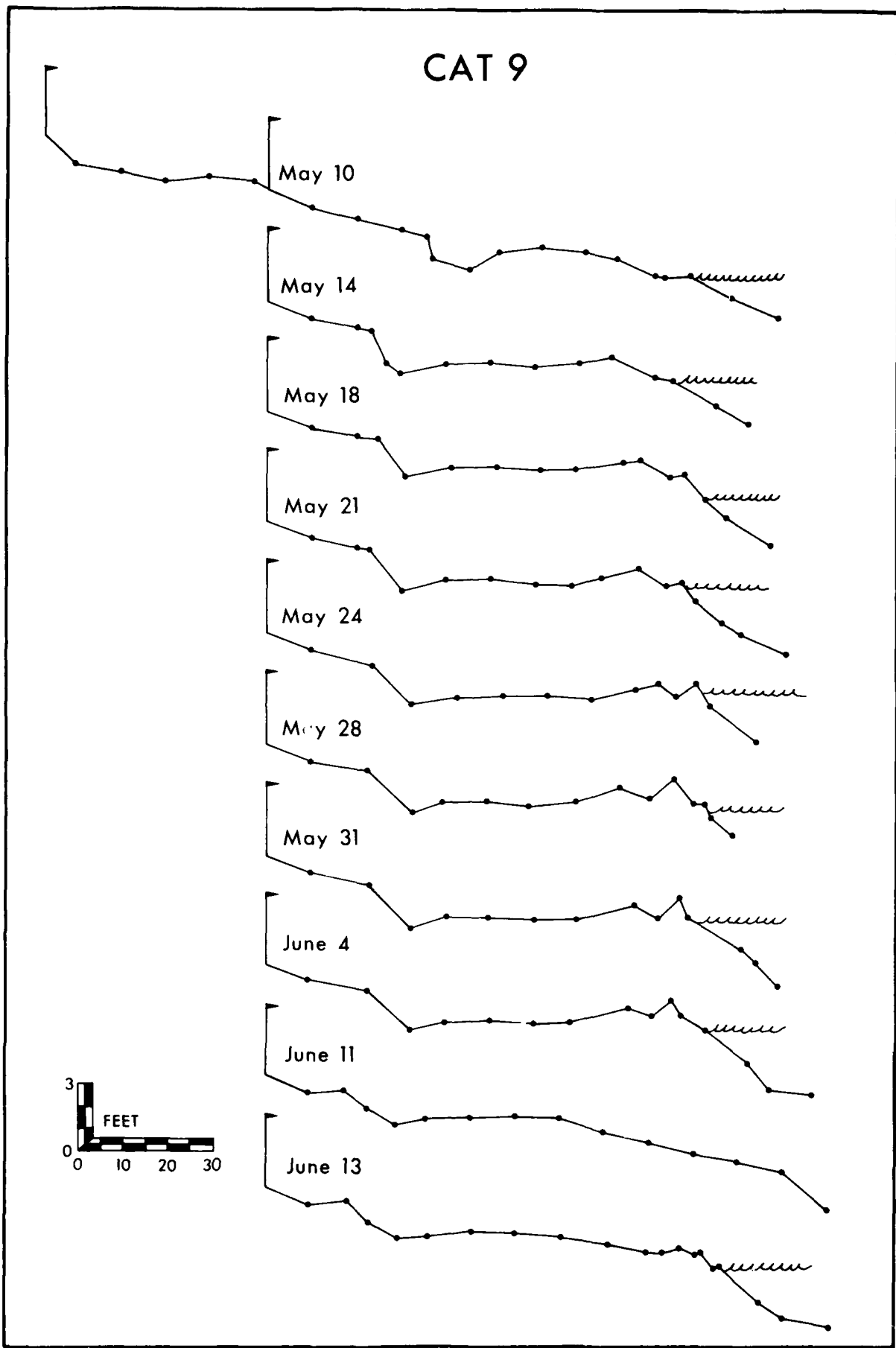
CAT 7



CAT 8



CAT 9



AD-A102 282

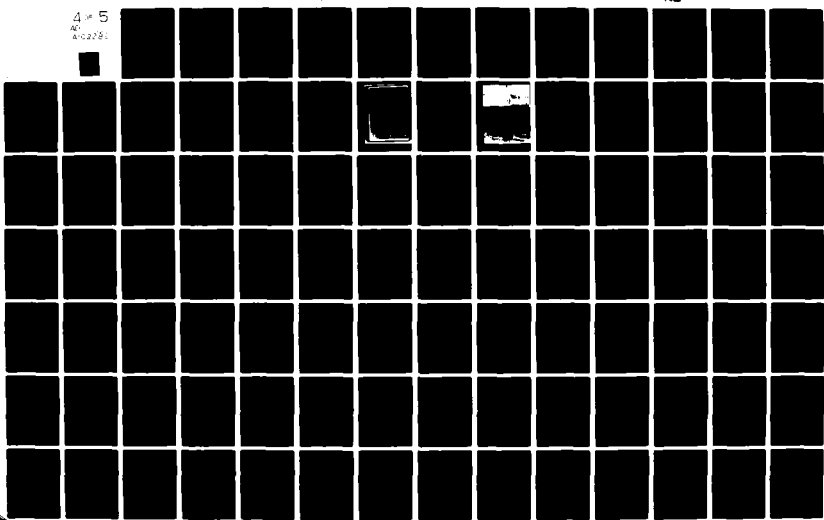
STATE UNIVERSITY OF NEW YORK COLL AT FREDONIA DEPT 0--ETC F/G 8/8
CATTARAUGUS CREEK HARBOR, NEW YORK GENERAL DESIGN MEMORANDUM, P--ETC(U)
MAR 76

DACW49-74-C-0118

NL

UNCLASSIFIED

4 x 5
NL
ad-a102 282



CAT 10

May 31

June 4

June 11

June 12

June 13



May 10

May 14

May 18

May 21

May 24

May 28

APPENDIX VI

APPENDIX VIIA

Concentration of Suspended Sediment in Surface Samples
from the Breaker Zone Obtained during the Storm of June 11, 1974

Sample Station	Concentration (ppm)
Cat. 1	3529
Cat. 3	2601
Cat. 5	124
Cat. 6	2688
Cat. 8	144
Cat. 10	913

APPENDIX VIIB

Concentration of Suspended Sediment in Cattaraugus Creek at the Buffalo Rd. Bridge. Obtained with a Depth-Integrated Suspended Sediment Sampler (DH-48) during a Small Flood in May.

Sample Station	Concentration (ppm)
1	601
2	518
3	606
4	662
5	614
6	505
7	508
8	525
9	510
10	541

APPENDIX VIII

Texture Parameters for Nearshore Sand in the Cattaraugus Embayment.

For computation of textural parameters this report follows Folk (1968, p. 44-47).

Sample Station	Mean Diameter, ϕ	Sorting ϕ	Skewness
Cat. 1A	2.16	0.41	0.50
Cat. 1B	2.33	0.43	0.43
Cat. 1C	2.47	0.52	1.10
Cat. 1D	2.45	0.55	1.24
Cat. 1E	2.44	0.48	0.90
Cat. 1F	2.42	0.55	1.25
Cat. 1G	2.41	0.43	0.30
Cat. 1H	2.41	0.40	0.15
Cat. 1I	2.60	0.56	1.08
Cat. 1J	2.63	0.56	0.95
Cat. 1K	2.58	0.56	1.04
Cat. 2A	2.32	0.40	0.29
Cat. 2B	2.46	0.37	0.24
Cat. 2C	2.41	0.38	0.16
Cat. 2E	2.37	0.35	0.08
Cat. 2F	2.49	0.38	0.06
Cat. 2G	2.56	0.49	0.37
Cat. 2H	2.56	0.53	0.98
Cat. 2I	3.01	1.08	5.88
Cat. 2J	2.57	0.54	1.15
Cat. 2K	2.58	0.54	0.92
Cat. 3A	2.14	0.33	0.23
Cat. 3B	2.28	0.42	0.09
Cat. 3C	2.40	0.53	0.64
Cat. 3D	2.47	0.55	1.02
Cat. 3E	2.98	0.98	3.73
Cat. 3F	4.83	2.20	8.22
Cat. 4A	2.07	0.31	0.13
Cat. 4B	2.38	0.35	0.17
Cat. 4C	2.37	0.36	0.15
Cat. 4D	2.52	0.43	0.25
Cat. 4E	2.64	0.61	0.92
Cat. 4F	2.64	0.61	1.05
Cat. 4G	2.93	0.92	4.37
Cat. 4H	2.69	0.52	0.72

Sample Station	Mean Diameter, ϕ	Sorting ϕ	Skewness
Cat. 5A	1.72	0.70	-2.68
Cat. 5C	2.05	0.44	0.30
Cat. 5D	2.12	0.50	0.47
Cat. 5E	1.75	0.55	0.20
Cat. 5F	2.11	0.51	0.76
Cat. 5G	3.03	1.53	13.58
Cat. 5H	2.98	1.13	4.77
Cat. 5I	3.18	1.28	6.26
Cat. 5J	3.87	1.35	0.63
Cat. 6A	1.55	0.66	-0.39
Cat. 6B	2.08	1.93	19.84
Cat. 6C	5.07	2.03	12.47
Cat. 6D	1.18	0.57	0.49
Cat. 6E	3.88	2.01	8.70
Cat. 6F	5.74	1.85	13.90
Cat. 6G	2.91	1.36	11.28
Cat. 7B	1.90	0.35	0.21
Cat. 7C	2.76	1.13	7.51
Cat. 7D	4.37	2.14	14.28
Cat. 7E	4.39	2.21	11.12
Cat. 7F	5.08	1.97	10.75
Cat. 7G	4.24	1.54	3.83
Cat. 7I	4.54	2.14	11.91
Cat. 7J	4.98	2.12	9.87
Cat. 8A	1.50	0.34	-0.09
Cat. 8C	2.38	0.37	0.12
Cat. 8E	2.65	0.63	1.20
Cat. 8G	3.33	1.51	11.84
Cat. 9A	1.72	0.32	0.10
Cat. 9H	6.89	1.85	4.06
Cat. 9I	6.65	1.83	4.57
Cat. 10A	1.75	0.39	0.43
Cat. 10I	7.30	1.52	5.03

APPENDIX IX

Textural composition of the Cattaraugus Beach sand fraction. For location of sample stations see Figure 56. Cumulative size-frequency curves for all sand samples are available upon request.

Sample Station	5	16	50	84	95	(% Coarser Than)
1	1.00	1.20	1.55	1.90	2.13	
2	1.25	1.45	1.75	2.06	2.27	
3	1.23	1.35	1.60	1.95	2.27	
4	0.15	0.60	1.10	1.68	2.00	
5	0.95	1.20	1.55	1.95	2.20	
6	0.50	0.95	1.40	1.88	2.10	
7	1.10	1.30	1.65	2.00	2.30	
8	0.85	1.15	1.45	1.93	2.30	
9	0.50	0.80	1.30	1.85	2.20	
10	-0.65	-0.25	0.30	1.10	1.60	
11	-0.60	0.00	0.35	0.80	1.10	
12	-0.25	0.60	0.85	1.40	1.85	
13	-0.75	-0.25	0.30	0.80	1.15	
14	0.25	0.65	1.05	1.54	2.00	
15	-0.30	0.15	0.70	1.20	1.60	
16	-0.10	0.05	0.28	0.70	1.25	
17	-0.50	0.00	1.05	1.52	1.85	
18	-0.60	-0.25	0.00	0.25	0.50	
19	-0.55	-0.20	0.20	0.50	0.70	
20	0.15	0.40	0.75	1.25	1.80	
21	0.50	0.75	1.15	1.65	2.25	
22	-0.25	0.50	1.20	1.70	2.15	
23	1.05	1.20	1.50	1.93	2.25	
24	0.20	0.85	1.30	1.85	2.15	
25	1.15	1.30	1.65	2.03	2.35	
26	-0.25	0.20	0.70	1.30	1.70	
27	-0.60	0.00	0.65	1.24	1.63	
28	-0.75	-0.20	0.75	1.30	1.65	
29	0.60	0.90	1.30	1.80	1.95	
30	-0.50	-0.25	0.10	0.65	1.30	
31	0.15	0.55	0.85	1.35	1.95	
32	-0.90	-0.50	0.25	1.05	1.45	
33	-0.85	-0.50	0.60	1.10	1.45	
34	-0.75	-0.40	0.50	1.05	1.80	
35	-0.30	0.55	1.10	1.55	2.05	
36	-0.75	-0.25	0.70	1.37	1.85	
37	-0.75	-0.40	0.20	0.65	1.20	

Sample Station	5	16	50	84	95	(% Coarser Than)
38	-0.25	0.45	1.10	1.57	1.85	
39	-0.50	0.30	1.20	1.60	1.92	
40	-0.85	-0.55	0.90	1.68	2.10	
41	-0.20	0.25	0.65	1.00	1.25	
42	-0.55	-0.25	0.30	1.05	1.45	
43	-0.25	0.00	0.30	0.70	1.05	
44	-0.50	-0.20	0.10	0.50	1.08	
45	-0.50	-0.25	0.00	0.20	0.35	
46	-0.15	0.50	0.75	1.18	1.40	
47	-0.75	-0.40	0.20	0.50	0.70	
48	-0.50	-0.15	0.15	0.50	0.85	
49	0.00	0.35	0.70	1.10	1.30	
50	0.15	0.40	0.80	1.27	1.55	
51	0.35	0.50	0.75	1.10	1.45	
52	0.90	1.05	1.27	1.60	1.87	
53	0.70	0.85	1.15	1.51	1.85	
54	1.05	1.15	1.30	1.60	1.85	
55	0.75	.80	1.00	1.27	1.50	

APPENDIX F

**SEDIMENT TRANSPORT
IN CATTARAUGUS CREEK**

CONTENTS

	<u>Page</u>
Abstract	i
Acknowledgements	ii
Illustrations	iii
Tables.....	iv
1. Introduction.....	v
2. Conditions at the Creek Mouth.....	1
3. Analysis of Sediment Transport.....	3
3.1. Basic data.....	13
3.2. Total sediment load.....	18
3.3 Meander migration rates.....	20
3.4. Gravel operations.....	25
3.5. Dredged traps.....	28
4. Theoretical Computations of Bed Material Transport.....	33
4.1. Basic approach.....	33
4.2. Hydraulic computations.....	34
4.3. Sediment transport computations.....	41
4.4. Results.....	42
5. Computer Simulation of Deposition in Cattaraugus Creek.....	51
5.1. Simulation technique.....	51
5.2. Sources of error.....	53
5.3. Results.....	55
5.4. Discussion of results.....	67
6. Conclusions.....	74

	<u>Page</u>
References.....	76
Appendix 1. Particle size analysis.....	77
Appendix 2. Cattaraugus Creek discharges, spring, 1975.....	83
Appendix 3. Irving pamphlet (historical account of early structure, circa 1837).....	84
Appendix 4. Data sources.....	89
Appendix 5. Hydraulic parameters.....	91
Appendix 6. Bedload computations.....	92
Plate I. Cattaraugus Creek Meanders 1938, 1958, and 1971.....	100

ABSTRACT

Rapid changes in morphology of the lower reaches of Cattaraugus Creek over the last century indicate that substantial bedload transport takes place. The proposed dredged turning basin at the mouth of the creek, therefore, could have a very short life expectancy.

Quantitative studies of sediment transportation on Cattaraugus Creek, based on cut bank migration rates, measurements of suspended sediment, estimation of sediment yield from the drainage basin, and computations of bedload transport from the river hydraulics and dredged sediment samples all indicate that the dredged turning basin would be filled within a period of less than ten years. Furthermore, natural scouring of the river bed in response to falling lake level would probably always maintain adequate navigation depth **without dredging**.

It is recommended that the proposed harbor dredging be omitted.

ACKNOWLEDGEMENTS

We wish to acknowledge the assistance of Mr. Norman Sackett in dredging sediment traps. Edward Bugliosi, Ignacio Orozco-Martinez, Herbert Buxton and Mary Earls, all students at S.U.N.Y., Fredonia; and Dr. Donald N. Peterson helped with fieldwork in blizzards and sun and with data reduction and analysis. Mr. B. Wojda of Sunset Bay pleasantly answered innumerable questions and requests for boats, launching facilities and parking. Mr. Ray Benacquista and Ms. Joan Pope of the Buffalo District of the Corps of Engineers provided many helpful suggestions. Section 3.3 was written jointly by Drs. Fahnestock and Nummedal, section 4 was done by Dr. Nummedal, section 5 by Dr. Apmann and Mr. Brownlie. The remainder of the report was written by Dr. Fahnestock. Mr. Hector DeJesus assisted with the sieve analysis and the computer modelling.

ILLUSTRATIONS

<u>Figure</u>	<u>Page</u>
1. Map of structure and bottom configuration of the mouth of Cattaraugus Creek in 1844.....	4-7
2. Water surface profiles for the lower reach of Cattaraugus Creek.....	9-10
3. Maps of Cattaraugus Creek mouth and the adjacent shoreline	11-12
4. Vertical current velocity profiles.....	14-15
5. Suspended sediment rating curves.....	16-17
6. Summary of meander bend erosion rates.....	22-23
7. Extent of gravel removing operations on Cattaraugus Creek	26-27
8. Rate of infilling of dredged sediment traps.....	29-30
9. Composite cross-section of river reach 0.0-0.75 miles....	35-36
10. Composite cross section of river reach 2.0-2.2 miles....	37-38
11. Depth (slope) versus hydraulic radius for the selected study reaches.....	39-40
12. Computed bedload rating curves.....	44-45
13. Potential transport rate vs. grain size.....	47-48
14. Cross section locations.....	68
Plate I Cattaraugus Creek meander migration 1958, 1958, 1971.	100

TABLES

Table

	<u>Page</u>
1. Suspended sediment load of Cattaraugus Creek for water year 1972.....	19
2. Parameters related to the estimation of bed material loads from the rate of meander bend migration.....	21
3. Summary data on dredged sediment traps in Cattaraugus Creek	31
4. Summary of computed bed material transport rates.....	43
5. Computed annual average sediment transport in Cattaraugus Creek.....	46
6. Sediment transport rates, 1971, low lake levels.....	59
7. Sediment transport rates, 1971, average lake levels.....	60
8. Sediment transport rates, 1971, high lake levels.....	61
9. Simulated bed changes for 1971 flows.....	62
10. Sediment transport rates, 1972, low lake levels.....	63
11. Sediment transport rates, 1972, average lake levels.....	64
12. Sediment transport rates, 1972, high lake levels.....	65
13. Simulated bed changes for 1972 flows.....	66
14. Design flow output summary.....	71
15. Estimates of mean annual sediment transport rates at the mouth of Cattaraugus Creek.....	75

V

LIST OF SYMBOLS

D	water depth
\bar{D}	arithmetic mean of a grain size interval
d_{35}	size of bed material for which 35% is finer
d_{50}	size of bed material for which 50% is finer
d_{90}	size of bed material for which 90% is finer
G_s	sediment transport rate for a grain size fraction
g_s	sediment transport rate per unit width of stream bed for a given size fraction
n	Manning's friction coefficient
U_*	$= \sqrt{\frac{\tau_0}{\rho}}$ shear velocity
Q_w	water discharge
q_s	bedload rate per unit time and unit width
R	hydraulic radius
R_h	hydraulic radius due to grain roughness only
S	slope
γ	specific weight of fluid
γ_s	specific weight of sediment
ρ	density of fluid
ρ_s	denisty of sediment
$(\tau_0)_{cr}$	critical shear stress
τ_0	$= \gamma \cdot R \cdot S$ bed shear stress
$\phi = \frac{g_s}{\gamma_s} \sqrt{\frac{\rho}{\rho_s - \rho}} \cdot \frac{1}{g \cdot d_{50}^3}$	transport intensity
$\psi = \frac{\rho_s - \rho}{\rho} \cdot \frac{d_{50}}{S \cdot R_h}$	flow intensity

1. INTRODUCTION

As long as ships have sailed Lake Erie, the mouth of Cattaraugus Creek has been a harbor. It has provided a haven for fishing boats, timber schooners and small ships of war. Ready access to the quiet waters of the river channel is denied when wave induced littoral drift blocks the river mouth. Until the mouth is reopened by flood in the creek only boats of very shallow draft have access. Permanent access requires improvement.

In addition to the building of breakwaters, the original design for improvement suggested dredging a 6 foot deep channel 4300 feet upstream from the river mouth and widening a portion of it for a turning basin (Army Corps of Engineers, 1966). Such a dredged channel would constitute an obvious departure from the normal hydraulic condition of the lower river with probable effects on sediment transport. The seriousness of these effects would depend on the quantity of transport and the efficiency of the sediment trap created. If the rate of bed material transport is small, the effects will take many years to prove harmful. If large, the effects may be apparent within a year. The purpose of this study is to determine the sediment transport rates on the lower river so these effects can be evaluated.

In order to estimate the amount of sediment likely to be trapped by the dredged turning basin a number of different approaches were taken. Traps were dredged in the stream bed to demonstrate the presence of bedload under the flow conditions existing in the spring of 1975; volume and size range of bed material set in motion by bank erosion was

determined; the amount of gravel removed by commercial sand and gravel operators was estimated; the total load of the stream was determined based on measured suspended sediment concentrations and known hydrographs. In addition to these direct estimates, the rates of bedload transport for natural and improved conditions near the river mouth were also calculated by existing bedload formulae and a computer model of sediment movement into and out of the proposed dredged basin.

2. CONDITIONS AT THE CREEK MOUTH

Problems with the bar at the mouth led to the construction of a structure in the 1830's similar to the one currently under consideration. Construction was begun about 1835, and before completion of the south bank jetty, scouring to a depth of 12 to 15 feet occurred along its inner face, according to the comment by R. P. Allen in the pamphlet on Irving (see Appendix 3, p. 46).

Examination of the depths shown in Figure 1 indicates the success of the completed structure and that sufficient depth exists near the river mouth without the "benefits" of dredging. No historic record or oral accounts indicate any problems with shoaling of the main channel anywhere but at the river mouth spit. Mr. B. Wojda, who has operated a marina at the mouth since 1960, including the extreme low lake level years of the early 1960's, indicates no problems where the river currents are unopposed by the waves and currents of the lake. Even where the river meets the lake it fails to maintain a channel of sufficient depth only during extended periods of low flow--moderate to high flows maintain a deep channel across the spit.

The present high lake levels and the estuarine appearance of the lower mile of the river deceptively combine to suggest to a casual observer that the coarse materials are not being transported through this reach. The sands and silts that floor portions of the reach also might appear to be indicators of low current velocities.

At river flows below 1000 cfs a quite perceptible current still exists to the mouth, and velocities in the narrow channel over the

Figure 1 A. Map of structure and bottom configuration of the mouth of Cattaraugus Creek in 1844. The simple structure of two parallel jetties of uneven length seems adequate in maintaining a harbor entrance. Note the channel depths.

M A P
OF
CATARAUGUS
H A R B O R



1

Reference: This map exhibits the condition of the public water of the Harbor in
Cattaraugus, State of New York, and the depth in feet of 10 fathoms in four fathoms.
The dotted lines represent horizontal lines of depth of 6, 7, 8, 10, & 12 fathoms.
The sounding lines represent a depth of 10 fathoms in the creek, and are indicated on
the map. The general depth was found to be 7 fathoms.

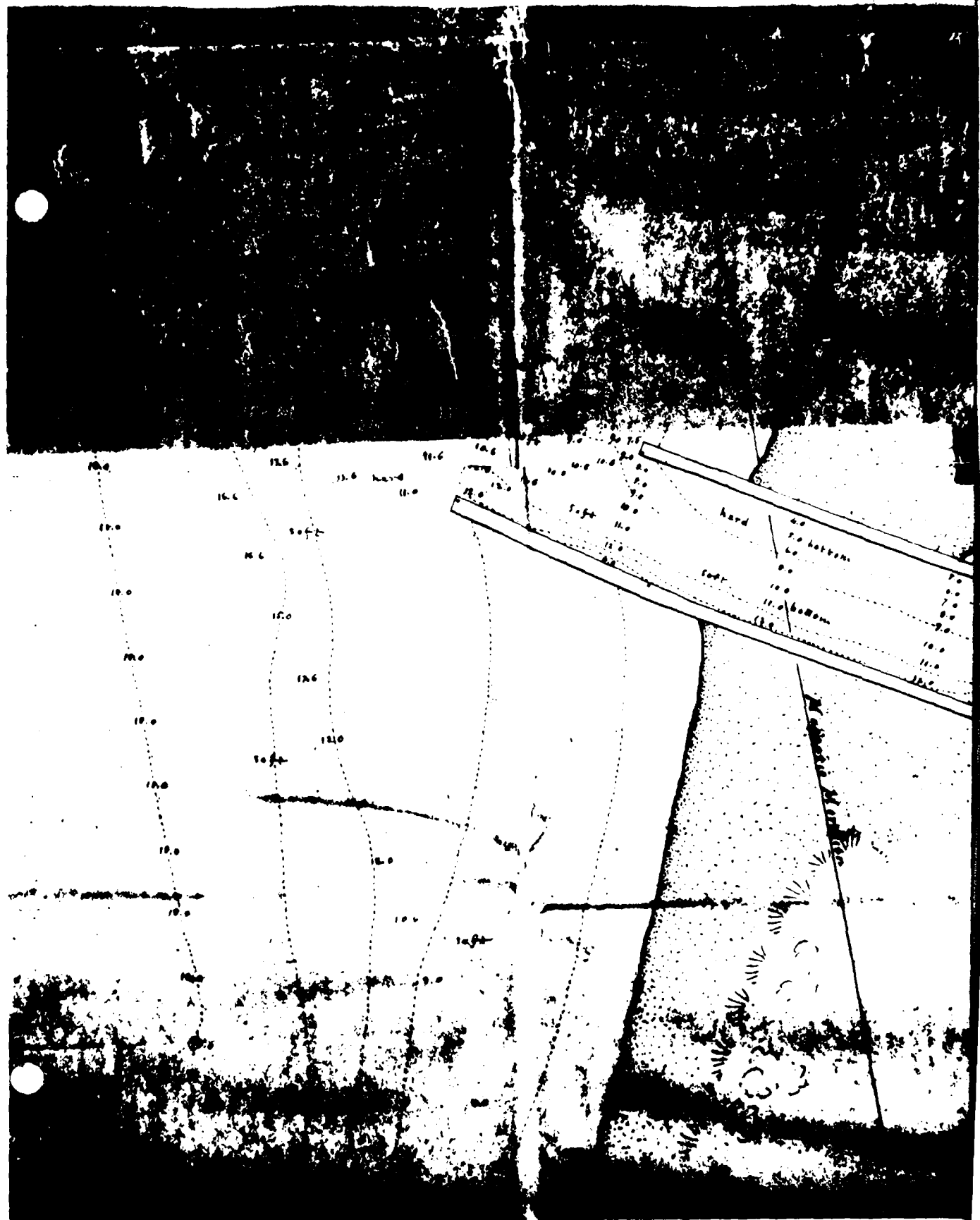
Surveyed and drawn under the direction of Capt. W. G. Williams, Capt. Top. Eng.
by Lieut. J. C. Woodward, Capt. Top. Eng. May 1864.

Eng. Dept. U. S. Army

1

Eng. Dept. U. S. Army

Figure 1 B. Enlarged portion of map shown in Figure 1 A. Depth soundings across the entrance indicate scour by the confined flow.



submerged portion of the spit may be more than five feet per second. Under these conditions, however, little sediment transport takes place in the lower mile, and only materials fine enough to be swept out by increasing flows are brought in.

Figure 2 shows the water surface slope measured at a low and a moderately high flow (approx. 12,000 cfs). The one measured at high flow is parallel to the bottom and to those slopes projected by the Army Corps to exist for intermediate regional and standard project floods (Army Corps of Engineers, 1968). Like those slopes, the measured one extends with imperceptible change all the way to the lake. Surface velocities of five feet per second were measured at places in the lower reach where the stream was more than 300 ft wide. The 12,000 cfs flow deposited appreciable quantities of sediment in all the dredged river bed traps which were not already filled.

Observations of channel migration for more than a hundred years indicate considerable erosion and deposition in the lower reach (Fig. 3). Changes in volume and shape of islands and bars in the lower reach of the river can also be noted by comparing maps and air photos for different years.

Probing and pile driving in the lower reach indicate an interlayering of silt, sand and gravel, as do exposures in the cut banks along most of the river. Gravel layers in the lower reach are clear indicators of the movement of quantities of gravel--at frequent intervals in the recent past. Gravel can be shown to be moving by a variety of evidence. The more quantitative lines of evidence developed for this report will be discussed in later sections.

Figure 2. Water surface profiles for the lower 3 miles of Cattaraugus Creek. Data on the Intermediate Regional, Standard Project, and the March, 1963, floods are from the Flood Plain Report (Corps of Engineers, 1968). Slope data for the smaller floods are based on field observations during different June, 1975, flood events. See Appendix 2 for a listing of the corresponding discharges. The channel bottom is represented by the wide hachured line. It is evident from the figure that a lowering of lake level must be accompanied by channel bed scour in order to maintain adequate conveyance.

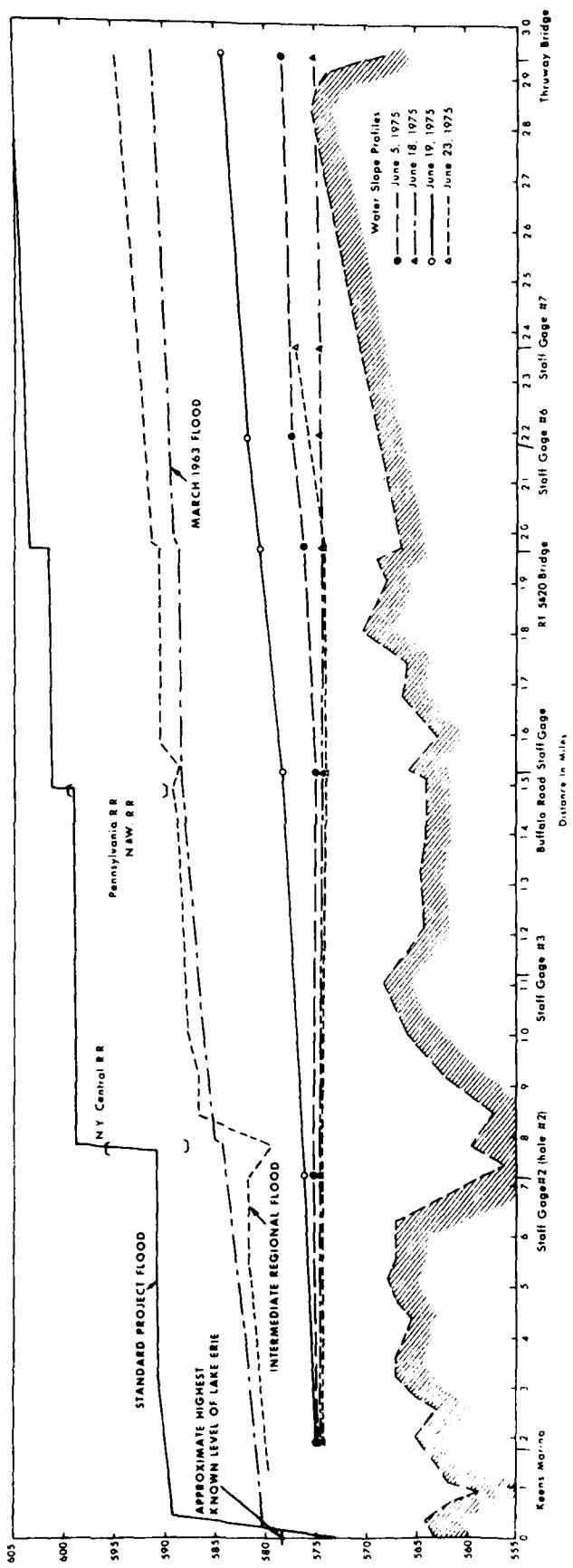
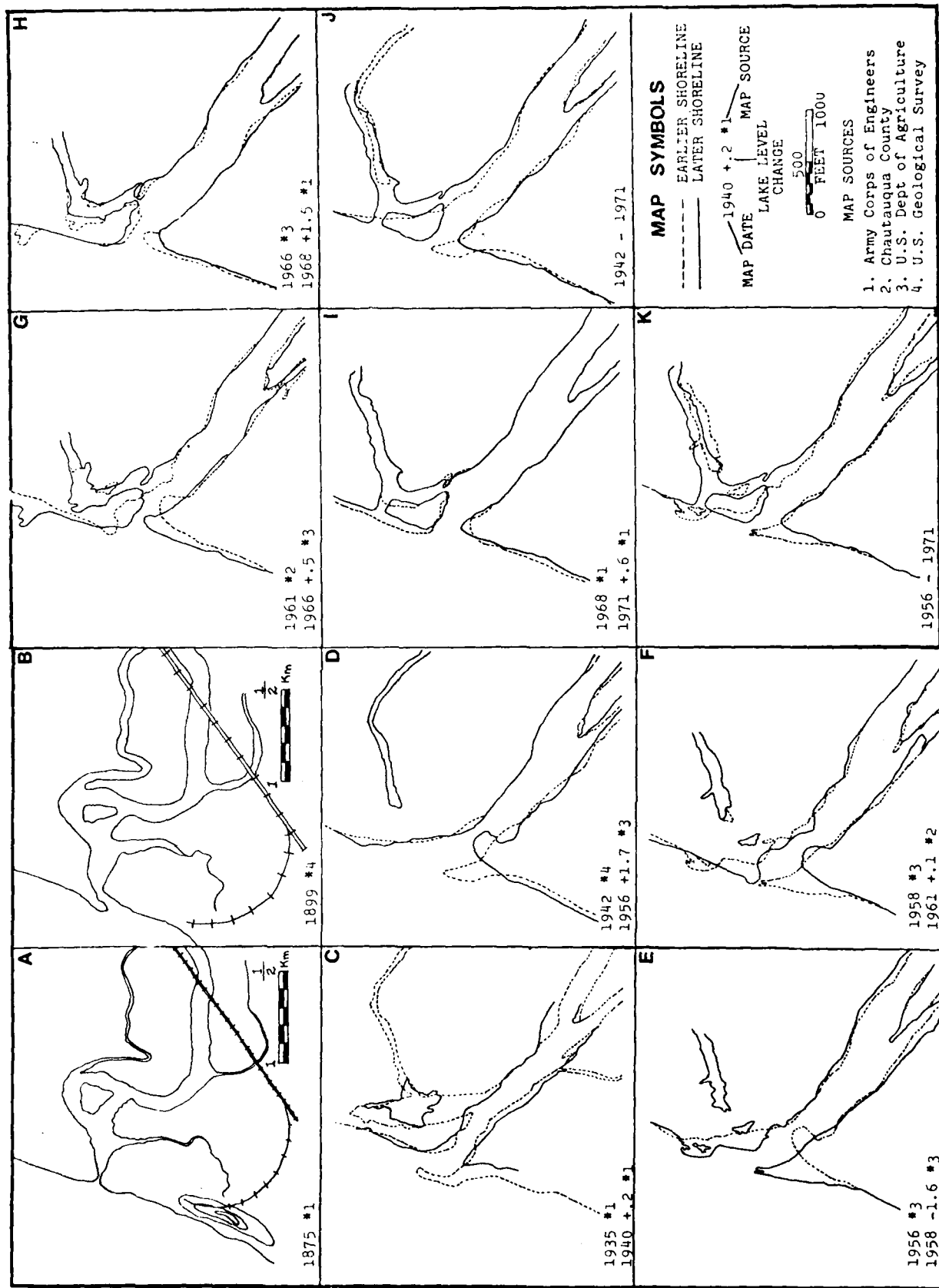


Figure 3. Maps of the mouth of Cattaraugus Creek and the adjacent shoreline from 1875 to 1971. Maps from a U. S. Army Corps report on "Littoral Processes and Sedimentation in the Cattaraugus Embayment, N. Y.," by Nummedal, Hayes and Fahnestock, 1974.



3. ANALYSIS OF SEDIMENT TRANSPORT

3.1. Basic data.

A variety of data were collected to allow analyses of sediment transport by as many methods as possible. The data used in more than one analysis have been compiled in the Appendices. Whenever possible, published data or data developed in earlier phases of the work or in concurrent studies are also utilized here. It is appropriate to review the general conclusions that can be drawn from these data.

Stream data include a daily hydrograph developed from the water stage strip chart at the U. S. Geological Survey Gauging Station in Gowanda (Appendix 2). (The computer data from the punch tapes is not yet available.) The strip chart recorder was removed in early June to make room in the gauge house for a telephone device, making it possible to learn instantly the river stage, but impossible to review the flow record of the last few days or weeks. For the month of June a partial hydrograph for two high flows was obtained by phone.

Velocity profiles and suspended sediment concentration were measured at the U. S. 20 & 5 bridge during the moderate flood on June 19th, 1975. Velocity profiles are presented in Figure 4; the depth integrated concentration data are part of the data used to establish the rating curve in Figure 5. The concentration data appear comparable to those obtained earlier by a pump sampler at Gowanda as part of the Lake Erie waste-water study presently in progress.

The materials dredged out of the river bed for construction of sediment traps and the sand and gravel subsequently filling these traps

Figure 4. Vertical current velocity profiles at the bridge of
U. S. 5 & 20 during a flood on June 19th, 1975.

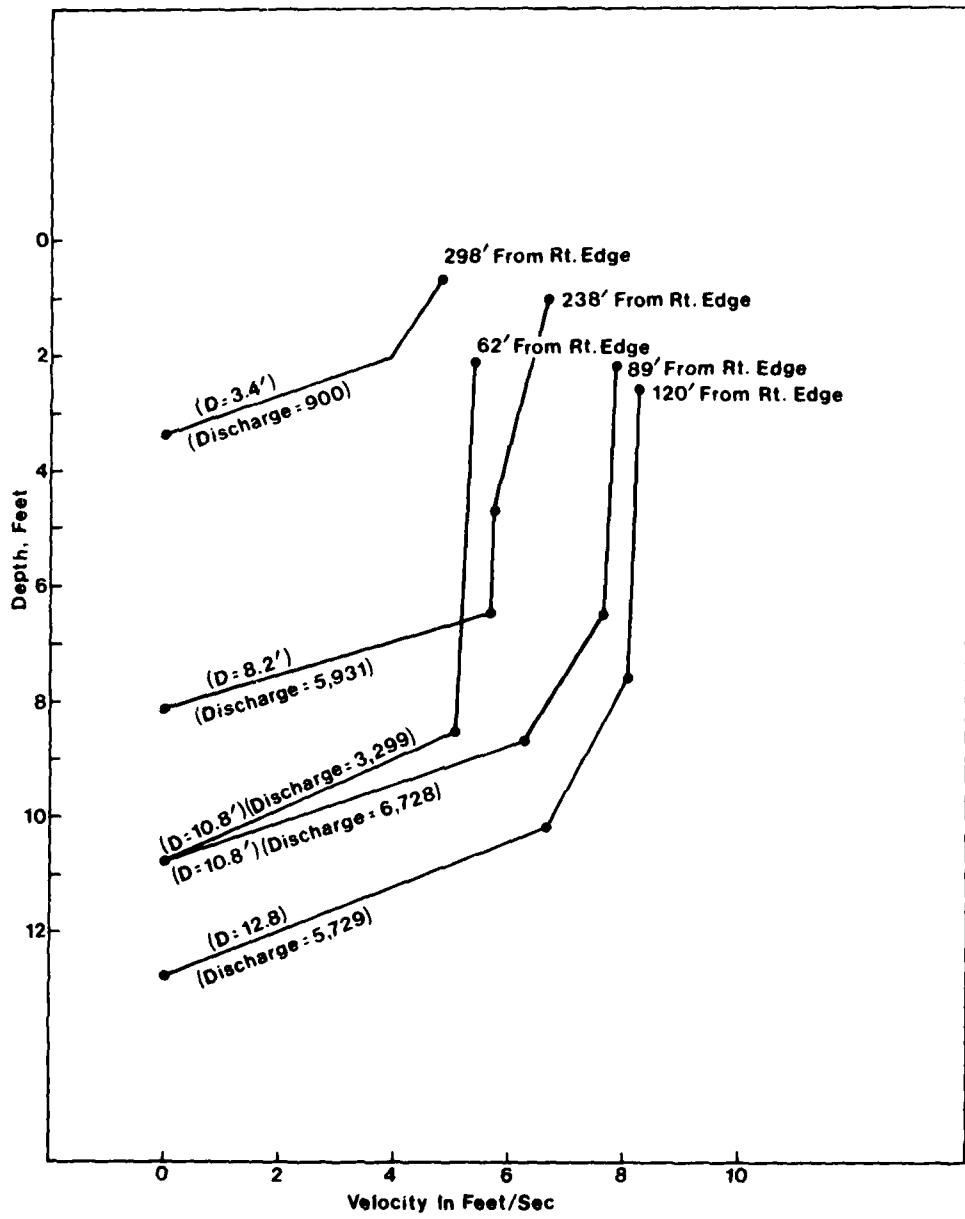
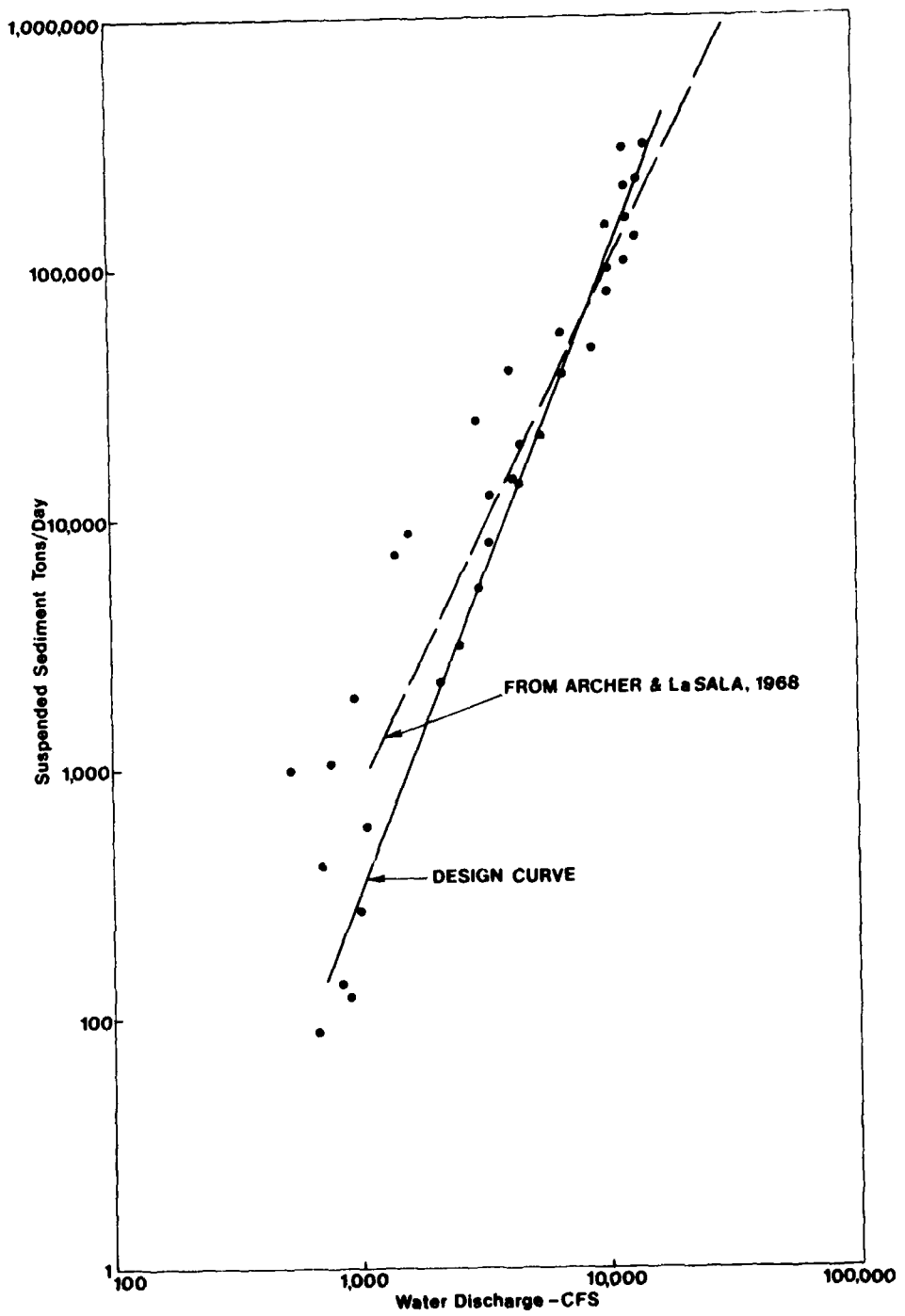


Figure 5. Suspended sediment rating curves at Gowanda, New York. Observations at the bridge of U. S. 5 & 20 during a June flood fall close to the Gowanda data. Despite the scatter of the observations, a design curve can be drawn. The one used in this report falls close to the one reported by Archer and La Sala, 1968.



were analyzed by sieving for their size-frequency distribution. Representative vertical sections of the cut banks were also sampled and sieved. All these results, summarized in Appendix 1, are used throughout the paper.

3.2. Total sediment load.

The total load of Cattaraugus Creek can be estimated from the known rating curve (Fig. 5) together with reported discharges for the 1972 water year (U. S. Geological Survey, 1972). Adjusted to the river mouth, the suspended load that year was about 1.43 million tons (Table 1). It can be seen that 45 percent of that was discharged during one day when the stream flow averaged 18,500 cfs and peaked at 25,300 cfs. Adding 10 percent, or 140,000 tons, for the bedload gives a total load for 1972 of 1.57 million tons of sediment.

The 10 percent increase for bedload is based on Archer and La Sala's (1968, p. 9) reference to previous work on the Genesee and the Potomac Rivers. Archer and La Sala's (1968) sediment discharge rating curve agrees well with our values (Fig. 5), although it is based on substantially less data. Rather than using one water year, Archer and La Sala used long term stream flow records, resulting in a total annual average sediment load at Gowanda of 610,000 tons. Adjusting for drainage area, this would correspond to about 780,000 tons at the mouth, including 10 percent for bedload.

Archer and La Sala (1968, p. 18) emphasize the sedimentation problems in the "deep, wide channel of the Buffalo River." They also point out that Gowanda's water supply reservoir on Point Peter Brook is almost

Table 1
 SUSPENDED SEDIMENT LOAD OF CATTARAUGUS CREEK
 FOR WATER YEAR OCTOBER 1971 - SEPTEMBER 1972

<u>Discharge (cfs)</u>	<u># of days per year*</u>	<u>tons per day</u>	<u>Tons</u>
17-19,000	1	500,000	500,000
15-17,000	0	--	--
13-15,000	0	--	--
11-13,000	0	--	--
9-11,000	1	115,000	115,000
7- 9,000	0	--	--
5- 7,000	1	40,000	40,000
3- 5,000	10	14,000	140,000
1- 3,000	52	5,000	260,000
<1,000 (av. 400)	300	200	60,000

Suspended Load at Gowanda = 1,115,000 Tons of Sediment per Year.

By adjusting to the mouth of the stream and adding 10 percent for bedload, the total load becomes:

1,570,000 tons per year

*From: U. S. Geological Survey, 1972.

completely filled with sediment and no longer provides adequate storage. The power plant reservoir on Cattaraugus Creek at Springville has lost much of its storage space and requires sluice flushing each spring to maintain its present limited capacity.

Another estimate of the total load supplied by the drainage basin has been made by the Soil Conservation Service (1974). Considering the erodability of the soils, the use of the land and the percentage of the area in each category, the SCS has estimated the total yearly sediment load of Cattaraugus Creek at 520,000 tons.

3.3. Meander migration rates.

The lateral movement of the stream channel, graphically portrayed on Plate 1, provides a minimum measure of the bed material transport rate if one considers that most of the coarse sediment removed from a cut bank is deposited on the point bar immediately downstream.

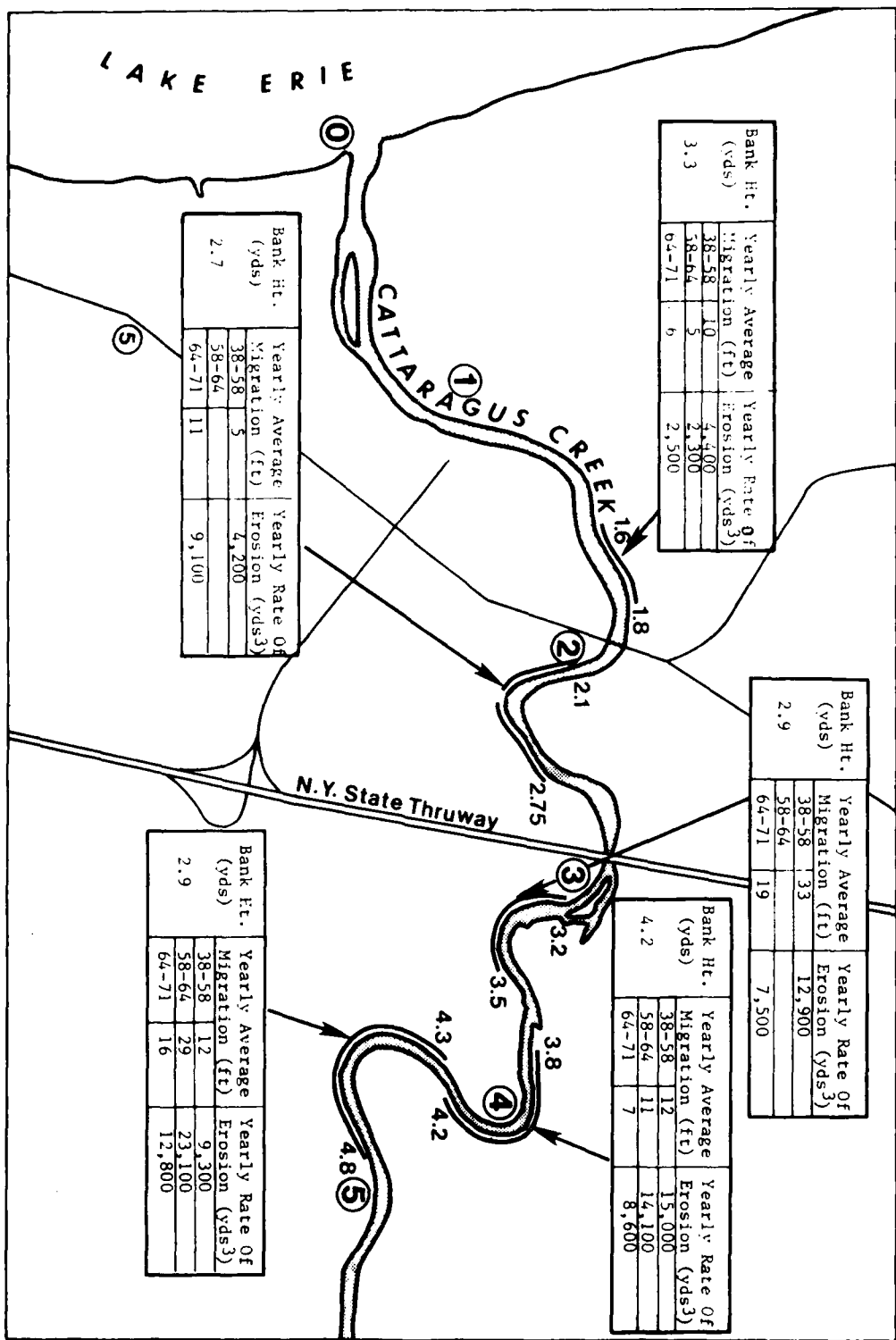
Measurements of the rates of bank retreat, the height of the cut banks and the estimated volume of sediments set in motion by the bank cutting are summarized in Table 2 and Figure 6. These data are based on field measurement of bank heights and composition and comparison of vertical aerial photographs taken in 1953, 1958, 1964, and 1971 (see Appendix 4 for data sources). With the exception of 1964, these river positions are indicated on Plate 1.

The basal portion of the cut banks consist almost entirely of gravel; the upper portions of sand and silt. Appendix 1 contains the relative proportions of these materials determined by sieve analysis of samples from the fine portion of three cut banks. The average amount of

Table 2
MEASURED AND COMPUTED PARAMETERS RELATED TO THE ESTIMATION OF BED MATERIAL LOADS FROM THE RATE OF MEANDER BEND MIGRATION

River Mile	Area (yd ²) Eroded By Cut Bank in Time Period 38-58 58-64 64-71	Bank Height (yds)	Yearly Rate of Erosion in (yds ³ /yr) 38-58 58-64 64-71	Composite			Length of Cut Bank (yds) 38-58 58-64 64-71	
				Rate of Erosion (yds ³ /yr)		Average Migration (feet/yr) 38-58 58-64 64-71		
				1938-1971 (yds ³ /yr)	38-71 38-58 58-64 64-71			
1.6-1.8	Total 26,700 4,100 5,400 4.3 5,700 8,800 3,300 5,900 10 5 6 13 1,213 404							
1.6-1.8	Bed Material	3.3	4,400 2,300 2,500	3,100				
2.1-2.8	Total 30,600 -- 23,600 4.2 6,500 -- 14,200 10,400 5 -- 11 14 -- 21 2,773 924							
2.1-2.8	Bed Material	2.7	4,200	9,100 6,700				
3.2-3.5	Total 88,900 -- 18,100 3.8 16,900 -- 9,900 13,400 33 -- 19 23 -- 30 1,221 407							
3.2-3.5	Bed Material	2.9	12,900	7,500 10,200				
3.8-4.2	Total 71,300 20,200 14,300 5.5 19,500 18,500 11,200 16,400 12 11 7 35 35 10 2,722 907							
3.8-4.2	Bed Material	4.2	15,000 14,100 8,600	12,600				
4.3-4.8	Total 63,800 47,700 30,800 4.2 13,400 33,400 18,500 21,800 12 29 16 38 33 2,461 70							
4.3-4.8	Bed Material	2.9	9,300 23,100 12,800	15,100				

Figure 6. Each meander bend used in the study of cut bank migration rates is indicated by a black line. River miles at the ends of each study reach are indicated, as are the integer river miles (circled numbers). Migration and volumetric erosion rates are computed for three time intervals--1938-58, 1958-64, 1964-71--and presented in tabular form for each study reach.



sand in the fine portion of the cut bank was taken as 30 percent. The volume of bed material released by erosion of a cut bank equals the product of the map area of erosion and the sum of the height of gravel in the cut bank plus 30 percent of the height of the upper fines. This product was divided by the time interval between photographs to get the volume of erosion per year. Similarly, the average bank recession per year equals the area divided by the length of bank and the time interval (Table 2).

Both volume of transport estimated by this method and bank recession per year appear to decrease somewhat in recent years and in the downstream direction, but the rates from different cut banks are similar enough to give credibility to the estimates (Table 2 and Fig. 6). Factors leading to the temporal decrease may include increasing rates of gravel removal for use in construction and decreasing agricultural land use as farms are abandoned in the uplands and revert to brush and trees. A decrease in the available sediment might have a stabilizing effect on the pattern if one can call 10 feet of bank erosion per year stability.

Perhaps there also are subtle hydrological effects such as a change in the height and duration of flood peaks that could have effects on the sediment transport rate but not be obvious from the daily or annual records.

The downstream changes in bed material transport rate appearing in Table 2 probably reflect an increase in sediment bypassing of the point bars with decreasing grain size rather than actual change in total bed

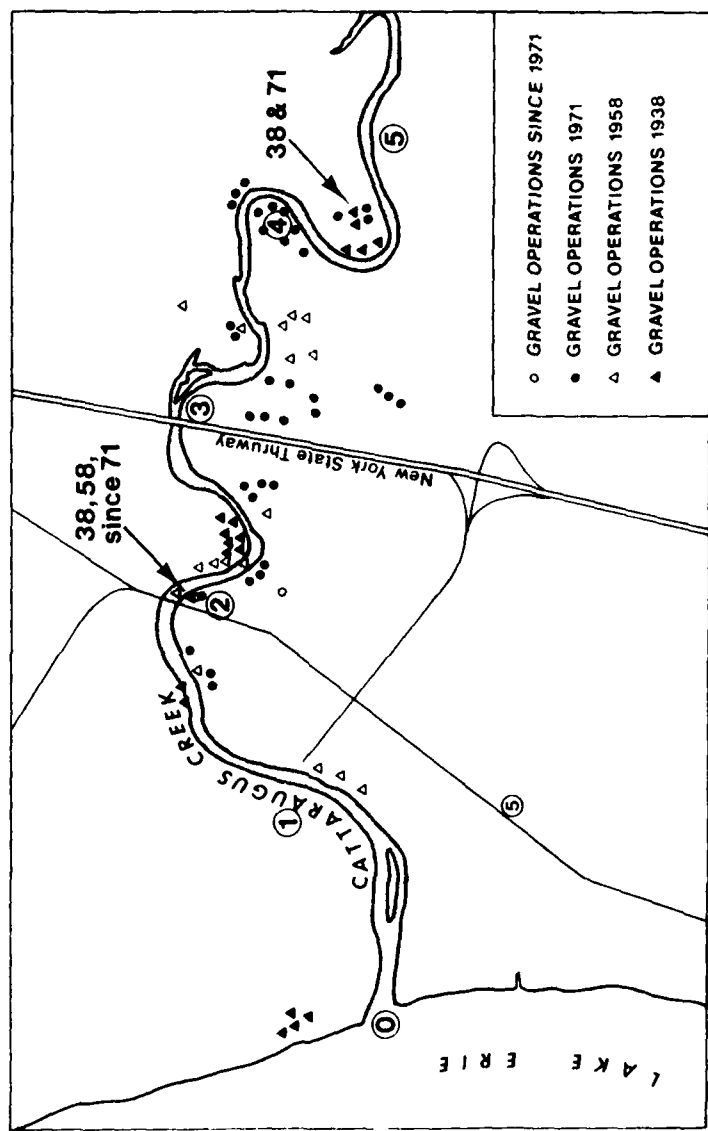
material transport rate. A typical rate of transport near the mouth of Cattaraugus Creek, therefore, would be represented by the average or by greater than the average of the rates listed in Table 2. We have chosen to use 10,000 cubic yards or 12,000 tons per day as a representative bed material transport rate near the mouth of Cattaraugus Creek for the 33 years of record.

3.4. Gravel operations.

The numerous gravel operations in and near Cattaraugus Creek demonstrate the existence of a large load of coarse sediment. Some volume estimates can be attempted from ongoing dredging operations. For example, the bar under the New York Thruway bridge, entirely removed, under permit, by a gravel operator in 1974, accreted about 4000 cubic yards between October, 1974, and June, 1975. In about the same time period, the point bar under the bridge of U. S. 20 & 5 added some 3000 cubic yards. A new replacement bar, infilling a previously excavated area, will grow till it attains the shape and size of the removed bar before there is any substantial bypassing of coarse bed material. The volumes quoted, therefore, suggest at least a minimum transport rate.

With the large number of gravel operations (Fig. 7) the amount removed from the entire river in one year is estimated to be between 25,000 and 50,000 cubic yards. The removal of all this material is thought to have a considerable stabilizing effect on the meander pattern, which might in part explain the decrease in transport rate with time found by the analysis in section 3.3. It might also reduce the rate of sediment deposition at the river mouth by a significant, but unknown, amount.

Figure 7. Map showing the extent of gravel removing operations on and near Cattaraugus Creek since 1938. The current average rate of the removal has been estimated at between 25,000 and 50,000 tons per year.



3.5. Dredged traps.

In order to demonstrate the transport of bed material throughout the system, a series of seven traps were dredged within the lower two river miles in late March, 1975. The rate of filling of the traps and the associated flow events are presented in Figure 8 and Table 3.

As demonstrated by grain size data presented in Appendix 2, the materials that filled the traps were finer than the materials removed from the bed during their dredging (Appendix 1). It may be inferred that the flows which were responsible for trap filling (7000-9000 cfs) carried less coarse materials than did the floods which had deposited the dredged sediments.

All the traps were dug with a dragline from the bank. On gentle bank slopes the dragline could work relatively far into the stream (holes 4 & 5, Fig. 8). Where high cut banks or deep water occurred (holes 1, 2, 3, 6, & 7, Fig. 8) the holes were limited in their cross-channel dimension by the length of the boom and the casting ability of the operator. Because of their proximity to the bank and their varying locations relative to the channel thalweg, the traps filled at different rates. The rate of sediment transport demonstrated by the filling of the traps, therefore, does not necessarily represent any "average" for the cross-section.

Figure 8 shows the location of the traps and a summary of the data on filling. All traps demonstrated some filling over the survey period; no. 4 filled almost immediately, whereas nos. 1, 2, 6 and 7 did not fill completely even after the June floods. Hole no. 5 and a big trench dug

Figure 8. The diagram summarizes the rate of infilling of the dredged sediment traps during the spring of 1975. The cross-hatched area within each circle is proportional to the amount of fill on the date of survey. Compare to Appendix 2 for information on the associated flow events.

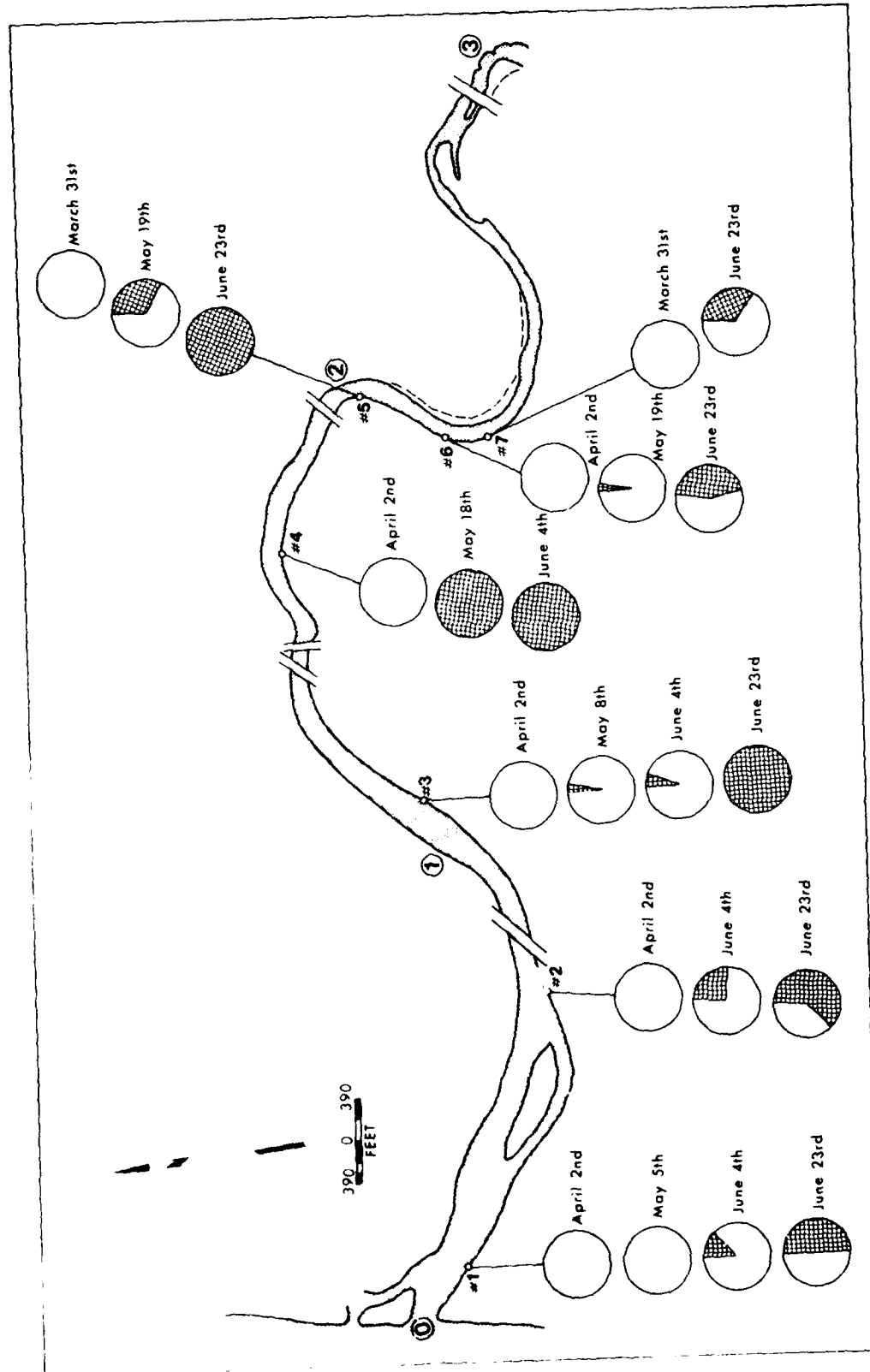


Table 3
SUMMARY DATA ON DREDGED SEDIMENT TRAPS IN CATTARAUGUS CREEK

Trap No.	River Mile	Width of Trap (ft)	Channel Width (ft)	D ₅₀		Percent Fill By May	Percent Fill By June 4	Percent Fill By June 23
				Dredging (mm)	Filling (mm)			
1	.1	35	400	---	.083	0	12	50
2	.7	30	290	12.0	<.062	---	25	61
3	1.1	40	250	---	.100	4 (May 8)	7	94
4	1.7	70	260	15.5	6.400	100 (May 18)	---	---
5	2.0	80	290	20.0	20.000	28 (May 18)	---	100
6	2.2	40	330	13.2	9.500	10 (May 19)	---	44
7	2.4	35	280	---	8.600	---	---	33

at the center of the adjacent point bar were both completely filled after the June floods.

The downstream traps appear to be filled first near the middle of the stream, indicating center line transport and a distant source.

4. THEORETICAL COMPUTATIONS OF BED MATERIAL TRANSPORT

4.1. Basic approach.

Estimates of sediment transport rates presented in section 3 rely on direct measurements and observations on the stream and are reliable indicators of what they are stated to represent. No direct measurement, however, pretends to give the mean annual bed material transport rate across the entire stream cross-section. Properly interpreted, the transport rates determined from meander migration rates (section 3.3) probably come the closest to that desired figure. It was, therefore, decided to supplement the observational data with theoretical computations of bed material load using bedload formulae commonly held to be reasonably reliable for gravel streams (Graf, 1971; Shen, 1971).

Bed material transport rates were computed for three stream segments: (1) river mile 2.0-2.2, (2) river mile 0-0.75 before improvement, and (3) river mile 0-0.75 after improvement (dredging). Computations on the upper section were performed in order to evaluate the methods against the results of the meander bend migration analysis. The two computations near the river mouth are used to evaluate the short term consequences of the proposed dredging.

Data required for sediment discharge computations include the cross-sectional geometry of the reach, energy slope as a function of discharge and bed material size gradation. Field data on mean current velocities are useful in establishing the proper frictional characteristics of the channel reach. Once the bed material rating curve has been established, total annual bed material transport can be easily determined

from the known hydrograph. It is important to note that the fine component of the total sediment load--the wash load--cannot be computed from the hydraulics of the stream because the concentration of fines is a function of sediment supply rather than the interaction between the flow and its bed.

4.2. Hydraulic computations

The composite cross-sectional geometry of the studied river segments are portrayed graphically in Figures 9 and 10. The geometry of river reach 0-0.75 mi is based on seven cross-sections between the mouth and the New York Central railroad bridge, all run by the Army Corps of Engineers, Buffalo District. Cross-sectional geometry of reach 2.0-2.2 miles is based on three sections surveyed by the authors during low water in October, 1974. Stage-discharge relationships for reach 2.0-2.2 miles and the unimproved river mouth are based primarily on observed and projected data presented in the Flood Plain Report (Army Corps of Engineers, 1968, Tables 7 & 8). Hydraulic radius can be computed directly as a function of stage from Figures 9 and 10 (Figure 11). Hydraulic radius is used throughout the computations because it is the depth parameter used in all bedload transport formulae.

Slope data were derived both from field measurements (Figure 2), projected backwater curves (Army Corps of Engineers, 1968), and computations specific to this study.

Mean current velocity in the study sections were computed two ways: (1) by use of the Manning equation, (2) by use of the bottom shear

Figure 9. Composite cross-section of reach 0.0-0.75 miles for natural and improved (dredged) conditions. The composite natural section is the "average" of sections 2 through 8 run by the Corps of Engineers in February-March, 1974. The improved cross-section was determined by superimposing the projected dredge channel on each of the seven natural sections. Water surface elevations at the mid-point of the study reach for 4 different discharges are indicated (Data from Army Corps of Engineers, 1968). Only the channelized portion of overbank flow was utilized in computations of sediment transport rates.

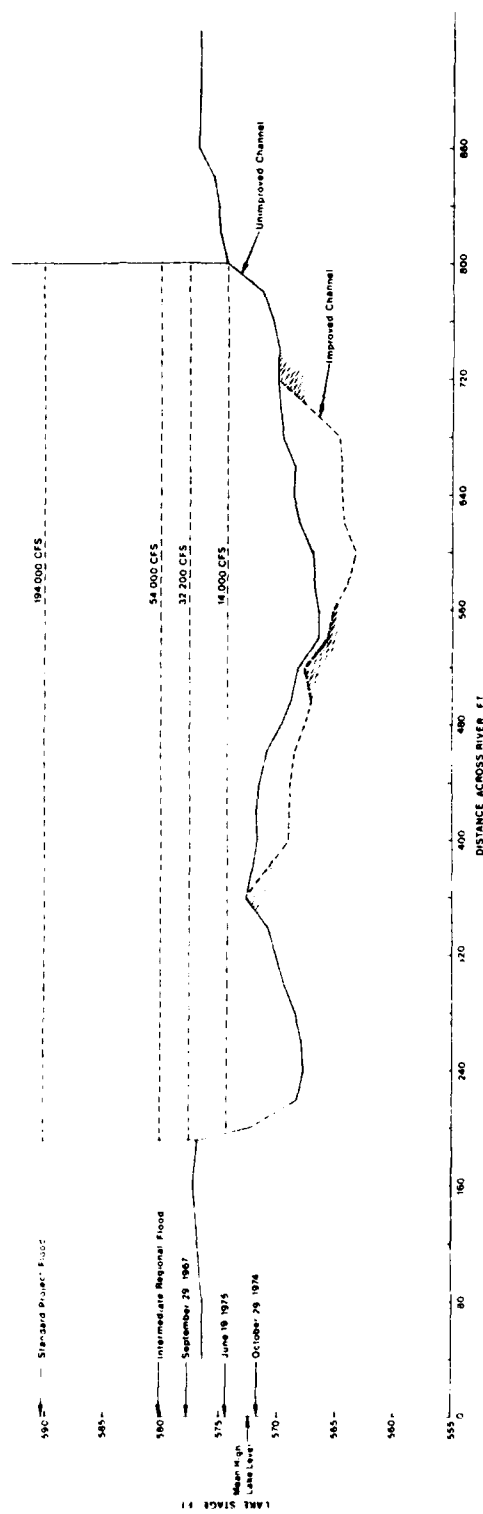


Figure 10. Composite of three surveyed cross-sections in river reach 2.0-2.2 mi. Sections were surveyed by the authors in October, 1974. Water surface elevations are based on field observations and data from the Flood Plain report (Corps of Engineers, 1968).

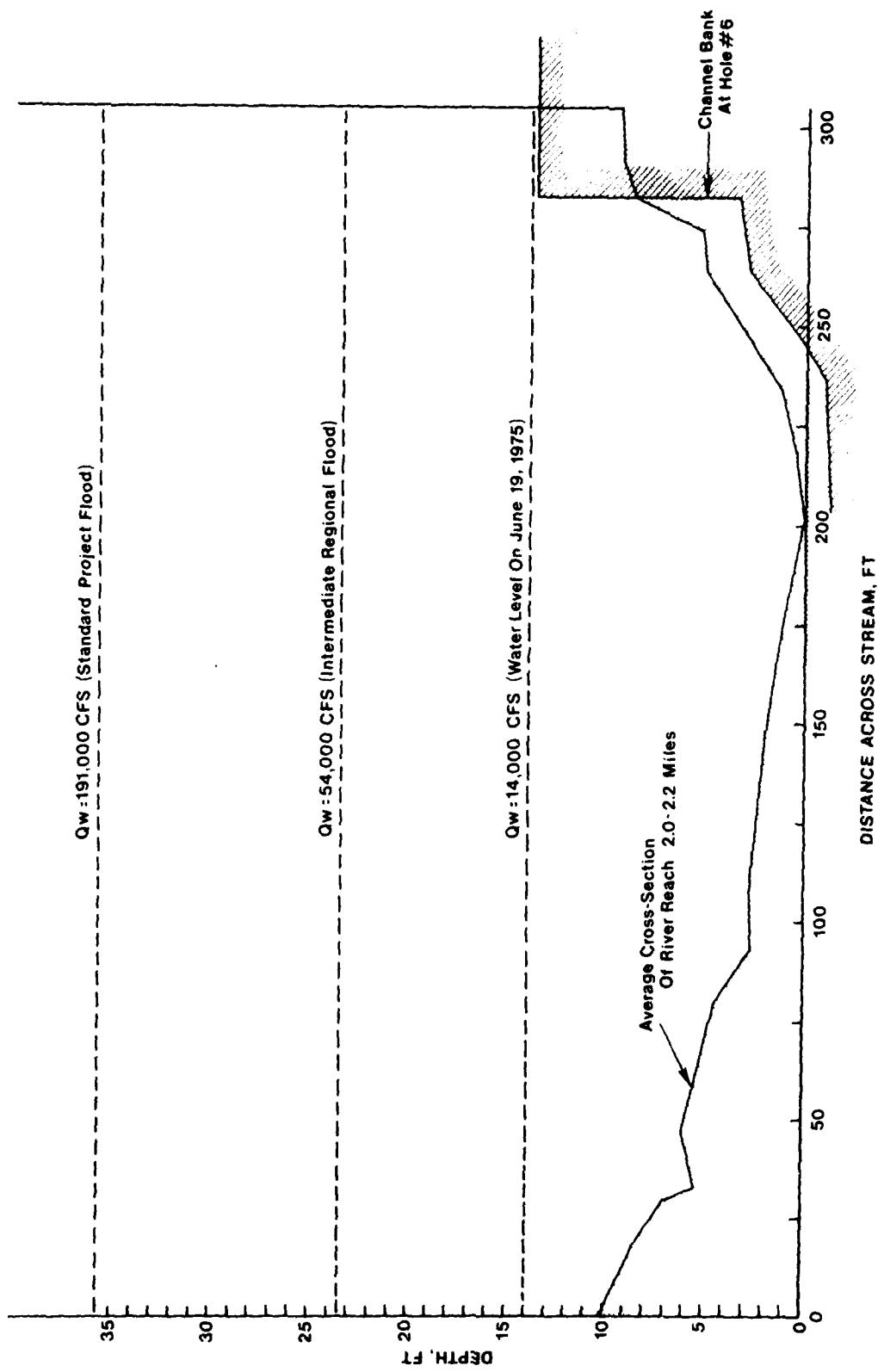
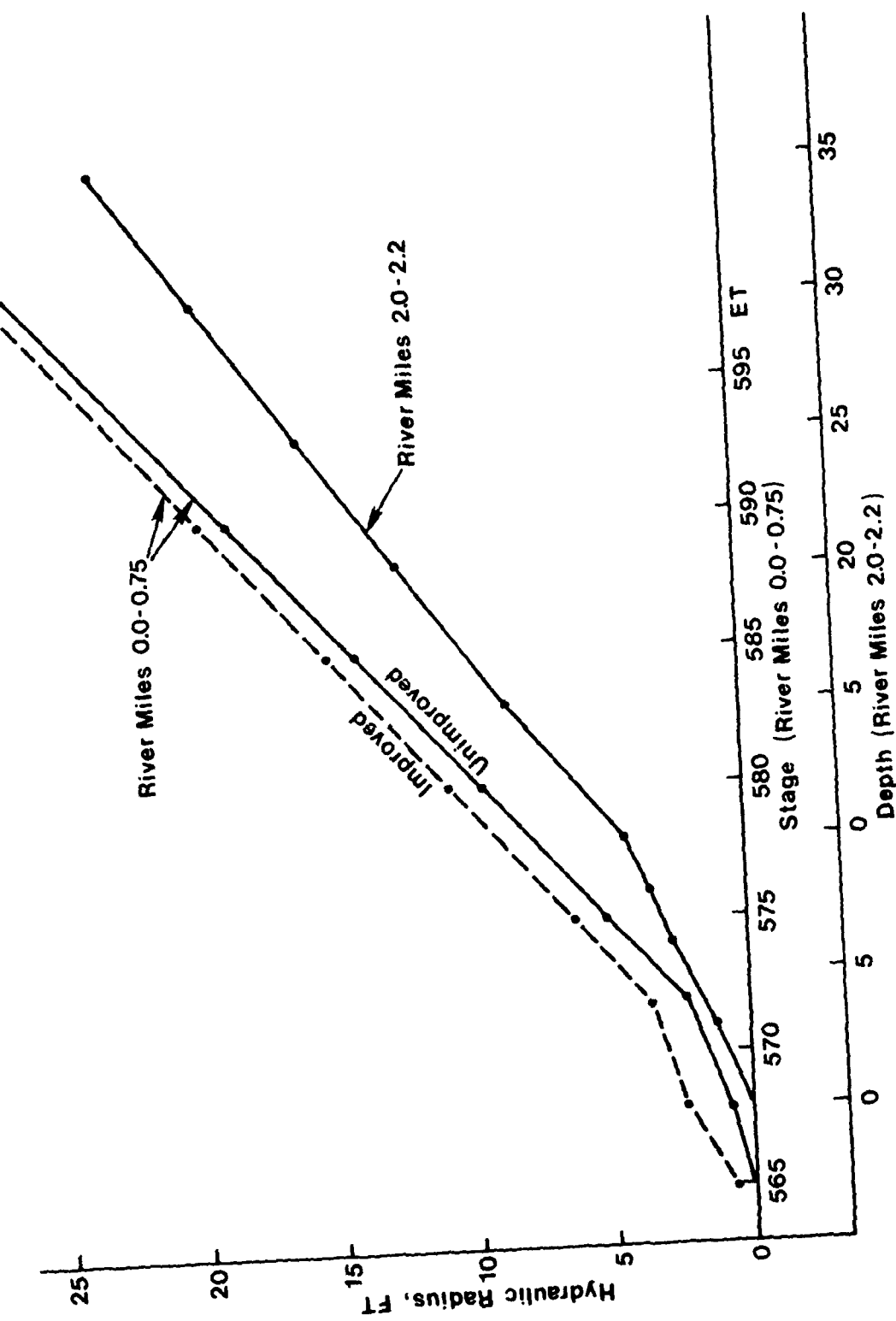


Figure 11. Relationship between channel depth (stage) and hydraulic radius used in the sediment transport calculations. The relations are derived from Figures 9 and 10.



velocity and an assumed logarithmic vertical velocity profile, as recommended by Einstein (1950). As demonstrated in Appendix 5, the two methods produce fair agreement. The appropriate Manning's n was determined from the observed mean current velocity and slope during a 12,000 cfs flood on June 18, 1975. This n , found to be 0.019 was subsequently used in all computations accepting the validity of the following assumptions: (1) no large-scale occurrence of bedforms; (2) for purposes of bed material entrainment, only the channelized portion is considered for overbank flow stages. All computed hydraulic parameters are summarized in Appendix 5.

4.3. Sediment transport computations.

There seems to exist a common opinion that for streams carrying coarse bedload, the rate of transport is best predicted by use of the equations proposed by Einstein (1950) or Meyer-Peter and Müller (1948). However, one cannot with certainty determine which existing method would be the most reliable for any given flow situation. In this study, therefore, initial computations based on Einstein (1950), Meyer-Peter and Müller (1948), Kalinske (1947) and Schoklitsch (1950) were carried out. The results of the Schoklitsch method proved to be unrealistically low and were therefore dropped in the final analysis. For a concise discussion of the procedural aspects of each individual method, the reader is referred to Graf (1971, pp. 123-159).

In order to represent the transport rate of each size component of the bed, the total sample was subdivided in five fractions, each containing 20 percent of the material. From the size-frequency diagrams

(Appendix 1, C) the corresponding size ranges and means were computed for each fraction. The potential load was computed by all three methods assuming the entire bed to consist of just one size range. The results are presented as "G_s" in the tables of Appendix 6. The total real load for any given discharge was then computed by summation of the G_s's for each size range and multiplying by .2.

Dredged material from hole #4 (Fig. 8) was considered representative for the lower reach (0-0.75 mi) of the creek; material from hole #6 (Fig. 8) was used in computations on the 2.0-2.2 mi reach. The computed results represent bedload and, therefore, exclude the washload and that portion of the bed material which moves in suspension. The river bed near the lake does not have a dramatic increase in fines compared to upstream (Appendix 1, C); therefore, it is assumed that bedload is the dominant factor in deposition in that lower reach. Because of rather minor changes in energy slope after channel improvement, that situation is assumed to remain essentially unchanged.

4.4. Results.

Details of bedload computations are presented in Appendix 6. The resulting bedload rating curves are presented in tabular form in Table 4 and graphically in Figure 12. Total annual bedload based on a listing of flow events over 25 years (Corps of Engineers, 1968, Table 4) and an unpublished flow frequency diagram (Corps of Engineers) is presented in Table 5 for the different methods used.

For water discharges in the intermediate and high flood range (20,000-80,000 cfs) the different bedload rating curves demonstrate good

Table 4
SUMMARY OF COMPUTED BED MATERIAL TRANSPORT RATES

River Mile	Discharge	Load in Tons/Day		
		Einstein	Meyer-Peter, <u>et al.</u>	Kalinske
0-0.75 mi unimproved	3,400	11	12.5	991
	16,000	5,201	3,952.0	4,727
	50,000	43,491	38,333.0	33,238
	100,000	88,327	77,868.0	59,569
0-0.75 mi improved	5,600	41	--	--
	23,000	7,883	--	--
	56,000	48,675	--	--
	107,000	104,800	--	--
2.0-2.2 mi	3,150	2,528	1,867.0	2,286
	17,000	14,820	11,620.0	10,560
	20,000	17,240	14,740.0	13,998
	33,000	28,120	23,832.0	20,893
	55,000	41,270	35,747.0	28,944

Figure 12. Computed bedload rating curves. Solid lines present the results of computations on river reach 0-0.75 miles by methods proposed by Einstein (1950), Meyer-Peter and Müller (1948) and Kalinske (1947). Dashed lines present results of similar computations on river reach 2.0-2.2 miles.

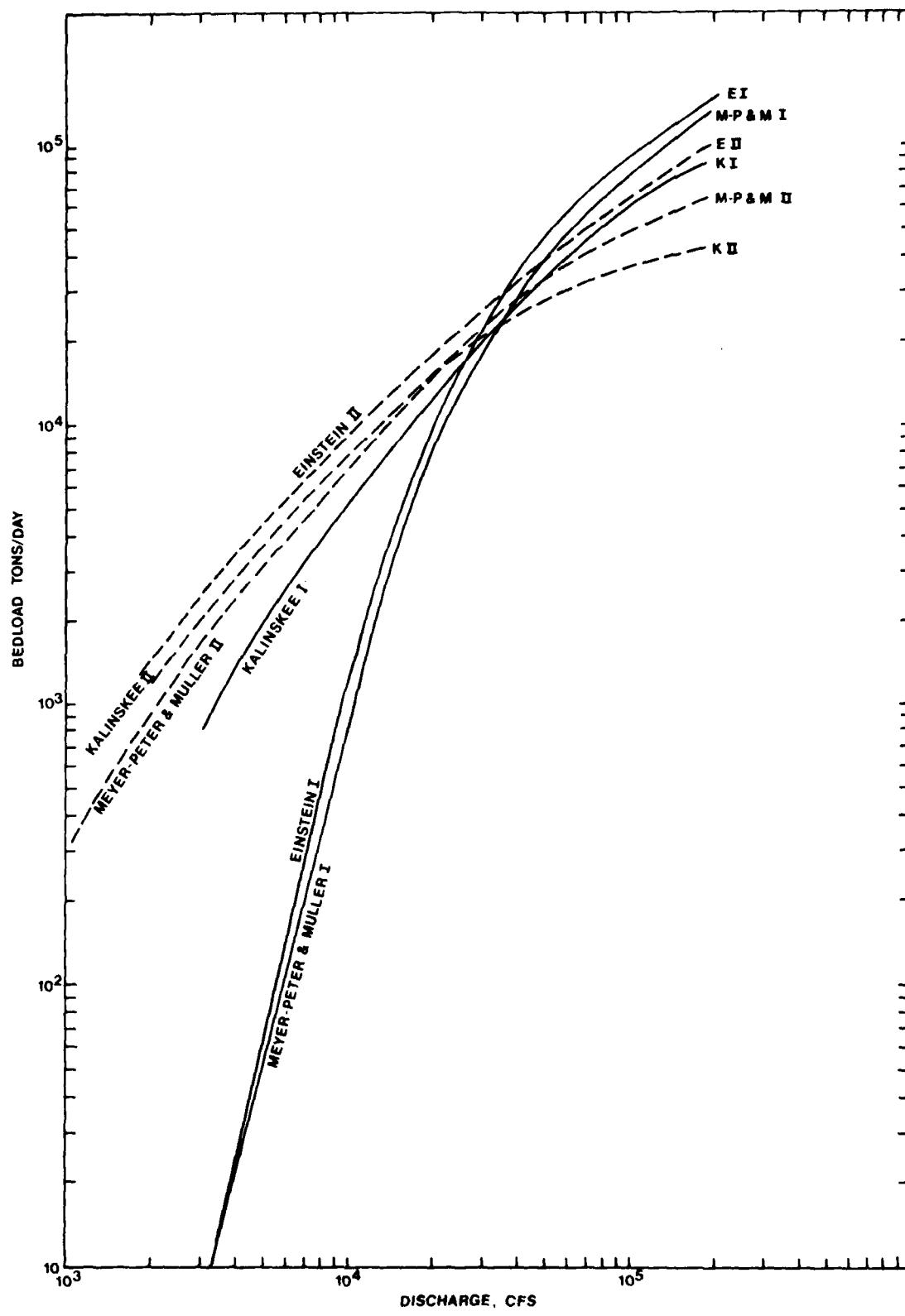


Table 5
COMPUTED ANNUAL AVERAGE SEDIMENT TRANSPORT IN CATTARAUGUS CREEK BASED ON 25 YEARS OF
WATER RECORDS (FLOW DATA FROM: CORPS OF ENGINEERS, 1968)

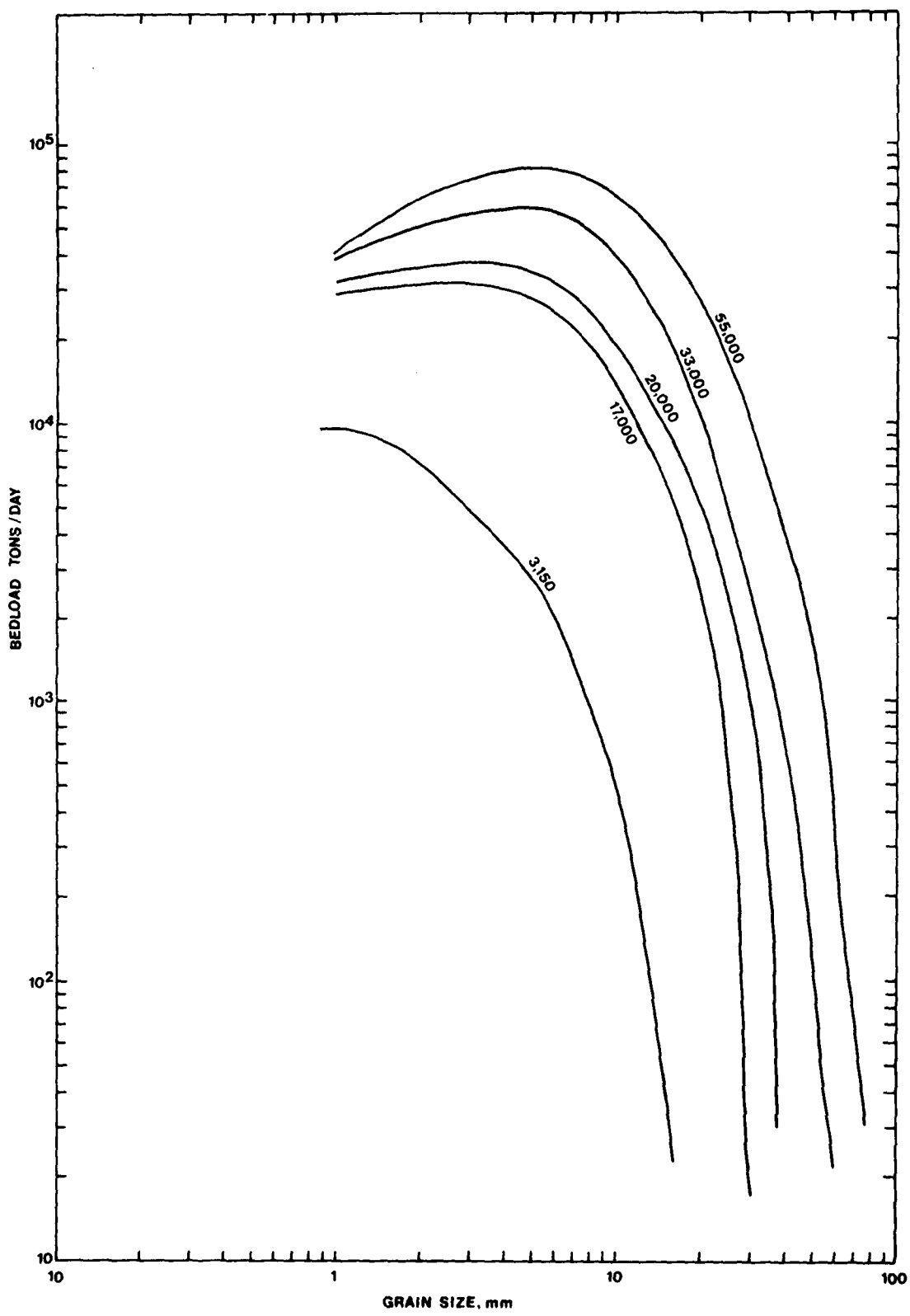
Discharge (cfs)	Number of Occurrences	Sediment Load, Tons					
		0-0.75 mi	0.75-2.0 mi	2.0-2.2 mi	Einstein	Meyer-Peter & Muller	0-0.75 mi
35,000	2	54,000	57,000	47,000	50,000	45,000	45,000
30,000	1	21,500	25,000	18,000	21,500	19,000	20,000
25,000	3	44,400	63,000	39,000	55,500	48,000	51,000
20,000	8	73,600	140,000	64,000	112,000	100,000	112,000
15,000	13	57,200	169,000	44,200	136,500	110,500	143,000
10,000	25	23,750	225,000	19,000	167,500	130,000	192,500
5,000	300	21,000	--	15,900	--	540,000	--
1,000	1,500	<1,500	--	<1,500	--	<15,000	--
25 yr total load, tons		295,450	--	247,100	--	992,500	--
Annual load, tons	11,818	27,160	9,884	21,720	29,700	22,520	

agreement. It seems that bedload transport rates for single major flow events can be predicted with reasonable accuracy. For lower, and much more frequently occurring, discharges the equations developed by Einstein and Meyer-Peter and Müller give similar transport rates, whereas Kalinskee's method predicts substantially larger rates for the lower reach of the creek. It is interesting to note that for low discharges--<20,000 cfs--all methods predict a larger transport rate for the upstream reach than for the mouth. This is due primarily to the steeper slope at mile 2 than mile 0; this difference becomes more pronounced the smaller the discharge. The slope used at the mile 2 reach was $7.5 \cdot 10^{-4}$ regardless of discharge. This is probably too steep for a flow of 5000 cfs or less. Consequently, sediment transport rates computed for low discharges of reach 2 are not used in estimating the mean annual sediment transport rate (Table 5).

Figure 13 presents the results of the computed potential transport rate at reach 2 as a function of grain size. At intermediate and high discharge (>20,000 cfs) one finds a maximum in transport rate for about 10 mm; for smaller grains the transport rate decreases. This probably reflects the incorporation of some of the smaller particles into the suspended load at such discharges. Undoubtedly, some of this coarse suspended load will settle out in the lower reach of the stream. The computed bedload, therefore, presents a minimum estimate of actual supply to the bed of the potential Cattaraugus Creek harbor site.

By integrating the sediment discharge for the last 25 years using the rating curves of Figure 12 and the listing of all significant flow events during this time period, one arrives at the mean annual transport

Figure 13. Potential transport rate versus grain size for five different water discharges (3,150 cfs - 55,000 cfs) on river reach 2.0-2.2 mi. For intermediate and high discharges maximum potential transport is found to occur for a size range of 5 to 10 mm. This indicates the transport of smaller particles in suspension for such discharges.



rates presented in Table 5. Because Kalinskee's method is the least sensitive to changes in water discharge, it predicts higher sediment transport rates for low, and frequent, flows than does either Einstein or Meyer-Peter. Consequently, Kalinskee predicts that the relatively frequent 5000 cfs flood is the most significant contributor to the long-term sediment discharge, whereas Einstein and Meyer-Peter and Müller indicate that the much more rare 20,000 cfs flood event is the one contributing the most sediment. The general consensus of all three methods for the stream segments investigated is that the mean sediment transport rate on the lower Cattaraugus Creek is a few tens of thousands tons per year.

As shown in Table 4, a separate rating curve was computed for improved (dredged) conditions near the river mouth. Given the approximate nature of the computations, the difference in transport rates for natural and improved conditions are not large enough to attempt an assessment of trap efficiency. In any event, the trap efficiency will depend a lot more on changes in lake level over the next few years.

5. COMPUTER SIMULATION OF DEPOSITION IN CATTARAUGUS CREEK

5.1. The Simulation Technique

The rates at which deposition could occur were calculated through using the computer program, 723-G2-L2470, "Scour and Deposition in Rivers," formulated by the U.S. Army Corps of Engineers, Hydrologic Engineering Center, Davis, California. Use of this program has the advantage of providing a more realistic simulation of the response of a river or harbor to changes in its configuration or in upstream conditions than can be feasibly gotten by hand calculations, assuming that the sediment transport equations used in the computer calculations accurately reflect the conditions which occur naturally.

The procedure for calculating deposition or scour is basically straightforward, based on the principle of conservation of mass of sediment. Dredging the harbor to greater than equilibrium depths decreases the capacity to transport sediment of the water which flows through the harbor. Nevertheless, the downstream improvements will not substantially affect the transport capacity upstream, with the net result that more sediment can flow into the dredged reach than is capable of being carried out. The amount deposited, or stored, equals the difference between the total amount of outflow and the total amount of inflow during the time period. Similarly, the storage rate equals the difference between inflow and outflow rates.

There are two different techniques for simulating deposition. One

is to calculate the storage which would occur if flow events of certain magnitude and frequency were to happen. In this case storms of several different return periods would be used as the hydrologic input to the program, with the output being the accreted volume in the harbor. Based on the number of floods of a certain frequency to be expected over a certain number of years, the average annual deposition to be expected from those floods could be calculated.

This simulation method has two drawbacks. First of all, it neglects the slow, but constant, transport of bed materials which occurs during the smaller flows of almost negligible return period. Secondly, using this method would be impractical to consider any other geometry for the harbor than its designed, dredged depth. For example, we do not know whether a 5-year flood would occur with the harbor partially filled with sediment or completely free. On the other hand the initial configuration of the harbor before the occurrence of a flood is very important, since that condition determines the trap efficiency of the harbor.

The other way of simulating deposition is to consider a series of actual flow events which have occurred. This has the advantage of following the naturally occurring sequence of events and of including even the most minor flows. In order to include the major flow events a long period of record has to be simulated or else the particular years in which large events occurred is chosen as the simulation period.

The latter method was the one used here. The water discharges at Gowanda for the years 1971 and 1972 were tabulated from the appropriate surface water records of the U.S. Geological Survey. The hydrograph record was leveled out in the form of a histogram so that the discharges

from January 1-4, for instance, were considered equal to 853 cfs for 4 days, and so on. This procedure saves considerable computer time and space, since a series of similar discharges, each of which act for a single day, are considered equivalent to a single average discharge acting for a number of days. The precision of the calculations is not significantly changed because of this. Table 6 shows that 1971 was divided into 20 different periods, one of which was 160 days long. The final step in choosing discharges was to increase the measured values at Gowanda by the multiplier 1.282, which is the ratio of watershed areas. Thus, it was assumed that the water discharge at the mouth of Cattaraugus Creek is proportionally larger than at Gowanda by the ratio of the watershed areas. That assumption is realistic, based on studies of other nearby rivers in the Great Lakes basin. The two-year sequence includes a flow event having a peak flow with a return period of about 10 years (instantaneous peak 25,300 cfs at Gowanda).

5.2 Sources of Error

Although the calculation procedure which has been outlined is straightforward, the calculations themselves are extremely complicated and likely to be imprecise. The amount of error to be expected is unknown. There are many natural factors which complicate the problem and too little is presently known about applying sediment transport theory to actual field problems. Computer simulation should not be relied upon as the sole method of analyzing sediment problems.

The fact is that the choice of a formula to calculate sediment transport capacity is critical to the results of any sediment study. Shulits and Hill made a very complete study of bedload formulas, at one point comparing

the convergence of a number of different equations. They wrote (Shulits and Hill, 1968).

"Interesting and very relevant is the range of grain sizes pertaining to each formula: 0.3 to 3.0 mm for Haywood, 3.0 to 7.0 mm for Meyer-Peter, and 0.3 to 7.0 mm for Schoklitsch. The three tables display where the Schoklitsch 1934 formula agrees again with 30%, with each of the other three formulas over the experimental and river data range. More important, it should be repeated that the Schoklitsch 1934 formula comes close to at least one of the other formulas over the entire range investigated. We would re-emphasize that the 30% limit extends into the range of river data as the tables show.

We, therefore, recommend, most particularly for design purposes, that of the Q-formulas the Schoklitsch 1934 formula be applied to actual problems. Yet without bedload measurements in the field, be they obtained from bedload traps, reservoir surveys or cross-sectional changes in the river, the computations would not further our knowledge. But with such measurements, coefficients or perhaps exponents can be altered to produce a more accurate formula, if only for one river or site.

We do not imply in any way that the Schoklitsch formula is the most accurate of all Q-formulas. What we affirm is that by using it one can be sure the result is within 30% of either the Haywood, Meyer-Peter or Schoklitsch 1943 formulas and so concentrate efforts on one formula... Again, finally and emphatically, only studies on actual rivers will give the answer."

In the HEC computer model either the Einstein bed material transport function or the Laursen function can be used. The Einstein method gives very similar results to the Meyer-Peter method. The former method is complicated and laborious but is based on a careful analysis of sediment transport theory based on fluid mechanics theory and flume experiments. Its precision was not studied by Shulits and Hill, but from other analyses it is expected that either the Einstein method or the Meyer-Peter method would work as well for gravel transport as any other calculation method.

Additional complexities have been mentioned. Perhaps the most important

the convergence of a number of different equations. They wrote (Shulits and Hill, 1968).

"Interesting and very relevant is the range of grain sizes pertaining to each formula: 0.3 to 3.0 mm for Haywood, 3.0 to 7.0 mm for Meyer-Peter, and 0.3 to 7.0 mm for Schoklitsch. The three tables display where the Schoklitsch 1934 formula agrees again with 30%, with each of the other three formulas over the experimental and river data range. More important, it should be repeated that the Schoklitsch 1934 formula comes close to at least one of the other formulas over the entire range investigated. We would re-emphasize that the 30% limit extends into the range of river data as the tables show.

We, therefore, recommend, most particularly for design purposes, that of the Q-formulas the Schoklitsch 1934 formula be applied to actual problems. Yet without bedload measurements in the field, be they obtained from bedload traps, reservoir surveys or cross-sectional changes in the river, the computations would not further our knowledge. But with such measurements, coefficients or perhaps exponents can be altered to produce a more accurate formula, if only for one river or site.

We do not imply in any way that the Schoklitsch formula is the most accurate of all Q-formulas. What we affirm is that by using it one can be sure the result is within 30% of either the Haywood, Meyer-Peter or Schoklitsch 1943 formulas and so concentrate efforts on one formula... Again, finally and emphatically, only studies on actual rivers will give the answer."

In the HEC computer model either the Einstein bed material transport function or the Laursen function can be used. The Einstein method gives very similar results to the Meyer-Peter method. The former method is complicated and laborious but is based on a careful analysis of sediment transport theory based on fluid mechanics theory and flume experiments. Its precision was not studied by Shulits and Hill, but from other analyses it is expected that either the Einstein method or the Meyer-Peter method would work as well for gravel transport as any other calculation method.

Additional complexities have been mentioned. Perhaps the most important

factor which has been neglected in this analysis is the role of waves and short term lake levels on sedimentation in the harbor.

Waves are capable of carrying sediment from the lake into the harbor, a process which occurs as the waves refract towards the shorelines and run into the embayment. Furthermore, the water level of the lake, which changes with winds and storms, strongly affects backwater curves and therefore the trap efficiency.

As mentioned before, the water discharges have been simulated as if the hydrograph were a histogram, so that one day is the shortest time period for which discharges are considered.

There are also limitations inherent in the computer program. It cannot simulate lateral variations in sediment transport across the channel. It cannot reproduce the conditions arising from channel curvature and it simulates conditions as if the channel were straight. It cannot accept more than 10 grain size fractions as bed material input. Since it takes 10 fractions to simulate all of the sand and gravel sizes, all of the potential silt and clay transport was neglected. Therefore, the results of the simulation do not include any potential silt and clay deposition.

5.3 Results

Despite the limitations mentioned in section 5.2, there were still many options and variables involved. Some of these include:

1. Specify number of iterations used in calculating bed material - a balance between computer time and precision.
2. Inflowing load - influences equilibrium of upstream sections.
3. High, average or low lake levels - influences velocity head and deposition.

4. Grain size distribution in bed - an important factor in calculating transport.
5. Peak floods - may be great sources of scour or deposition.
6. Series or parallel discharges - the program is capable of either taking up to 10 discharges at a time (in parallel) followed by 10 more, etc. or taking one at a time (series). Calculating in series allows readjustment of the bed after each event.

Number 4 requires discussion. We were provided with several grain size distributions taken at different locations at different times. When an actual series of these distributions was fed into the model, a great deal of instability occurred. It was felt that the arbitrariness of locating the grab samples was the cause. This was supported by distinct variations in the samples which were taken at the same location on different occasions. After much experimentation, two bed gradations were used. First, an actual distribution, consisting of very fine sand up to very coarse gravel and a small amount of finer material, was used at each cross-section. Second, an actual distribution taken from the proposed dredging project area was used. This sample contained a greater amount of fine material but very little gravel. A proportion of gravel was gradually added at each section towards the upstream direction, since this type of trend had been shown in the grab samples, to finally agree at the upstream section with the bed material distribution there.

Finally, ten runs were made. Each run used either 30 or 60 iterations to calculate bed material, the modified inflowing load, sediment gradation, water discharge table, and all 20 discharges in series. The runs were as follows:

1. First bed gradation.
 - a. 1972 discharges - low lake levels
 - b. 1972 discharges - average lake levels
 - c. 1972 discharges - high lake levels
 - d. Highest flood of record - average lake levels
 - e. 100 year - design flood - average lake levels
2. Second gradation.
 - a. 1972 - low lake levels
 - b. 1972 - average lake levels
 - c. 1972 - high lake levels
 - d. Highest flood of record - average lake levels
 - e. 100 year flood - average lake levels

During high discharges both bed gradations yielded similar results.

However, during high discharges, the extra fines present in the downstream sections of the second gradation tended to increase the transport in those sections. The result was a scouring in the dredged area. It was felt that although the gradation might vary in the flow direction during low discharges it would be much more uniform during high flows. Since high flows are the most important to sediment transport, only the first gradation is presented in this report.

A summary of the results is presented in Tables 6 through 13. Calculations for the 1971 year are presented in Tables 6, 7, 8, and 9. The first three of those tables present the chronologic sequence of transport rates for the given water discharges, together with the trap efficiency of the harbor at the end of the flow events. Table 9 presents the calculated bed changes for each section as of the end of the 1971 year.

Table 6
Sediment Transport Rates Based on
1971 Discharges for Low Lake Levels

<u>Flow</u>	<u>Discharge (cfs)</u>	<u>Duration (Days)</u>	<u>Transport Rate (tons/Day)</u>	<u>Trap Efficiency</u>
1	853	4	0	0.99
2	3538	1	81	-0.22
3	615	46	0	-0.21
4	2158	6	8	-0.06
5	7692	1	1595	0.07
6	6384	1	716	0.02
7	3077	1	43	0.01
8	1256	13	1	0.01
9	7327	2	1304	0.08
10	3205	1	46	0.05
11	1205	14	1	0.05
12	4405	2	167	0.08
13	1906	6	6	0.08
14	3494	4	73	0.12
15	6481	2	778	0.13
16	837	76	0	0.13
17	206	160	0	0.13
18	4282	2	171	0.14
19	1202	21	1	0.14
20	4212	2	149	0.14

Average yearly cumulative transport rate = 5140 tons/Year

Final trap efficiency = 0.14

Table 7

Sediment Transport Rates Based on
1971 Discharges for Average Lake Levels

Flow	Discharge (cfs)	Duration (Days)	Transport Rate (tons/Day)	Trap Efficiency
1	853	4	0	1.00
2	3538	1	82	0.52
3	615	46	0	0.52
4	2158	6	7	0.57
5	7692	1	1571	0.29
6	6384	1	695	0.23
7	3077	1	32	0.24
8	1256	13	0	0.24
9	7327	2	1277	0.23
10	3205	1	34	0.24
11	1205	14	0.0	0.24
12	4404	2	138	0.27
13	1906	6	4	0.27
14	3494	4	60	0.31
15	6481	2	743	0.30
16	837	76	0	0.30
17	206	160	0	0.30
18	4282	2	172	0.31
19	1202	21	0	0.31
20	4212	2	145	0.32

Average yearly cumulative transport rate = 4960 tons./year

Final trap efficiency = 0.32

Table 8

Sediment Transport Rates Based on
1971 Discharges for High Lake Levels

<u>Flow</u>	<u>Discharge (cfs)</u>	<u>Duration (Days)</u>	<u>Transport Rate (tons/Day)</u>	<u>Trap Efficiency</u>
1	853	4	0	1.00
2	3538	1	65	0.91
3	615	46	0	0.91
4	2158	6	4	0.93
5	7692	1	1572	0.43
6	6384	1	684	0.52
7	3077	1	25	0.53
8	1256	13	0	0.53
9	7327	2	1244	0.40
10	3205	1	48	0.41
11	1205	14	0	0.41
12	4405	2	141	0.44
13	1906	6	1	0.44
14	3494	4	52	0.48
15	6481	2	746	0.51
16	837	76	0	0.51
17	206	160	0	0.51
18	4282	2	146	0.52
19	1202	21	0	0.52
20	4212	2	137	0.53

Average yearly cumulative transport rate = 4865 tons/Year

Final trap efficiency = 0.53

Table 9
Simulated Bed Changes by Section in Feet for 1971 Flows

Section	Low Lake Levels	Average Lake Levels	High Lake Levels	Average Value
Upstream ↑				
18.0	0.23	0.46	0.60	0.43
17.0	-0.03	-0.02	-0.07	-0.04
16.0	-0.06	-0.04	-0.04	-0.05
15.0	0.02	-0.02	0.02	0.02
14.0	-0.07	-0.04	-0.05	-0.05
13.0	-0.01	-0.05	-0.02	-0.03
12.0	-0.04	-0.03	0.01	-0.02
11.0	0.04	0.05	0.09	0.06
10.0	0.09	0.13	0.10	0.11
9.0	-0.02	-0.02	0.01	-0.01
8.0	0.02	0.07	0.12	0.07
7.0	0.01	0.09	0.19	0.10
6.0	0.02	0.03	0.01	0.02
5.0	-0.05	0.00	0.00	-0.02
4.2	0.00	0.01	0.01	0.01
3.8	0.01	0.01	0.01	0.01
3.4	0.18	0.08	0.07	0.11
3.0	0.04	0.05	0.14	0.08
2.8	0.01	0.02	0.01	0.01
2.4	-0.02	0.00	0.00	0.01
2.3	0.00	0.01	0.00	0.003
2.2	0.02	0.02	0.01	0.02
Downstream ↓	2.0	0.06	0.03	0.03

Average Change, Sect. 2.0-8.0

+0.02 +0.03 + .04 +0.03

Table 10
Sediment Transport Rates Based on
1972 Discharges for Low Lake Levels

<u>Flow</u>	<u>Discharge (cfs)</u>	<u>Duration (Days)</u>	<u>Transport Rate (tons/Day)</u>	<u>Trap Efficiency</u>
1	723	61	0	0.98
2	12820	1.00	5735	0.05
3	6461	1.00	575	-0.12
4	3077	20.0	44	-0.05
5	1538	20.0	3	-0.05
6	2602	10.0	20	-0.04
7	800	15.0	0	-0.04
8	2936	2.0	36	-0.04
9	620	43	0	-0.04
10	6115	1.0	447	-0.02
11	23717	1.0	55004	0.12
12	6282	1.0	661	0.06
13	2367	3.0	13	0.06
14	432	101	0	0.06
15	3872	1.0	127	0.06
16	779	26	0	0.06
17	4192	1.0	147	0.06
18	1340	31	1	0.06
19	10320	1.0	2651	0.06
20	1801	25	3	0.06

Average yearly cumulative transport rate = 65,467 tons/Year

Final trap efficiency = 0.06

Table 11

Sediment Transport Rates Based on
1972 Discharges for Average Lake Levels

<u>Flow</u>	<u>Discharge (cfs)</u>	<u>Duration (Days)</u>	<u>Transport Rate (tons/Day)</u>	<u>Trap Efficiency</u>
1	723	61	0	1.00
2	12820	1.00	5734	0.11
3	6461	1.00	569	0.04
4	3077	20.0	41	0.13
5	1538	20.0	1	0.13
6	2602	10.0	17	0.14
7	800	15.0	0	0.14
8	2936	2.0	36	0.15
9	620	43	0	0.15
10	6115	1.0	409	0.15
11	23717	1.0	55667	0.16
12	6282	1.0	540	0.14
13	2367	3.0	12	0.14
14	432	101	0	0.14
15	3872	1.0	89	0.14
16	779	26	0	0.14
17	4192	1.0	128	0.14
18	1340	31	1	0.14
19	10320	1.0	2657	0.14
20	1801	25	4	0.14

Average yearly cumulative transport rate = 65905 tons/Day

Final trap efficiency = 0.14

Table 12

Sediment Transport Rates Based on
1972 Discharges for High Lake Levels

<u>Flow</u>	<u>Discharge (cfs)</u>	<u>Duration (Days)</u>	<u>Transport Rate (tons/Day)</u>	<u>Trap Efficiency</u>
1	723	61	0	1.00
2	12820	1.00	5728	0.24
3	6461	1.00	529	0.23
4	3077	20.0	28	0.32
5	1538	20.0	0	0.32
6	2602	10.0	11	0.33
7	800	15.0	0	0.33
8	2936	2.0	21	0.34
9	620	43	0	0.34
10	6115	1.00	403	0.35
11	23717	1.00	55648	0.17
12	6282	1.00	528	0.17
13	2367	3.0	6	0.17
14	432	101	0	0.17
15	3872	1.0	82	0.18
16	779	26	0	0.18
17	4192	1.0	124	0.18
18	1340	31	0	0.18
19	10320	1.0	2674	0.18
20	1801	25	3	0.18

Average yearly cumulative transport rate = 65785 tons/Year

Final trap efficiency = 0.18

Table 13
Simulated Bed Changes by Section in Feet for 1972 Flows

	<u>Section</u>	<u>Low Lake Levels</u>	<u>Average Lake Levels</u>	<u>High Lake Levels</u>	<u>Average Value</u>
Upstream	18.0	0.54	0.32	0.66	0.51
	17.0	-0.01	-0.04	-0.04	-0.03
	16.0	-0.11	-0.09	0.02	-0.06
	15.0	-0.17	-0.13	-0.12	-0.14
	14.0	-0.08	-0.04	-0.03	-0.05
	13.0	-0.11	-0.07	0.03	-0.05
	12.0	-0.03	0.08	0.10	0.05
	11.0	0.09	0.21	0.07	0.12
	10.0	0.21	0.09	0.16	0.15
	9.0	-0.45	-0.30	0.01	-0.25
Existing conditions	8.0	0.26	0.23	0.20	0.23
	7.0	0.10	0.15	0.42	0.22
	6.0	0.10	0.07	0.11	0.09
	5.0	-0.02	0.05	0.04	0.02
	4.2	0.00	0.03	0.06	0.03
	3.8	0.02	0.09	0.06	0.06
	3.4	0.29	0.15	0.17	0.20
	3.0	0.17	0.35	0.30	0.27
	2.8	0.08	0.12	0.12	0.11
	2.4	0.03	0.06	0.03	0.04
Improved conditions	2.3	-0.16	0.14	0.05	0.01
	2.2	0.06	0.39	0.12	0.19
	2.0	0.36	0.82	0.25	0.48
Average Bed Change, Sect. 2.0-8.0					
+0.10 +0.20 +0.15					

Sections 2.0 through 8.0 are the dredged harbor, or improved conditions, while 8.0 through 18.0 represent existing conditions. The average bed change in the dredged harbor for that dry year is between +0.02 feet and +0.04 feet, depending on lake levels.

A similar sequence is followed for Tables 10 through 13, which apply to the 1972 year. In this case, average deposition rates in the dredged section range from +0.1 to +0.2 feet. The high lake levels cause deposition in the reach above the dredged section, accounting for the lower average value.

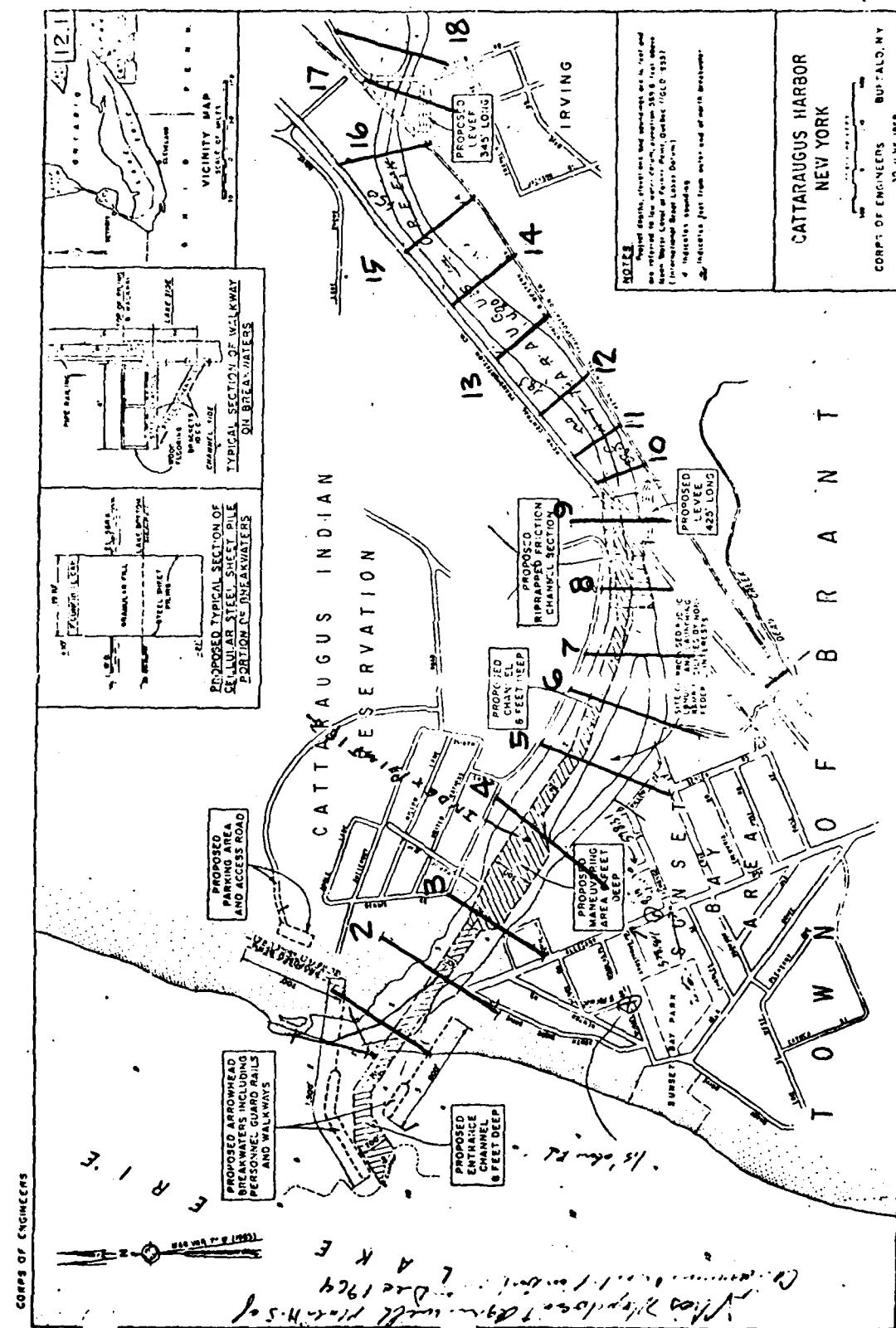
These accretion rates would increase if it were possible to include silt transport in the calculations.

The two-year sequence, 1971-1972, includes one exceptionally dry year and a wet year, and this was the reason for choosing the two. As a crude approximation, the average annual bed-load transport could be considered as the average of the two total transport rates, approximately 35,000 tons/year. In order to obtain a more realistic figure, a larger number of years ought to be simulated. Since 1972 does include a 10-year event, the average load for the two years is probably somewhat too large.

An important test was run to verify the model. The 1972 discharges were run with average lake levels, for the existing conditions of the creek. This was an attempt at verification of the model. It was felt that if the model was working correctly it would show that the existing conditions were approximately in an equilibrium state. The model did in fact show that. The final trap efficiency was 0.00, as it should be.

5.4 Discussion of Results

The results, in general, are quite consistent. A deposition rate of 0.1 to 0.2 feet per year would seem in order for the dredged sections



X - Section Location Map

for the hydrologic conditions simulated here. (See Figure 5,1 for location of sections.)

As might be expected the water levels of the lake had a pronounced effect on the deposition rates and trap efficiencies. During extreme low lake levels the final trap efficiency at the end of the year was reduced to 0.06 (Table 10), due to higher velocities in the dredged area. The final trap efficiency was 0.14 during average levels (Table 11), and 0.18 during extreme high lake levels (Table 12).

Deposition patterns were generally expected. Fluctuations in upstream sections reflected the dynamics of a meandering stream bed. Sections of low minimum elevation (Sects. 12.0 and 18.0) tended to build up. Sections with high minimum elevations (13.0 and 16.0) tended to scour. Scour also occurred in section 9.0, the last section before dredging, as would be expected, except for the high lake level condition. Highest deposition rates occurred in sections 8.0, 3.0, and 3.4, where dredging began and deepened, respectively. High deposition rates in section 2.0 and 2.2 are somewhat misleading. These sections are only 100 feet long, each, and very susceptible to slight changes in transport rates. Section 2.1 was only 10 feet long and had to be eliminated.

It is important to note that for high lake levels deposition occurred primarily close to the original channel reach upstream of the dredged section, a pattern which was not typical of the other lake level cases.

The flows 35,900 cfs and 57,000 cfs represent the peak and design flows for Cattaraugus Creek. The final trap efficiencies obtained were 0.03 and 0.05 respectively. The runs were made with a lake elevation 572.5 and for a duration of 1.0 day. A more precise prediction of the effects of these high flows would result from using flood hydrographs

instead of the method used. Unfortunately, those hydrographs were not available to us. A copy of the computer output summary for the design flow has been included as Table 14. These flows are really instantaneous peak discharges and do not have a 1.0 day duration. A comparable daily discharge would have to be reduced from those figures by multiplying by a factor of approximately 0.8.

From that table the total sediment inflow of 295.24 acre-feet for that 1.0 day flow is accompanied by an outflow of 281.44 acre-ft. The difference represents an average accumulation of about 0.25 feet. From the output summary it appears that about 5. feet of deposition occurs at section 15, a situation which appears unlikely and which, in the computer calculations, created scour in the downstream sections. This extreme non-uniformity may represent natural conditions or it may very well be due to the inability of the model to deal with curvature and abrupt changes in width, factors which are important to that section.

Returning to the principal results, the computer simulation indicates that although very substantial rates of sediment are carried in Cattaraugus Creek, the trap efficiencies of the proposed harbor are relatively small. Trap efficiency represents the proportion of inflowing sediment which is deposited in the reservoir. In this case the trap efficiency comes about from the program calculating the outflowing sediment load at section 2.0 and comparing that load to the inflowing load at section 18.0. Another method, somewhat crude, is to use a trap efficiency curve. From the capacity-inflow ratio of the proposed harbor, and using Brune's curve (Vanoni, 1973) a trap-efficiency of between 0.10 and 0.20 ought to be expected. This range agrees closely with the numbers presented in Tables 6-12.

Table 14
Design Flow Output Summary

Accumulated AC-FT by Entry Point Days		Inflow	Sand Outflow	Trap Eff.
1.00		295.24		
Total =	18.000	295.24	281.44	.05
	2.000			
Section ID NO	Bed Change Feet	WS Elev. Feet	Thalweg El Feet	Q CFS Sediment Load in Tons/day
18.000	.51	588.78	561.11	57000 597224
17.000	.06	587.69	562.46	57000 597021
16.000	2.13	586.73	566.63	57000 586655
15.000	5.05	586.07	566.05	57000 569489
14.000	1.77	585.42	567.37	57000 563045
13.000	~.07	585.30	566.73	57000 563490
12.000	~.27	584.50	563.23	57000 564900
11.000	~.93	580.87	561.77	57000 567937
10.000	~.88	580.60	557.92	57000 570416
9.000	~.55	580.72	559.55	57000 572061
8.000	~.12	579.14	561.48	57000 572898
7.000	.14	579.65	561.74	57000 571758
6.000	.25	579.30	561.85	57000 570322
5.000	.17	578.67	561.77	57000 568999
4.200	.10	578.23	561.70	57000 567947
3.800	.12	578.01	561.72	57000 567088
3.400	.13	577.73	559.73	57000 566273
3.000	.15	577.46	559.75	57000 565653
2.800	.04	577.35	559.64	57000 565471
2.400	~.27	576.14	559.33	57000 567285
2.300	~.40	575.00	559.20	57000 568908
2.200	~.60	574.42	559.00	57000 569993
2.000	~.08	572.50	559.52	57000 570067

On the other hand, our experiences with the bed load traps which were dug across Cattaraugus Creek appears to conflict with the calculated deposition rates in the dredged reach. The traps filled up quickly, even though water discharges during the period were relatively low. If the trap efficiencies of the harbor are roughly in the range which was mentioned, then a fault in the calculations may be in the input for gravel transport rates. These actually may be substantially higher than the amounts calculated in the program. Additional information is needed on the relation of active bed load transport to water discharge.

This page intentionally left blank.

6. CONCLUSIONS

Eight different estimates of sediment transport rates on Cattaraugus Creek all indicate substantial volumes (Table 1'). It is very difficult to assess the reliability of each method except to say that the theoretically computed transport rates and the results of the meander bend migration analysis all indicate minimum values.

If the present channel bed represents a short term equilibrium configuration for high lake levels, the proposed dredged channel will act as a relatively efficient sediment trap. With the bedload transport rates suggested by Table 6, the proposed dredged basin is likely to be filled within a period of less than ten years and more quickly if there is any trapping of suspended load. Because of the present high lake level, the desired project depth--6 feet--is attained over most of the lower river without any dredging. The expected rate of sediment transport suggests, therefore, that the dredged basin would be filled before there would be a real need for it. Furthermore, there is no known historic record of problems with navigation depths in the river channel at any lake level. For adequate conveyance the bed must be scoured during periods of low water.

It is, therefore, strongly recommended that the proposed dredging be omitted from the initial construction and not undertaken unless called for by problems encountered at lower lake stages.

Table 15
ESTIMATES OF MEAN ANNUAL SEDIMENT TRANSPORT
AT THE MOUTH OF CATTARAUGUS CREEK

Method	Total Load tons/year	Bedload tons/year
Meander migration rates (sect. 3.3) (upstream of river mile 2).....	--	12,000
Suspended sediment concentration (sect. 3.2) This report 1972 water year.....	1,570,000	140,000
Archer & La Sala, 1968.....	780,000	71,000
Sediment yield of drainage basin (sect. 3.2) U.S.D.A., 1974.....	520,000	--
Bedload transport equation, 25 yr average (sect. 4.3)		
Einstein.....	12,000	
Meyer-Peter & Müller.....	10,000	
Kalinske.....	40,000	
Computer simulation (sect 5.3).....	35,000 ¹	

¹This probably includes some suspended load.

REFERENCES

Archer, R. J. and A. M. La Sala, Jr., 1968, A reconnaissance of stream sediment in the Erie-Niagara basin, New York: New York State Water Resources Commission, Basin Planning Report ENB-5.

Einstein, H. A., 1950, The bedload function for sediment transportation in open channel flows: U. S. Dept. of Agriculture, Soil Conservation Service, Technical Bull. No. 1026.

Graf, W. H., 1971, Hydraulics of sediment transport: McGraw-Hill, N.Y.

Kalinske, A. A., 1947, Movement of sediment as bedload in rivers: Trans. Am. Geophysical Union, v. 28.

Meyer-Peter, E., and R. Muller, 1948, Formulas for bedload transport: Proc. Internat. Assoc. Hydr. Res., 2nd Meeting, Stockholm.

Schoklitsch, A., 1950, in Graf (1971, p. 136).

Shen, H. W., 1971, Total sediment load: Ch. 13 in River Mechanics, H. W. Shen (ed), H. W. Shen, Ft. Collins, Colo.

Shulits, S. and R. D. Hill, Jr., 1968, Bedload formulas: Pennsylvania State Univ., Dept. of Civil Engineering, Hydraulics Laboratory Bulletin.

U. S. Army Engineer District, Buffalo, 1966, Interim report on Cattaraugus Creek Harbor, New York, Revised ed.

_____, 1968, Flood plain information, Irving, Sunset Bay and Gowanda.

U. S. Department of Agriculture, Soil Conservation Service, 1974, Erosion and sedimentation inventory, Cattaraugus Creek, New York.

U. S. Geological Survey, 1972, Water resources data for New York.

Vanoni, V. A., 1973, Sediment control methods: D. reservoirs: J. Hydr. Div., Am. Soc. Civil Engineers, v. 99, no. HY4, p. 620.

Appendix 1, Table A
PARTICLE SIZE ANALYSIS

Material	#	Role	Percent Retained on Sieve No.															
			3"	2"	1½"	1"	3/4"	1/2"	3/8"	1/4"	4	10	20	40	70	140	200	230
Dredged	2	0.00	0.00	5.65	--	16.85	15.50	11.90	8.00	7.58	4.10	6.45	2.85	2.43	2.40	1.65	2.50	11.50
	4	0.00	5.96	10.86	--	17.12	9.74	11.40	5.72	7.15	3.94	7.12	6.08	6.83	6.38	1.02	0.20	0.20
	5	15.00	0.00	9.63	--	16.37	9.96	8.12	4.15	4.82	3.55	6.77	6.12	4.95	6.25	1.44	1.12	1.58
	6	13.56	8.14	9.66	--	5.95	5.00	8.20	8.06	8.57	5.38	9.80	5.20	3.22	5.42	1.12	1.18	1.45
Fill in traps	1	0.00	0.00	--	0.00	0.00	0.00	0.00	0.00	0.50	0.60	0.40	2.80	6.30	17.50	20.50	43.30	
	2	0.00	0.00	--	0.00	0.00	0.00	0.00	0.00	0.00	0.10	0.40	1.10	22.30	7.90	10.00	58.10	
	3	0.00	0.00	--	0.00	0.00	0.00	0.00	0.00	0.00	0.35	0.43	6.30	17.90	20.00	17.30	16.25	
	4	0.00	0.00	--	4.72	3.77	7.48	13.37	9.33	13.23	9.18	16.02	4.42	4.20	10.98	1.67	0.47	0.87
	5	0.00	3.99	--	17.49	12.61	18.39	18.96	8.31	7.55	3.97	4.50	0.94	0.13	0.15	0.56	0.70	1.53
	6	0.00	11.15	--	15.68	2.17	7.15	7.95	5.27	6.18	4.58	7.76	4.90	6.20	5.35	2.17	8.10	4.88
	7	0.00	0.00	--	1.75	8.13	12.27	15.30	9.83	11.40	7.75	14.37	8.82	4.92	3.43	0.60	0.48	0.55
Cut bank 6-7																35	1.00	
Cut bank at power poles																25	5.00	
Cut bank																35	5.00	
<u>Discharge (cfs)</u>																		
Suspended Load, June, 1975, Flood Sample																5	95.00	
Archer and La Sala, 1968, p. 15 (also see Table 3)																9,030	74.00	
																14,100	78.00	
																18,100	83.00	
																1,000	79.00	

Appendix 1, Table B
 PARTICLE SIZE ANALYSES OF SUSPENDED SEDIMENT FROM CATTARAUGUS CREEK
 AT GOWANDA, AND TONAWANDA CREEK AT BATAVIA

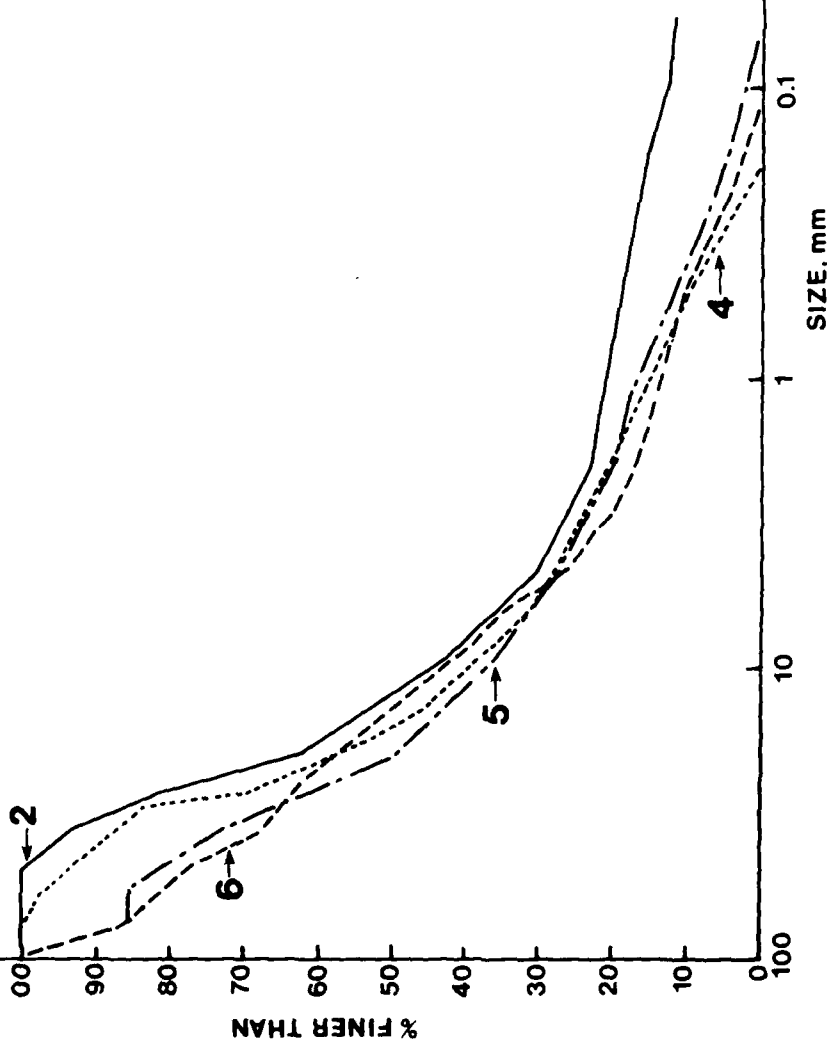
(Methods of analysis: B, bottom withdrawal tube; C, chemically dispersed; M, mechanically dispersed; N, in native water; S, sieve; W, in distilled water)

Date of collection	Time (24-hour)	Discharge (cfs)	Water temperature (°F)	Concentration or sample (ppm)	Suspended sediment						Methods of analysis		
					Percent finer than indicated size, in millimeters			Sieve diameters					
					0.002	0.004	0.008	0.016	0.031	0.062	0.125	0.250	0.500
2135. Cattaraugus Creek at Gowanda, New York													
3/25/63	1830	9,030	38	3,970	23	28	39	49	60	74	85	92	97
3/27/63	0030	14,100	--	5,090	25	31	42	53	70	78	87	94	98
3/ 5/64	0845	18,100	35	5,310	25	34	45	58	73	83	92	96	99
3/ 5/64	0845	18,100	35	5,310	12	16	26	40	60	79	89	94	99
2170. Tonawanda Creek at Batavia, New York													
3/27/63	1245	3,430	--	442	63	78	93	88	91	93	96	98	99
4/20/63	1550	824	51	1,260	48	58	75	88	96	99	100	100	100

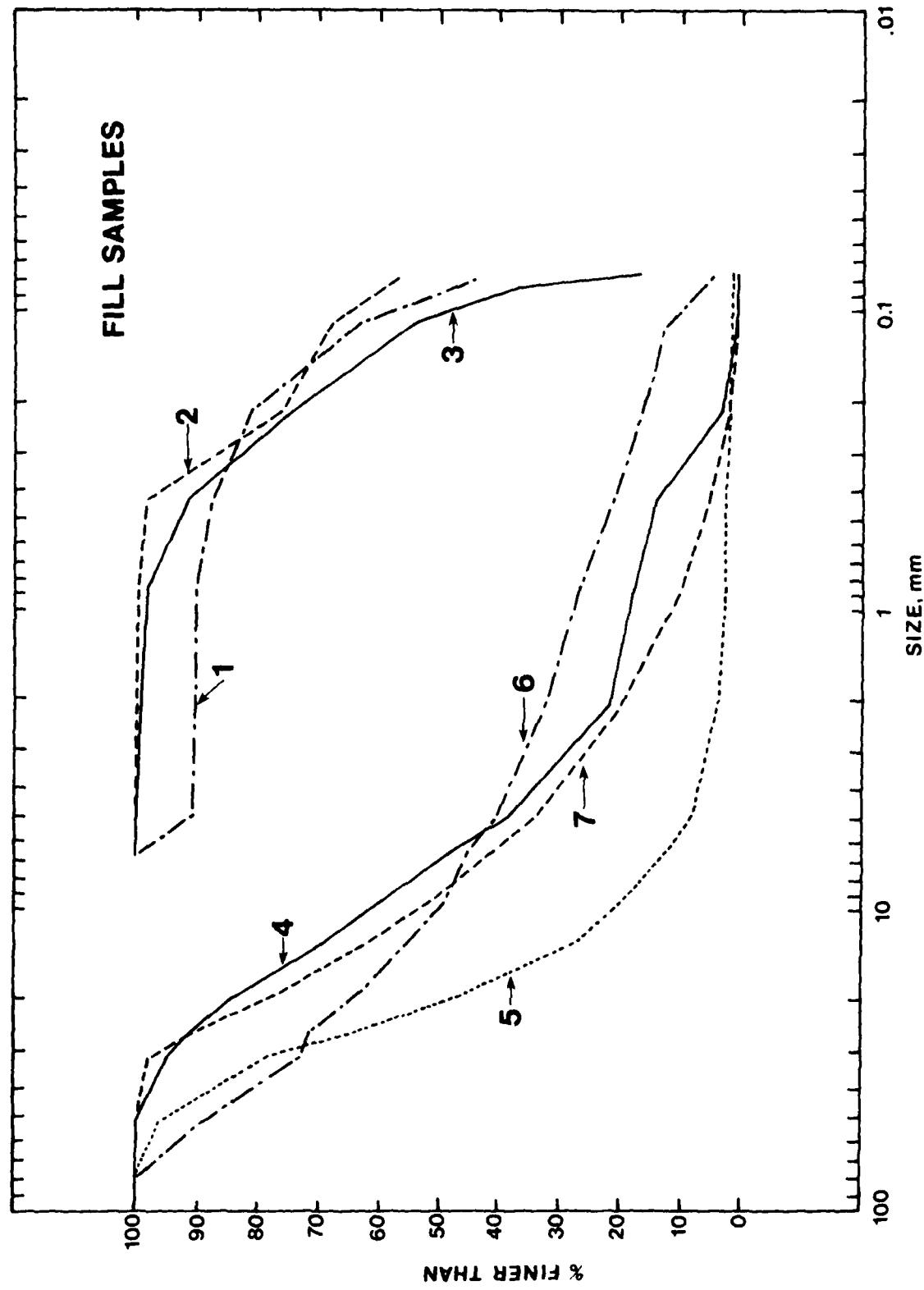
From Archer, R. J. and La Sala, A. M., Jr., 1968, p. 15.

Appendix 1 C. Size-frequency curves of bed material dredged from sediment traps nos. 2, 4, 5 and 6. For location of traps, see Figure 8.

DREDGED SAMPLES



Appendix 1 D. Size-frequency curves of bed material infilling traps
1 through 7 during the spring of 1975.



AD-A102 282

STATE UNIVERSITY OF NEW YORK COLL AT FREDONIA DEPT 0--ETC F/6 8/8
CATTARAUGUS CREEK HARBOR, NEW YORK GENERAL DESIGN MEMORANDUM, P--ETC(U)
MAR 76

DACW49-74-C-0118

NL

UNCLASSIFIED

5 = 5
AF
4-42281

END
9 81
DTIC

Appendix 2
1975 DAILY DISCHARGES: CATTARAUGUS CREEK
BASED ON INTERPRETATION OF STRIP CHART

<u>Day</u>	<u>Jan.</u>	<u>Feb.</u>	<u>March</u>	<u>April</u>	<u>May</u>	<u>June</u>	<u>Time</u>	<u>Discharge</u>
1	580	1,200	990	960	400		06:00	528
2	560	850	810	930	710		13:00	3,230
3	810	720	710	1,010	450		15:00	4,120
4	900	550	650	930	510		18:00	6,680
5	840	600	620	770	790	7,000	19:00	9,960
6	740	600	560	850	1,170	4,500	20:00	10,550
7	850	530	630	710	2,210		21:00	9,960
8	460	460	1,360	570	1,150			
9	1,280	560	850	790	1,700			
10	1,470	440	790	870	640			
11	5,190	490	690	960	570		06:00	5,540
12	3,470	470	720	1,050	510		13:00	4,180
13	1,510	400	2,080	870	570		16:00	3,960
14	980	370	1,220	790	510			
15	790	420	850	1,250	450			
16	760	470	700	1,360	400			
17	630	570	770	1,250	400	1,850	13:00	9,710
18	660	1,510	1,180	1,050	340	1,850	14:15	12,900
19	690	1,200	3,130	1,470	340	1,850	15:15	13,150
20	630	810	6,800	860	300	9,000	15:50	13,490
21	440	650	5,910	640	300		16:00	14,020
22	580	760	1,640	710	345		16:25	14,540
23	530	2,790	1,580	450	870			
24	480	9,790	1,560	870	1,050			
25	710	6,660	2,420	960	510			
26	1,680	2,340	1,620	710	400			
27	910	1,520	1,120	570	450			
28	770	1,120	1,000	510	330			
29	4,620		1,240	510	340			
30	5,230		1,250	450	250			
31	1,910		960		250			

Appendix 3

IRVING.

IRVING, at the mouth of Cattaraugus, is situated partly on a flat, interlaced by arms and channels of the creek, and partly, on a beautiful slope commanding a land and water prospect, extending to the out-let of Lake Erie, 30 miles below.

The Cattaraugus, is by far the largest tributary of the lake in the state of New-York, and embays Islands of more than 20 acres extent, having depth of water above them sufficient for the largest class of ships, affording the only inner or river harbor, between the port of Buffalo and the head of Lake Erie, on the American shore. [See Memorial to Congress, page —.]

The United States are now connecting, by parallel piers, this inner haven, with the bay or outer anchorage off the mouth; long known as a place of refuge during storms. These works, when finished, will afford a convenient road-stead of some hundreds of acres, wholly free of rock, the Engineers having sunk piles five and twenty feet below the surface, and some eighteen feet through alternate strata of clay and gravel.

IRVING, is the first port West of Buffalo, and fifteen miles above the ice-bank, which some times forming at the out-let cuts short the whole Erie Canal from water communication with the lake in spring. [See Williams' Register.]

The state having authorized the *widening* of the canal at the estimated cost of 12 millions, its *extension* likewise "to some harbor above the ice," seems not only necessary to accomplish the purpose of widening it, but has already attracted executive recommendation. [See Gov. Marcy's last (1836) message.]

From Buffalo and Erie County Historical Society Pamphlet, 1836,
Irving Land Development Company. Pamphlet original in the Buffalo and
Erie County Historical Society.

valuable water privileges, will undoubtedly become an important manufacturing district.
This harbor is as yet entirely unimproved, and though occasionally resorted to for the purpose of lying up vessels during the winter, or of taking on board passengers. During the early part of the navigation it is customarily visited by only few vessels employed in transporting lumber and other produce of its immediate vicinity.

The Creek, offering at all times complete protection from the storms of the Lake, the principal improvements required for the convenience of the general commerce, are the construction and preservation of a channel sufficiently wide and deep to admit any vessel navigating the Lakes, and the erection of suitable beacon lights. Whatever means may be employed in the construction of this channel, its preservation must be effected by the current. And as this may hereafter (either by exertions of persons or by a combination of natural causes,) be so regulated as to wear away the bed of the Creek, above the point at which it would under present circumstances be advisable to terminate the improvement, it is necessary to secure a velocity sufficient to carry on whatever may be brought from above; or in other words, to provide for a current sufficiently powerful to not only preserve but create the required dimensions.

The force of the stream in common stages of the water, being insufficient to completely effect the object in view, reliance must be placed upon the scuds, and the dimensions proper for the channel will be determined by the amount of water passed, and the character of the bottom.

There is rock bottom in the Lake one-third of a mile above the mouth, and at about the same distance below. Examinations were made of the bed of the Creek, and of the Lake opposite its mouth, by boring to the depth of 23 feet below the surface of the water.

To the depth of 18 feet the bottom is composed of sand and common gravel—below 18 feet of common gravel and very hard cemented gravel in alternate strata.

REPORT OF THE ENGINEER APPOINTED TO MAKE THE FIRST SURVEY.—DEC. 1535.

Sir—Having made an examination of the Harbor at the mouth of Cattaraugus Creek, in the State of New-York, I have the honor to submit the following report: The Cattaraugus, which rises in the south-west part of Genesee county, and during a course of 45 miles receives the waters of several tributary streams, empties into Lake Erie at a point 30 miles in a south-western direction from Buffalo, and 15 in an easterly and north-easterly direction from Dunkirk.

Deriving its supplies from a high and some what broken country, it is subject to sudden and very considerable freshets. Its banks, generally bold, are low in the immediate vicinity of the Lake, and subject to occasional inundations. Its width, near the mouth, varies from 200 to 350 feet, its depth from 4 to 10 feet. The channel at its mouth is frequently obstructed, and sometimes closed by bars. In heavy gales from north-west and south-west, the Lake rises from 3 to 5½ feet.

The Lake at this point is usually clear from ice, earlier than is the harbor at Buffalo. Statement upon this subject are various. From a point 14 miles above the mouth, this stream falls 200 feet, to the level of the Lake, and in less than 30 miles the waters of the south branch descends 700 feet, to the level of the Lake Erie.

The back country is rapidly increasing in population

and in wealth, and from its affording so many and so val-

High water marks were ascertained at various points, the corresponding slopes and sections measured, and calculations based on these data, were instituted to ascertain the amount passed in units of high water. From these it appears that the freshets have afforded from 6000 to 9000 cubic feet per second, and that in the great freshet of November last, there passed more than 20,000 cubic feet per second.

It is believed that by preventing the spread and consequent gradual subsidence of the waters, the freshets may be so controlled as to produce a very considerable increase in the depth of the stream, and that by contracting the width to 230 feet, a depth of 12 to 15 feet will be secured.

It is proposed to commence the improvement at a point 2000 feet from the lake.

To depend upon the action of the current to secure the required depth of water.

To contract the channel in the creek to the width of 234 feet.

To construct two piers parallel to each other, at the distance of 234 feet, extending from the shore to 14 feet water in the lake—and to erect a beacon light at the extremity of the southern pier.

Abstracting from these considerations, the communication of lateral motion, the stream after passing through any contraction, will be subject at first, to the causes which produce the *vena contracta*, and afterwards, to the law of inverse ratio between space and velocity.

If then, the distance between the contractions, be

diminished and the mean velocity increased one-sixth, and upon arriving at the second aperture, the stream will have acquired its original conditions. As the intervals between the wings become filled with deposit, the shores will gradually approximate to the desired form, and acquire a natural and permanent character.

The wings can be readily made by driving rows of contiguous piles from each shore to the side of the proposed channel.

The embankment should be 8 feet above the level of the lake, and calculated for a head of 6 feet above common low water.

The latter manner of contracting the width of the channel, being least expensive—and being adequate to the purposes of general utility, is deemed preferable, and is the one proposed. The southerly pier should be 1016 feet in length, 25 feet in width, raised from a foundation 14 feet below, to the height of 8 feet above the surface of the water; and have a channel-face, protected by piles, extending from the surface of the water to the depth of 23 feet.

The northerly pier should be 1105 feet in length, 15 feet in width, and protected by piles. It is believed that this pier may be built upon the natural bed of the lake; that the abutment should be settled below the frost, of the same height as the piers, 10 feet in width, and protected by piles.

The action produced by the proposed contraction, will probably be gradual, commencing near the mouth of the Harbor and extending with each successive freshet, till through the whole length of the improvement an equilibrium shall have been established between the force of the current, and the resistance opposed by the bottom.

The current extends to a considerable distance into the lake, and will probably carry along with it the lighter materials, which, when deposited, will assume the natural slope of the bed of the lake.

The heavier substances, will be deposited nearer the extremities of the piers, and spread over the bottom, or removed by the action of the waves, as has been the

EXTRACTS

FROM THE OFFICIAL CORRESPONDENCE OF LIEUT. R. F. M.
LEN, U. S. AGENT FOR CERTAIN PUBLIC WORKS
ON LAKE ERIE.

13

case heretofore, when the freshets confined by ice, have torn away the bed of the creek—and carried into the lake, immense quantities of matter similar to that now to be removed.

In arranging the plans now submitted to your consideration, advantage has been taken, as far as was possible, of the experience of other similar works, and comparisons instituted between the effects produced here, under given circumstances, and those designed to be effected on the measures now suggested, and although from the many influences to which works of this kind are subjected, it may happen that the consequence of the measures now proposed, may not, in all respect correspond with those anticipated, it is believed that sufficient precautions have been taken, in the selection and application of the data upon which the opinions advanced have been founded, to warrant a reasonable degree of confidence in the general results, of the means by which it is proposed to effect an important and permanent improvement of this Harbor.

[Detail of estimates omitted.]

All which is respectfully submitted, by

Your obedient servant,
(Signed) JOHN S. STODDARD.
To HENRY SMITH, Esq., Capt. U. S. A.,
Superintendent Public Works, Lake Erie. }

"August 10, 1836.
* * * * The mouth of the Cattaraugus appears formerly, to have been further to the N. E. The channel passing near the bluff, (shown in plan) and to have been changed by the action of the S. W. winds.

I would recommend the construction of piers as marked in sketch, to rectify the channel, and turn the mouth of the creek more to the north, as less liable, in this position, to be effected by the severe south-westerly blows, and at the same time, the waves would tend to remove any deposit the creek might bring out, towards the N. E."

"August 29, 1836.
* * * * My plan for this work, was first to construct the *southern* pier until we should reach twelve feet water: then to turn the course of the creek; and after the spring freshets had widened and deepened the channel, to determine the proper width to be given to the harbor, and then construct the northern pier, at the same time finishing the southern one.

The piers, once constructed upon this plan, and the channel cleared, the sediment brought down would be carried past by the prevailing lake-current, which sets directly across the harbor entrance, which is so disposed, that none of the prevailing winds can beat into it. This plan would give [ainner] harbor 3,000 feet in length, and probably 300 feet in breadth, *perfectly safe at all seasons*, with sufficient depth of water."

3

P 415

"Sept, 8, 1836.

* * * Another plan might be adopted, thus : let the piers be carried out so that the alluvial matter from the creek may be carried off to strike N. E., then construct the proposed western break-water, commencing at the shore, and connect the outer harbor with the inner, by slips; those would answer as entrances to the inner harbor, and might be so constructed that they would never fill up."

"Jan. 1837.

* * * At Cattaraugus, the first crib was sunk 4th October. There are now nine cribs 30 feet long, forming a pier 210 feet in length. The effect of this work is already beginning to be felt by the stream.

The channel is deepening and widening in the proper direction.

200 feet more of crib-work, will give this channel a permanent position, and prevent its being filled by the lake. * * * This length of pier will be put down before the lake opens in the spring.

The form of work adopted at this place, appears to be perfect; nearly all the cribs now down, having been exposed while empty, to severe storms, and not one having been moved.

These cribs are not fastened to the piles, but are allowed to settle as the sand washes out from beneath, the piles only serving to keep them in position. Within a few days after each crib was sunk, the water deepened on its channel-face to 12 and 15 feet, whilst on the other it shoaled to 2 or 3 feet.

A large quantity of timber is on hand, a considerable quantity being already framed and ready for putting together. * * *

This harbor, when fully improved, will be one of the best on this lake."

[In reply to inquiries submitted by a stranger.]

January, 1837.

* * * A harbor might be made at the mouth of the Cattaraugus, carry of recks, perfectly safe at all seasons.

47

for the amount of the estimate presented to Congress last winter, but a full improvement of the harbor will require a much larger amount.

Of the importance of that harbor to the commerce of Lake Erie, no one at all acquainted with the subject can entertain a doubt. It is well known that a harbor at that place, is indispensable to the well-being of the lake commerce.

The harbor at Cattaraugus will not cost half the sum expended upon that of Buffalo; and when finished, will lose nothing by a comparison.

(Signed)

R. T. P. ALLEN,

U. S. Agent, &c.

Appendix 4

SOURCE OF DATA

A. Map References

Date	Number or Title	Source/Holder
Changes from 1813-1845 " " 1927-1938	Map Showing Erosion of Cattaraugus Creek (scale 100' = 1")	E. H. Keyes - Surveyor Forestville, New York
-1929-	?	E. H. Keyes Forestville, New York
Prior to August 1845	Map of Irving Village (scale 1" = 264')	John B. Preston - Surveyor; Altered by William Clogher - Surveyor
May, 1844	Map of Cattaraugus Harbor (copy of 1" = 200')	Lt. J. C. Woodruff, Corps of Top. Eng. Photostat in National Archives.
June, 1940	Cattaraugus Creek, New York. Survey and Examination of Creek Mouth. 1" = 200'	U. S. Engineer Office Army Corps of Engineers
1935, Dec. 24	Cattaraugus Creek, New York. Survey 1" = 200'	U. S. Army Corps of Engineers, Drawer #72, 11-A-76

Map showing erosion of Cattaraugus Creek from the railroad bridge
to the mouth in 1939, 1927, 1845 and 1813. Scale 1" = 100'. Holder:
E. H. Keyes - Forestville, New York.

Appendix 4

B. Airphoto References

<u>Date</u>	<u>Photo Number</u>	<u>Source/Holder of Negative</u>
11-1-38	ARN26-95 + 97 27-3	S.U.N.Y Fredonia Library/National Archives
4-16-68	NY-10-1539-628	Corps of Engineers, Buffalo, New York
5-17-71	369-15-445	Chautauqua County Planners, Mayville, New York.
10-25-64	V-VAP62 USN340	U. S. Navy Corps of Engineers, Buffalo, New York.

Appendix 5

SUMMARY OF HYDRAULIC PARAMETERS ON CATTARAUGUS CREEK PERTINENT TO BED MATERIAL
 TRANSPORT COMPUTATIONS. ASSUMED CONSTANT LAKE LEVEL: 572' ABOVE L.W.D.

River Mile	Stage (ft)	Area (ft)	Hydraulic Radius (ft)	Discharge (cfs)	Slope	Mean Velocity	
						Shear Velocity Relationship (fps)	Manning's Relationship (fps)
0-0.75 mi							
unimproved	573.5	2,280	3.80	3,400	6 • 10^{-5}	.39	.43
	575.0	3,180	5.03	16,000	4.5 • 10^{-4}	4.56	4.96
	580.0	6,230	9.64	50,000	7.1 • 10^{-4}	8.72	9.69
	585.0	9,280	14.15	100,000	7.1 • 10^{-4}	11.13	12.57
0-0.75 mi							
improved	573.5	3,080	5.08	5,600	6 • 10^{-5}	.55	.59
	575.0	3,980	6.23	23,000	4.5 • 10^{-4}	5.27	5.74
	580.0	7,030	10.77	56,000	7.1 • 10^{-4}	9.36	10.41
	585.0	10,080	15.20	107,000	7.1 • 10^{-4}	11.63	13.16
2.0-2.2 mi							
	8.0	--	3.50	3,150	7.5 • 10^{-4}	3.99	--
	15.0	--	8.53	17,000	7.5 • 10^{-4}	6.31	--
	16.2	--	9.57	20,000	7.5 • 10^{-4}	7.61	--
	19.7	--	12.33	33,000	7.5 • 10^{-4}	9.84	--
	23.8	--	15.21	55,000	7.5 • 10^{-4}	11.56	--

Appendix 6
RESULTS OF SEDIMENT TRANSPORT CALCULATIONS
AT RIVER MILES 0-0.75 AND 2.0-2.2

EINSTEIN CALCULATIONS FOR RIVER MILES 2.0-2.2

Size (mm)	Q _w (cfs)	Ψ	Φ	g _s (kg/m ³ ·s)	G _s (tons/day)
$\bar{D} = 77.5$	100-55	3,150	159.80	$\ll 10^{-4}$	$<10^{-2}$ <80
		17,000	65.55	$\ll 10^{-4}$	$<10^{-2}$ <80
		20,000	58.43	$\ll 10^{-4}$	$<10^{-2}$ <80
		33,000	45.34	$\ll 10^{-4}$	$<10^{-2}$ <80
		55,000	36.78	$\ll 10^{-4}$	$<10^{-2}$ <80
$\bar{D} = 38.5$	55-22	3,150	79.40	$\ll 10^{-4}$	$<10^{-2}$ <80
		17,000	32.55	$<10^{-4}$	$<10^{-2}$ <80
		20,000	29.04	$<10^{-4}$	$<10^{-2}$ <80
		33,000	22.51	$1.2 \cdot 10^{-3}$.096 787
		55,000	18.24	$7.0 \cdot 10^{-3}$.563 4,621
$\bar{D} = 15.5$	22-9	3,150	31.96	$<10^{-4}$	$<10^{-2}$ <80
		17,000	13.09	$4.0 \cdot 10^{-2}$.822 6,746
		20,000	11.68	$5.5 \cdot 10^{-2}$	1.131 9,283
		33,000	9.06	$1.3 \cdot 10^{-1}$	2.673 21,940
		55,000	7.35	$2.7 \cdot 10^{-1}$	5.552 45,570
$\bar{D} = 5.6$	9-2.2	3,150	11.15	$7.0 \cdot 10^{-2}$.312 2,561
		17,000	4.72	$7.5 \cdot 10^{-1}$	3.343 27,440
		20,000	4.20	$9.5 \cdot 10^{-1}$	4.242 34,820
		33,000	3.28	1.60	7.145 58,730
		55,000	2.65	2.30	10.271 84,300
$\bar{D} = 1.45$	2.2-.7	3,150	2.98	1.85	1.088 8,930
		17,000	1.22	6.40	3.765 30,900
		20,000	1.09	7.10	4.177 34,280
		33,000	.84	9.60	5.648 46,360
		55,000	.68	11.00	6.472 53,120

EINSTEIN CALCULATIONS FOR RIVER MILES 0-0.75.

UNIMPROVED CONDITIONS

Size (mm)	Q _w (cfs)	Ψ	Φ	g _s (kg/m·s)	G _s (tons/day)
$\bar{D} = 33.5$	3,400	801.00	$\ll 10^{-4}$	$\ll 10^{-3}$	$\ll 20$
	16,000	80.28	$\ll 10^{-4}$	$\ll 10^{-3}$	$\ll 20$
	50,000	26.48	$1.5 \cdot 10^{-4}$	$9.8 \cdot 10^{-3}$	156
	100,000	18.04	$9 \cdot 10^{-3}$.590	9,431
$\bar{D} = 13.25$	3,400	316.00	$\ll 10^{-4}$	$\ll 10^{-3}$	$\ll 20$
	16,000	31.76	$\ll 10^{-4}$	$\ll 10^{-3}$	< 100
	50,000	10.47	$7.5 \cdot 10^{-2}$	1.218	19,469
	100,000	7.12	$2.4 \cdot 10^{-1}$	3.901	62,354
$\bar{D} = 7.15$	3,400	171.00	$\ll 10^{-4}$	$\ll 10^{-3}$	$\ll 20$
	16,000	17.13	$1.3 \cdot 10^{-2}$.083	1,327
	50,000	5.64	$5.4 \cdot 10^{-1}$	3.479	55,608
	100,000	3.84	1.2	7.731	123,570
$\bar{D} = 3.0$	3,400	71.70	$\ll 10^{-4}$	$\ll 10^{-3}$	$\ll 20$
	16,000	7.19	$2.6 \cdot 10^{-1}$.455	7,273
	50,000	2.37	2.7	4.728	75,572
	100,000	1.61	5.0	8.755	139,940
$\bar{D} = .64$	3,400	15.30	$1.9 \cdot 10^{-2}$	$3.28 \cdot 10^{-3}$	52
	16,000	1.54	5.3	.914	15,041
	50,000	.49	17.0	2.933	46,881
	100,000	.34	24.0	4.141	66,190

EINSTEIN CALCULATIONS FOR RIVER MILES 0-0.75.

IMPROVED CONDITIONS

Size (mm)	Q_w (cfs)	Ψ	ϕ	g_s (kg/m.s)	G_s (tons/day)
$\bar{D} = 33.5$	5,600	594.000	$\ll 10^{-4}$	$\ll 10^{-3}$	$\ll 20$
	23,000	64.700	$\ll 10^{-4}$	$\ll 10^{-3}$	$\ll 20$
	56,000	23.700	$8.5 \cdot 10^{-4}$	$2.9 \cdot 10^{-2}$	463
	107,000	16.790	$1.8 \cdot 10^{-2}$	1.170	18,701
$\bar{D} = 13.25$	5,600	235.000	$\ll 10^{-4}$	$\ll 10^{-3}$	$\ll 20$
	23,000	25.600	$2.4 \cdot 10^{-4}$	$3.9 \cdot 10^{-3}$	62
	56,000	9.350	$1.1 \cdot 10^{-1}$	1.787	28,563
	107,000	6.620	$3.4 \cdot 10^{-1}$	5.525	88,312
$\bar{D} = 7.15$	5,600	126.000	$\ll 10^{-4}$	$\ll 10^{-3}$	$\ll 20$
	23,000	13.800	$3.8 \cdot 10^{-2}$.243	3,884
	56,000	5.050	$6.1 \cdot 10^{-1}$	3.929	62,801
	107,000	3.570	1.45	9.342	149,320
$\bar{D} = 3.0$	5,600	53.200	$\ll 10^{-4}$	$\ll 10^{-3}$	$\ll 20$
	23,000	5.770	$5.0 \cdot 10^{-1}$.875	13,986
	56,000	2.130	2.90	5.077	81,151
	107,000	1.470	5.40	9.455	151,130
$\bar{D} = .64$	5,600	11.350	$6.8 \cdot 10^{-2}$	$1.17 \cdot 10^{-2}$	187
	23,000	1.217	6.50	1.120	17,902
	56,000	.452	17.50	3.020	48,272
	107,000	.321	25.00	4.310	68,891

MEYER-PETER AND MÜLLER COMPUTATIONS

FOR RIVER MILES 2.0-2.2

<u>Size (mm)</u>	<u>Q_w (cfs)</u>	<u>g_s (kg/m·s)</u>	<u>G_s (tons/day)</u>
100-55 $\bar{D} = 77.5$	3,150	0	0
	17,000	0	0
	20,000	0	0
	33,000	0	0
	55,000	0	0
55-22 $\bar{D} = 38.5$	3,150	0	0
	17,000	0	0
	20,000	0	0
	33,000	0	0
	55,000	.475	3,899
22-9 $\bar{D} = 15.5$	3,150	0	0
	17,000	.836	6,862
	20,000	1.283	10,531
	33,000	2.677	21,973
	55,000	4.464	36,641
9-2.2 $\bar{D} = 5.6$	3,150	.292	2,397
	17,000	2.399	19,691
	20,000	3.011	24,714
	33,000	4.766	39,119
	55,000	6.873	56,414
2.2-0.7 $\bar{D} = 1.45$	3,150	.742	6,090
	17,000	3.200	26,266
	20,000	3.869	31,757
	33,000	5.755	47,237
	55,000	7.984	65,533

MEYER-PETER AND MÜLLER COMPUTATIONS

FOR RIVER MILES 0-0.75

<u>Size (mm)</u>	<u>Q_w (cfs)</u>	<u>g_s (kg/m³·s)</u>	<u>G_s (tons/day)</u>
50-17 $\bar{D} = 33.5$	3,400	0	0
	16,000	0	0
	50,000	0	0
	100,000	.421	6,729
17-9.5 $\bar{D} = 13.25$	3,400	0	0
	16,000	0	0
	50,000	1.421	22,713
	100,000	3.746	59,876
9.5-4.8 $\bar{D} = 7.15$	3,400	0	0
	16,000	.0658	1,052
	50,000	2.459	39,305
	100,000	5.118	81,806
4.8-1.2 $\bar{D} = 3.0$	3,400	0	0
	16,000	.399	6,377
	50,000	3.265	52,188
	100,000	6.129	97,966
1.2-0.08 $\bar{D} = .64$	3,400	$3.58 \cdot 10^{-3}$	57
	16,000	.659	10,533
	50,000	3.756	60,036
	100,000	6.730	107,570

KALINSKEE CALCULATIONS FOR RIVER MILE 2.0-2.2

Size mm	Q _w cfs	τ_{cr}/τ_o	q _s /U*D	q _s * $\tau_s = g_s$ kg/m*s	G _s tons/day
100-55	3,150	9.6000	10^{-3}	10^{-2}	80
	17,000	3.9600	10^{-3}	10^{-2}	80
$\bar{D} = 77.5$	20,000	3.5100	10^{-3}	10^{-2}	80
	33,000	2.7300	10^{-3}	10^{-2}	80
$(\tau_o)cr = 7.7 \text{ kg/m}^2$	55,000	2.2100	$6 \cdot 10^{-3}$.2990	1,879
55-22	3,150	4.8000	10^{-3}	10^{-2}	80
	17,000	1.9800	.014	.1980	1,625
$\bar{D} = 38.5$	20,000	1.7500	.030	.4520	3,710
	33,000	1.3600	.098	1.6700	13,707
$(\tau_o)cr = 3.85 \text{ kg/m}^2$	55,000	1.1000	.200	3.7900	31,108
22-9	3,150	1.9800	.018	.0661	542
	17,000	.7970	.420	2.3900	19,617
$\bar{D} = 15.5$	20,000	.7070	.500	3.0300	24,870
	33,000	.5490	.680	4.6900	38,496
$(\tau_o)cr = 1.55 \text{ kg/m}^2$	55,000	.4450	.780	5.9500	48,838
9-2.2	3,150	.6980	.510	.6770	5,474
	17,000	.2880	1.100	2.0600	16,908
$\bar{D} = 5.6$	20,000	.2550	1.350	2.9600	24,296
	33,000	.1980	1.500	3.7300	30,616
$(\tau_o)cr = .56 \text{ kg/m}^2$	55,000	.1600	1.600	4.4200	36,279
2.2-.7	3,150	.1810	1.550	.5330	4,375
	17,000	.0746	2.250	1.2000	9,849
$\bar{D} = 1.45$	20,000	.0662	2.300	1.3100	10,752
	33,000	.0514	2.300	1.4800	12,148
$(\tau_o)cr = .145 \text{ kg/m}^2$	55,000	.0416	2.300	1.6400	13,461

KALINSKEE COMPUTATIONS FOR RIVER MILES 0-0.75

Size mm	Q _w cfs	τ_{cr}/τ_o	q _s /U _{st} ·D	q _s · γ _s = g _s kg/m·s	G _s tons/day
50-17	3,400	47.8000	10^{-3}	10^{-3}	20
	16,000	4.7800	10^{-3}	$7.155 \cdot 10^{-3}$	114
$\bar{D} = 33.5$	50,000	1.5800	.05	.636	10,166
$(\tau_o)_{cr} = 3.3 \text{ kg/m}^2$	100,000	1.0800	.21	3.262	52,140
17-9.5	3,400	18.8000	10^{-3}	10^{-3}	20
	16,000	1.8800	.02	.0583	931
$\bar{D} = 13.25$	50,000	.6200	.60	3.0340	48,495
$(\tau_o)_{cr} = 1.3 \text{ kg/m}^2$	100,000	.4200	.90	5.5300	88,391
9.5-4.8	3,400	10.3000	10^{-3}	10^{-3}	20
	16,000	1.0300	.24	.3770	6,026
$\bar{D} = 7.15$	50,000	.3400	1.20	3.2740	52,331
$(\tau_o)_{cr} = .71 \text{ kg/m}^2$	100,000	.2300	1.45	4.8080	76,851
4.8-1.2	3,400	4.3500	10^{-3}	10^{-3}	20
	16,000	.4300	.90	.5930	9,478
$\bar{D} = 3.0$	50,000	.1400	1.70	1.9460	31,105
$(\tau_o)_{cr} = .30 \text{ kg/m}^2$	100,000	.1000	1.90	2.6430	42,246
1.2-0.08	3,400	.8690	.32	.2820	4,507
	16,000	.0869	2.20	.3090	4,939
$\bar{D} = .64$	50,000	.0287	2.30	.5620	8,983
$(\tau_o)_{cr} = .06 \text{ kg/m}^2$	100,000	.0196	2.35	.6970	11,141

Plate I. Cattaraugus Creek meander positions 1938, 1958, 1971.

(This page is to be replaced with
Plate I which has been furnished
separately.)

DATE
FILMED
- 8